The Mechanism of ER to Cytosol Retrotranslocation of Proteins Targeted to ERAD (ER Associated Degradation)

Thesis

UNRESTRICTED

The mechanism of ER to cytosol retrotranslocation of proteins targeted to ERAD (ER Associated Degradation)

Gianluca Petris

A Thesis Submitted in Fulfilment of the Requirements of the Faculty of Life Science of the Open University (UK) for the Degree of Doctor of Philosophy

International Centre for Genetic Engineering and Biotechnology
(ICGEB)
Trieste, Italy

Director of Studies: Dr. Oscar R. Burrone

External Supervisor: Dr. Lawrence Banks

September 2013

DATE OF SUBMISSION: 27 SEPTEMBER 2013
DATE OF AWARD: 25 NOVEMBER 2013

ProQuest LLC.
789 East Eisenhower Parkway
P.O. Box 1346
Ann Arbor, MI 48106 – 1346

Contents

Abstract....4
Introduction....5
1.The ER from protein synthesis to ERAD....5
1.1 ER general aspects....5
1.2 ER protein synthesis and translocation....5
1.3 Protein folding in the ER....11
1.4 From ER quality control to ERAD....18
1.5 Unfolded protein response....19
1.6 ERAD substrate recognition and demannosylation....23
1.7 ERQC compartment....25
1.8 A channel model to ERAD....26
1.9 Cytosolic ERAD steps....29
1.10 Ubiquitination and proteasomal degradation....31
1.10.1 Ubiquitin structure and conjugation....32
1.10.2 Deubiquitination....37
1.10.3 Proteasome function, structure and location....39
1.11 Specific ERAD pathways for different ERAD substrates....43
2.HCMV induced degradation of MHC class I....45
2.1 MHC class I structure and function....45
2.2 Folding of MHC class I molecules....47
2.3 Immuno evasion: HCMV and MHC class I down regulation....48
2.4 US11 and US2 activity....49
3.The ERAD model Null Hong Kong α1 antitrypsin (NHK-α1AT)....52
4.Folding and ERAD of immunoglobulin heavy and light chains....55
5.Vpu induced degradation of CD4 and Tetherin....58
5.1 Vpu....58
5.2 ER associated degradation of CD4....59
5.3 Vpu induced Tetherin degradation....61
6.Calreticulin: ER and non-ER functions....64
7.Protein biotinylation as a tool to label cytosolically exposed proteins....68
8.Tobacco Etch Virus protease (TEVp) as biotechnological tool....70
Materials and methods....72
Results....79
1.BirA localization in eukaryotic cells....79
2.Retrotranslocation of MHC-Iα....83
2.1 Proteasome inhibition increases biotinylation of MHC-Iα....87
2.2 Determination of MHC-Iα retrotranslocation by ELISA....90
2.3 Trypsin sensitivity of biotinylated MHC-Iα....91
2.4 Cell fractionation of biotinylated MHC-Iα....93
2.5 The extracellular domain of biotinylated-glycosylated MHC-Iα is fully exposed to the cytosol....95
3.Retrotranslocation of secretory proteins....99
4.Retrotranslocation of calreticulin....102
5.Analysis of protein folding during dislocation....104
5.1 Biotinylation of dislocated CD4 and Tetherin....105
5.1.1 Retrotranslocation of CD4....106
5.1.2 CD4 retrotranslocates with intrachain oxidised disulphide bonds....112
5.1.3 Retrotranslocation of Tetherin....114
5.1.4 Tetherin retrotranslocates with oxidized disulphide bonds....118

5.2 The non-secreted immunoglobulin κ light chain NS1.....125
6.The role of the p97 ATPase activity in ERAD.....130
7.TEVp as second reporter of ER to cytosol retrotranslocation.....135
7.1 TEVp in the analysis of MHC-Iα ERAD.....136
7.2 TEVp and NS1 retrotranslocation.....139
Discussion.....141
Acknowledgments.....161
References.....162

Abstract

Retro-translocation from the endoplasmic reticulum (ER) to the cytosol of secretory and membrane proteins takes place on misfolded molecules targeted for proteasomal degradation, in a process called ER associated degradation (ERAD). Because of the difficulties in clearly discriminating the fraction of molecules already retro-translocated from the ones in the ER, we took advantage of the *E. coli* biotin-ligase (BirA) expressed in the cytosol of mammalian cells, to specifically biotin-label proteins that undergo retro-translocation. The method was validated using four different model proteins, known to undergo retro-translocation upon different conditions: the MHC-Iα chain, the non-secretory null-Hong Kong mutant of α1 antitrypsin, the immunoglobulin γH chain and calreticulin. The specific mono-biotinylation of only cytosolically dislocated molecules resulted in a novel quantitative method to determine the extent of retro-translocation.

The method was used to study dislocation of CD4 and BST-2/Tetherin, two membrane proteins targeted to degradation by the HIV-1 protein Vpu. It was found that CD4 retro-translocates with oxidised intra-chain disulphide bridges that only upon proteasomal inhibition accumulates in the cytosol in reduced and de-glycosylated form. Similarly, BST-2/Tetherin is first exposed to the cytosol as a dimeric-oxidised complex, which then becomes de-glycosylated and reduced to monomers. Experiments with the non-secreted NS1 Ig-κ light chain showed that also this ERAD model protein is retro-translocated with oxidised cysteines. The role of VCP/p97-ATPase in retro-translocation was investigated. In contrast to what previously reported, it was found that it is not required to dislocate ERAD substrates from the ER lumen to the cytosol, while it is required for efficient de-glycosylation and proteasomal degradation of ERAD substrates. The results obtained indicate that complete cysteine reduction and unfolding is not strictly required for retro-translocation, suggesting alternative mechanisms of the ERAD pathway. In addition, the role of VCP/p97-ATPase was found associated to stages downstream of membrane crossing.

Introduction

1. The ER from protein synthesis to ERAD

1.1 ER general aspects

The endoplasmic reticulum (ER) is a eukaryotic organelle, spread in the cell cytoplasm from the nuclear membrane to the Golgi apparatus. This organelle is formed by an interconnected network of membrane delineated structures such as tubules, vesicles and cisternae.

The environment within the ER apparatus is widely different from other cell compartments such as the cytosol, with a high Ca^{2+} concentration and a more positive redox potential.

Many different functions are associated with the ER and those are reflected in the different ER subdomains like the nuclear envelope, the rough ER, the smooth ER and the ER-Golgi intermediate compartment (ERGIC) (Lavoie and Paiement, 2008). The rough ER is where secretory proteins are synthesized and reach their primary folding, while the smooth ER is the site of lipid and steroid synthesis, carbohydrate metabolism, calcium level regulation and drug detoxification (Lavoie and Paiement, 2008).,

The ER altogether is responsible for the synthesis, processing and trafficking of about one third of the proteins encoded by the human genome.

1.2 ER protein synthesis and translocation

Secretory proteins and many transmembrane proteins are synthesized on ribosomes bound to the ER membrane. The translation of those proteins initiates in the cytosol on free ribosomes involving a number of initiation and elongation factors (Preiss and Hentze, 2003). If the nascent polypeptide has a signal sequence (a short hydrophobic sequence of around 20 amino acids) the protein complex SRP (the Signal Recognition Particle consists of a 7S RNA molecule of 300 nucleotides and six protein subunits: SRP72, SRP68, SRP54, SRP19, SRP14 and SRP9) bind it through the methionine-rich M-domain of its 54kDa subunit (SRP54), while the interaction with the ribosome promotes the

loading of GTP on the G-domain of the SRP complex (Krieg t al., 1986; Lutcke et al., 1992; Luirink and Sinning, 2004).

The complex docks onto the translocon, a heterotrimeric protein complex called Sec61p, through the SRP receptor (SRα-SRβ) promoting the interaction of the ribosome to the translocon pore, formed by the transmembrane of its three Sec61α-, β- and γ-subunits (Rapoport et al., 1996; Chen et al., 2010).

After the release of SRP and SRP-receptor they are recycled and separated through GTP hydrolysis (Connoly and Gilmore, 1993), while the nascent protein is synthesized by the ribosome directly on the ER allowing a co-translational translocation within the ER lumen (Fig.1). In this process the GTP hydrolysis is believed to be required for chain elongation by the ribosome but not for the polypeptide movement through the channel (Connoly and Gilmore, 1986; Rapoport, 2007).

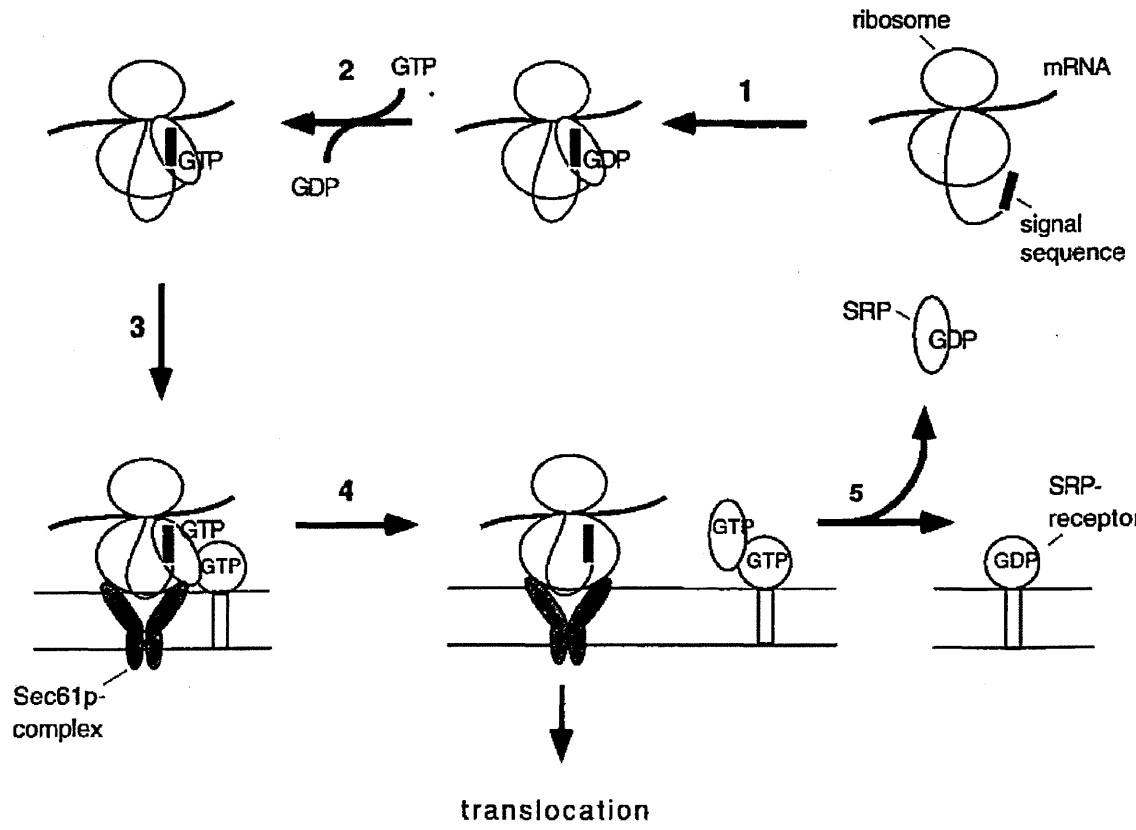

Figure 1. Scheme of the SRP cycle in the first steps of the translocation process (Rapoport et al., 1996). When the signal sequence of a growing polypeptide chain has emerged from the ribosome, SRP bind both the nascent chain and the ribosome (step 1). Then GDP associated with SRP is replaced by GTP (step 2). This complex interacts with the ER membrane through the SRP receptor (which also is binding a GTP molecule) and the Sec61p

complex (step 3). After ribosomal docking the SRP complex is released (step 4), while the membrane-secretory protein start to get translocated. Finally the SRP cycle terminates (step 5), through GTP hydrolysis in both SRP and SRP receptor, and SRP is released.

The Sec61 α-subunit, a 10 membrane-spanning domains containing protein, forms the aqueous pore of the channel, but, when targeting is completed, this pore is not open to the lumen until the nascent chain length reaches about 70 residues (Simon and Blobel, 1991; Crowley et al., 1993, 1994.).

The structure of the Sec61 α-subunit is evolutionary conserved through the species and the pore, formed by a single α-subunit, has an estimated maximum dimension of 15 X 20 angstrom (Å), according to the crystal structure of a bacterial SecY complex (Van den Berg et al., 2004; Breyton et al., 2002). In such a small channel the nascent polypeptide can only form a α-helix, but not tertiary structure (Kowarik et al., 2002). Despite that, fluorescence quenching experiments during cotraslational protein translocation have indicated that the pore is rather larger (40-60 Å) (Hamman et al., 1997), suggesting the possibility that two or more Sec61/SecY complexes can be associated fusing their pore into a large channel. Even though experiments of disulphide-bridge cross-linking found that, during translocation, both the signal sequence and the mature region of the polypeptide are located in the same SecY molecule (Rapoport 2007; Osborn and Rapoport, 2007). While in the heterotrimeric translocon complex the Sec61γ subunit, a small type two membrane protein of 7kDa, is in tight contact with Sec61α functioning as a sort of hinge for the channel, clamping the two halves of alpha subunit (TM1-TM5 and TM6-TM10), the type two membrane protein Sec61β seems to have a more peripheral localization (Van den Berg et al., 2004) (Fig. 2). Indeed Sec61β has a less pivotal role during translocation as is not required for cell viability in *S. cerevisiae* and in *E. coli* as observed for the Sec61α and γ, however this subunit is thought to interact directly with the ribosomal protein Rpl17 in all ribosomal translocon complexes (Pool, 2009). Probably its function is minimally required to stabilize ribosomal association with ER membranes, a role predominantly performed by the C-terminal tail and loop 8 of Sec61α (Raden et al., 2000; Cheng et al., 2005). Rather, Sec61β activity is to facilitate the transfer of the nascent chain from SRP to the translocon, reasonably driving the signal

sequence towards the ER lumen after release from the SRP (Kalies et al., 1998; Jiang et al.,2008; Pool, 2009).

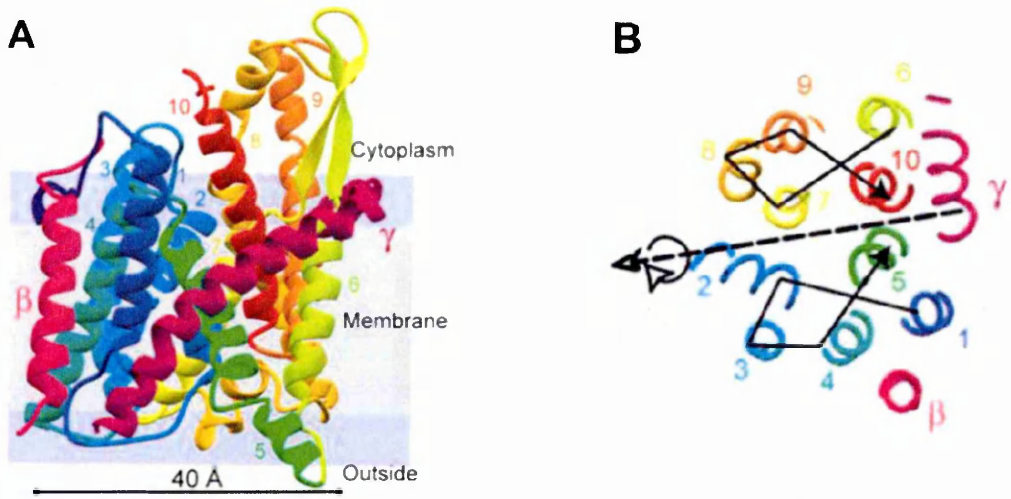

Figure 2. Architecture of membrane domains in SecY complex (adapted from Van den Berg, 2004). (A) Lateral organization of SecY complex in the ER membrane. Protruding cytosolic loops of α-subunit are probably involved in ribosomal binding. Membrane is shown in grey in the background. (B) Top view sliced through the middle of the membrane. The image shows the bridge form by γ transmembrane subunit between the two halves of α-subunit, and the peripheral localization of β-subunit in the complex. The solid lines represented the connection of the transmembranes from the N to the C terminus in the two halves of α subunit; the dotted arrow shows the axis of internal symmetry.

Many ER resident proteins assist the entry of the polypeptides. These include the translocon-associated protein complex (TRAP), a protein with still an unclear function (Rapoport, 2007), and the translocating-chain associating membrane protein (TRAM), a multispanning membrane protein. The latter has been detected in proximity to short nascent polypeptide chains, in cross-linking experiments, after their transfer from SRP into the ER membrane. Moreover TRAM was found to be required for the cotranslational translocation of most polypeptides in vitro (Gorlich et al., 1992; Gorlich and Rapoport, 1993). In addition to TRAM many other proteins are associated with the translocon and interact with the nascent polypeptide. The tetrameric Sec62/Sec63 complex (Panzner et al., 1995) has been coupled with a population of proteins post-translationally inserted in the ER lumen or in the periplasm in bacteria. The post-translational translocation occurs in particular in simpler organisms, i.e. yeast and bacteria, but also in higher eukaryotes. This pathway is used mostly by soluble proteins with a signal sequence not highly hydrophobic, that allows

them to escape the recognition by SRP during synthesis (Ng et al., 1996; Huber et al., 2005a).

This class of proteins need to remain unfolded or loosely folded after their release from the ribosome (Huber et al., 2005b) through the binding of many cytosolic chaperons, which are removed when translocation begins (Plath and Rapoport 2000).

Sec63 has in its luminal portion the J-domain, which interacts with the ATP-loaded peptide-binding domain of the protein BiP, a member of the Hsp70 family, resulting in the binding of the ER-chaperon with the translocation substrate through ATP hydrolysis (Misselwitz et al.,1998).

The J-domain-activated BiP has a low binding specificity, thus it can interact with most of the polypeptide segments emerging from the channel. In this case BiP promotes the translocation through a ratcheting mechanism, because, while the polypeptide is sliding in the translocon by Brownian motion, the binding of BiP prevents a movement back of the substrate, resulting in a forward translocation driven by a subsequent interaction of another BiP to the next sequence of the polypeptide (Matlack et al., 1999). This proceeds until the polypeptide is fully translocated, when an exchange of ADP to ATP releases BiP (Fig.3).

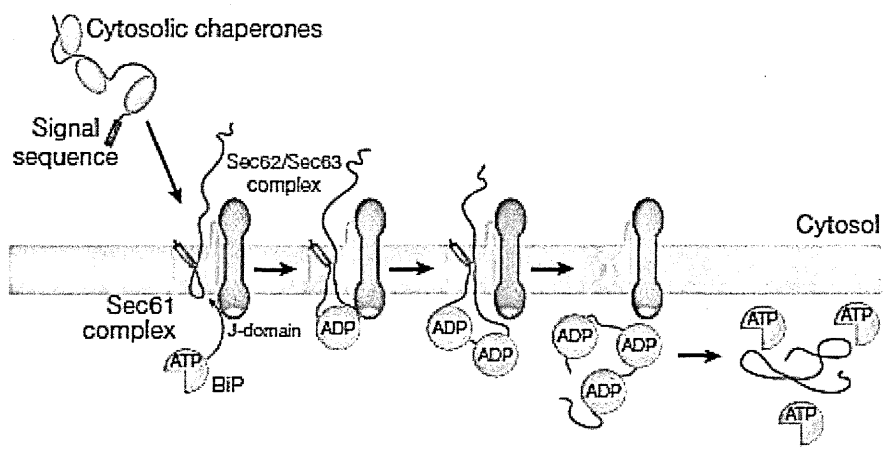

Figure 3. Representation of role of BiP in the post-translational translocation (Rapoport, 2007). In the ratcheting model BiP is believed to bind the entry polypeptide through ATP hydrolysis stimulated by the J-domain of Sec63, preventing a reverse movement of the substrate back to the cytosol.

The membrane insertion of many transmembrane proteins occurs through the same targeting and translocation machinery used for secretory proteins; if the

translocating polypeptide bears a hydrophobic α-helix domain this acts as an anchor signal and provokes the exit of the nascent membrane protein from the translocon to become embedded into the phospholipid bilayer.

In this process, at the early phases, the membrane anchor interacts with both the Sec61 and the lipid bilayer, but also in some cases with the TRAM protein (Martoglio et al., 1995; Heinrich et al., 2000). In particular the association of the hydrophobic domain with the membrane occurs through the gate formed by four short transmembrane segments of Sec61 linking the two halves of the molecule; from this joint the transmembrane domain of the new protein can reach the lipid phase (Van den Berg et al., 2004). In general in the absence of an N-terminus leader peptide, the orientation of the transmembrane domains, having the N terminus oriented to the luminal or cytosolic side, depends on the amino-acid sequences around this protein region. Indeed, when a hydrophobic polypeptide portion emerges from the ribosomal tunnel, if it is long and its N terminus is not retained in the cytosol by positive charges or by already folded domains it can flip across the channel and subsequently exit it laterally into the lipid phase, giving rise a type one membrane protein even without a classical leader peptide at the extreme N-terminus. In contrast, the N-terminus is usually retained in the cytosol if in this portion are already present folded structures or in close proximity to the hydrophobic domains are located positively charged amino acids. In this case the polypeptide chain is further elongated, inserting the C-terminus of the polypeptide as a loop through the channel in the ER lumen (Rapoport, 2007). However a membrane proteins can have several transmembrane domain but the exact mechanisms leading to their appropriate insertion in the ER membrane are still not completely understood. Usually in those multi-spanning membrane protein the first transmembrane domain dictates the orientation of the subsequent ones (Wessel, 1988), although there are exceptions where a transmembrane domain has its own preferred orientation (Rapoport 2004). For example if N-glycosylation sites are present and recognized these impose final luminal localization to the glycosylated protein domain (Goder et al., 1999).

1.3 Protein folding in the ER

When the nascent secretory protein reaches the ER lumen a group of proteins in charge of the folding dock to the new protein, catalysing the post-translational modifications typical of the ER compartment. First the protease signal peptidase, a complex of five different proteins (in mammals) with serine-peptidase activity (Evans et al., 1986), removes the leader peptide, generally cleaving at a site that has small aliphatic residues at position -1 and -3 (Paetzel et al., 2002). The cut secretion signal is then further degraded by the protein signal peptide peptidase (SPP) (Weihofen et al., 2002).

Second the oligosaccaryltransferase (OST) complex transfers an oligosaccharyl moiety from the dolichol intermediate to Asn of the nascent polypeptide in the sequence context Asn-X-Ser/Thr, where X can be any amino acid other than Pro (Bause and Hettkamp, 1979). N-glycosylation occurs when the site reaches a distance of at least twelve amino acids from the luminal side of the membrane (Nilsson and Heijne 1993) and when the translated NXS site is already distant 65–75 amino acids, depending on the tendency of the nascent chain to adopt an α helix conformation in the ribosome-translocon channel, from the ribosomal P site (Mingarro et al., 2000; Deprez et al., 2005). The OST is a heteromeric, multisubunit complex in the ER membrane, characterized by the presence of many different proteins. The most characterized ones are ribophorin I, ribophorin II, OST48, DAD1, while the yeast homologous are respectively named Ost1p, Swp1p, Wbp1p, Ost2p (Yan and Lennarz, 2005). Among them a pivotal role has been assigned to Ost1p/ribophorin1 which was found to be cross-linked to many other OST components, probably playing an important role in the assembly of the enzyme complex (Yan et al., 2003). It is important to underline that the presence of an N-glycosylation consensus sequence is necessary but not sufficient to determine the glycosylation of a secretory protein, in particular amino acid residues adjacent to the consensus sequence modulate the binding of the polypeptide substrate with the OST complex. This suggests that the substrate-binding site on the enzyme recognizes a particular conformation formed by several amino acids rather than just the two Asn and Ser/Thr residues (Petrescu et al., 2004).

The preformed oligosaccharide in the N-glycosylation is formed by $Glc_3Man_9GlcNAc_2$ (Khalkhall and Marshall 1975) (Fig.4).

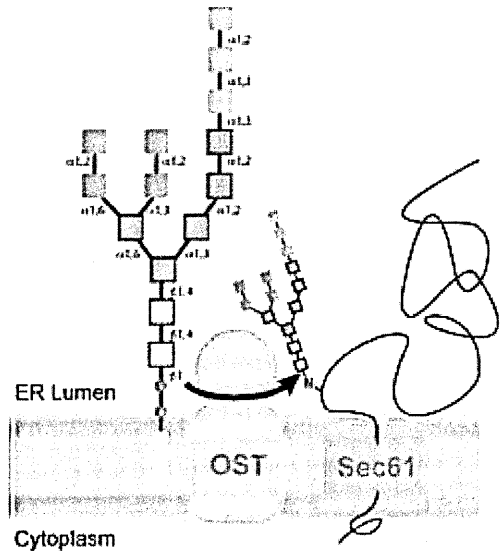

Figure 4. Scheme of the cotranslational N-glycosylation process. The preformed $Glc_3Man_9GlcNAc_2$ sugar moiety is transferred by the OST complex from the dolichol to Asn residues of the nascent polypeptide.

After the conjugation with the protein substrate the N-glycosylation tree is rapidly rearranged by the removal of the two outermost glucose residues by the enzymes glucosidase I (GI) and II (GII) (Parodi, 2000). The type-II membrane enzyme GI is a Mannosyl-oligosaccharide glucosidase, which cleaves in a highly specific manner the distal alpha 1,2-linked glucose residue from the $Glc_3Man_9GlcNAc_2$ oligosaccharide precursor; this enzyme is believed to be tightly associated to the OST complex (Caramelo and Parodi, 2008). Indeed its reaction occurs almost simultaneously with glycan transfer (Hubbard and Robbins, 1979; Deprez et al., 2005). After the first terminal glucose is trimmed by GI, the GII can remove both the two residual glucose residues. GII is a soluble dimeric protein both in yeast an in mammals. The catalytic activity resides in the α subunit, while the β subunit bears a KDEL-like sequence at its C-terminus, retaining the dimeric complex in the ER (Trombetta et al., 1996; Caramelo and Parodi, 2008). Of note the cleavage of the final glucose requires the expression of the β subunit, for which a regulatory role has been proposed at least in yeast (Wilkinson et al., 2006). GII cleavage of these two α1,3 glucoses is thought to not happen, however, in the same consecutive reaction, probably because of the different structural orientation in the chain of glucose α1,3 glucose and glucose α1,3 mannose (Caramelo and Parodi, 2008). This separation between the GII cleavages of the N-glycan probably allows

recognition of the monoglucosylated protein by calnexin and calreticulin (Deprez et al., 2005).

Indeed once cleaved the second glucose, the Glc1Man9GlcNAc2–protein is rapidly recognized by the lectin-like chaperones calnexin and calreticulin that intervene to favour the folding process.

Calnexin is a type-I ER resident membrane protein (Ahluwalia et al., 1992; Williams, 2006), while calreticulin is a soluble enzyme that has the signal KDEL at its C-terminus. The KDEL sequence promotes calreticulin retention in the ER through the binding with the multi-spanning KDEL-receptor protein (Fliegel et al., 1989; Wada et al., 1991; Pelham, 1990).

When the GII removes the remaining glucose residue, if the protein is finally folded, it can exit from the ER through COPII vesicles that bud from the ER surface (Lotti et al., 1996; Barlowe, 2002). COPII-coated vesicles bud from specific areas of the so called transitional ER, where the ER exit sites (ERES) are located (Bannykh, et al., 1996; Budnik and Stephens, 2009). The assembly of the COPII coat initiates with the activation of the small GTPase Sar1 by Sec12 (a transmembrane protein which acts as a guanine exchange factor), leading to Sar1 attachment to the ER membrane. This process is mediated by the exposure of an N-terminal amphipathic helix of Sar1 when is loaded with GTP, causing per se a local deformation or the ER membrane (Bielliet al., 2005). This membrane-linked Sar1 recruits the heterodimer formed by Sec23 and Sec24 (Hughes and Stephens, 2008). Sec23 act as a linker between Sar1 and Sec24 (Yoshihisa et al., 1993), which is instead required for the majority of cargo enrolment through its multiple independent cargo binding sites (Miller et al., 2002 and 2003). At this point a pre-budding complex is formed and in the cytosolic side of the ER membrane are recruited a minimum of 24 heterotetrameric complexes, composed each by two Sec13–Sec31 pairs, which are organised to form the outer cage of the budding COPII vesicle (Lederkremer et al., 2001; Hughes and Stephens, 2008). The full coat assembly drives vesicle scission through a not well defined mechanism involving Sar1–GTPase activity (Yoshihisa et al., 1993; Budnik and Stephens, 2009). The vesicles are then fused to the ER–Golgi intermediate compartment (ERGIC), before final protein sorting to the appropriate destination in the secretory pathway through the Golgi compartment (Appenzeller-Herzog and Hauri, 2006).

The third post translational modification that occurs on proteins during folding or even co-translationally in the ER lumen, is performed by proteins belonging to the thioredoxin superfamily, as the protein disulfide isomerase (PDI). Those enzymes are involved in the formation of intra-molecular and inter-molecular disulfide bonds in almost any newly synthesized polypeptide possessing cysteines in a luminal compartment (Ellgaard and Ruddock, 2005). Interestingly most PDI family members contain both catalytic and non-catalytic thioredoxin like domains (Kozlov et al., 2010). The active domains contain catalytic CXXC motifs, which are able to react with the thiols of cysteines. The non-catalytic domains although structurally similar to the active ones do not present catalytic cysteines. Instead, they are usually responsible for substrate recruitment (Denisov et al., 2009)

Currently it is believed that the major route for the oxidation of reduced cysteine (-SH) to oxidized cysteine (S-S) is via the oxidation of PDI by members of the Ero1 sulfhydryl oxidase family, followed by the oxidation of the substrate reduced cysteine by PDI (Lappy and Ruddok, 2011).

PDI proteins are not only required to catalyse the S-S bridge formation, but they are also enzymes able to isomerase or reduce also already formed disulfide bonds (Kozlov et al., 2010). Remarkably, independently of its redox activity, proteins of the PDI family can also act as a chaperone both in vitro and in living cells (Cai et al., 1994; McLaughlin and Bulleid, 1998). Among the members of the PDI superfamily, ERp57 was reported to be important in the oxidative folding during the protein folding cycles associated with calnexin and calreticulin (Oliver et al., 1999).

Indeed calnexin and calreticulin, facilitating the interaction between the newly synthesized protein and ERp57, favour indirectly the oxidative folding of their substrates, preventing protein aggregation, not only acting as chaperones but also in this way (Williams, 2006; Russell et al., 2004; Frickel et al., 2002). Other than ERp57 and PDI, in the PDI family several disulfide isomerases have been described in mammalian cells, most of which are ubiquitously expressed (Kozlov et al., 2010). Each PDI protein has a peculiar binding affinity with Ero1 and some family members have extra domains driving the disulfide isomerase to its specific class of substrates in the ER lumen, thus influencing the redox reactions in the different sub-compartments of the ER (Feige and Hendershot, 2011). For example ERdj5 is a PDI protein with a DnaJ-like domain which

favours its interaction with BiP (Ushioda et al., 2008). BiP binding, and also interaction with EDEM, influences the activity of ERdj5 toward misfolded proteins favouring their reduction before degradation.

In addition some ER-secretory proteins bear at the C-terminus a signal for the attachment of the glycosylphosphatidylinositol (GPI) anchor, which bind the mature protein to the outer layer of the membrane (Paulick and Bertozzi, 2008). The GPI signal peptide is sufficient to induce the GPI-anchoring when attached to the exposed C-terminus of a soluble secreted protein. Of the GPI anchor signals is known that they are usually formed by eight to twenty hydrophobic residues preceded by 6–12 hydrophilic "spacer" residues, rich in charged amino acids and proline (Eisenhaber et al., 2001; Orlean and Menon, 2007). At the N-terminus of this last region is present an amino acid residue with a small side-chain (Gly, Ala, Ser, Asn, Asp or Cys), called x, to which, after the cleavage performed by the GPI-transamidase between the x and x+1 sites, the GPI-anchor is linked. Around this amino acid x the x+1 residue can be any amino acid except a Pro, and the x+2 position is usually a small amino acid such as Gly, Ala or Ser (White et al., 2000).

The GPI-transamidase is believed to form transient intermediates with the precursor before the GPI-anchor is attached to the carbossilic terminal group of the substrate protein (Maeda and Kinoshita, 2011). Under defective biosynthesis of GPIs, precursor proteins may be released from the GPI-transamidase, but retained by chaperone molecules, being then targeted to proteasomal degradation, or the processed protein may be even secreted in a soluble form (Ashok and Hegde, 2008; Wilbourn et al., 1998).

The GPI anchor has a complex structure conserved in most eukaryotes formed by an initial phosphoethanolamine, which act as a linker between the GPI and the protein C-terminus (Fig. 5); this phosphoethanolamine is covalently bound to position 6 of the first mannose. The glycan part of the GPI anchor is made of three mannose (linked α1–2 and α1–6) followed by a glucosamine liked α1–4. The final glucosamine is bound α1–6 to a single myo-inositol (Maeda and Kinoshita, 2011). In all mammalian GPI anchors at least one additional phosphoethanolamine is present, in particular linked to 2-position of the mannose linked to the glucosamine (Orlean and Menon, 2007). Other modification and sugar residues can be added on this glycan core structure, as

the addition of galactose, N-acetyl-galactose and mannose. The inositol in the GPI anchor is further linked in position 1 to a phospholipid which can vary in their saturation state and length from 14 to 28 carbons. Additional lipids such as palmitic acid can be present on the 2-hydroxyl group of the inositol ring; the presence of this extra fatty acid renders the GPI anchor resistant to cleavage by PI-PLC an enzyme exploited also in vitro during analysis of presumed GPI anchored proteins (McConville and Ferguson, 1993). Despite the structural complexity of the GPI anchors, up to now, their only confirmed biological function is the stable anchoring to membranes of the GPI-lated protein and their modal localization in the elusive and not well characterized lipid raft domains at the plasma membrane (Paulick and Bertozzi, 2008).

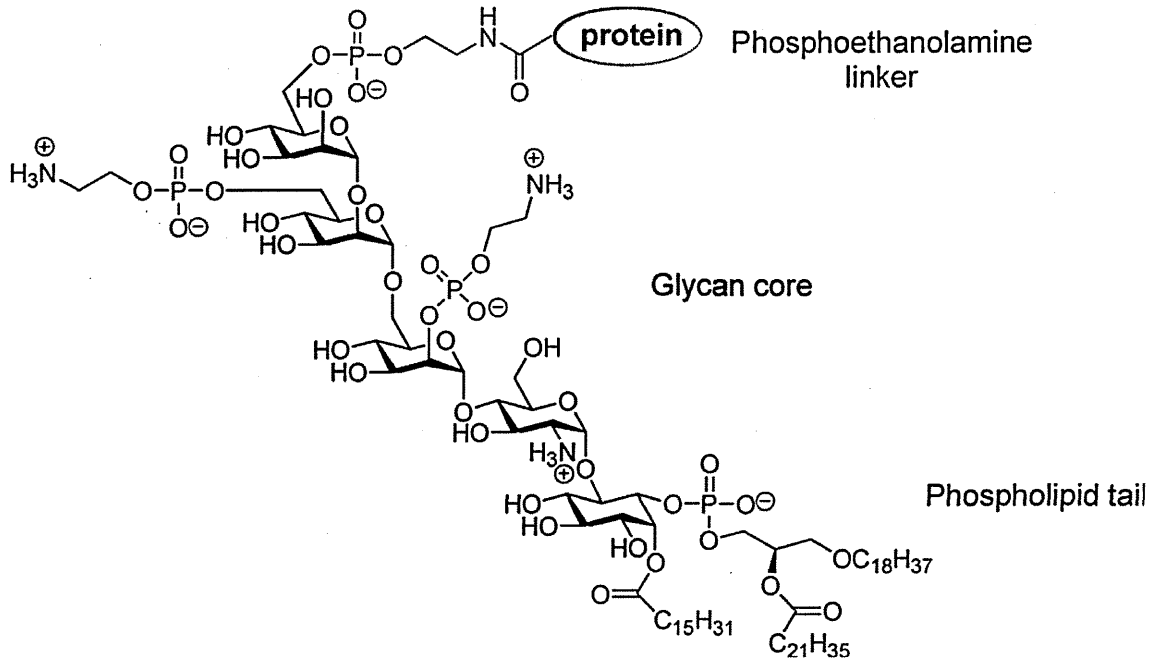

Figure 5. Example of the GPI anchor from human erythrocyte acetylcholinesterase (Paulick and Bertozzi, 2008). In red is indicated the phosphoethanolamine linker with the protein, glycans are shown in black and phospholipid tail and extra phosphoethanolamine are indicated in blue.

As in the cytosol, also in the ER lumen during the folding of a protein the prolyl-peptide bonds are rearranged to the cis or trans isoform by peptidylprolyl cis-trans isomerases (PPIase), allowing a correct conformation to the nascent polypeptide (Bose and Freedman, 1994). This effect of PPIase on protein folding can be either direct or indirect, as in the case of FK506-binding protein

23 (FKBP23), a soluble ER resident PPIase protein. Indeed FKBP23 is able to influence directly protein folding of BiP through its PPIase activity on Pro117cis/trans conformation in a calcium regulated manner (Zhang et al., 2004). However, this conformational change of BiP suppresses the ATPase activity of the chaperon and thus FKBP23 PPIase activity can influence indirectly the folding of several BiP regulated substrates (Feng et al., 2011).

Even though is not well established how chaperones monitor protein folding, this process is believed to occur either through detection of exposed hydrophobic patches, or through excessive surface dynamics associated with the non-compact structure characteristic of partially folded proteins, or both (Malhotra and Kaufman, 2007).

Hydrophobic domains are commonly buried in folded proteins, otherwise they display a tendency to form insoluble aggregates that can have toxic effects.

Chaperones such as those belonging to the family of the heat shock proteins primarily recognise hydrophobic amino acid side-chains exposed by non-native proteins and promote their folding through ATP-regulated cycles of binding-release (Gething 1999; Mayer and Bukau, 2005).

Among them the protein BiP is not only pivotal to post translational translocation, but it is also an important chaperone in the next step of protein folding.

Indeed BiP was originally found associated with immunoglobulins (Haas and Wabl, 1983) and, through ATP hydrolysis, after a different number of binding-release folding cycles, it can ensure the proper protein folding (Gething, 1999).

BiP was also found to keep the substrate in a conformation that ensures PDI has access to the cysteines involved in a disulphide bond formation, so favouring the PDI activity (Mayer et al., 2000; Panter et al., 2000).

If protein folding is delayed, proteins are subjected to additional folding cycles or, when the protein has become irreversibly unfolded, are targeted for proteasomal degradation through ER-associated degradation (ERAD) (Lippincott-Schwartz et al., 1988).

1.4 From ER quality control to ERAD

At the end of the folding process, if a protein has not been folded correctly, it can be recognized through its exposed hydrophobic patches or because it harbours an insufficiently compact structure.

For these proteins the so called calnexin cycle occurs. This process is characterized by one, or rarely more, cycles of deglucosylation-reglucosylation which take place in the ER lumen, mediated by activities of the glucosidase-II (GII) and of the UDP-glucose glycoprotein glucosyltransferase (UGGT or GT). The latter enzyme can add back a glucose residue to the N-linked glycan (Caramelo et al. 2003) and in humans are known two soluble forms (HUGT1 and 2), both retained in the ER via a KDEL-like signal. Of them the most catalytically active, at least *in vitro*, seems to be the HUGT1 (Arnold et al., 2000). In the case of glucose re-addition the protein re-enters in the calnexin-calreticulin cycle (Caramelo and Parodi, 2008; Ellgaard et al., 1999), while the removal of all the glucose by the GII promote release from the cycle to further processing and maturation through the secretory pathway (Fig. 6). Calnexin and calreticulin bind, as lectins, glycosylated proteins substrates, but it was shown that they can act as chaperones preventing also aggregation of non-glycosylated proteins (Ireland et al, 2008). It is believed that, when calnexin and calreticulin release a protein which still exposes hydrophobic regions, those protein segments and the present glycan moieties can be recognized directly by UGGT, which through the re-glucosilation retarget them again toward the two lectins preventing escaping of misfolded proteins (Sousa and Parodi 1995; Pearse et al., 2008).

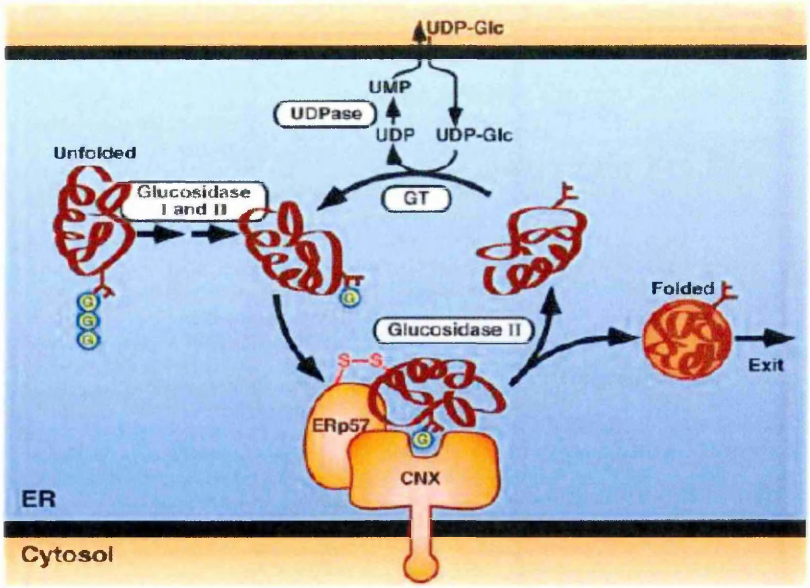

Figure 6. Schematic representation of the calnexin cycle (Ellgaard et al., 1999). Newly synthesized N-glycosylated proteins are initially deglucosylated by GI and GII leaving a single glucose on the N-glycosylation sugar moiety, which is recognised by a chaperone like Calnexin (CNX). With assistance of other proteins, as the oxidoreductase ERp57, a fist attempt of substrate folding is performed. In case of success the folded substrate is released through the secretory pathway by the deglucosylation of the GII, otherwise the deglucosylated protein is recognised by GT, re-glucosylated end retargeted to Calnexin.

1.5 Unfolded protein response

The accumulation of aberrant proteins can be fatal to a cell system, but to overcome this issue cells can activate a process known as unfolded protein response (UPR). The UPR is an ER-to-nucleus and ER-to-cytosol signalling pathway (Schroder and Kaufman, 2005), that result in an enhanced transcriptional synthesis of chaperones and enzymes required for protein folding, trafficking and degradation (Harding et al., 2002).

Apart from that, globally the process causes the attenuation of protein synthesis to prevent a worse ER engulfment and to allow the clearance of the misfolded proteins.

Three UPR pathways are known, in all of them a pivotal role for BiP was proposed. In this hypothesis UPR initiate when the misfolded proteins induce BiP dissociation from the ER transmembrane proteins IRE1 (inositol-requiring

enzyme-1), ATF6 (Activating transcription factor 6) and PERK (PKR-like ER kinase), which function as UPR transducers (Fig. 7) (Ron and Walter, 2007).

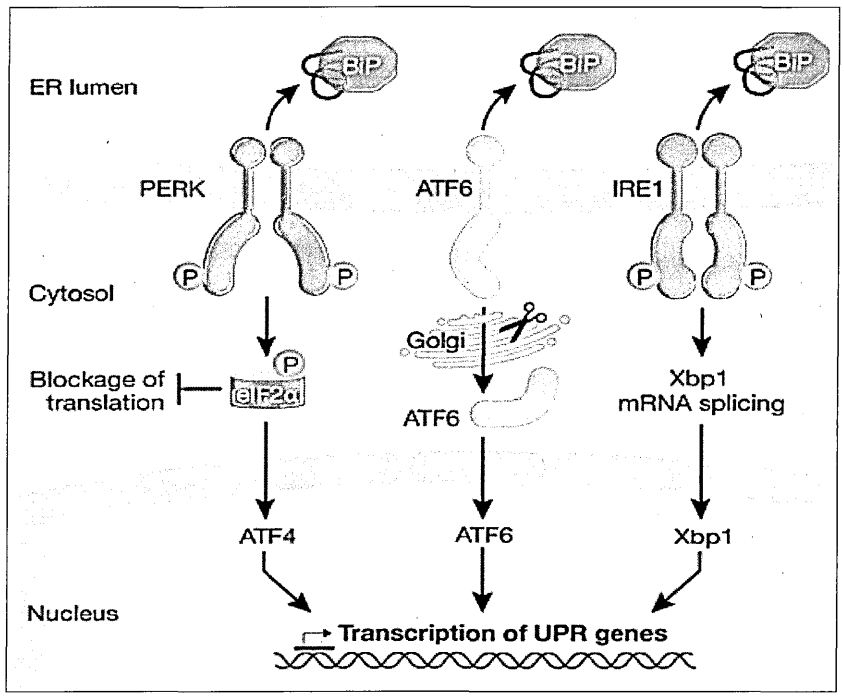

Figure 7. Representation of the three main UPR pathways (Cyr and Hebert, 2009). In the presence of unfolded polypeptides BiP dissociate from the UPR sensors PERK, ATF6 and IRE1. This is believed to cause activation of the sensors, which through phosphorylation or proteolytic cleavage induce the beginning of the UPR pathway, leading to phosphorylation of eIF2α (impairing translation), splicing of Xbp1 and translocation of resulting transcription factors to the nucleus to boost transcription of UPR genes.

However the transmembrane ribonuclease/kinase and UPR sensor protein IRE1 can be activated also by direct binding to unfolded proteins, as in its luminal domain is present a peptide binding pocket, which upon dimerization, form a groove with a structure resembling the one present in the major histocompatibility complex molecules (Credle et al., 2005). IRE1 bounds to unfolded proteins could trigger its oligomerization and thus its activation (Walter and Ron, 2011). According to this view the BiP binding to IRE1 prevent the oligomerization of the UPR sensor under physiological conditions in the presence of low levels of misfolded proteins, thus stabilizing the appropriate concentration of free IRE1 monomers available (Pincus et al., 2010).

Interesting results were observed recently using mutants and deletion mutants of IRE1 luminal domain, which showed sensitivity, similar to wild type, towards

depletion of the membrane lipid component inositol and deletion of genes involved in lipid homeostasis; therefore showing that somehow IRE1 cytosolic or transmembrane domains can sense also membrane aberrancy (Promlek et al., 2011). After its activation through oligomerization and trans-phosphorylation on its cytosolic domains, IRE1 performed an unusual cytosolic splicing of XBP1 (X-box-binding protein 1) mRNA (Yoshida et al., 2001). The spliced XBP1 mRNA generates a new longer C-terminus on the Xbp1 protein, which in this form behaves as a transcription activator, targeting genes encoding for enzymes involved in ER protein disposal and triggering growth arrest and apoptosis (Lee, et al. 2003; Ron and Walter, 2007).

IRE1 was also reported to cleave other mRNAs, in addition to XBP1, coding for ER targeted proteins and mediating their degradation (Hollien and Weissman, 2006). The observation could be explained considering the homology of IRE1 to ribonuclease L, an RNase with reduced specificity (Dong et al., 2001). This activity was interpreted as a more rapid response, compared to gene transcription, to decrease ER overload under stress conditions (Hollien and Weissman, 2006). In a similar way IRE1β, a second mammalian homolog of IRE1, was found able to cleave 28S ribosomal RNA and thus by ribosomal perturbation, it decreases the total synthesis of new proteins on the ER membrane (Iwawaki et al., 2001).

A second UPR cascade involves ATF6, a mammalian protein complex formed by the closely related type-II transmembrane proteins ATF6α and ATF6β. The complex can be either homo- and hetero-dimeric, and following dissociation from BiP, it can be transported to the Golgi, where it is cleaved by the S1P and S2P proteases (Haze et al., 2001). The released cytosolic N-terminal dimeric fragment possesses a basic leucine zipper domain (Haze et al., 1999; Ye et al., 2000). This fragment act as a transcriptional factor that translocates to the nucleus activating ER stress response genes, as for instance, several chaperones like BiP, PDI, and glucose-regulated protein 94 (GRP94) (Yoshida et al., 1998; Schroder and Kaufman, 2005; Walter and Ron, 2011). Of note a predominant role for ATF6α, rather than ATF6β, was reported as the transcription factor generated from this protein is required for transcription induction of major chaperons and ERAD components; in addition ATF6α heterodimerizes with Xbp1 again for the induction of ER-associated degradation

components (Yamamoto et al., 2007 Adachi et al., 2008). This crosstalk between the two pathways generate an ATF6-XBP1 heterodimer which can bound to the cis-acting UPRE (Unfolding Protein Response Elements: consensus sequence TGACGTGG/A) with an 8-fold higher affinity than the XBP1 homodimer (Yamamoto et al., 2007). UPRE are located in promoters of several components of the ER-associated degradation system that can deal with unfolded proteins in the ER (Yamamoto et al., 2004).
The other cis-acting response element, present in the promoter region of several chaperons and ERAD components, recognized by either Xbp1 and/or ATF6 are the ERSE (ER stress response element, consensus sequence CCAAT-N9-CCACG), which control the expression of ER-localized molecular chaperones, such as for instance BiP, and ERSE-II (consensus sequence ATTGGNCCACGT), which was discovered only in the promoters of the human homocysteine-induced endoplasmic reticulum protein (HERP) and in the one of the arginine rich, mutated in early stage of tumours protein (ARMET) (Kokame et al., 2001; Yamamoto et al., 2004; Mizobuchi et al., 2007).

However comparing these two, ATF6 and IRE1, distinct UPR activation pathways in HeLa cells, it was shown that ATF6 fragment was already detectable 30 min after the addition of thapsigargin (a non-competitive inhibitor of SERCA, a class of Ca^{2+} ATPase), while the protein produced by the XBP1 spliced mRNA was detected only after three hours (Yamamoto et al., 2004). This different temporal response and the presence of an overlapping crosstalk could offer mammalian cells more option for a more fine regulated tuning of the ER stress response.

In the third pathway, which, as the one involving ATF6, is present only in mammals, the type-I transmembrane protein kinase PERK is auto activated upon oligomerization through *trans*-auto-phosphorylation, when is released by BiP. The PERK pathway is phylogenetically related, similar in structure and function with IRE1 UPR. Indeed these two pathways resulted even experimentally interchangeable (Bertolotti et al., 2000; Ron and Walter, 2007). However PERK phosphorylates not only itself, but also other proteins, such as the α-subunit of eukaryotic translation initiation factor-2 (eIF2α) at Ser51. As consequence of this phosphorylation, the eIF2 pentameric complex gets

inactivated. Low levels of active eIF2 caused a global decreased translation, thus reducing also the amount of newly synthesized proteins on the ER associated ribosomes (Harding et al.,1999; Harding et al., 2000). Interestingly, some mRNAs contain short open reading frames in their 5' UTR (untranslated region) which are preferentially translated when active eIF2 is lacking. The best known one encodes the transcription factor ATF4. The leucine zippers of ATF4 protein enhances the expression of genes containing the cAMP response element (CRE, consensus sequence GTGACGT[AC][AG]) present in many cellular promoters. Among them the overexpression of CHOP (transcription factor C/EBP homologous protein), a transcription factor involved in apoptosis, can lead stressed cells to death, if they are not able to restore rapidly their homeostasis. Even though PERK activity seems to acts as a trigger for apoptosis, this should not be considered an absolute and general rule as several ATF4 cellular targets are known and not every cell type respond to PERK activation in the same exact way (Lin et al., 2007).

For the PERK pathway a regulatory cycle is formed by expression of GADD34 (growth arrest and DNA damage–inducible 34), which encodes a regulatory subunit of the protein phosphatase PP1C. PP1C can counteract PERK activity because dephosphorylate eIF2α (Walter and Ron, 2011).

The PERK pathway was also involved in regulation of amino acid metabolism and resistance to oxidative stress (Harding et al., 2003). PERK high expression levels and its dependent signalling were also found particularly relevant in secretory organs. Indeed, PERK knockout mice showed severe defects in one of them, as they develop diabetes mellitus and exocrine pancreatic dysfunction after birth (Harding et al., 2001).

1.6 ERAD substrate recognition and demannosylation

Misfolded proteins and non-assembled proteins are retained in the ER lumen bound to chaperons such as Hsp70 family, calnexin and calreticulin or other lectins. These proteins have to drive the misfolded protein towards the degradation machinery; if glycosylated these substrates are often labelled in the cell through demannosylation (Lederkremer, 2009). For example in mammalian cells N-glycosylated ERAD substrates are processed to M6 and M5 by removal

of almost all the mannose residues linked α1,2 to the N-glycosylation tree (Avezov et al., 2008). Removals of mannose prevent irreversibly the re-glucosilation of the N-glycosylated protein, precluding calnexin binding and thus taking out permanently the protein from the calnexin/calreticulin cycle (Lederkremer, 2009).

Demannosylation is consequence of the activity of members of the glycosyl-hydrolase 47 family, such as the ER α1-2 mannosidase I (ERManI), the three EDEM proteins (ER degradation-enhancing α mannosidase-like proteins) and the Golgi ManI-A, I-B and I-C (Molinari, 2007). Among them however the most catalytically active ERAD-associated demannosilase for the production of M6-5 sugar moieties seems to be ERManI, which was also reported to concentrate in the ERQC (endoplasmic reticulum quality control) compartment where also ERAD substrates are prone to localize before proteasomal degradation (Avezov et al., 2008).
About the EDEM proteins is still under debate whether they act really as mannosidase or just as cofactors of ERManI for the efficient trimming of some of the mannose branches (Lederkremer, 2009). Nevertheless the role of the EDEM1 protein is particularly interesting because, through its mannosidase activity and interaction with calnexin can interrupt the calnexin cycle of the unfolded protein (Oda et al., 2003). Moreover EDEM1 regulation of ERAD through acceleration of protein de-mannosylation was reported to prevent the formation of intermolecular disulphide-bonded dimers or other kind of aggregates (Olivari et al., 2006). This function is carried out by EDEM1 through its specific association with the PDI family member Erdj5.

The three related type-I membrane proteins VIPL, VIP36 and ERGIC53 have luminal carbohydrate recognition domain with high affinity for deglucosylated high mannose N-glycosylated proteins and are involved in ER-Golgi transport of secretory proteins (Kamiya et al., 2008). Once in the Golgi compartment the Golgi ManI-A, I-B and I-C produce the same M5 structure produced in the ER by ERManI/EDEM1 activity. Nonetheless in this case their trimming activity is believed to release the glycoprotein from the ER-Golgi shuttles lectins, allowing further maturation of substrate proteins through the secretory pathway (Lederkremer, 2009). Interestingly, it is possible that this class of Golgi

mannosidase, and in mammals also ERManI (Pan et al., 2013), can cycle between the ER and the Golgi compartments or that some ERAD substrates can arrive to the Golgi before delivery to ERQC compartment and thus to final ERAD steps (Haynes et al., 2002; Hosokawa, 2007; Pan et al., 2013).

At the end of ERManI/EDEM1 activity the N-glycosylation tree of misfolded proteins expose a terminal α 1,6 bonded mannose. This residue is recognized by mannose 6-phosphate receptor homology-domain (MRH-domain) proteins such as the OS-9 proteins (homologs of yeast Yos9) and XTP3-B (Quan et al., 2008; Clerc et al., 2009). Of note those kind of lectins can interact also with non-glycosylated proteins, their linked chaperones (i.e. BiP and GRP94), and ERAD components; indeed, they were suggested to act as a sort of scaffold for the formation of a multi protein ERAD complex together with Sel1L and HRD1 for the ubiquitination and degradation of their substrates (Alcock and Swanton, 2009; Hosokawa et al., 2008; Christianson et al., 2008).

1.7 ERQC compartment.

Some years ago the existence of a perinuclear microtubule-dependent ER portion called ERQC (ER quality control) compartment was proposed; this compartment was reported to be highly enriched upon proteasomal inhibition and several misfolded ERAD protein substrates are known to accumulate there (Kamhi-Nesher et al., 2001; Spiliotis et al., 2002; Wakana et al.; 2008; Shenkman et al., 2013). Bap31, a multi spanning protein, cycles between the peripheral ER and the ERQC and was proposed to be a membrane protein included in the vesicular system responsible of the delivery of misfolded proteins to the ERQC compartment (Wang et al., 2008; Wakana et al., 2008). Overexpression of both Arf1 (associated to COP-I retrograde transport) and Sar1 (associated to COP-II anterograde transport) and their mutants affected Bap31 cycling to the ERQC compartment (Wakana et al., 2008). Considering also that the COP-II component p137 was found able to relocate to the ERQC compartment (Spiliotis et al., 2002) and that ERQC system seems to be mostly unaffected by brefeldin A (Kamhi-Nesher et al., 2001) (this molecule causes ER–Golgi fusion inhibiting transport of proteins from ER to Golgi), it is possible

that during ER stress, or even at lower rates during physiological conditions, a subfamily of COP-II vesicles is responsible of targeting of the substrates and of the appropriate protein components to this ERAD associated compartment.
Even upon ER stress, in the ERQC compartment not every ERAD involved component can reside, indeed while ERManI, calnexin, calreticulin and several UPR components localize there, other proteins such as BiP, PDI, GT or ERp57 are excluded (Kamhi-Nesher et al., 2001; Kondratyev et al., 2007; Frenkel et al., 2004). It is possible that several critical steps of recognition (due to the presence of pivotal chaperones), demannosylation (for ERManI/EDEM1 localization) and ERAD targeting (OS-9 and XTP3-B) happen in the ERQC compartment (Leitman et al., 2013). Moreover the finding of numerous components of the UPR pathways and of proteins involved in several membrane associated and cytosolic ERAD steps (such as: HRD1, Derlin-1, Herp, Sec61β, p97, proteasome, SCF^{Fbs2}, PERK, IRE1 and eIF2a-P) localized to the ERQC compartment (Leitman et al., 2013; Groisman et al., 2011; Kondratyev et al., 2007), suggests that this might be the restricted cellular location where actually retrotranslocation takes place (Kondratyev et al., 2007).

1.8 A channel model to ERAD

The membrane separation of the unfolded protein and the site of degradation requires the clustering of a large number of protein enzymes and open the possibility to the existence of channels responsible to misfolded protein dislocation. Such channels should allow the retrotranslocation of both ER luminal and ER membrane misfolded proteins to the cytosol where the proteasome resides.
Essentially many multi-spanning ER protein was nominated to be the (or one of the possible) ERAD channel.
A putative retrotranslocation channel was indicated in the same Sec61 translocon (Schmitz et al., 2000), but it was also associated to proteins like Derlin 1, an ER resident multispanning protein, which was found to be involved in the retrotranslocation process (Lilley and Ploegh, 2004; Ye et al., 2004).
In the case of Sec61 it was found associated to MHC class I before its delivery to the proteasome when it is co-expressed with two immunoevasins, US2 and

US11, of the human cytomegalovirus (HCMV) (Wiertz et al., 1996a and 1996b).
Also other proteins such as Cholera toxin are able to reach the cytosol binding the Sec61 translocon, however in this case after a previous endocytosis and retrograde transport to the ER (Schmitz et al., 2000).
However data about translocation indicates the inability of the Sec61 to allow the movement of partially folded proteins (Rapoport et al., 1996) and some experimental indications (i.e. Fagioli et al., 2001) induced some authors in the ERAD field to postulate protein unfolding as a prerequisite to retrotranslocation. But even in the case of a full protein unfolding occurring before dislocation, usually the ER proteins are usually glycosylated and such a large structure should be too bulky to pass across the narrow translocon channel (Hiller et al., 1996; Wiertz et al., 1996a and 1996b).
So adding this pivotal point to some other experimental evidence, like the reported efficient retrotranslocation of a recombinant MHC-I, bearing at the N-terminus the tightly folded dihydrofolate reductase domain (DHFR) (Tirosh et al., 2003), the requirement of a complete unfolding is under debate and eventually appear to be mostly not required (Bagola et al., 2010).
This indicates that if the Sec61 is the retrotranslocation channel to some class of substrates, it is somehow adapted not only to function in the opposite direction, but also to accommodate large folded proteins.
In a similar scenario, it is possible that more than a Sec61 molecule participate to the process and that different Sec61 binding partners realize these kinds of adaptations (Kalies et al., 2005)

Regarding the involvement of the Derlin proteins as possible retrotranslocation channels, it was found that the yeast Der1p, homologue of Derlin1, was necessary in misfolded protein degradation (Lilley and Ploegh, 2004; Ye et al., 2004; Hitt and Wolf, 2004; Kirst et al., 2005).
Interestingly siRNA of Derlin-1 in C. elegans provokes ER stress (Lilley and Ploegh, 2004), while its down-regulation prevent CFTRαF508 degradation (Sun et al., 2006).
Moreover Derlin-1 was described to be important also in HCMV induced MHC class I degradation (Lilley and Ploegh, 2004). In this case being Derlin-1 able to associates with peptide-N-glycanase in the cytosolic side of the ER membrane, it can justify the well described appearance of a deglycosylated MHC-I in the

cytosolic fraction of HCMV infected cells (Katiyar et al., 2005).

In addition Derlin-1 interacts also with the ATPase p97, a cytosolic protein indicated as the major source of ATP hydrolysis during dislocation (DeLaBarre and Brunger, 2005), and through this binding it can associate with the ubiquitin ligases HRD1 and gp78 (Lilley and Ploegh, 2005; Ye et al., 2005).

In vitro experiments of retrotranslocation with the fluorescent pro-alpha factor and anti-derlin1 antibodies further indicates it possible function as a retrotranslocation channel (Wahlman et al., 2007).

Also other members of the Derlin family, Derlin2 and 3, were found to be regulated under UPR, to be required for degradation of misfolded glycoproteins and to associate with some crucial ERAD partners like p97 and EDEM1 (Oda et al., 2006).

However recently it was reported that Derlins are not as believed a family of protein with four transmembrane domains, but they are, instead, inactive members of the rhomboid family of intramembrane proteases (Olzmann and Kopito, 2011). In particular it was shown that Derlin-1 mutants within the rhomboid domain are able to stabilize the ERAD substrate α-1 Null Hong Kong antitrypsin, but only as an intermediate after retrotranslocation in the cytosolic face of the ER membrane. Moreover the convincing membership of Derlins to the rhomboid family, of which is known to lack any ability to form transmembrane pores, is inconsistent with a channel-like function of Derlins (Olzmann and Kopito, 2011).

Another putative retrotranslocation channel could be build up by Hrd1p oligomerization. In this case the transmembrane segments of Hrd1p have been demonstrated to be required for efficient protein degradation, probably due to its activity in dislocation of proteins from ER to cytosol (Omura et al., 2008a; Omura et al., 2008b).

Among the other central proteins in the ER membrane associated with the retrotranslocation pathway it was found that also TRAM1 and BAP31are involved.

The association of TRAM1, previously characterized in translocation (Gorlich et al., 1992, Gorlich and Rapoport, 1993), with ERAD born by finding that TRAM1 is important for the disposal of membrane substrates and its absence leads to an increased UPR (Ng et al., 2010).

Regarding BAP31, it is a three membrane spanning ER protein, involved in protein sorting (Ng et al., 1997). From the ERAD point of view BAP31 knock down cause an increase amount of CFTRαF508 but its lack cause a decrease of the interaction between CFTRαF508 and Derlin-1 (Wang et al., 2008)

1.9 Cytosolic ERAD steps

In order to reach the cytosol and be degraded, misfolded proteins that are substrates for degradation, have not only to be detected in the ER lumen, but they should also be tagged with ubiquitin molecules to be recognised by a series of ubiquitin binding proteins that facilitate movements of the substrates from the ER membrane to the proteasome (Elsasser and Finley, 2005; Raasi and Wolf, 2007).

The published data suggest that misfolded proteins are ubiquitinated during retrotranslocation, but immediately after the ubiquitin chains are removed by the activity of deubiquitinating enzymes (DUBs), to allow an efficient degradation by the proteasome.

Despite this transient presence, the ubiquitination of the ERAD substrates appear to be really important to link, for instance, the substrate to the ATPase p97 (cdc48 in yeast). This ATPase is supposed to be recruited to the ER membrane to supply the energy for the dislocation or for the release of substrates that have been already retro-translocated (Hitchcock et al., 2001).

P97 consists of six subunits each containing two ATPase domains, that are arranged in a ring, which undergo to wide conformational changes during ATP hydrolysis (DeLaBarre and Brunger, 2005; Davies et al., 2008), and where the central pore could accommodate the dislocating protein (DeLaBarre et al., 2006).

Regarding p97 interactions with the ER membrane, this protein can have different binding partners as UFD1 (Ubiquitin fusion degradation protein 1) and NPL4 (Nuclear protein localization protein 4 homolog), two proteins containing many ubiquitin binding domains. Those ubiquitin binding domains could facilitate the interaction between p97, the ubiquitinated proteins and the proteasome (Schmidt et al., 2005; Besche et al., 2009).

Indeed the complex of p97 with those two ubiquitin binding proteins was found

implicated in ER dislocation and degradation of misfolded protein substrates (Stirling and Lord, 2006, Ye et al., 2001, Rabinovich et al., 2002).

One more link between p97 and ERAD is its association with Derlin1 and SEL1L, another component quality control and dislocation complex (Lilley and Ploegh, 2005).

Recently a small myristoylated protein named SVIP (small p97/VCP interacting protein), whose over-expression causes cellular vacuolation due to the dilation of the ER (Nagahama et al., 2003), was indicated as a p97 regulator.

Indeed, SVIP can form a complex with Derlin1 and p97 and could act as an endogenous inhibitor of ERAD, reducing the association of ERAD substrates with p97 and the gp78 ubiquitin ligase (Ballar et al., 2007).

In the cytosol the activity of peptide N-glycanase (PNGase) could favour the proteasomal degradation by removing N-linked glycans, even though this step is not absolutely required and PNGase can act either before or after proteasomal cleavage of polypeptides (Kario et al., 2008). PNGase was discovered in yeast and is responsible for the deglycosylation of N-linked glycoproteins, but being those proteins usually in the ER lumen, only molecules dislocated to the cytosol become substrates of PNGase (Suzuki et al., 2002). For this reason its activity has been used widely in the literature as reporter of retrotranslocation and the percentage of ER to cytosol dislocated molecules is often calculated through the ratio between the deglycosylated protein and the total. However, de-glycosylation is a finely regulated cellular event and appears not to be essential for retro-translocation (Blom et al., 2004).

PNGase was identified to be an interactor of Rad23 (Suzuki et al., 2001) and that this interaction occurs through on the PNGase N-terminus in 1:1 ratio (Biswas et al., 2004). Rad23 is a protein that can bind the 26S proteasome through its N-terminus ubiquitin like domain (Schauber et al., 1998).

Therefore, PNGase creates another link between the dislocated protein substrates and the proteasome (Katiyar et al., 2004).

Rad23 can interact with the 26S proteasome through its ubiquitin-like domain (UBL) (Schauber et al., 1998), while its ubiquitin associated domain (UBA) serve to bind mono ubiquitin and poly ubiquitin chains (Hofmann and Bucher, 1996). Due to the presence of UBL and UBA domains Rad23 act as a ubiquitin receptor, creating a bridge from the ubiquitinated protein substrate to the

proteasome (Saeki, et al., 2002; Verma et al., 2004; Kaplun et al., 2005). Moreover the interaction of Rad23 with ataxin-3, a proteasome-associated factor, that associate with the almost ERAD essential p97ATPase (Doss-Pepe et al., 2003), highlighted the presence of a relevant network of interaction connecting they key players (PNGase, p97 and the proteasome) acting in the cytosolic steps of the ERAD pathway. It was also demonstrated a direct interaction of PNGase PUB (PNGase/UBA (ubiquitin-associated) or UBX (ubiquitin-regulatory X)) domain with the last 10 amino acid residues of the C terminus of p97, which is both necessary and sufficient for the binding, only if Tyr805 (in mouse p97) is not phosphorylated (Zhao et al., 2007). The formation of a ternary complex of PNGase PUB domain with p97 and simultaneously with HR23 UBL (ubiquitin-like) domain was reported (Kamiya, et al., 2012). However this ternary interaction might occurs mainly after engaging of p97 in the retrotranslocation complexes escorting ERAD substrates to the cytoplasm as it has been proposed that the p97 substrates are first recognized by substrate-recruiting cofactors and then processed by substrate-processing cofactors (Rumpf and Jentsch, 2006) as indeed is the PNGase.

1.10 Ubiquitination and proteasomal degradation

The proteasomal system is believed to be one of the major degradation routes in cells (Hochstrasser 1996; Pickart and Cohen 2004). A protein targeted for proteasomal degradation has to be labeled by the appropriate conjugation to ubiquitin molecules, which are attached by proteins of the ubiquitin ligase (E3) family in a cytosolic environment (Tsai et al., 2002; Hirsch et al., 2009). Through ubiquitination, proteins committed for proteasomal degradation are targeted to this multiprotein complex, in a highly specific and regulated way. The proteasomal pathway has been exploited by cells to tune indirectly several cellular processes as for instance: cell cycle, development, DNA repair, tumorigenesis, metabolism, signal transduction, cell death, protein quality control, viral infections and antigen cross presentation (Voges et al., 1999; Varshavsky, 2005; Ciechanover, 2006; Kobayashi et al., 2013; Tu et al., 2012; Choi et al., 2013; Contin et al., 2011).

The process of ubiquitin mediated proteasomal degradation requires the energy

released by ATP hydrolysis, both for protein substrate unfolding and for movements that allow its access to the active proteasomal proteolytic core (Pickart and Cohen, 2004).

1.10.1 Ubiquitin structure and conjugation

In eukaryotic cells there is a class of small proteins with a remarkable similar structure, all included in the ubiquitin-related protein family. Those proteins are involved in several cellular processes and have the peculiar feature to be covalently attached to other proteins through a C-terminal di-glycine motif, which is conjugated to amino group of the target protein (Pickart and Eddins, 2004). In addition to ubiquitin several other members of the ubiquitin protein family have already been identified, such as SUMO proteins 1, 2 and 3, Nedd8, ISG15, Atg8, Atg12, FUBI, FAT10, Urm1, Hub1 and UFM1 (Hochstrasser, 2009). Some of these proteins have, as ubiquitin, a broad number and diversity of substrates, but several others have a much more limited range of known substrates (Kerscher et al., 2006). All those ubiquitin like proteins have functions in many cellular pathways like cell cycle control, transcription, splicing, signal transduction, DNA repair, nutrient sensing and autophagy (Kerscher et al., 2006). So far Fat10 seems to be the only ubiquitin like protein involved in ubiquitin-independent proteasomal degradation (Hipp et al., 2005).

Among these kinds of proteins, ubiquitin, the prototype founder of the family, is certainly the most studied and characterized. Ubiquitin is a small protein (76 amino acids) with a major role in several cellular processes, either related to degradation or not, caused by its covalent conjugation to proteins (Schreiber and Peter, 2013; Pinder et al., 2013; Tanno and Komada, 2013). Ubiquitin is encoded by four different genes (Archibald et al., 2003). UBB and UBC genes express each a polyubiquitin precursors formed by several exact repetition of the single ubiquitin subunit. While RPS27A and UBA52 genes code for a single copy of ubiquitin fused to the ribosomal proteins S27a and L40, respectively. Single free ubiquitin subunits are generated by post-translational cleavage of polyubiquitin and ubiquitin fusion proteins by the catalytic activity of specific proteases (Jonnalagadda et al., 1989; Baker et al., 1992; Ha and Kim, 2008). The process of covalent linkage single ubiquitin molecules, to proteins is called ubiquitination; ubiquitination takes place mainly on the amino groups of Lys and

on the free amino group the protein N-terminus, but it can also involve the thiol group of Cys and the hydroxyl group of Ser, Thr and probably Tyr (Pickart, 2001; Ciechanover and Ben-Saadon, 2004; Cadwell and Coscoy, 2005; Wang et al., 2007; McDowell and Philpott, 2013). Upon single ubiquitination the protein substrate can often be further modified by addition of other ubiquitin molecules, either on other free ubiquitination sites on the target protein or on the available Lys of the first conjugated ubiquitin, leading to the formation of polyubiquitin chains. Formation of polyubiquitin chains occurs only on the seven Lys residues (Lys6, Lys11, Lys27, Lys29, Lys33, Lys48 and Lys63) or the N-terminus of Met1 of ubiquitin (Komander and Rape, 2012). Of note, each Met and Lys residue involved in formation of polyubiquitin chains is exposed in the surface of the ubiquitin and in the three dimensional structure points to different direction (Fig. 8).

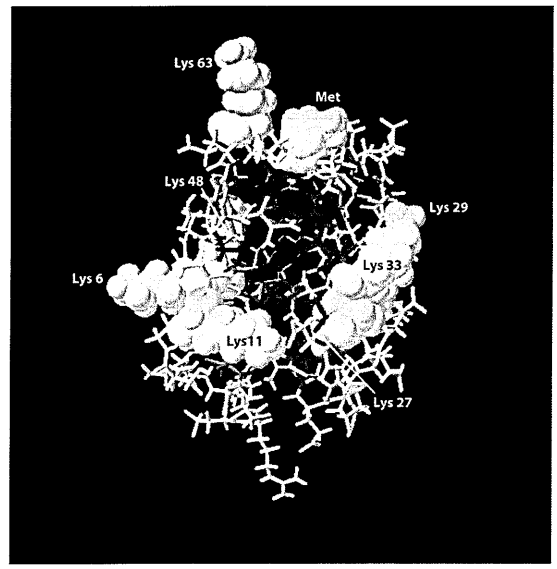

Figure 8. Ubiquitin structure . Adaptation of an ubiquitin molecular structure (a single ubiquitin subunit from polyubiquitin-C polyprotein) from pdb 2k39 (Lange et al., 2008), colours represent accessibility of the amino acid residues (yellow highly accessible, dark blue hidden amino acid side chain). Figure shows the Lys and Met amino acid involved in the formation of polyubiquitin chains.

Modification of proteins with ubiquitin monomers is connected to cellular non-proteolytic processes (Hicke, 2001), while the presence of polyubiquitin chains (even more than ten moieties) could lead both to a proteolytic and to a non-proteolytic pathways. This depend on the particular Lys (or Met1), used for the

development of the polyubiquitin chains; obviously different linkage lead to diverse structures. Moreover in the same polyubiquitin chain more than one Lys residue of the several ubiquitin was reported to be involved in the formation of the poly-conjugated protein (Komander and Rape, 2012). This results in the various different topologies of ubiquitin chain: homogenous, branched or mixed topology. In addition, preformed polyubiquitin chains not conjugated to protein substrates are present in cells with relevant biological function in some cellular pathways (Strachan et al., 2012). Among the several polyubiquitin conformations the canonical Lys48-linked chain adopts a compact conformation, similarly to Lys6 and Lys11-linked chains; whereas the Lys63 and Met1 linkage form a more extended conformation with higher levels of freedom (Komander and Rape, 2012). The features of the chain determine the fate and the biological function of the modified protein substrate.

Ubiquitination through Lys11, Lys29, Lys48 and Lys63 have roles in proteasomal degradation. In this pathway however the K48 linkage, in particular if in long chains, seems to be the most prevalent.

In addition K48 is the only essential K of ubiquitin in yeast, and gp78, one of the major ERAD involved ubiquitin ligase, also trigger this kind of polyubiquitination (Chau et al., 1989; Li et al., 2007). K11 linked chains are involved in proteasomal degradation of proteins essential to the proceeding of the cell cycle (Matsumoto 2010). The role of the other Lys (K63 and K29) was reported to lead to proteasomal degradation only in few peculiar cases (Saeki et al., 2009; Koegl et al., 1999).

Ubiquitination can be also the signal that trigger endocytosis and might also target the protein towards lysosomes. In this case a monoubiquitination on a cytosolic tail of a protein substrate drives its relocalization from the plasma membrane to an endosomal compartment by recognition of different ESCRT (Endosomal Sorting Complexes Required for Transport) complexes (Mukhopadhyay and Riezman, 2007). K63 polyubiquitin linked chains are prevalently known to facilitate endocytosis (Galan and Haguenauer-Tsapis, 1997; Mukhopadhyay and Riezman, 2007) but they were also involved in the transport toward lysosomes and autophagosomes (Komada and Kitamura, 2005; Kirkin et al., 2009). Moreover K63 linkage seems to play relevant roles in DNA damage tolerance, inflammatory response, and ribosomal protein synthesis (Friedberg et al., 2005, Pickart and Fushman, 2004; Mukhopadhyay

and Riezman, 2007).

In the literature a detailed analysis of function of other K-linked ubiquitin chains and on the probable presence of complex mixed K-conjugation chains is still missing.

The ubiquitination process is mediated by the activity of three main type of enzymes, namely E1, E2 and E3 (Pickart and Eddins, 2004). In some cases an E4 protein was also reported to be involved.

The E1 enzyme activates ubiquitin by binding it and MgATP. Through ATP hydrolysis E1 catalyses the C-terminal acyl-adenylation of ubiquitin. This initial ubiquitin-adenylate intermediate reacts with a cysteine residue of an E1 protein (Fig. 9), forming an E1~Ubiquitin thiol ester ("~" represents a high-energy covalent complex) (Schulman and Harper 2009).

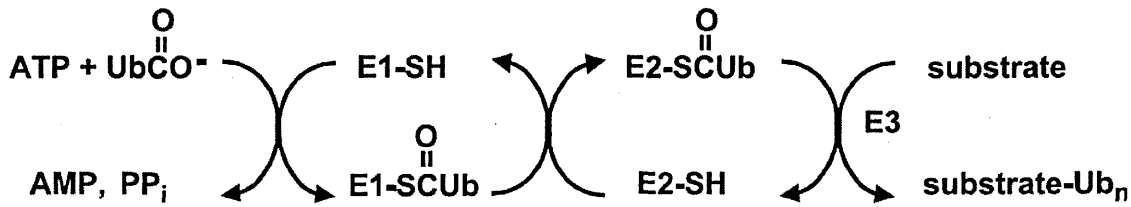

Figure 9. The main ubiquitination steps (adapted from Pickart and Eddins 2004). Through ATP hydrolysis ubiquitin is activated by the E1 enzyme, and then loaded by the E2, which in collaboration with the E3 conjugate ubiquitin to substrate protein.

In general, each ubiquitin like protein has a single dedicated E1 enzyme, which forms the thioester bridge between the cysteine in the active centre of E1 and the terminal Gly76 of ubiquitin (Pickart and Eddins, 2004). In humans, eight E1 proteins are known to initiate the conjugation of ubiquitin like proteins. Interestingly not all of these E1 enzymes share the same subcellular localization, but, up to now, the precise functions of the different isoforms are still not fully elucidated (Grenfell et al., 1994; Schulman and Harper, 2009).

Several (35 in humans) E2 ubiquitin conjugating enzymes are available in the cell for receiving the activated ubiquitin from the E1 enzyme forming a similar thioester bond (van Wijk and Timmers, 2010). The E2 enzymes can influence the specificity of the ubiquitination, as individual E2 enzymes interact with specific E3 enzymes. Moreover the E2 proteins are the main determinants for selection of the lysine on which to construct the polyubiquitin chains, thus

controlling the cellular fate of the substrate (van Wijk and Timmers, 2010).

Eventually, E3 enzymes promote the ligation of ubiquitin (or ubiquitin-like proteins) to the substrates. In eukaryotic cells a large number of E3-ligase are present (more than a thousand). Initially, E3 ligases were proposed to be the bridging factors that group together the E2 and the substrate (Hershko et al., 1983). However, it is now known that E3-ligases can work either as catalytic intermediates in the ubiquitination pathway (similarly to E1 and E2) or they can mediate direct transfer of ubiquitin from the E2~Ub complex to the substrate (Metzgeret al., 2013). Based on their structure and activity E3 enzymes can be assigned into two major groups: the HECT (homology to E6AP C-terminus) E3 ligases, which form a trans-thiol bond with ubiquitin before conjugation to the substrate, and the RING (Really Interesting New Gene) E3 ligases, which instead link the substrate to the E2~Ub, which directly conjugate ubiquitin to the protein target (Metzgeret al., 2013). RING finger E3 ligases are the most abundant in mammalian cells, and are further subdivided in two subfamilies named RING-type E3, if they can coordinate two Zn^{2+} ions through cysteines and histidines to create the appropriate binding site for the E2 protein, and RING-like U-box E3, if they create a related structure for the binding of E2s without coordinating Zn^{2+} ions (Metzgeret al., 2013; Hatakeyama and Nakayama, 2003). After ubiquitin conjugation the substrate is released by the E3 ligase or the ubiquitination steps can be repeated for further ubiquitin chain elongation. Polyubiquitination can be catalysed not only by the same E3 enzyme that performed the first conjugation, but also by specific ubiquitin elongating factors called generally E4 enzymes, which, apparently, are either other E3 ligases or cofactors needed for efficient ubiquitin chain elongation (Koeglet al., 1999; Metzger et al., 2010). RING E3 ligases can also promote their own auto-ubiquitination and thus degradation (Carroll and Hampton, 2010). Interestingly some RING-type E3 were reported to be able to dimerize or to form oligomers through domains separated from the RING. For this reason some of them involved in ERAD were proposed to be or to be associated to a hypothetical retrotranslocation channel during ER to cytosol dislocation (Hirsch et al., 2009; Nakatsukasa and Brodsky, 2008).

In the proteasomal degradative pathway it was reported that the minimal signal for an efficient proteasomal targeting and degradation is a tetraubiquitin chain (Thrower et al., 2000). Once recognised by the 26S proteasome complex the

polyubiquitinated protein is inserted into the catalytic portion of the degradation machinery, where a series of proteases can rapidly degrade it into peptides (Voges et al., 1999).

Ubiquitin conjugation is certainly essential for the degradation of ERAD substrates and it was proposed to be also essential for the ER to cytosol retrotranslocation step. This conclusion was drawn because disruption of the ubiquitination machinery causes inhibition of the complete cytosolic solubilization of ER resident protein substrates (Kikkert et al., 2001; Shamu et al., 2001; Jarosch et al., 2002).

Among the RING-type E3 the SCF (Skp, Cullin, F-box containing) E3 ligase complex is particularly interesting. In the SCF complex cullin1 forms the scaffold for the simultaneous interactions with the adaptor subunit Skp1, the RING-finger protein Roc1/Rbx1 and a specific E2 (Cardozo and Pagano, 2004). Skp1 can bind one of the F-box proteins (69 in humans) through their F-box domain (Yoshida and Tanaka, 2010). Some years ago Fbs1/Fbx2 and Fbs2 were identified as a glycoprotein-specific F-box protein; these lectins recognize high mannose and complex-type glycans of misfolded glycoproteins, probably interacting with the innermost chitobiose (a dimer of β1,4-linked N-acetyl-glucosamine) located at the base of the N-glycosylation moiety, a portion usually masked in the folded polypeptides (Yoshida et al., 2002; Yoshida et al., 2005). A role of these E3-ligase-associated-lectins in ERAD was proposed as they can prevent premature deglycosylation of the substrates by peptide:N-glycosidase, promoting also substrate ubiquitination (Yoshida et al., 2002; Groisman et al., 2011; Shenkman et al., 2013).

1.10.2 Deubiquitination

Deubiquitinating enzymes (DUBs) and ubiquitin-like specific protease (ULP) are proteases responsible for the production of ubiquitin and ubiquitin-like monomers from their precursors and from proteins conjugated with ubiquitin or ubiquitin-like proteins (Ha and Kim, 2008). This activity cleaves at the at the C-terminal glycine residue of ubiquitin subunits, which are involved in the isopeptide bond linkage to the Lys of the substrate protein. Several dozens of human DUB acting on ubiquitin, classified into two main classes of cysteine

proteases and metalloproteases, have already been identified. The cysteine protease class can be further subdivided into four distinct subfamilies (Ha and Kim, 2008).

The largest and most diverse class of these DUBs is the USP (ubiquitin-specific protease). Their catalytic domain is sized around 40 kDa with conserved cysteine and histidine boxes (Ha and Kim, 2008).

Second members of the cysteine protease group are UCH (ubiquitin C-terminal hydrolase); these DUBs possess a catalytic site resembling the papain cysteine protease (Johnston et al., 1997). They are generally smaller in size than USP and target mainly short polypeptides, small adducts of ubiquitin and some ubiquitin proproteins, but not large ubiquitin-protein conjugates or long polyubiquitin chains (Larsen, et al., 1998).

Belonging to the ovarian tumour proteins superfamily, the otubain (OTU-domain Uba-binding) proteases (OTUs) are proteins containing a deubiquitinating domain of approximately 130 amino acids in size, also related to the papain proteases family (Messick et al., 2008). This OTU domain is highly conserved from yeast to mammals and is also present in viral proteins (Messick et al., 2008; Frias-Staheli et al., 2007). Members of the OTU family like Otu1 and A20 can bind preferentially polyubiquitin chain analogues, hydrolysing longer polyubiquitin chains with K48 and K 63 linkages (Messick et al., 2008; Wertz et al., 2004). Among viral OTUs it is worth mentioning the 169 amino acids long OTU domain from the N-terminus of Crimean Congo haemorrhagic fever virus-L protein (CCHFV-L) and related viral OTU proteins, which can directly de-conjugates ubiquitin and the ubiquitin-like-protein ISG15 from protein substrates (Frias-Staheli et al., 2007). The CCHFV-L OTU and some other viral OTUs are able to inhibit NF-kB activation affecting immune pathways regulated by ubiquitination (Capodagli et al., 2011). The CCHFV-L OTU can cleave both K48- and K63- linked poly-ubiquitin chains into monomers but probably is not be able to cleave K6- K11- or K27- linked poly-ubiquitin conjugates (Frias-Staheli et al., 2007; Capodagli et al., 2011).

The last members of the cysteine protease DUBs, called MJD (Machado-Joseph disease protease) are also related to the papain protease superfamily (Ha and Kim, 2008). The best characterized of them is ataxin-3 and is pivotal in the Machado-Joseph neurodegenerative disease, a cerebella ataxia (Doss-Pepe et al., 2003).

Differently from other DUBs, the ubiquitin-specific JAMM/MPN domain containing metalloproteases family has the peculiar feature to bind Zn^{2+} ions (Ha and Kim, 2008). To this DUB family belong Rpn11 (described below), a subunit of the lid of the 19S proteasome, COP9 signalosome (CSN), a conserved multiprotein complex regulating the activity of SCF and other cullin-RING ligase families of ubiquitin E3 complexes (Wei et al., 2008), and the translation initiation factor 3 (eIF3) complexes, which is the largest of the eukaryotic translation initiation factors (Querol-Audi et al., 2013). Despite eIF3, proteasome lid, and CSN complexes share a common spatial organization no DUB activity is expected from the eIF3 MPN domains as they cannot coordinate metal ions (Sanches et al., 2007).

Considering the essential roles of ubiquitin and ubiquitin-like modifiers in several essential pathways in eukaryotic cells, from proteasomal degradation to regulation-signalling activities, it is obvious that DUBs are key functional regulators of them.

1.10.3 Proteasome function, structure and location

The proteasomal complex 26S is the cellular machinery responsible for a large fraction of protein degradation within cells. Its catabolic activity is crucial for the efficient generation of the antigenic peptides loaded on MHC-I molecules (Goldberg et al., 2002).

The proteasome degrades substrate proteins that are labeled through the addition of polyubiquitin chains and requires energy consumption. The proteasome consist of two major subunits, the 19S regulatory particle of about 700kDa, which recognize and unfold, through ATP hydrolysis, ubiquitinated proteins before transferring them forward into the second 20S subunit (Baumeister et al., 1998). This larger multiprotein complex of around 750kDa is the proteolytic core of the proteasome, where the active sites of protein degradation are located. Interestingly the 20S subunit can bind more than a single 19S regulatory particle, one at each side, forming a so called 30S proteasomal complex with a cylindrical caterpillar-like structure (Yoshimura et al., 1993). Each 19S complex can be further divided in an external lid and a base in contact with the major proteasomal subunit (Fig. 10).

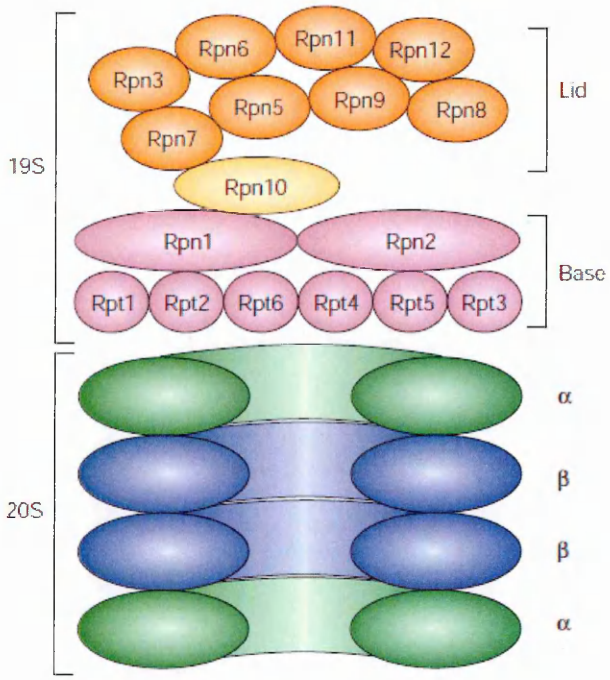

Figure 10. Subunit composition of the 19S and 20S complexes of *Saccharomyces cerevisiae* (adapted from Pickart and Cohen 2004). Several proteins, constituting the lid and the base portion of 19S regulatory particle, are shown. The α- and β-rings of the 20S proteasome are also included. Rpn are regulatory particle non-ATPase proteins, while are named Rpt the regulatory particle ATPases.

The 20S complex is constituted by several related α and β subunits. The α subunits form the two outer heptameric rings, while other two heptameric rings organized by the β subunits constitute the innerpart of the 20S particle with the proteolytic active sites (Fig. 10 and 11). Protein substrates can access the 20S cylinder through axial pores, with a diameter of up to 2 nM and too narrow to allow the entry of fully folded polypeptides; pores can be regulated from an open to a completely closed form by the N-terminal domain of the α subunits (Groll et al., 1997; Whitby et al., 2000; Groll et al., 2000). From the pores three main separate chambers are axially opened in the central part of the 20S complex (Pickart and Cohen, 2004) (Fig. 11).

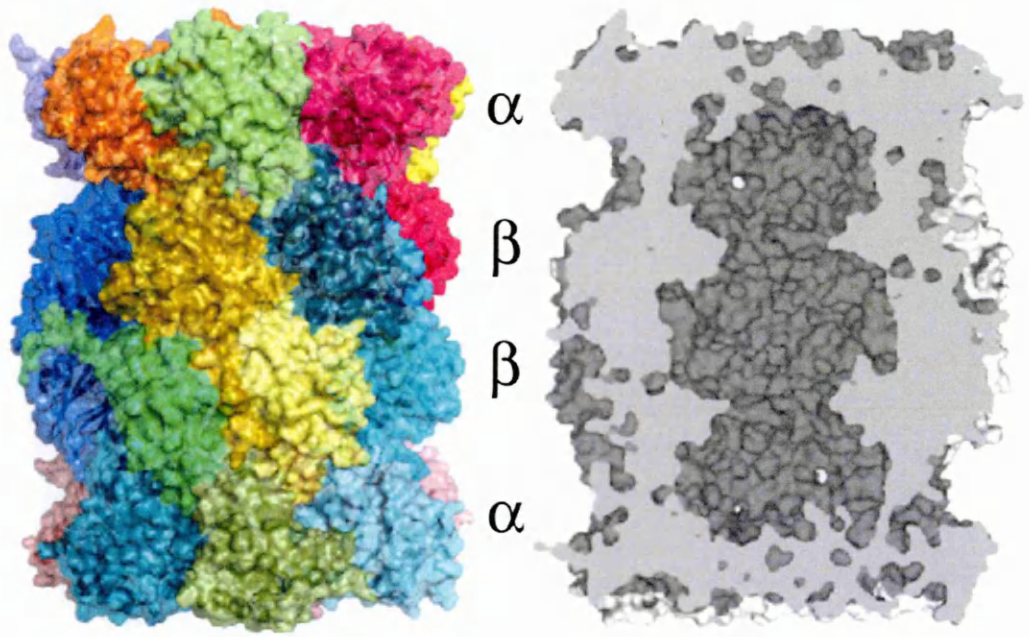

Figure 11. Cristal structure of yeast 20S subunit (adapted from Kunjappu and Hochstrasser 2013). Left panel: the yeast proteolytic core structure is shown with each single protein subunit differently colored. Right panel: internal view of the catalytic particle illustrating the linked chambers containing the proteolytic active sites.

The two lateral chambers (59 nm^3) are believed to have the function to hold a considerable mass of substrate or (partial) digestion products and to regulate their entry to the central proteolytic chamber.

Faced to the central chamber (84 nm^3) are located the protease catalytic sites. The proteases subunits β1, β2 and β5 of eukaryotic proteasome cleave preferentially after acid, basic and hydrophobic residues (Kunjappu and Hochstrasser, 2013). It is clear that the presence of a similar array of proteases with caspase-like, trypsin-like and chymotrypsin-like activities guarantees the ability of the proteasomal complex to efficiently degrade a broad range of polypeptides, producing a heterogeneous mixture of peptides rather than single amino acids (Kisselev et al., 1999).

The binding of the 19S regulatory particle to the core particle induces the opening of the channel in the 20S (Smith et al., 2005). Indeed, in the isolated 20S proteasomal subunit negligible protease activity and very limited peptidase activity was reported. The transformation of these latent enzymes into efficient proteases requires the presence of the 19S regulatory complexes and its active ATPase subunits (Pickart and Cohen, 2004).

Between the base and the lid in the 19S complex are contained at least

seventeen different subunits. In the base are present six ATPases (Rpt1, Rpt2, Rpt3, Rpt4, Rpt5 and Rpt6), belonging to the AAA protein family (ATPases-associated-with-different-cellular-activities) plus two non-ATPase (Rpn1 and Rpn2) subunits with scaffold functions (Fig. 10). These non-ATPase subunits of the base and the entire lid of the 19S complex are not present in bacterial proteasomes (Kunjappu and Hochstrasser, 2013). Two ubiquitin receptors Rpn10 and Rpn13 are associated with the base (Finley, 2009). However several other proteins, containing UBL (ubiquitin-like) and UBA (ubiquitin-associated) domains, can mediate ubiquitin recognition to the proteasome (i.e. Rad23) (Elsasser et al., 2004; Finley, 2009).

In general Rpn10 is considered already a subunit of the lid as it can associate with both the two parts of the 19S regulatory complex, connecting the distal lid with the proximal base (Glickmanet al., 1998).

The lid is essential for the degradation of ubiquitinated proteins and, other than Rpn10, it is formed by nine subunits. Among them the best characterized one is Rpn11 (Poh1 in humans), a Zn^{2+}-dependent deubiquitinating (DUB) enzyme pivotal for the proteasomal function in eukaryotes (Yao and Cohen, 2002). In fact proteasome substrates to be degraded need to be cleaved from the targeting polyubiquitin chains and apparently the early steps of proteasomal associated deubiquitination are mediated almost entirely by Rpn11. This DUB was reported to be able of releasing K48- and K63-linked polyubiquitin chains from substrates targeted to the proteasome for degradation (Yao and Cohen, 2002; Cooper et al., 2009). As Rpn11 require ATP in its proteasomal-associated activity it is possible that other 19S subunits serve to activate, position, or regulate the specificity of Rpn11 (Yao and Cohen, 2002). Little is known about the other lid subunits: Rpn11 and Rpn8 contain an MPN domain (Mpr1, Pad1 N-terminus) of unknown function (Finley, 2009). Of note in this MPN is located the catalytic site of Rpn11, but the related Rpn8 lacks DUB activities.

Notably in addition to Rpn11/Poh1 other DUBs such as the ubiquitin C-terminal hydrolase, Uch2/Uch37 and Doa4, and the ubiquitin specific protease Ubp6/Usp14 can be recruited and associated to the proteasome (Stone et al., 2004). These DUBs can either favour proteasomal degradation or rescue from it. In the latter case it is believed that DUBs activity provoke the release from the proteasome of proteins with too short polyubiquitin tails (D'Arcy and Linder, 2012).

The subunits Rpn3, Rpn5, Rpn6, Rpn7, Rpn9, and Rpn12 contain a common so called PCI module (Proteasome, COP9, Initiation factor 3), that has been observed also in subunits of the COP9 signalosome and the translation initiation factor eIF3. In general protein containing this PCI subunits are highly connected (Förster et al., 2010).

The localization of the proteasome in eukaryotic cells is nuclear and cytosolic (Wilkinson et al., 1998; Reits et al., 1997). Among the cytosolic proteasomal population a fraction that can interact with the ER membranes directly binding the Sec61 complex was proposed to be involved in ERAD (Kalies et al., 2005; Ng et al., 2007).

Apparently, despite proteasomes rapidly diffuse both in the cytoplasm and in the nucleus, there is little exchange between the nuclear and cytoplasmic pools, except in mitosis (Reits et al., 1997; Kunjappu and Hochstrasser, 2013).

1.11 Specific ERAD pathways for different ERAD substrates

Both in yeast and mammalian cells several ERAD pathways, sometimes overlapping (Bernasconi et al., 2010; Shenkman et al, 2013), have been described (mainly in yeast) and are also emerging in mammals, depending on the localization of the misfolded moiety, on the type of protein substrate (i.e. soluble or membrane anchored) and on the eventual presence of N-linked glycans (Vembar and Brodsky, 2008; Taxis et al., 2003; Vashist and Ng, 2004; Bernasconi et al., 2010; Christianson et al., 2012; Ninagawa et al., 2011).

In yeast depending on where the protein lesion is located, cytoplasmic, luminal or membrane-spanning domains, three different pathways were envisaged: ERAD-C, ERAD-L and ERAD-M, respectively (Vembar and Brodsky, 2008). For example, in yeast ERAD-L requires the activity of the E3 ubiquitin ligase Hrd1p (homologous of HRD1) and the adaptor protein Hrd3p (homologous of Sel1L) (Bordallo et al., 1998). In the complex with Hrd1p was reported to be present also Usa1p, a double-spanning membrane protein, which seems to bridge Hrd1p to Der1p (homologous of Derlin1) (Carvalho et al., 2006). Apparently also ERAD-M involved Hrd1p, even though is independent from Usa1p and Der1 (Vashist and Ng 2004). Instead, ERAD-C substrates are reported to involve a complex that contains the ubiquitin ligase Doa10 and is independent from

Usa1p and Der1p (Carvalho et al., 2006).

In mammals the ERAD-L, ERAD-M and ERAD-C pathways are not as clearly defined as in yeast. In higher eukaryotes several more ERAD players than in yeast are present and a global picture of the different pathways is still missing (Vembar and Brodsky, 2008), despite the fact that with the some model substrates a defined ERAD network was mapped. (Christianson et al., 2012).

Of note almost all ERAD pathways seems to converge to the cdc48/p97 ATPase consistently with its pivotal role in ERAD (Vembar and Brodsky, 2008; Christianson et al., 2012), even though must be addressed that not every kind ER to cytosol retrotranslocation requires its activity. For instance, in the case of cholera toxin (Lencer et al., 2003; Kothe et al., 2005; McConnell et al., 2007) its retro-translocation does not lead to degradation, a feature apparently shared also by calreticulin, which despite being synthesized and transported to the lumen of the ER, entail other functions in the nuclear/cytosolic compartments after retrotranslocation, without a relevant rapid degradation of the dislocated fraction (Afshar et al., 2005).

Considering the existence of different retrotranslocation pathways and the several differences among the retrotranslocation/ERAD substrates, it is mandatory to consider several models to draw a comprehensive picture of the process and to validate new methods that enable to determine substrate localisation during the crossing of the ER membrane, one of the most unclear step of ERAD.

2. HCMV induced degradation of MHC class I

2.1 MHC class I structure and function

Under the name MHC class I (Major histocompatibility complex class I protein) there is a family of type-I membrane glycoproteins responsible of transplant rejection and involved in immunodetection of virally infected cells or transformed cells.

MHC-I proteins are able to load a broad variety of peptides, originated both from intracellular and extracellular protein portions (even the same processed leader peptide of the MHC-I molecule), but mainly derived from proteasomal produced proteolytic fragments (Hewitt 2003). The bound peptides are then displayed by the mature MHC-I molecules (formed by the polymorphic class I α chain and the monomorphic β2-microglobulin) at the cell surface to be recognised by antigen specific receptor complexes located in the plasma membrane of cytotoxic T cells (Germain, 1994).

In humans, the MHC-Iα chains are encoded in chromosome 6 in three different loci (HLA-A, HLA-B and HLA-C; HLA: human leukocyte antigen). They are among the most polymorphic genes in the whole genome. Indeed, according to the IMGT-HLA database, a large number of variant alleles are known at each of the three class I loci.

More in detail MHC class I molecules are formed by an α chain, a transmembrane glycoprotein of about 44-47 kDa formed by three main immunoglobulin domain (α1, α2, α3, Fig. 12) associated non-covalently with the β2 microglobulin, a non-polymorphic protein with a weight of about 12 KDa. The association between α chain and β2 microglobulin is required to membrane expression of MHC-I molecules.

The association between α chain and β2 microglobulin is required for membrane expression of MHC-I molecules.

The MHC-I α chain can bear, through a binding-pocket of around 25Å x10Å x11Å, a broad array of peptides of 8-11 amino acids long in an extended conformation.

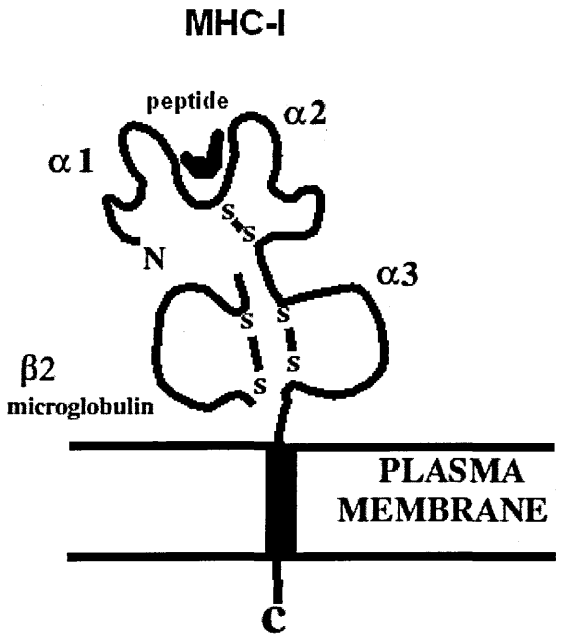

Figure 12. Scheme of MHC class I molecule. MHC-I α chain is shown, with indicated its three extracellular immunoglobulin domains α1, α2 and α3, in association with β2 microglobulin. The α chain creates a pocket for the binding of the peptide.

These peptide-presenting molecules are expressed in every cell and usually they display peptides originating from cytosolic proteins. However in professional antigen-presenting cell (APC) like dendritic cells, MHC-I can display also peptides that derive from exogenous and secretory antigens exploiting the cross-presentation pathway.

In cross-presentation exogenous antigens are internalised in endosomes and processed in a lysosomal/phagosomal compartment, containing some ER resident proteins and probably also ER lipids, or retrotranslocated to the cytosol for proteasomal degradation before loading onto MHC-I molecules (Joffre et al., 2012). In the latter case the ERAD machinery was found to be involved with a pivotal role for p97 ATPase (Ackerman et al., 2006). Links between antigens, internalising receptor and the ERAD machinery are known, as in the case of cross presentation of model antigen ovalbumin through binding to the mannose receptor, which is polyubiquitinated to induce recruitment of p97 towards the phagosomal membrane and retrotranslocation to the cytosol for proteasomal degradation (Zehner and Burgdorf, 2013).

The binding to a peptide increases the stability and the surface expression of the MHC-I molecules, where they display peptides to the Cytotoxic T lymphocytes (CTLs) (Momburg and Tan, 2002; Garbi et al. 2005).

CTLs are CD8+ T cells restricted to the recognition of a defined peptide bound to a defined MHC-I allele through the membrane TCR (T-Cell Receptor) complex, formed by either a TCR alpha/beta or TCR gamma/delta heterodimer coexpressed with the invariant subunits of CD3 (named γ, δ, ε, ζ, and η). Upon recognition of the peptide peptide-MHC-I complex on membrane of APC, naïve T CELLS proliferate and differentiate into competent CTLs. Once activated, CTLs interacting with the same peptide-MHC-I complex on target cells, perform their cytotoxic activity by secreting a number of toxic granules containing molecules, such as perforin and granzymes, which kill the target cell. Most viruses are potent inducers of CTL responses, directed to viral proteins produced in the infected cells, which following degradation by the proteasome end up displayed on the cell surface bound to MHC-I complexes. The capability of CTLs to recognize and destroy virally infected cells is, in some cases, counteracted by viruses through the development of mechanisms that allow escape to recognition by the immune system. This is achieved, for instance, by directly interfering with the antigen presentation pathway (Lorenzo et al., 2001; Hewitt, 2003).

2.2 Folding of MHC-I molecules

During translation MHC-I molecules are N-glycosylated at the end of the α1 domain and are bound by calnexin and its associated protein ERp57, a member of the protein disulphide isomerase family, which arranges the appropriate disulphide bridges (Ellgaard and Ruddock, 2005; Peaper et al., 2005).

Then the MHC-I α chain associates with β2 microglobulin and to the chaperon calreticulin (Momburg and Tan, 2002; Garbi et al. 2005, Peaper and Cresswell, 2008a).

At this point MHC-I form the peptide loading complex (PLC), with β2 microglobulin, ERp57, calreticulin, tapasin, TAP (antigen peptide transporter) and Bap31.

In the PLC tapasin is linked to ERp57 through a disulphide bond and it is pivotal

to connect MHC-I to TAP and to the other components of the PLC (Peaper and Cresswell, 2008b; Garbi et al., 2003; Leonhardt et al., 2005).

Peptides presented on MHC class I usually derived from immuno-proteasomal degradation, thus with a prevalence of intracellular peptides.

Only some class of peptides can be accommodated in the groove of MHC-I, usually of 8-11 amino acids, which are trimmed to this dimension by the activity of some ER associated peptidases, because TAP transports often longer peptides. In humans two ER amino peptidase have been described:: ERAP1 cleaves peptides with hydrophobic residues, while ERAP2 cleaves peptide with basic residues (Saric et al., 2002; Saveanu et al., 2005; Chang et al., 2005).

Once assembled, the peptide / MHC-I α chain / β2 microglobulin complex is a mature and stable molecule, which can traffic from the ER to the cell membrane through a process that involves Bap31 and possibly other export receptors (Paquet, Cohen-Doyle et al. 2004).

2.3 Immuno evasion: HCMV and MHC class I down regulation

Human cytomegalovirus (HCMV) is a widely spread virus that affects around 50-70% of the human population with usually no serious pathological consequences.

Nevertheless, HCMV can cause serious diseases in immunosuppressed or immunodeficient patients.

The tropism of HCMV is towards many cell types including: epithelial cells, glial fibroblasts, endothelial cells, monocytes and macrophages, where it replicates slowly and establishes a latent state with periodic reactivation.

HCMV is so diffused because is well adapted in escaping from the immune system, in particular down-regulating MHC-I display on the membrane of infected cells (Ploegh, 1998).

In the HCMV genome there is the unique short region S component (US), which encodes for eight membrane glycoproteins involved in immunoevasion (Jones et al.,1995), termed immunoevasins.

Expression of those immunoevasins is fine-tuned during the viral life cycle and together they strongly affect the cell surface expression of MHC-I. After infection, US3 is the first one expressed and prevents the trafficking of newly

synthesized MHC-I molecules to the cell surface (Jones et al., 1996).
US6, instead, blocks TAP enzymatic activity, preventing the peptide loading on MHC-I (Hengel et al. 1996). Another immunoevasin, US10 was found to delay MHC class I trafficking towards the cell membrane (Lin et al., 2007).
Instead, proteins US2 and US11 are both able to induce specific proteasomal degradation of MHC-I either associated or not with the β2 microglobulin (Jones et al., 1995; Wiertz et al., 1996a and 1996b).
US2 and US11 degrade MHC-I promoting its dislocation from the ER lumen to the cytosol, exploiting some components of the ERAD pathway used to degrade misfolded proteins (Meusser et al., 2005; Sayeed and Ng, 2005) (Fig.13)
When the MHC-I reaches the cytosol the N-glycanase can remove the N-glycan favouring the molecule to be degraded by the proteasome (Suzuki et al., 2000; Hirsch et al., 2003; Sayeed and Ng, 2005).

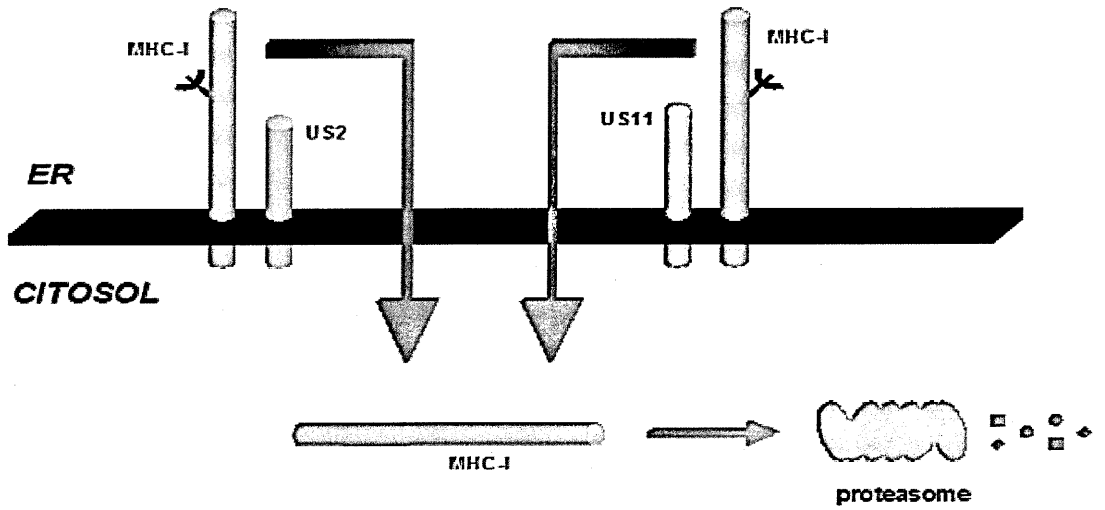

Figure 13. Scheme of MHC-I degradation induce by US2 and US11 activity. The process involves a dislocation step followed by deglycosylation and proteasomal degradation.

2.4 US11 and US2 activity

US11 is a type I glycoprotein of about 25 kDa with an N-terminal glycosylated ER luminal domain, a transmembrane and a short cytoplasmic tail.
US11 induces down regulation of MHC-I molecules, interacting with the α1 and α2 luminal domains of MHC-I, being particularly specific for HLA-A2 and HLA-C

alleles (Huard and Fruh, 2000; Barel et al., 2003).

US11 seems to target MHC-I molecules independently of its folding structure (Blom et al. 2004) and to promote its polyubiquitination of MHC-I (Shamu et al., 2001; Furman et al., 2003).

Through a Gln residue at position 192 in its transmembrane domain, US11 is able to interact with Derlin-1 exploiting its role in an ERAD pathway that involves also HRD1 and SEL1L (Lilley and Ploegh, 2004; Mueller et al., 2006).

Expressed in a cell, US11 was found to induce UPR, but this happened only through the interaction of US11 and Derlin-1 transmembrane domains (Tirosh et al., 2005).

US2 (23 kDa) shares a common topology with US11, but it suffers of an inefficient ER translocation, due to the presence of a non-cleavable signal peptide that causes the formation of a non-glycosylated cytosolic form of the protein (Wiertz et al., 1996a; Gewurz et al., 2002)

US2 recognises MHC-I molecules binding its α2 and α3 domains, without interacting with the β2 microglobulin or the peptide (Fig. 14), and is able to down-regulate HLA-A2, HLA-B27 and HLA-G alleles (Barel et al., 2003).

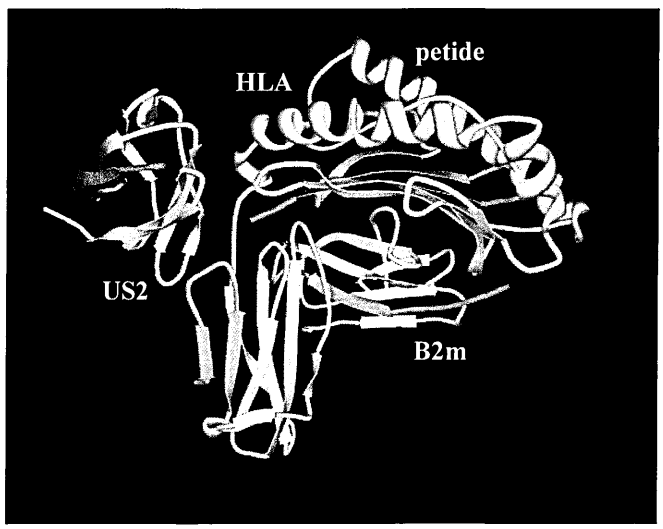

Figure 14. 3D folding of MHC-I and US2. Cristal structure MHC-I α luminal domain associated with the β2 microglobulin, the peptide and US2 (Gewurz et al., 2001)

Following interaction with US2, MHC-I molecules are dislocated to the cytosol, where also in this case steps of deglycosylation and proteasomal degradation take place (Jones et al., 1996; Wiertz et al., 1996a).

A critical portion of US2 resides in its cytoplasmic tail, where some amino acids

(Cys 187, Ser 190, Trp 193 and Phe 196) have been indicated as involved in the interaction with the host retrotranslocation machinery.

Thus, upon the tight interaction between US2 and MHC-I, the cytoplasmic tail of US2 engages the cellular retrotranslocation machinery (Oresic et al., 2006)

Indeed it was previously found that creating a chimeric protein with the cytoplasmic tail of US2 and US3, enables US3 to degrade MHC-I. In this process it was found that the cytosolic tail of US2 was involved in the recruitment of the p97 ATPase, which is considered the main power supply of ERAD (Chevalier et al., 2002; Chevalier and Johnson, 2003).

The US2 pathway requires also the activity of the signal peptide peptidase (SPP) (Loureiro et al. 2006) and of a functional ubiquitin system, (not required in the case of US11 (Hassink et al., 2006)), in particular with the presence of the TRC8 E3 ligase (Stagg et al., 2009).

US2 promote the degradation preferentially of properly folded MHC-I molecules (Blom et al., 2004), which upon US2 contact are modified with 3-5 ubiquitins (Shamu et al., 2001; Furman et al., 2003).

3 The ERAD model Null Hong Kong α1 antitrypsin (NHK-α1AT)

The serine protease inhibitor alpha1-antitrypsin (α1AT) is a cellular secreted glycoprotein factor belonging from the serpin protein family (Kroeger et al., 2009). Serpins are suicide inhibitors of several intracellular and extracellular proteases (Lomas and Mahadeva, 2002). In the case of α1AT its major physiological role of is to protect elastic fibers in the lung from excessive hydrolysis by neutrophil elastase, as genetic deficiency of this enzyme lead mainly to the development of emphysema; but α1AT can also irreversibly inhibits several other proteases such as trypsin, chymotrypsin and plasminogen activator (Sifers et al., 1988). The protein is also abundantly secreted by hepatocytes and by interacting one to one with substrates is responsible for 90% of the protease inhibitory capacity in the serum (Sifers et al., 1988). Several different mutations of α1AT have been reported in the literature. One of these mutants called Null Hong Kong alpha1 antitrypsin (NHK-α1AT), characterized from a patient lacking completely the protein in the serum, has been widely used as an ERAD model. The relevant alteration on NHK-α1AT is a frame-shift mutation, because of a dinucleotide deletion in the codon for Leu318, which causes a premature termination at residue 334, producing a truncated protein of 45 kDa containing three well recognized N-glycosylation sites (Sifers et al., 1988). As the inhibitory site of α1AT is located in Ser359 (Johnson and Travis, 1978) NHK-α1AT lacks protease inhibitory activity; moreover the mutant protein is retained within the endoplasmic reticulum and degraded through the proteasomal pathway (Liu et al., 1999). This ERAD model, because of the presence of the three glycan moieties, was useful in understanding the role of rearrangement of the distal N-glycan sugar residues and the activity of mannosidases in the selection and recognition of ERAD substrates. Indeed it was initially discovered that the plant alkaloid kifunensine, an inhibitor of ERManI was able to arrest turnover of the misfolded glycoprotein. Instead, inhibition of glucosidase II, by castanospermine, favoured NHK-α1AT interaction with calnexin, causing an increased degradation of the glycoprotein by the proteasome (Liu et al., 1999). A type-II ER membrane lectin, called EDEM1 (ER degradation enhancing α-mannosidase-like protein), was reported to participate, most likely indirectly, in mannose trimming of NHK-α1AT.

EDEM1 is a protein reported to do not have enzymatic mannosidase activity in vitro (although evidence for its trimming of alpha1,2-linked mannose on the C branch of N-glycans was reported in living cells: Hosokawa et al., 2010), but whose overexpression accelerates NHK-α1AT degradation in the absence of kifunensine (Hosokawa at al., 2001). Moreover a synergic effect of EDEM1 and ERManI was shown to promote degradation of NHK-α1AT (Hosokawa et al., 2003). Interestingly EDEM1 was reported to favour release of misfolded glycoproteins from calnexin cycle (Molinari et al., 2003). Through its binding activity EDEM1 is believed to inhibit the formation of a spurious NHK-α1AT homo-dimer through the single Cys present in the mature protein at position 256; of note wild type α1AT does not from a related dimer (Hosokawa et al., 2006).

In addition to ERManI and EDEM1 also the Golgi a1,2-mannosidase IA, IB, and IC and γ-COP (a subunit of COP-I retrieval vesicles) seam to accelerate turnover of NHK-α1AT, suggesting the involvement of early Golgi compartments (ERGIC) in mannose trimming and retention of NHK-α1AT (Hosokawa et al., 2007; Pan et al., 2013).

Even though it was a bit debated (Hosokawa, et al., 2008; Christianson et al., 2008), it seems that among the ERAD components involved in NHK-α1AT degradation, is present a complex formed by at least one of the ER-resident lectins OS-9 and XTP3-B, which contain the mannose 6-phosphate receptor homology domain (MRH) believed to be required not for substrate recruitment, but for binding to the ER type-I transmembrane protein SEL1L (also this protein bear a MRH domain). SEL1L further interacts with the ubiquitin ligase Hrd1 and in the complex probably joins also the ER chaperone GRP94. This protein chaperon, together with Hrd1 and SEL1L were reported to favour the degradation of NHK-α1AT (Christianson et al., 2008).

Also a role for BiP in such complex was described, but only for the artificial NHK-QQQ mutant (with all the glycosylated Asn residues mutated to Gln) as differences in ERAD of the two isoforms, with or without sugars, were reported (Hosokawa, et al., 2008).

Recently, a protein called Herp was found in the Hrd1 complex involved in ERAD of NHK-α1AT. This protein contains a UBL (ubiquitin-like) domain required for its association with Hrd1, which promotes a more efficient

ubiquitination and degradation of NHK-α1AT (Kny et al., 2011).

A role for the TRAP (translocon-associated protein) complex in the late stages of NHK-α1AT degradation was reported, as RNA interference of single subunits (α, β or γ) apparently causes a delayed degradation of misfolded proteins (Nagasawa et al., 2007).

Recently it was reported the participation of malectin in regulating negatively protein export from the ER for glycoproteins such as NHK-α1AT under stress conditions (Galli et al., 2011). It was proposed that malectin might act upstream or concomitantly to the calnexin cycle as this lectin can bind only G2M9 sugar chains (Chen et al., 2011).

4 Folding and ERAD of Immunoglobulin heavy and light chains

Immunoglobulin (Ig) molecules are the key components of the humoral immune system, which relies on both the membrane and secretory forms for B cells activation and antigen targeting in the effector phage, respectively.

Immunoglobulins are in general multimeric protein complexes and their folding requires the presence of several molecular chaperones (Lee et al., 1999). Excluding the peculiar case of homo-heavy chain immunoglobulins expressed mainly in camelids and sharks (Wesolowski et al., 2009), immunoglobulins are formed by at least two identical pairs of heavy (HC) and light chains (LC) stabilized by interchain and intrachain disulphide bridges (Fig. 15) (Lee et al., 1999). In some cases, as for secretory IgA and IgM a complex of higher order can be formed which is stabilized through disulphide bonds by the cysteine-rich J-chain protein (Horton and Vidarsson 2013).

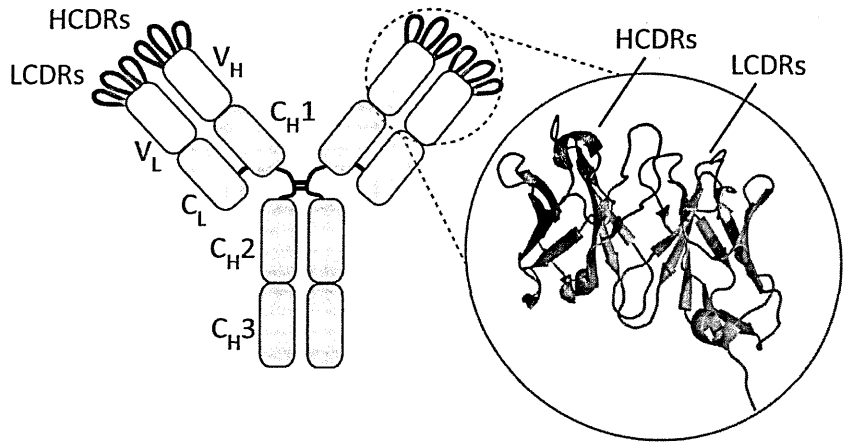

Figure 15. Organization of an immunoglobulin (adapted from Lee et al., 2013). Scheme of an antibody molecule and its immunoglobulin subunits in the light and heavy chain. Black lines represent the hinge region and the interchain disulphide bonds (S-S) present on it between the first (C_H1) and the second (C_H2) constant domain of the heavy chain and also the interchain S-S bonds between constant domain of the light chain (C_L) and C_H1. In the variable regions of the heavy chain (V_H) and light chain (V_L) the complementarity-determining regions (respectively HCDRs in blue and LCDRs in red) are highlighted and shown as are positioned in the crystal structure of Herceptin mAb antigen-binding domains (pdb 1N8Z, Cho et al., 2003).

Each immunoglobulin chain is formed by two to five Ig domains independently folded and stabilized by a single disulphide bond into a compact structure (Lilie et al., 1995; Amzel and Poljak, 1979). In all Igs at the N-terminus is present an Ig domain called variable region. Within this region are present three

complementarity-determining regions (CDR) with an amino acid sequence extremely variable and long between three and twenty-five amino acids (Kabat and Wu, 1991; Hofle et al., 2000). The CDRs of the LC and HC are exposed on the 3D structure of immunoglobulins forming together the surface for antigen binding (figure 16) (Kabat and Wu, 1991).

When expressed in the absence of the LCs, as in the B lymphocyte stage of pre-B cells, the HCs do not traffic to the cell membrane and get retained in the ER because of their association with the ER resident chaperone grp78/BiP, which binds to the first constant domain (C_H1) (Bole et al., 1986; Lee et al., 1999). In the absence of LC the C_H1 domain is not able to fold correctly, remaining also reduced, because of its binding to BiP. LCs provoke the release from BiP allowing C_H1 folding, which therefore binds to the C_L domain, thus allowing secretion of the whole immunoglobulin (Lee et al., 1999). Forcing the release of BiP from isolated heavy chains resulted in oxidation of the C_H1 domain, but this was not properly folded (Vanhove et al., 2001). Instead the presence of folded LCs interacting with HCs C_H1 provoke oxidation, probably by an inducing a proline isomerization in the C_H1, and correct secretion (Feige et al., 2009). The unassembled ER-retained Ig HCs were reported to be degraded by cytosolic proteasomes through the ERAD pathway (Mancini et al., 2000; Ho et al., 2000).

LCs are usually able to fold readily and to be secreted independently as monomers or dimers (Dul et al., 1996; Leitzgen et al., 1997). However, there are LCs unable to be secreted in the absence of HCs, probably because of defective folding of only the V_L domain (Skowronek et al., 1998). In fact it was proposed that those V_Ls require the assistance of an already folded V_H domain to reach the appropriate conformation (Feige et al., 2009). Among this class of non-secreted LCs, NS1 expressed by a HC loss variant of the mouse plasmacytoma cell line MOPC 21 (Cowan et al., 1974) is one of the most studied models (Skowronek et al., 1998; Shimizu et al., 2010). The non-secretory phenotype of NS1 is the consequence of a replacement of the conserved Phe/Tyr in position 87 with His (Dul et al., 1992).

Interestingly, also on the retention of these partially folded LCs, which are reported to become ERAD substrates and degraded by the proteasome, the protein responsible is BiP. It was proposed that degradation takes place while exiting from the ER lumen (Chillaro´n and Haas 2000). This conclusion was

drawn because in murine plasmacytoma cells, NS1 was not completely reduced upon proteasomal inhibition. In particular, at least the C_L domain was already folded. Moreover, during cell fractionation experiments, in conditions of impaired proteasomal degradation, NS1 remained mainly bound to the microsomal fraction, not displaying cytosolic exposure, since it was not sensitive to trypsin digestion and remaining apparently completely bound to BiP (Chillaro´n and Haas 2000). However, this might not be true in other cells. For instance, in NIH/3T3 cells it was recently observed that upon proteasomal inhibition the NS1 protein is released from BiP and relocated by the activity of the lectin XTP3-B and of EDEM1 in the ERQC compartment (Shenkman et al., 2013), an area of the ER where probably takes place the dislocation step. Ubiquitinated NS1 was found to be formed mainly by a partially reduced form (with the C_L domain still oxidized). In addition, ubiquitination occurs mainly in the reduced V_L domain and can interest several amino acid residues, mainly Ser and Thr, other than the classical Lys (Shimizu et al., 2010). Moreover, it was shown that at least part of this ubiquitination was performed by the E3 RING type ubiquitin ligase Hrd1 (Shimizu et al., 2010). Derlin1 was found associated to NS1 as well as Herp (a multi-spanning membrane protein with a cytosolic N-terminal ubiquitin-like domain) following proteasomal inhibition (Okuda-Shimizu and Hendershot, 2007). This protein is known to interact with the ATPase p97 and the ubiquitin ligase Hrd1 (Schulze et al., 2005). Moreover, Herp was reported in a complex also with ubiquitinated proteins and with the 26S proteasome (Okuda-Shimizu and Hendershot 2007). A remarkable stabilization of NS1 was shown when co-expressed with the p97 ATPase incompetent dominant negative mutant (Okuda-Shimizu and Hendershot, 2007).

5 Vpu induced degradation of CD4 and Tetherin

5.1 Vpu

The HIV-1 (human immunodeficiency virus type 1) accessory protein Vpu is a small (around 80 amino acids, depending from the viral strain) oligomeric type-I membrane phosphoprotein (Strebel 2013). The protein is structurally formed by a very short luminal domain (3-12 amino acids), followed by a transmembrane domain that functions also as a signal peptide, and a cytoplasmic tail of about 47-59 amino acids (Maldarelli et al., 1993). Apparently through the transmembrane domain Vpu can cluster into pentamers in particulary in the Golgi or in intracellular vesicles, but not in the ER, and these oligomers can functionally form a channel for monovalent cations such as Na^+ and K^+ (Ewart et al., 1996; Hussain et.al., 2007; Mehnert et al., 2007). Nevertheless a clear functional significance for this Vpu property is still missing (Strebel, 2013).

In the cytoplasmic tail of Vpu contains motifs influencing its membrane localization through all the secretory pathway, but the protein resides mainly in the ER, trans Golgi network and endosomal compartments (Hussain et.al., 2007; Dubé et al., 2010; Iwabu et al., 2009). Indeed in the cytosolic portion of the protein are present an YXXΦ tyrosine motif (where Φ is a hydrophobic amino acid) and a dileucine motif (D/EXXXLL/I/V) both involved in endocytic/lysosomal targeting (McCormick-Davis et al., 2000; Bonifacino and Traub 2003).

Regarding the cytoplasmic domain it has been predicted that contains two main α-helix interconnected by a flexible loop, encoding for a conserved DSGNESEGE sequence, which is phosphorylated on both Ser52 and Ser56 residues by the casein kinase II (CKII, consensus S/TXXD/E) (Schubert et al., 1994). The constitutive phosphorylation of these two Ser, in the context $DS^PG\Phi XS^P$ (Dubè et al., 2010), provoke the continuous binding of Vpu with a β-TrCP-containing SKP1, Cullin, F-box protein (SCF) E3 ubiquitin ligase complex (SCF^{TrCP}) (Margottin et al., 1998). Interestingly while usually a contact between the E3-ligase and the phosphorylated protein causes the degradation of the latter, but this is not the case for Vpu, which is not ubiquitinated in the process (Schubert et al., 1994; Strebel, 2013). The Vpu interaction with SCF^{TrCP} is responsible, at least in part, of several of the Vpu mediated functions such as

the selective induction of proteolysis of newly synthesized membrane proteins, the favouring of virus release from the cell surface (i.e. CD4 and Tetherin/BST-2 degradation) (Margottin et al., 1998, Mangeat et al., 2009) and the inhibition of NFκB activation (because of its interference with SCF^{TrCP} mediated degradation of IκB) (Bour et al., 2001; Strebel, 2013).

5.2 ER associated degradation of CD4

CD4 is a type-I membrane protein expressed by thymocytes, helper T lymphocytes, cells of the macrophages/monocytes lineage, and hematopoietic progenitor cells, playing a crucial role during antigenic stimulation by antigen presenting cells exposing MHC-II and function as receptor for IL-16 (Bowers et al., 1997; Wilson et al., 2004). CD4 contains two N-glycosylation moieties and four extracellular immunoglobulin-like domains, three of which are stabilized by an intrachain disulphide bridge, and a 40 amino acids long cytosolic tail, where five Cys residues are present. Some of them (Cys420 and Cys422) are involved in the formation of membrane proximal disulphide bonds mainly in a tetraspanin-enriched plasma membrane fraction of the protein (Fournier et al., 2010), while others Cys in the juxtamembrane domain (Cys394 and Cys397) are known to be palmitoylated (Crise and Rose, 1992). CD4 is the major component of the receptor complex exploited by HIV for infection. At the same time the virus promotes also CD4 down regulation in at least two different ways: i) by internalization from the plasma membrane mediated by HIV Nef protein and ii) by ER retention and degradation mediated by the expression of gp160 and Vpu (Bowers et al., 1997). It was shown that the coexpression of Vpu and gp160 resulted in increased degradation of CD4 (Willey et al., 1992), probably because of the synergic effect on ER retention which favours the ERAD promoted by Vpu.

Vpu induced degradation of CD4 requires the interaction of their respective transmembrane domains and of its two cytoplasmic α-helices to some cytoplasmic sequences of CD4 (Magadán et al., 2010; Margottin et al., 1996), comprised mainly between amino acids 414 and 419 in the sequence LSEKKT (Bour et al., 1995; Vincent et al., 1993; Lenburg et al., 1993). Of note the association of Vpu to CD4 in not sufficient to trigger its degradation, because

the phosphorylation of Vpu Ser52 and Ser56 is required for efficient recruitment of β-TrcP-1 and β-TrcP-2, which through their F-box domain are able to mediated CD4 ubiquitination by the SCF^{TrCP} complex (Dubè et al., 2010). Interestingly, ubiquitination of CD4 can occur on multiple types of amino acids: Lys, Ser and Thr (Magadán et al., 2010). The mechanism of CD4 ERAD induced by Vpu is apparently atypical as the SCF^{TrCP} complex was previously reported to act on non-ERAD substrates such as IκB (Bour et al., 2001) and β-catenin (Latres et al., 1999). Nevertheless several proteins usually involved in ERAD such as the p97 ATPase and its associated cofactors UFD1L and NPL4 were reported to be pivotal in Vpu-mediated CD4 degradation (Fig. 16) (Magadan et al., 2010).

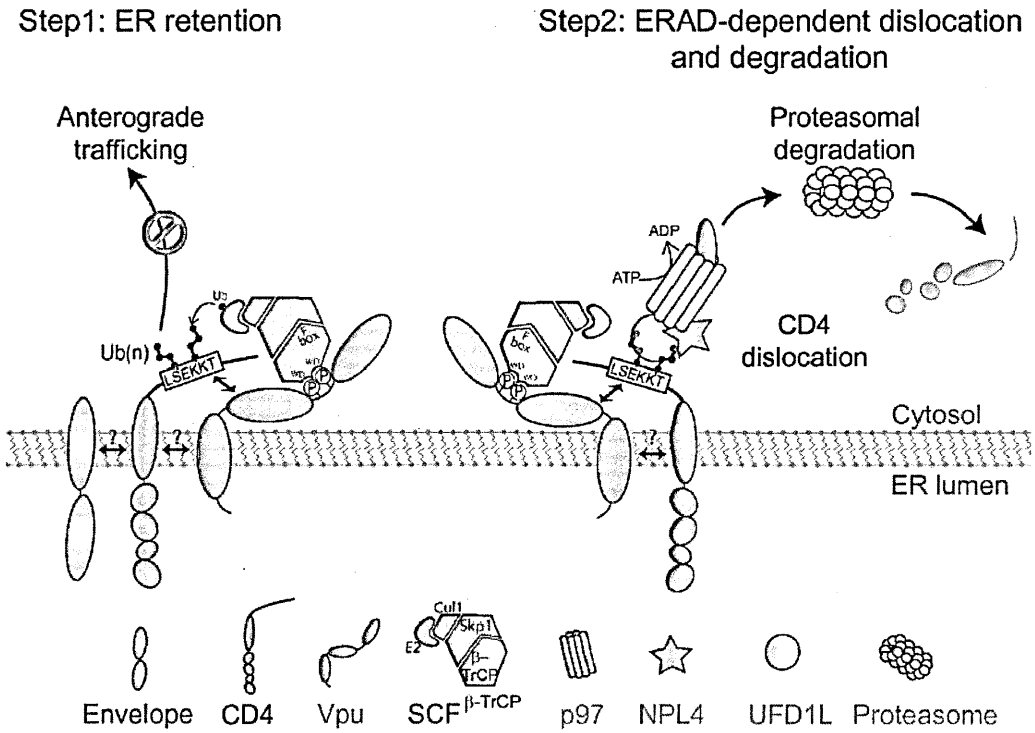

Figure 16. Model of Vpu induce ERAD of CD4 (adapted from Magadan et al., 2010). The scheme pictures the two major steps of CD4 associated degradation during HIV infection: the protein is first retain in the ER by the synergic effect of gp160 and Vpu on the membrane and cytosolic domains, then the polyubiquitination of CD4 cytosolic tail, triggered by the phosphorylated Vpu recruitment of SCF^{TrCP} complex via the F-box domain of β-TrCP, results in a dislocation and proteasomal degradation mediate by the p97-UFD1L-NPL4.

5.3 Vpu induced Tetherin degradation.

One of the most relevant Vpu effect is promoting a more efficient release of viral particles from several HIV infected cells (Dubè et al., 2010). Indeed in the absence of Vpu release of HIV-1 was highly impaired in HeLa cells, in macrophages, and in primary T helper cells, but an efficient release of viral particles was reported in COS, CV-1, HEK293T, and Vero cells (Schubert et al.,1995; Sakai et al., 1995; Geraghty et al., 1994).

Interestingly Vpu was found able to enhance release also of other retrovirus like MLV (murine leukemia virus) and Visna virus (Gottlinger et al., 1993), but even viral-like particles from the unrelated Ebola virus and several other enveloped viruses (Neil et al., 2007; Douglas et al., 2010). It was also observed that viruses were not released because tethered to the plasma membrane and that could be released by protease treatment (Neil et al., 2006). Moreover the proteinaceous tethering factor was found to be inducible by type 1 interferon treatment (Neil et al., 2007) and was identified in the BST-2/Tetherin protein (Van Damme et al., 2008). Tetherin is a peculiar type-II transmembrane glycoprotein with two glycosylation sites, a short cytosolic N-terminal domain, an ectodomain of around 120 amino acids, forming a rod-like α helical structure long 16-17 nm, and a C-terminal GPI anchor (Strebel 2013; Swiecki et al., 2011). Tetherin efficiently forms parallel homodimers, which can be stabilized by at least one of the three available disulphide bonds located in the ectodomain (Perez-caballero et al., 2010). Tetherin dimerization through Cys is essential for efficient tethering of viral particles on the plasma membrane, where Tetherin seem to localize in the same cholesterol-enriched lipid domains home of budding for several enveloped viruses (Perez-caballero et al., 2010; Strebel, 2013). Among the several possible models, virus retention is apparently performed through the localization of one membrane anchored domain, probably mainly the N-terminus (Lehmann et al., 2011), of each Tetherin dimer in the budding viral particle, while the other is embedded in the plasma membrane; apparently Tetherin can even form small chains of viral particles bound one to the other to the plasma membrane (Fig. 17). This mechanism of viral retention is probably mainly due to the structure of Tetherin rather than a really specific amino acid sequence, as a structurally related protein chimera with totally different amino acids composition was capable of inhibit release of

viral particles from the plasma membrane (Perez-caballero et al., 2010).

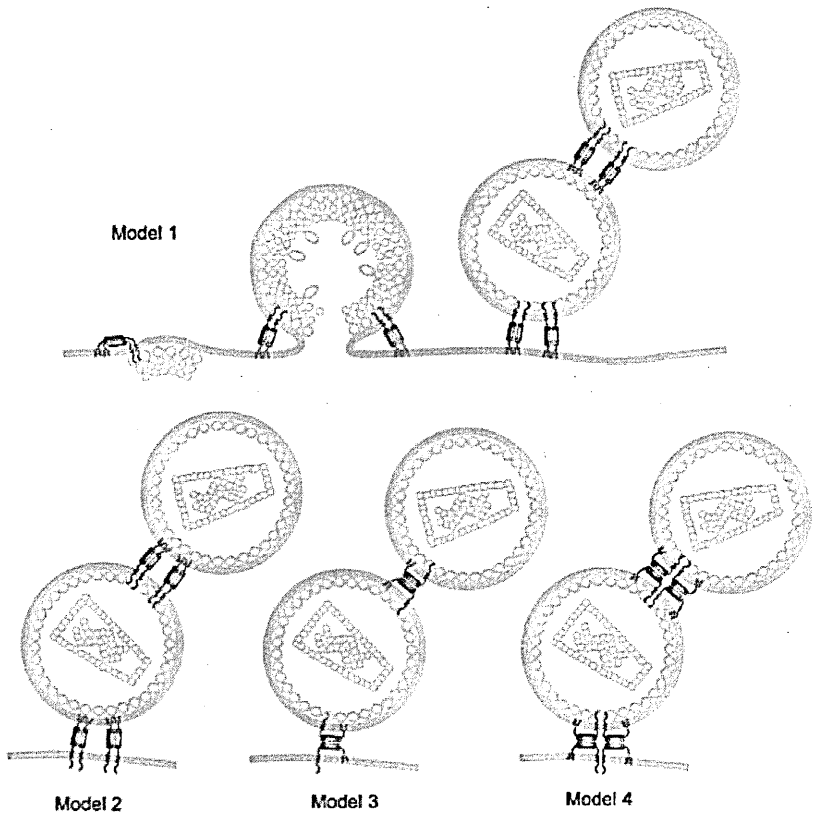

Figure 17. Possible models for Tetherin mediate viral particles retention (Perez-caballero et al., 2010). In model 1 the transmembrane domain of tetherin localizes to the site of formation of the viral particles, being thus incorporated into the envelope and tethering it to the plasma membrane through the GPI anchor. Model 2 illustrate a reverse possible viral anchoration. Model 3 picture a retention mechanism where only one tetherin molecule in the dimer has both membrane anchors incorporated into the budding envelope. In model 4 a multimeric hypothesis for Tetherin action is shown.

How exactly Vpu mediates down regulation of cell surface Tetherin promoting virions release is still debated and it was suggested that both relocalization of Tetherin in the plasma membrane and decrease display of the protein at the cell surface could be sufficient to circumvent its antiviral activity (Strebel, 2013).

It is quite clear that Vpu physically interacts with Tetherin through their respective transmembrane domains (Iwabu et al., 2009). However various contradictory evidences are showing that Vpu can affect the supply of newly synthesized Tetherin, but also its resupply by recycle, to the plasma membrane. Published data claim that Vpu acts on Tetherin either retaining it in the ER, degrading the protein through the proteasome (Goffinet et al., 2009; Mangeat et al., 2009), or relocalising it to a trans-Golgi perinuclear compartment (as judge

for instance by colocalization with the TGN46 marker protein: Dubé et al., 2010) before endo-lysosomal degradation (Andrew et al., 2011; Mitchell et al., 2009). Similarly to Vpu mediated ERAD of CD4, in Vpu induced Tetherin degradation a role for the ubiquitin ligase SCF^{TrCP} complex was found but, surprisingly, it seems to interest both the lysosomal and the ERAD pathway (Mitchell et al., 2009; Mangeat et al., 2009). Probably these discrepancies are due to the several different cell lines used and to the different ways of Tetherin and Vpu expression (i.e. endogenous/viral or overexpressed) (Douglas et al., 2010). Nevertheless, probably the preferential degradative pathway of Tetherin trigger by Vpu during HIV infection involve mainly the lysosomes, but proteasomal degradation cannot be fully excluded (Dubé et al., 2010). However, for Tetherin degradation it has been clearly established that the ERAD pathway is pivotal when this protein is overexpressed. As in the case of CD4, Vpu induced ERAD of Tetherin requires phosphorylation of Vpu residues (Ser52 and Ser56), exploits the ubiquitin ligase SCF^{TrCP-2} complex and ubiquitination of Tetherin cytosolic tail interest several Cys, Ser and Thr residues other than Lys (Mangeat et al., 2009; Tokarev et al., 2011). Also for Tetherin ERAD a pivotal role of p97 ATPase was reported (Mangeat et al., 2009).

6 Calreticulin: ER and non-ER functions

Calreticulin is a highly expressed soluble protein of about 46 kDa, present in every cell of higher eukaryotes, excluding erythrocytes (Krause and Michalak, 1997). There is no calreticulin gene in yeast and prokaryotes, yet this protein is essential in mammals, as calreticulin knockout mice are not viable because of embryonic lethality for cardiovascular defects (Mesaeli et al., 1999). This observation was not surprising considering calreticulin involvement in a number of diverse and important functions, the best known of which are its roles as a pivotal ER chaperone and as the major Ca^{2+}-binding protein within the ER lumen (Michalak et al., 1999). The protein is inserted in the ER through a leader peptide, has a KDEL retention signal at the C-terminus and can be divided into three main distinct functional and structural domains (Fig. 18) (Michalak et al., 2009). The N-domain of calreticulin is similar to the chaperone-lectin domain present also in calnexin, thus contain polypeptide and sugar binding sites (Michalak et al., 2009). Moreover in the N-domain is present a disulphide bridge and a Zn^{2+} binding site (Baksh et al., 1995). The folding of calreticulin is highly influence by Ca^{2+} concentration, for example the N-domain is resistant to proteolysis in the presence of Ca2 (Corbett et al., 2000).

The second calreticulin domain is called P-domain (proline-rich) and it is probably involved together with N-domain in chaperone-lectin functions (Michalak et al., 2009). As the N-domain, also the P-domain of Calreticulin shares a common structure with the homologous domain of calnexin and both the proteins can boost their chaperone functions using it to interacts with the oxidoreductase ERp57 (Martin, et al., 2006).

This P-region of calreticulin binds Ca^{2+} with a relatively high affinity (Kd 1μM), but low capacity (1mol of calcium/1mol of protein) (Baksh and Michalak, 1991).

In the highly acid C-domain of calreticulin are located several Ca^{2+} binding sites with a global high capacity (18-25 mol of calcium/1mol of protein), but low affinity (Kd 2 mM) (Baksh and Michalak 1991). Of note, calreticulin with its Ca^{2+} binding sites is the major responsible of Ca^{2+} storage in the ER lumen (Michalak et al., 2009).

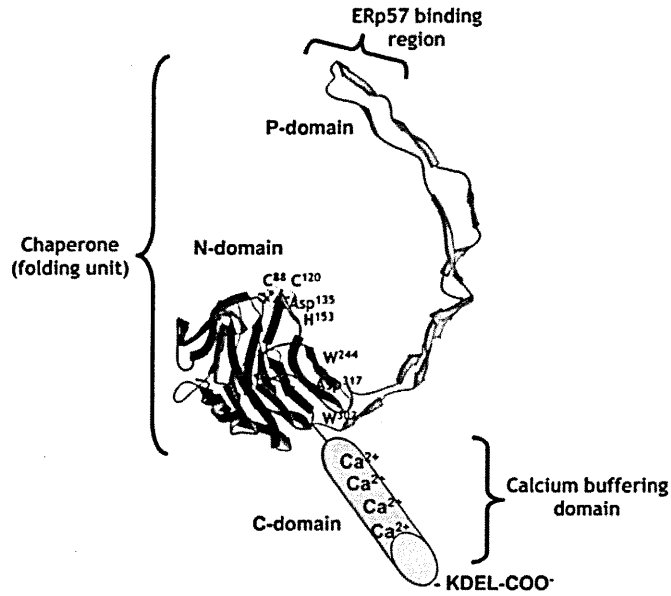

Figure 18. Structural model of calreticulin N- and P-domains and schematic representation of the C-domain (adapted from Michalak et al., 2009). In blue is depicted the globular N-domain (Cys residues involved in S-S bridge are highlighted in yellow), in red the central P-domain with indicated the ERp57 binding area. The N- and P-domains are responsible of the chaperone-lectin properties (Asp135, His153, Trp244, Trp302 and Asp317 the most critical residues for those functions are indicated). In orange is represented the highly acid calcium buffering C-domain.

Within the lumen of the ER, calreticulin is well known to play several roles in folding of proteins in with other ER-resident chaperones and lectins, preventing also protein aggregation and participating to the protein quality control system which mediates degradation of target proteins. Moreover from the ER calreticulin is pivotal regulator of calcium homeostasis, which influences a large variety of cellular functions (Michalak et al., 2009).

Unpredictably calreticulin was found ectopically in the cell, outside of its putative ER localization (Gold et al., 2009). If the localization of this protein at the plasma membrane might be explain by a leakage of the KDEL receptors system, this surface population of calreticulin has been indicated to have several serious functions in antigen complement activation, presentation, clearance of apoptotic and cancer cells and wound healing, to quote only few of its believed extracellular roles (Gold et al., 2009).

Interestingly it was also reported that following retro-translocation or partial insertion, calreticulin has regulatory functions both in the cytosolic and nuclear compartments (Holaska et al., 2001, Shaffer et al., 2005, Afshar et al., 2005).

For example, calreticulin was described to bind the cytoplasmic tail of α-integrins (Reilly et al., 2004), to be a component of the nuclear matrix in hepatocellular carcinomas (Yoon et al., 2000), to have a role in nuclear export of the glucocorticoid receptor, influencing thus transcription (Holaska et al., 2001; Shaffer et al., 2005) and to bind histones in mitotic chromosomes (Kobayashi et al., 2006). More surprisingly, calreticulin was believed to be able to influence translation by RNA binding activities on both viral (Atreya et al., 1995; Yocupicio-Monroy et al., 2003) and cellular mRNAs (Timchenko et al., 2002; Iakova et al., 2004).

These ectopic functions of calreticulin are believed to depend on physical interactions with substrates and hence cannot be explained only by indirect effects. These interpretations were confirmed, for instance, by the effects of increasing insertion efficiency in the ER lumen influenced glucocorticoid receptor-mediated gene activation (Shaffer et al., 2005) and by rescue cell adhesion in calreticulin knock out cells by the expression of a cytosolic version of calreticulin (Afshar et al., 2005). To support a retrotranslocation mechanism from the ER as the source of calreticulin, it was found that the C-terminal domain of calreticulin is both necessary and sufficient for the retrotranslocation (Afshar et al., 2005). In trypanosome this retrotranslocation was reported to be triggered by ER calcium depletion, but not by increasing of cytosolic calcium levels, and that the effect of calcium was strictly dependent on presence of the C-terminal domain, even in fused proteins (Afshar et al., 2005; Labriola et al., 2010). Only a fraction of dislocated calreticulin is known to be targeted to rapid proteasomal degradation (Afshar et al., 2005; Labriola et al., 2010). A clear direct evidence of calreticulin cytosolic localization is the posttranslational N-terminal arginylation of a calreticulin cellular fraction (Decca et al., 2007). This modification is performed by arginyl-tRNA protein transferase, an enzyme, present also in yeast and expressed in two isoforms (ATE1 and ATE2) in mice and humans, with a cytosolic and nuclear localization. ATE proteins can attach an Arg to the N-terminal Glu, Asp or Cys residue of protein substrates (Kwon et al., 1999). This calreticulin arginylation was found dependent from ATE1, increased in condition of calcium sequestration and decreased in the of the ion; of note in the presence only of cellular stress (combined EGTA and thapsigargin treatment) that lead to a reduction of intracellular Ca^{2+} levels the arginylated cytosolic calreticulin was localized in cytoplasmic stress granules (Decca et al.,

2007; Carpio et al., 2010). Interestingly, a recent report described a function for the arginylated calreticulin in response to stress at the plasma membrane, where it seems to act as a preapoptotic signals (Sambrooks et al., 2012).

7 Protein biotinylation as a tool to label cytosolically exposed proteins

Detection of retro-translocated molecules relies usually on the separation of the cytosolic soluble fraction or identification of the fraction deglycosylated by the cytosolic PNGase and accumulated in the cytosol upon proteasome inhibition (Hassink et al., 2006; Wiertz et al., 1996b).

A limitation of this technique could be represented by a low efficiency in the detection of retro-translocated substrates, because of incomplete proteasome inhibition or the inability to identify possible glycosylated, yet retro-translocated molecules.

In an attempt to improve the detection of retro-translocated substrates, we developed a method of specific in living cells labelling of retro-translocated proteins, by selective biotinylation in the cytosolic compartment (Petris et al., 2011, Vecchi et al., 2012). This in living cells biotinylation approach has also been recently used to study cytosolic/luminal localization of prion protein isoforms (Emerman et al., 2010).

Biotinylation of proteins in cells can be easily achieved by co-expression of the E. coli derived biotin-ligase BirA and the protein of interest tagged with a 15 amino acid (GLNDIFEAQKIEWHE) biotin-acceptor-peptide (BAP) (Barker and Campbell, 1981; Beckett et al., 1999).

BirA enzyme catalyses the biotinylation reaction through two ATP-dependent steps that allow the formation of a covalent linkage between the amidic group of the lysine residue in the BAP sequence, and the carboxylic group of biotin. During the biotinylation reaction, ATP hydrolysis causes the formation of the intermediate biotinyl-AMP which is hydrolysed in order to transfer the biotin to the lysine residue of the substrate (Fig. 19) (Abbott and Becket, 1993; Beckett et al., 1999).

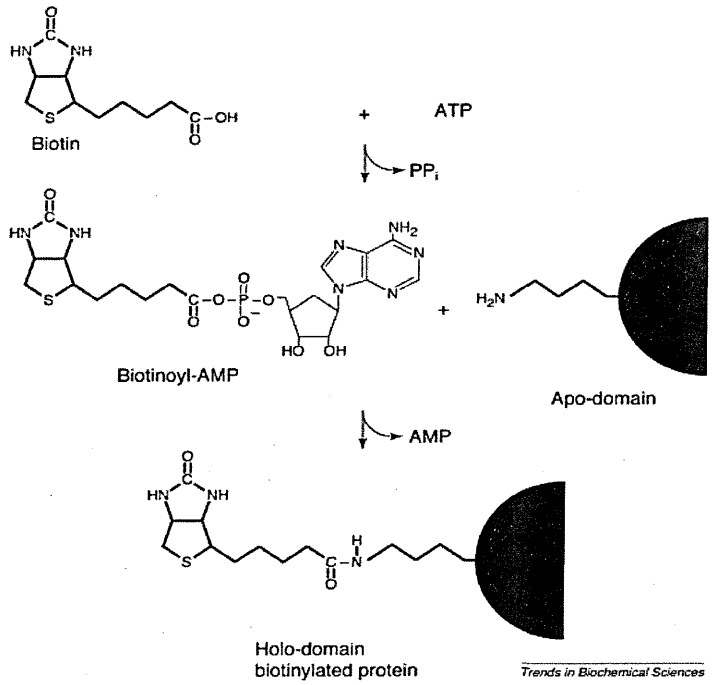

Figure 19. Illustration of the biotinylation reaction. During biotinylation BirA enzyme catalyses the biotinylation of the substrate through two ATP-dependent steps (modified from Chapman-Smith and Cronan, 1999).

It was previously shown that, because of its cytosolic localization, BirA needs to be engineered with a signal leader peptide, in order to translocate to the ER lumen and to achieve efficient biotinylation of proteins within this restricted compartment (Predonzani et al., 2008).

Thus exploiting the strong affinity of streptavidin, from Streptomyces avidinii, or avidin, a glycoprotein present in eggs, the biotinylated molecules can be easily detected.

The binding between avidin or streptavidin and biotin, despite the high affinity, is a non-covalent interaction and a single streptavidin or avidin molecule, being a homotetramers, can bind until four biotins one to each monomeric subunit (Livnah et al., 1993).

For these reasons the streptavidin-biotin interaction is widely exploited in protein science.

8 Tobacco Etch Virus protease (TEVp) as biotechnological tool

Tobacco Etch Virus (TEV) is a non-envelope positive-sense, single-stranded RNA virus, which belongs from the Potyviridae family and can infect several plant species.

Its genome codifies for a single polyprotein of 346 kDa (Allison et al, 1986). From the N-terminal portion of the polyprotein are generated by auto-catalysis the proteases P1 and HC-pro, while the viral protease NIa (*Nuclear inclusion A*) releases all the other proteins. After these maturation cleavages a minimal (27 kDa) active form of the NIa protease (NIa-pro), called also TEVp, is released (Dougherty and Parks, 1991).

TEVp is homologous to serine-proteases, but unlike these it has a cysteine residue in its catalytic site, indeed the single point mutation C151A completely abolish the protease activity (Parks et al., 1995).

The minimal TEVp substrate specificity is encoded in a small seven amino acid long sequence E-X-X-Y-X-Q-S/G (TEVp cleavage site or TS), where X can be any amino acid (Carrington and Dougherty, 1988). However up to now, despite this apparent low specificity and the variety of peptides which could be included as TS, the best recognized and cleaved TEVp epitope is identical to the protease's natural substrate peptide (ENLYFQ/G) (Kostallas et al., 2011). The proteolytic cleavage occurs between the Q and the short aliphatic G residue (Parks et al., 1994). A TS is also present in TEVp itself. Indeed in the C-terminal portion of the molecule a GHKVFM/S sequence is intramolecularly recognised and cleaved (Parks et al., 1995; Kapust et al., 2001). The generated protein fragments are almost proteolytically inactive and resemble a general inactivation mechanism common among several proteases. To overcome the problem of auto cleavage several mutants of TEVp were characterized, of them the S219V seems to have the best ration between catalytic activity and auto-cleavage (Kapust et al., 2001).

Due to its remarkable specificity, stability and activity in several buffer conditions TEVp is widely used in the biotechnology industry as a reagent for endoproteolytic removal of affinity tags (Melker, 2000; Sun et al., 2012),

While in viral infection TEVp accumulates mainly in the nucleus of plant cells before being released from the full length NIa, if expressed alone it localise largely in the cytoplasm (Ceriani et al., 1998). In addition the expression of

TEVp, not only in plant cells, but also in bacteria and yeast was found to be safe (Henrichs et al., 2005; Taxis et al., 2009). Even in Drosophila, the ubiquitous or tissue specific expression of TEVp has no notable phenotypes (Pauli et al., 2008). In HeLa cells micro-injection of the TEVp had no discernible effect on viability or cell proliferation (Satoh and Warren, 2008). Because of these features TEVp is suitable to be used, in place of BirA, as a new tool to label, through its proteolytic activity, the fraction of retrotranslocated ERAD substrates.

Materials and methods

Constructs

MHC-Iα

The human MHC-Iα allele A2 cDNA (accession number U02935) was PCR amplified from RNA extracted from anonymous healthy donors lymphocytes and inserted into pcDNA3 expression vectors (Invitrogen) containing the coding sequences for a secretion signal, the SV5 tag (GKPIPNPLLGLD) and the biotin acceptor peptide BAP (GLNDIFEAQKIEWHE, Beckett et al., 1999). Two plasmids were generated, one containing the SV5 and BAP sequences at the amino terminal side of MHC-Iα (pcDNA-BAP-MHC-Iα) and one with BAP and SV5 sequences fused to the carboxyterminal side of MHC-Iα (pcDNA-MHC-Iα-BAP). US2 and US11 plasmids were kindly provided by Domenico Tortorella.

α1-antitrypsin

The cDNA for the human α1-antitrypsin (α1AT, accession number K01396) was similarly PCR amplified and inserted in a vector that adds the SV5 and BAP sequences at the carboxyterminal end (pcDNA-α1AT-BAP). The vector expressing the NHK mutant of α1AT (Sifers et al., 1988) was generated by substituting the wild type α1AT sequence in the pcDNA-α1AT-BAP vector with a sequence containing a two-base deletion after codon 318 of the mature protein resulting in the insertion of 14 frame-shifted codons (pcDNA-NHK-α1AT-BAP).

γ heavy chain

The plasmid expressing the mouse γ heavy chain was obtained by inserting the coding sequence in the pcDNA vector with the SV5 and BAP sequences at the carboxyterminal end (pcDNA-HC-BAP).

Calreticulin

The vectors expressing the full-length and truncated calreticulin were generated by inserting the PCR amplified cDNAs of human calreticulin (accession number NM_004343) or the calreticulin truncated after codon 285 of the mature protein in the vector with the SV5 and BAP sequences at the amino terminus (pcDNA-

BAP-Crt and pcDNA-BAP-Crt-ΔC).

CD4

CD4 cDNA was modified by inserting at the N-terminus the coding sequences for a secretion signal, the SV5-tag and the Biotin Acceptor Peptide and cloned into pcDNA3 vector (Invitrogen), yielding BAP-CD4. To obtain a CD4 with membrane-proximal BAP (18 amino acids from transmembrane domain, CD4-BAP), the BAP-tag was introduced immediately after Ser382. A codon optimized version of gp160 was cloned into pcDNA3 and used in all experiments with CD4.

Tetherin

Human Tetherin was tagged with SV5 and BAP immediately upstream of the GPI-anchor signal (Tetherin-BAP) and cloned into pcDNA3. Tetherin ectodomain, including amino acids 45–160 of wild type human Tetherin (Swiecki et al., 2011) and containing the added SV5 and BAP tags, was amplified and cloned into pcDNA3. Tetherin cyt-ecto cDNA was modified by inserting at its N-terminus the coding sequence for a secretion signal to obtain a secreted version of Tetherin ectodomain (sec-ecto).

Tetherin with the membrane proximal BAP (12 amino acids from transmembrane domain, BAP-Tetherin) was obtained by inserting the BAP-tag after Ala48. Vpu from viral clone NL4-3, was expressed from a pcDNA3 vector containing an N-terminal leader peptide followed by SV5-tag.

NS1

NS1 SV5-BAP tagged plasmids were generated amplifying wild type, NS1C and NS1STK- sequences (kindly provided by Linda Hendershot, as the p97 and p97QQ plasmids) cloning them in pcDNA3 vectors, codifying an immunoglobulin leader peptide, upstream the coding sequence for the BAP and SV5 tag or in between the two tags. No additional Ser, Thr or Lys (excluding the K site of biotinylation) were introduced at the N-terminus during cloning and tagging of NS1STK-. OTU plasmid was kindly provided by Adolfo García-Sastre.

TEV protease and TS tagged plasmids

NIa TEV protease (TEVp) coding sequence was codon optimized for expression in eukaryotic cells and cloned into pcDNA3. A C-terminal SV5 tagged TEVp in pcDNA3 was also produced.

TEVp C151A mutant was obtained by PCR using the QuikChange Site-Directed Mutagenesis Kit (Stratagene). For experiment with TEVp were realised pcDNA3 SV5-BAP-MHC-Iα-TS-RT and pcDNA SV5-TS-MHC-Iα-RT. These two vectors codify for a MHC-Iα C-terminally tagged with the roTag epitope: SISSSIFKNEG (RT) and contain the seven amino acids (ENLYFQ/G) TEVp cleavage site (TS) at the N-terminus downstream the SV5 tag (pcDNA SV5-TS-MHC-Iα-RT) or at the C-terminus upstream the RT tag (SV5-BAP-MHC-Iα-TS-RT).

A doubled TS and BAP tagged pcDNA3-SV5-BAP-TS-MHCIα-RT was obtained inserting a RT at the C-terminus of SV5-BAP-MHCIα and a TS between BAP and MHCIα.

Starting from pcDNA-NS1(STK)-BAP-SV5 it was obtained a vector (pcDNA-NS1(STK-)-BAP-SV5-TS-RT) expressing NS1STK-mutant tagged at the C-terminus with the BAP, a GGSGS linker followed by the SV5, TS and RT tags.

Cell culture and transfection

HEK293 cells were grown in Dulbecco's modified Eagle's medium (DMEM), supplemented with 10% fetal calf serum (FCS).

Cells were co-transfected in 6-well plates (about $5x10^5$ cells/well) by standard calcium phosphate technique (Sambrook et al., 1989). When indicated, US2 or US11 plasmids (kindly provided by D. Tortorella) were co-transfected. In transfection experiments involving mouse γHC, a vector expressing a mouse κLC was co-transfected, where required. 18 h after transfection, medium was discarded and replaced by 2 ml of serum free medium supplemented with 0.1 mM biotin and further incubated for at least 8 h. When required, after 4 h incubation with biotin, the proteasome inhibitors MG132 (Sigma) or Bortezomib (Selleck Chemicals) were added at a concentration of 50 μM for 4 h, or at 10 μM for 16 h (MG132).

In experiments with CD4 and Tetherin, when indicated, the Vpu-expressing plasmid was co-transfected. pEGFP-N1 plasmid was co-transfected as a loading control. In all experiments shown with CD4 was cotransfected gp160.

Approximately 18 hours after transfection, medium was discarded and replaced with 2 ml of medium supplemented with 0.1 mM biotin and cells were further incubated for at least 7-8 hours. When indicated, with CD4, Tetherin and NS1 after 4 hours of incubation with biotin, the proteasome inhibitor MG132 (Sigma) was added in serum free medium at a concentration of 10 μM for 4 hours, or at 5 μM for 12 hours or overnight. Chloroquine (Sigma) was used at 50 μM for 4 hours. The PNGase inhibitor Z-VAD(OMe)-fmk (IMGENEX) was used for 4 hours at 100 μM.

Cell extracts, gel retardation assays and Western blotting

HEK293 transfected cells were lysed directly in the transfection plates, after collecting medium and washing with PBS to remove free biotin with 100 μl/well of SDS-lysis buffer (100 mM Tris-HCl, pH 6.8, 6% SDS) and subsequently sonicated to disrupt nuclear DNA; for analysis of the presence of disulphide bridges cells were washed with 20 mM N-ethylmaleimide (NEM) (Fluka) in PBS pH 6.8 and lysed in SDS buffer containing 20 mM NEM. For experiments with TEVp SDS-lyses buffer was supplemented with protease inhibitor mixture (Sigma). Proteins were separated by standard SDS-PAGE in reducing (25 mM Tris-HCl, pH 6.8, 1% SDS, 10% glycerol and 175 mM b-mercaptoethanol or 0.1mM dithiothreitol (DTT) or non-reducing loading buffer (25 mM Tris-HCl, pH 6.8, 1% SDS, 10% glycerol) before to be transferred to PVDF membranes.

Bi-dimensional SDS-PAGE

For 2D gel analysis, samples were first run on a non-reducing SDS-PAGE gel. The lane of interest was then cut and incubated with reducing loading buffer for 15 minutes at room temperature, before being run in a second gel under reducing condition.

Gel retardation assays

For gel retardation assays, samples denatured in SDS-gel-loading buffer (25 mM Tris-HCl, pH 6.8, 1% SDS, 10% glycerol, 175 mM β-mercaptoethanol) were boiled for 10 min, cooled to RT and incubated with 1 μg of StrAv (Sigma) for 15-30 min before separation on SDS-PAGE and transferred to PVDF membranes.

Immunoblotting and immunoprecipitation

Gels were transferred to PVDF membranes for immunodetection with anti-SV5 mAb followed by incubation with HRP-labeled anti-mouse whole IgG (Jackson) and ECL reaction. Where indicated, WB of rabbit anti-EGFP (Life Technologies) was used as loading and transfection control. WB of mouse anti-p97 was used to verify overexpression of p97 (BD Bioscience). In WB of cell fractionation experiments rabbit anti-actin (Sigma), mouse anti-calnexin (BD Bioscience) and rabbit anti-Derlin1 (Sigma) were used according to manufacturer instructions.

Quantification of bands was performed with the image processing software Image-J 1.43u (National Institutes of Health, USA) or using UVItec Alliance detection system. Purification of biotinylated material was carried out by incubating the lysates in SDS-PAGE loading buffer with StrAv-coated magnetic beads (Dynabeads, Invitrogen) and eluting by boiling for 10 min. Where indicated, eluted material was treated with Peptide-N-Glycosidase-F (PNGase-F, New England Biolabs) according to manufacturer indications.

Immunoprecipitations were carried out by incubating lysates, diluted 3 times in TNN buffer (100 mM Tris-HCl pH 8.0, 250 mM NaCl, 0.5% NP40, 20mM N-ethylmaleimide, 1% protease inhibitors cocktail (Sigma)) with anti-SV5 and Protein A-agarose (Repligen) for 2 hours at 4°C. Immunoprecipitated proteins were eluted from agarose beads by boiling in SDS buffer. For immunoprecipitation of plasma membrane fractions, intact cells were first incubated with anti-SV5 for 1 hour on ice, then washed with cold PBS, and lysed in TNN buffer. Post-nuclear supernatants, were incubated with Protein A-agarose (Repligen) for 30 minutes and, after washing, bound proteins were eluted by boiling in SDS buffer. Biotinylated material in the purified fraction was detected in Western Blot with streptavidin-HRP (Jackson). Where indicated, cellular lysates or eluted material were treated with Peptide-N-Glycosidase-F (PNGase-F) or Endoglycosidase Hf (Hf) (New England Biolabs) according to manufacturer instructions. Where indicated, WB of anti-EGFP was used as loading and transfection control.

Cytofluorimetric analysis

Cells were, 24 h after transfection, incubated either with the anti-SV5 mAb followed by fluorescein-conjugated anti-mouse IgG (KPL), or with QuantumDot$_{655}$-Streptavidin (Invitrogen) and analysed in a FACSCalibur (Becton Dickinson).

Trypsin sensitivity assay and cell fractionation

Microsome-containing lysates were obtained by resuspending cells in buffer 50 mM Tris-HCl pH 8.0, 250 mM sucrose and 10 mM N-ethyl-maleimide (for cells transfected with MHC-Iα and NHK-α1AT), or in buffer 20 mM Tris-HCl pH 7.4, 250 mM sucrose and 30 mM N-ethyl-maleimide (for cells transfected with CD4 and Tetherin), freezed and thawed once (MHC-Iα and NHK-α1AT) or lysed by 12 passages through a 23Gx1" needle (CD4 and Tetherin). After low speed centrifugation (500-5000xg for 5 min at 4°C) to discard nuclei and cell debris. Supernatants (microsome-containing lysates) for trypsin sensitivity assays were incubated with 1 μg trypsin (Sigma) for 1 h at 37°C and when indicated NP40 was added at 0.5% final concentration. While for cell fractionation, 1000xg supernatants were further centrifuged at 100.000xg for 1 hour at 4°C. Supernatants represented cytosolic material and pellets the microsomal-ER fraction. After a delicate wash in fractionation buffer, pellets were resuspended in the same buffer enriched with 1.2% SDS.

Quantification of retro-translocation by ELISA

Samples in SDS-lysis buffer were treated with 0.15 M β-mercaptoethanol and boiled for 10 min. Free β-mercaptoethanol was then quenched by diluting with an equal volume of iodoacetamide 0.15 M in buffer Tris-HCl 0.1 M, pH 8.0. Serial dilutions of these lysates in buffer TNN (50 mM Tris-HCl, pH 8.0, 250 mM NaCl, 0.5% NP-40), starting from 10 μl/well, were applied to polystyrene microplates (Nunc Maxisorp C96) coated with 0.2 μg/ml of anti-SV5 mAb in buffer $NaHCO_3$-Na_2CO_3 50 mM, pH 9.5 (100 μl/well). Proteins were bound to

the plates for 1 h at RT and then reacted with either HRP-labeled StrAv (Jackson Immunoresearch) or anti-roTag (scFv in SIPε_{S2} format [40]) followed by HRP-labeled anti-human IgE (KPL), and developed with TMB reagent (Sigma). After blocking with H_2SO_4, the O.D. at 450 nm was read on a BioRad microplate reader 550. To calculate the proportion of retro-translocated molecules, the ratio between the slopes derived from the linear region of the serial dilutions curves developed with StrAv and anti-roTag was first determined for the 100% biotinylated sample (MHC-Iα co-expressed with sec-BirA), and termed reference factor, F_{100}. The same factor was then determined for each sample (F_x). The biotinylated fraction was thus calculated as (F_x/F_{100}) x 100.

[^{35}S]-Methionine labelling

Cells were first starved for 30 minutes in Methionine/Cysteine free medium, supplemented with 10% dialyzed FCS and 0.1 mM biotin, then labeled for 10 or 15 minutes, as indicated, with 200 µCi/ml of [^{35}S]-Methionine/Cysteine (Perkin Elmer), and chased for the indicated times in biotin-containing fresh medium. Cells were lysed in 100 µl of SDS-lysis buffer, diluted with 400 µl of TNN and digested with DNaseI (Promega) for 1 hour at 37°C. SV5 tagged proteins were immunoprecipitated with anti-SV5 and Protein A-agarose (Repligen), eluted by boiling in SDS-lysis buffer and samples were resolved on a non-reducing or reducing 10% SDS-PAGE. Purification of biotinylated material was performed with StrAv-coated magnetic beads (Dynabeads, Invitrogen) and the elution obtained by boiling. Gels were fixed in 10% acetic acid, 10% methanol, incubated for 20 minutes in Amplify fluorographic enhancer (GE Healthcare), dried and exposed for autoradiography on Kodak BioMax XAR films.

Results

1. BirA localization in eukaryotic cells

Determining the localization of proteins within eukaryotic cells is often challenging, in particular when the polypeptide studied could be present in more than one cellular compartment. In investigating Endoplasmic Reticulum Associated Degradation (ERAD), a process where secretory and membrane proteins are targeted to proteasomal degradation, the essential requirement needed is to know precisely their localization discriminating between the Endoplasmic Reticulum (ER) lumen and the cytosolic compartment, where the final clearance of the dislocated polypeptides occurs (Zhong and Fang, 2012; Hampton and Sommer, 2012).

In the literature are described biochemical and physical methods to discriminate whether an ERAD substrate is on the luminal or cytosolic side of the ER membrane, evaluating the presence or absence of characteristic post-translational modifications typical of one of the two compartments (i.e. N-glycosylation or ubiquitination), performing cell fractionation by differential centrifugation or protease sensitivity assays (Zhong and Fang, 2012). However, even if all those techniques are certainly powerful methods to localize proteins, many of them require extensive sample manipulation and, as a consequence, are difficult to execute. Despite the few interesting recently developed techniques based on fluorescence reconstitution of split GFP to analyse ERAD in fluorescence experiments in intact cells (Zhong and Fang, 2012; Grotzke et al., 2013), there is still a need for user friendly and reliable methods to biochemically label in living cells, proteins retrotranslocated from the ER to the cytosol. In this thesis are described, analysed and validated two new methods to localize proteins during ERAD, both of them based on the expression of reporter enzymes in the cytosol of eukaryotic cells, which can modify a specific short target sequence added on a luminal domain of model ERAD protein substrates. The two enzymes used in living cells to label retrotranslocated proteins are the E. coli biotin ligase BirA (biotinylation) and the Tobacco Etch Virus protease NIa (TEVp) (cleavage). As many aspects of the ERAD pathway are still unclear or controversial for both membrane and soluble proteins, the two new methods were used to investigate unexplored aspects in this field.

The *E. coli* biotin ligase BirA is a 35 kDa well characterized protein. In bacteria its major function is to activate biotin to form biotinyl-5'-adenylate and transfer the biotin moiety to biotin-accepting proteins, involved in several metabolic pathways, that must contain a biotin carboxyl carrier protein (BCCP) subunit (Bekett et al., 1999). To exploit BirA enzymatic biotinylation for biotechnological purposes it was developed a small 15 amino acid long (GLNDIFEAQKIEWHE) Biotin Acceptor Peptide (BAP) (Bekett et al., 1999). This mono-biotinylation is highly specific and almost irreversible, as the only known de-biotinylating activity in cells takes place on short peptides derived from degraded proteins and in particular by the activity of biotinidases, a class of enzymes that remove biotin preferentially from biocytin (Biotinyl-L-lysine) (Wolf, 2005).

BirA is not secreted by bacterial cells, does not contain any hydrophobic leader peptide and, if transfected in eukaryotic cells, has a cytosolic localization. Indeed already from a simple experiment of co-transfection of the 12 amino acids SV5 (GKPIPNPLLGLD) C-terminal tagged version of BirA with the ER marker Derlin1-EGFP (Lilley and Ploegh, 2004), analysed by immunofluorescence, showed a diffuse cellular distribution and generally does not overlap with the ER resident protein (Fig. 20).

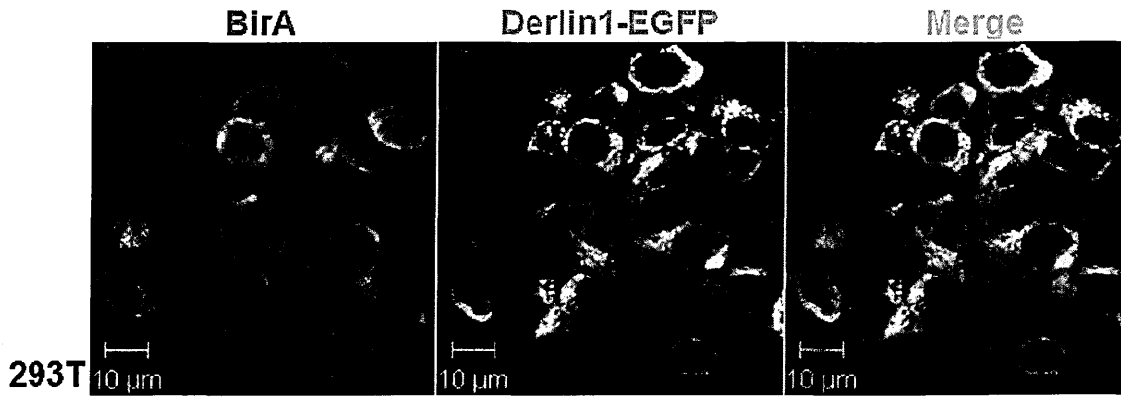

Figure 20. BirA has a diffuse pattern and generally does not overlap with the ER marker Derlin1-EGFP. 293T cells were co-transfected with plasmids expressing BirA-SV5 (red) and Derlin1-EGFP (green); BirA expression was observed by the mAb ā-SV5.

This assumption on BirA localization was also confirmed by analysis of its enzymatic activity on a few secreted and membrane proteins (Predonzani et al, 2008). While the presence of the BAP tag in a cytosolic domain of model proteins was found completely biotinylated in the presence of BirA, the localization of BAP in a luminal domain of secreted or membrane proteins results in no biotinylation. However, after expression of an engineered version of BirA, containing an N-terminal leader signal peptide (sec-BirA), such proteins can get fully biotinylated (Predonzani et al, 2008). To discriminate between the biotinylated and the non-biotinylated isoforms of the protein tagged with the BAP a technique based on a Western blotting retardation assay (Wb-ra) was developed. In this assay denatured samples are incubated with streptavidin (StrAv); this protein is resistant to SDS-PAGE conditions and forms a molecular complex with biotinylated molecules that is retarded in relation to the non-biotinylated ones that do not bind StrAv.

Evidence of compartmental restriction of BirA catalytic activity were confirmed also on MHC-Iα, a well characterized molecule, which is an ERAD model substrate in the presence of different viral immunoevasins (Hansen and Bouvier, 2009; Lilley and Ploegh, 2005). In figure 21A is shown an analysis by WB-ra of total cellular extracts from HEK293T cells co-transfected with BirA and either the N- or C-terminus BAP tagged MHC-Iα. As expected, while BAP-MHC-Iα was essentially not biotinylated, C-tagged BAP MHC-Iα (MHC-Iα-BAP) yielded complete biotinylation (Fig. 21A). Likewise, BAP-MHC-Iα was almost completely biotinylated by sec-BirA (Fig. 21B). Thus, the catalytic activity of BirA expressed in the cytoplasm of mammalian cells can be used to discriminate localization of protein domains bearing the BAP between the ER lumen and the cytosol.

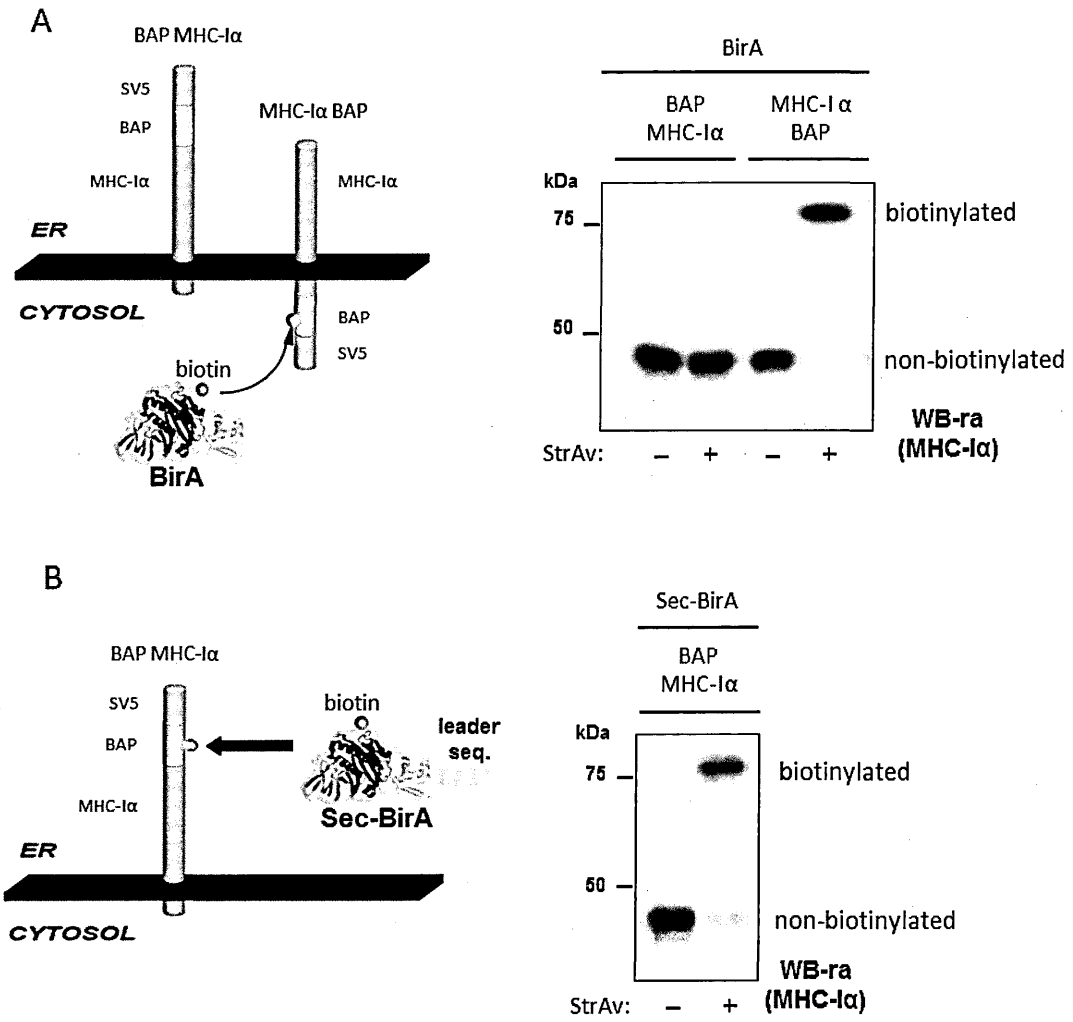

Figure 21. Compartment restricted activity of cytosolic BirA. On the left schemes of the experiments of biotinylation in living cells, for the evaluation of compartment specific BirA activity, and on the right WB-ra of cellular extracts of HEK293 cells transfected with: (A) BAP-MHC-Iα and MHC-Iα-BAP, co-expressed with cyt-BirA; (B) BAP-MHC-Iα co-expressed with sec-BirA, as indicated.

2. Retrotranslocation of MHC-Iα.

In experiments where BAP MHC-Iα was co-expressed with BirA and either of the two immunoevasins US2 or US11 to induce retro-translocation and degradation, we observed a significant increase in the amount of biotinylated BAP-MHC-Iα, as compared to co-expression with an irrelevant protein (Fig. 22A). This was clearly evident despite a reduction in the total amount of BAP-MHC-Iα, suggesting that molecules biotinylated by BirA corresponded to the retro-translocated ones. Co-expressing BAP-MHC-Iα with three different retro-translocation incompetent mutants, namely, US11-Q192L (Lilley and Ploegh 2004), US2-C133S (Lee et al., 2010) and US2-ΔC (lacking the cytosolic domain amino acids 186-199: Chevalier 2002), did not affect MHC-Iα levels and showed much lower biotinylation levels than wild type immunoevasins (Fig. 22A). This evidence represents a clear indication that, indeed, the biotinylated material represents molecules exposed to the cytosol that become substrate of BirA. This conclusion was further supported by cytofluorimetric analysis (FACS) of the mature, cell-surface exposed MHC-Iα co-expressed with cyt-BirA (and US2 or US11) or sec-BirA (Fig. 22B). Levels of MHC-Iα on the cell membrane were reduced, as expected, when co-expressed with either US2 or US11, but were not affected by co-expression of BirA or sec-BirA, as revealed by detection with anti-SV5 mAb (Fig. 22B, left panel). When the same set of transfected cells was instead analyzed with streptavidin-QuantumDot to exclusively detect biotin-labeled MHC-Iα, positive staining was observed only when co-expressed with sec-BirA and not with cyt-BirA (Fig. 22B, right panel). Thus, in cells expressing BirA all the MHC-Iα exposed on the cell surface (regardless whether expressed alone or with US2 or US11) was not biotinylated, further demonstrating the intracellular localization of the biotinylated molecules. Furthermore, when a negative control secretory BAP-bearing protein (scFv-BAP, Predonzani et al., 2008 BMC), which does not interact with US2 or US11 was co-expressed with BAP-MHC-Iα, BirA and US2 or US11 the secreted material was found not biotinylated, although somehow reduced with US11 (Fig. 22C), thus confirming the specificity of biotinylation in the cytosolic compartment. Similarly, a truncated version of human membrane IgE (t-BAP-mIgE), irrelevant to US2 or US11, that is otherwise fully biotinylated by sec-BirA Predonzani et al., 2008, was also

essentially not biotinylated by BirA (Fig. 22D). The small amount of biotinylated molecules found with US2 was likely due to the immunoevasin induced cellular stress.

These results demonstrated that molecules within the ER lumen, either membrane bound or secretory, are protected from the biotinylating activity of cytosolic BirA. A small fraction of biotinylated BAP-MHC-Iα, when expressed either alone or with an irrelevant protein was frequently detected, most likely representing the fraction of misfolded molecules that have spontaneously entered the ERAD pathway. This was not due to post-lysis biotinylation since cellular extracts were prepared by directly resuspending cells in SDS-containing lysis buffer to immediately denature proteins and block BirA's activity. In addition when cells expressing BirA, BAP-MHC-Iα and US11 were co-transfected with Derlin1-EGFP, we observed a decreased level of biotinylation and an increased abundance of MHC-Iα, in agreement with the reported dominant negative activity of this form of Derlin1 on the US11 induced MHC-Iα dislocation (Lilley and Ploegh, 2004). Thus, from these experiments, where MHC-Iα was co-transfected with functional and non-functional immunoevasins or with the repressor of the US11 induced MHC-Iα ERAD (Delin1-EGFP) we obtained levels of biotinylation consistent with the expected retrotranslocation.

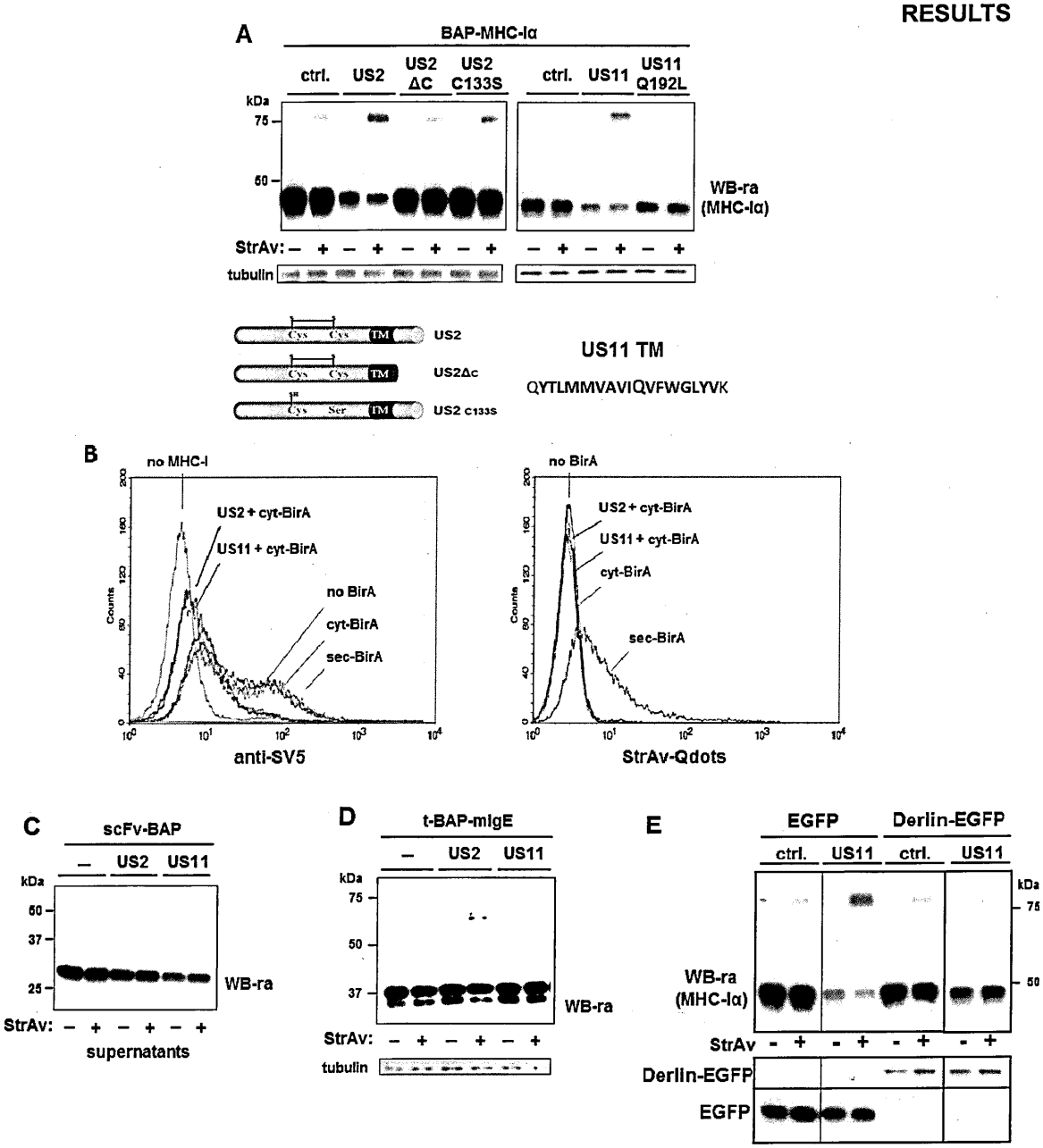

Figure 22. Retro-translocation of MHC-Iα. (A) WB-ra of cellular extracts of HEK293 cells transfected with BAP-MHC-Iα, BirA and US2 or the US2 mutants US2-ΔC and US2-C133S (left panel), or US11 or US11 mutant US11-Q192L (right panel), as indicated. Lower panel show a scheme of the immunoevasin mutants. (B) Cytofluorimetry of HEK293 cells co-transfected with BAP-MHC-Iα and either cyt-BirA (alone or with US2 and US11), or sec-BirA, and stained with anti-SV5 mAb (left panel) or Streptavidin-QuantumDot (right panel). (C) WB-ra of supernatants of HEK293 cells co-transfected with a secretory BAP-tagged scFv control protein and cyt-BirA, BAP-MHC-Iα and US2 or US11. (D) WB-ra of cellular extracts of HEK293 cells co-transfected with t-BAP-mIgE, cyt-BirA and US2 or US11, as indicated. (E) WB-ra of cellular extracts of HEK293 cells transfected with BAP-MHC-Iα, BirA with or without US11 in the presence of either EGFP or Derlin1EGFP, as indicated. All blots were developed with anti-SV5 mAb, and anti-tubulin or anti-GFP where indicated.

Similar experiments to evaluate MHC-Iα induced retrotranslocation by biotinylation in living cells were also performed in additional cell lines. In HeLa cells, as shown in figure 23A and B, we observed an induced ERAD of MHC-Iα comparable to HEK293T cells, where US2 appear to be more efficient than US11. Whereas in the non-human cell line CHO, US11 was much more effective to promote MHC-Iα degradation and in this cell extract the residual amount of MHC-Iα is fully biotinylated, thus already exposed to the cytosolic environment (23C). As US2 and US11 proteins are derived from human CMV their activity in non-human cell lines could be different as we observed.

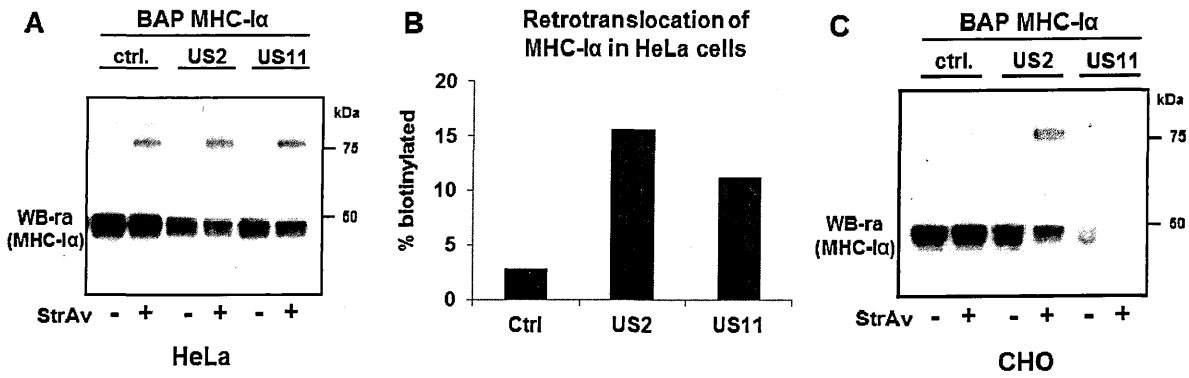

Figure 23. Retro-translocation of MHC-Iα in HeLa and CHO cells. (A) WB-ra of cellular extracts of HeLa cells transfected with BAP-MHC-Iα, BirA and US2 or US11. (B) Quantification of the experiment shown in A. (C) WB-ra of cellular extracts of CHO cells transfected with BAP-MHC-Iα, BirA and US2 or US11.

Results similar to the ones shown above with WB-ra were also obtained by performing [^{35}S]-Methionine pulse-chase labelling experiments, followed by analysis of immunoprecipitated MHC-Iα in a gel retardation assay. While total cell lysates display accumulated protein material, pulse-chase labelling approaches allow to detect proteins immediately after synthesis and to follow their fate during time. As shown in Fig. 24, while in cells expressing US2 30% of the [^{35}S]-Methionine-labeled MHC-Iα was biotinylated after the 30 min pulse labelling period, the proportion of biotinylated molecules increased to around 55% after the 2 h chase, despite a decrease in total MHC-Iα. These results are consistent with the progressive retrotranslocation and degradation of MHC-Iα in the presence of US2.

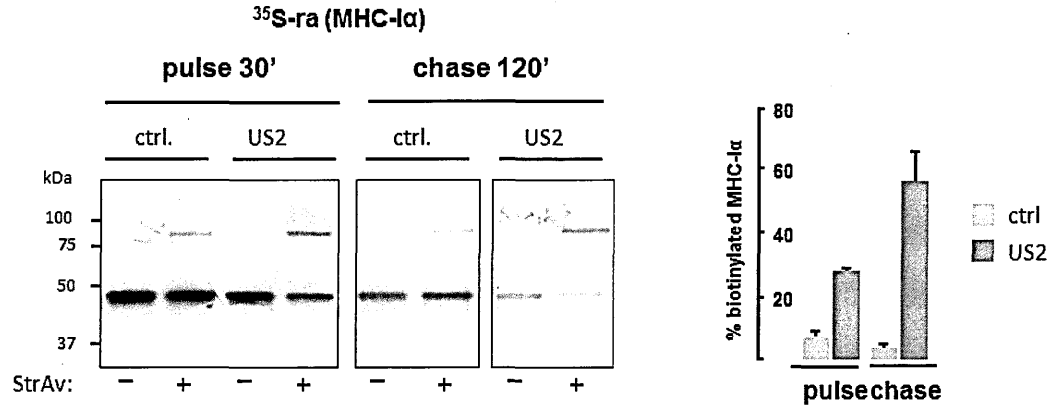

Figure 24. Pulse-chase labelling of retro-translocated MHC-Iα. Left panel, [^{35}S]-Methionine/Cysteine PAGE retardation assay of anti-SV5 immunoprecipitated cellular extracts of HEK293T cells co-transfected with BAP-MHC-Iα and BirA and, where indicated, with US2. Right panel, quantification of the BAP-MHC-Iα biotinylated band, expressed as percentage of the total immunoprecipitated BAP-MHC-Iα (biotinylated + non-biotinylated). Histograms show the results of three independent experiments; error bars indicate one standard deviation.

2.1 Proteasome inhibition increases biotinylation of MHC-Iα

According to our results the biotinylated MHC-Iα corresponds to the fraction dislocated to the cytosol and not yet degraded by the proteasome. To further support this interpretation we tested the effect of proteasome inhibitors MG132 (50μM for 4h) and Bortezomib (50μM for 4h). As shown in figure 25 upon proteasome inhibition an increased amount of around 5-6 folds of biotinylated molecules was detected, both in the absence and presence of US2 and US11 (Fig. 25A). In addition, although the total amount of BAP-MHC-Iα was reduced when either US2 or US11 were present, the proportion of biotinylated molecules accumulated upon proteasome inhibition was much increased. Quantification of the relative intensities between retarded (biotinylated) and non-retarded bands of Fig. 25A (displayed in Fig. 25B) showed in fact that, while less than 1% of BAP-MHC-Iα expressed alone was found biotinylated in non-treated cells, upon proteasome inhibition this proportion increased to 3-4% with MG132 or Bortezomib; when co-expressed with US2 or US11 the proportion of biotinylation raised from 13% (US2) - 27% (US11) up to 43-52% following proteasome inhibition (Fig. 25B).

In the presence or absence of proteasomal inhibitor the BirA levels in the total

cell extracts were found minimally changed (Fig. 25C), thus indicating that the increased amount of biotinylation is not due to a relevant increase in the abundance of the enzyme. The effect of proteasomal inhibition appeared slightly stronger in rescuing total amount of MHC-Iα probably due to the higher proportion of retrotranslocating molecules in the presence of US11.

For MHC-Iα, it has been shown that, after dislocation in U373 cells, de-glycosylation by the cytosolically localized cellular PNGase takes place just before engagement by the proteasome, although de-glycosylation appears not to be essential for retro-translocation (Bloom et al., 2004). In HEK293T cells de-glycosylated MHC-Iα was less apparent, particularly with US11. In the presence of proteasome inhibitors (Fig. 25A), a band corresponding to de-glycosylated material was more evident and found to be, as expected, completely biotinylated. This de-glycosylated from of MHC-Iα could not be a non-glycosylated isoform due to an inefficient ER insertion of the molecule, as de-glycosylated MHC-Iα was not present when it was expressed in the absence of the immunoevasins, but cells were treated with proteasome inhibitors, and to our knowledge was never reported a misinsertion in the ER lumen of MHC-Iα or other molecules caused by these CMV immunoevasins.

However, within the glycosylated fraction, a consistent amount was also biotinylated. Indeed, figure. 25D shows the composition of biotinylated MHC-Iα, after affinity-purification with StrAv-coated beads from extracts of cells co-expressing US2, incubated with or without MG132. In MG132-treated samples the presence of de-glycosylated material, in addition to a relevant amount of glycosylated one, was clearly observed (right panel), while in the absence of MG132 MHC-Iα was mostly glycosylated. *In vitro* PNGaseF treatment in both cases was used to confirm the state of glycosylation of the purified material. Similar results were obtained for US11. This demonstrates that a significant number of molecules already retro-translocated to the cytosol and not yet de-glycosylated (also evident in figure 22) have already become biotinylated. These results also indicate that in these cells retro-translocation occurs more rapidly than de-glycosylation, consistently with a regulated post dislocation activity of cytosolic PNGase in late ERAD steps.

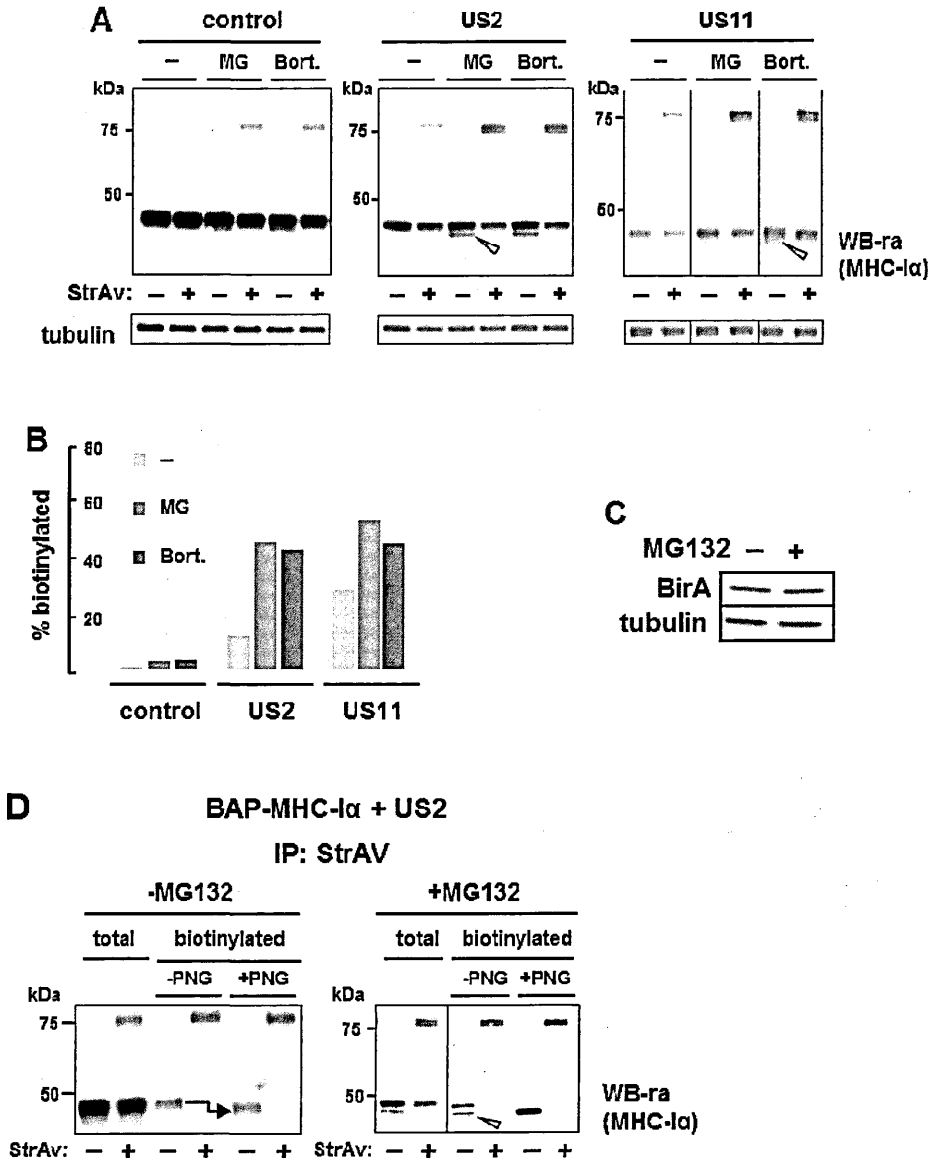

Figure 25. Proteasome inhibition effect on biotinylation of MHC-Iα. (A) WB-ra of cellular extracts of HEK293T cells co-transfected with BAP-MHC-Iα and BirA (control) and, where indicated, with US2 or US11 in the absence (-) or presence of MG132 (MG; 50μM for 4h) or Bortezomib (Bort.; 50μM for 4h). (B) Quantification of the relative levels of biotinylated MHC-Iα shown in (A) calculated as the ratio between biotinylated vs. non-biotinylated form in a given lane. (C) Analysis by WB of cells transfected with BirA-SV5 and treated or not with MG132. (D) WB-ra of PNGaseF (PNG) treated, affinity-purified biotinylated BAP-MHC-Iα, derived from MG132-treated and untreated cells co-expressing US2. All blots were developed with anti-SV5 mAb and where indicated with anti-tubulin. Open arrowheads indicate de-glycosylated BAP-MHC-Iα.

2.2 Determination of MHC-Iα retrotranslocation by ELISA

Biotinylation also allows detection and quantification by ELISA of the level of retro-translocation as well as the proportion of dislocated molecules, making therefore possible to determine the level of retro-translocation with a technique more suitable for large screenings and in general more quantitative than a WB-ra. The assay was set up by coating plates with anti-SV5 to capture all MHC-Iα molecules regardless of their state of biotinylation, and then revealed: i) with HRP-conjugated StrAv to determine the level of biotinylation, or ii) with HRP-conjugated StrAv (for the biotinylated fraction) and in parallel, with a second antibody (for the total amount of protein) to determine the proportion of retro-translocated molecules (Fig. 26A). In our case we used a BAP-MHC-Iα construct that contained, in addition to the SV5 at the N-terminus, a second tag (roTag) at the C-terminus (BAP-MHC-Iα-roTag). To normalize the assay, we used an extract of cells co-transfected with the same BAP-MHC-Iα-roTag construct and sec-BirA (SEC), since in that case all molecules are biotinylated (Fig.26D). A rough estimation of retro-translocation was therefore determined as the fraction of biotinylated molecules (revealed with StrAv) relative to the total amount of MHC-Iα in the sample (revealed with anti-roTag). Figure 26B shows the levels of biotinylation of MHC-Iα expressed with US2 or US11 in the absence and presence of MG132, while figure 26C shows a plot of the percentage of dislocated MHC-Iα in cells co-expressing US2 or US11. The values in figure 26C are quite consistent with those obtained, for the same samples, with the WB-ra (% biotinylated MHC-Iα: 1% (-), 30% US2, 26% US11) (Fig. 26D).

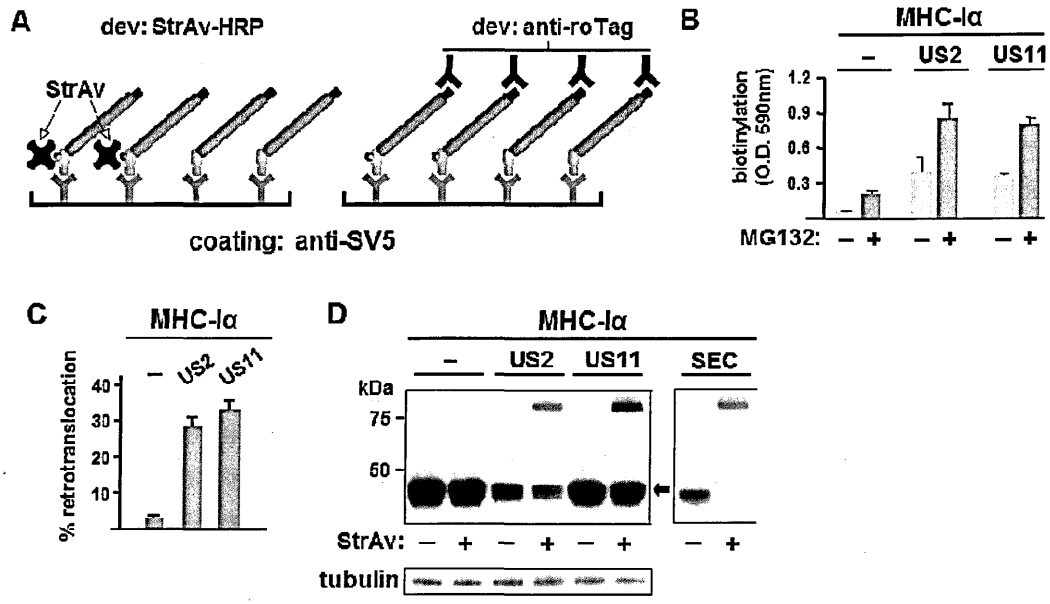

Figure 26. Determination of retro-translocation by ELISA. (A) Scheme of the ELISA used to monitor biotinylation of the retro-translocated fraction. Anti-SV5 mAb coating ensures capture of both, biotinylated and not-biotinylated BAP-MHC-Iα, which are then revealed with HRP-conjugated StrAv (only biotinylated MHC-Iα) and with anti-roTag (total MHC-Iα). (B) Retro-translocation levels (developed with HRP-conjugated StrAv) of BAP-MHC-Iα in HEK293 cells transfected alone or with US2 or US11, in the presence or absence of MG132 (50μM for 4h), as indicated. (C) Proportion of retro-translocated BAP-MHC-Iα (developed in parallel with HRP-conjugated StrAv and anti-roTag) in HEK293 cells transfected alone or with US2 or US11, expressed as the fraction of biotinylated BAP-MHC-Iα relative to the total amount of BAP-MHC-Iα. Histograms show the results of three independent experiments; error bars indicate one standard deviation. (D) WB-ra of samples used in (C), developed with anti-SV5 mAb or anti-tubulin. SEC indicates cotransfection with sec-BirA. The arrow indicates the position of the non-biotinylated MHC-Iα.

2.3 Trypsin sensitivity of biotinylated MHC-Iα

To further demonstrate the specificity of biotinylation occurring only on molecules that have been exposed to the cytosolic side, trypsin-sensitivity experiments were performed on microsomes-containing cell lysates. Cells co-expressing MHC-Iα, BirA and US2 or US11 were gently lysed in an appropriate buffer to preserve the ER structure and then treated with trypsin. As shown in figure 27, the non-biotinylated material obtained with both US2 (Fig. 27A) or US11 (Fig. 27B) was trypsin-resistant (except for the removal of the cytosolic C-

terminal tail, that results in a faster migrating band), as expected for molecules protected because of their localisation in the luminal side of the ER. The biotinylated material, however, was degraded by trypsin, thus demonstrating that the biotinylated MHC-Iα molecules are exposed to the cytosolic side.

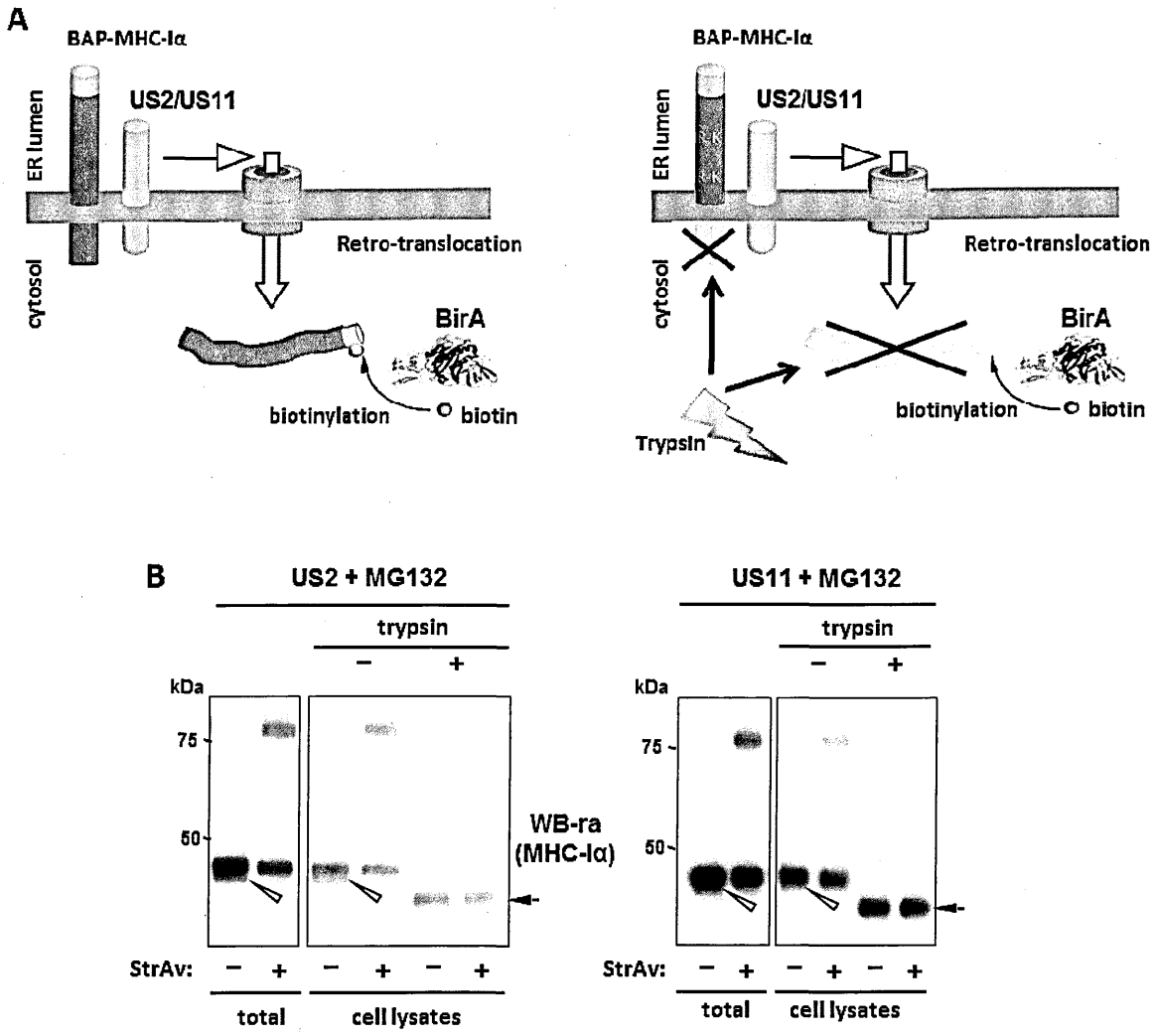

Figure 27. Trypsin sensitivity of biotinylated MHC-Iα. (A) Scheme of BAP-MHC-Iα dislocation, in the presence of BirA and US2 or US11, before and after a trypsin sensitivity assay. (B) WB-ra of microsomes-containing cell lysates (microsomes) derived from cells expressing BAP-MHC-Iα, BirA and US2 or US11 and treated or not with trypsin, as indicated. As a control, an aliquot of cells was directly lysed in SDS sample buffer (total). Before lyses cells were treated with 10μM MG132 for 16h. Open arrowheads indicate de-glycosylated molecules, while arrows indicate MHC-Iα with the cytosolic C-terminal tail digested by trypsin. All blots were developed with anti-SV5 mAb.

2.4 Cell fractionation of biotinylated MHC-Iα.

According to trypsin sensitivity assays the biotinylated fraction of MHC-Iα represents the retrotranslocated cytosolically exposed population. To know whether those isoforms are still associated with the ER membranes or fully solubilized and dislocated in the cytosolic milieu, cell fractionation experiments were performed. For such experiments cells co-expressing MHC-Iα, BirA and US2 or US11, treated with the proteasome inhibitor were gently lysed in an appropriate buffer to preserve the ER structure (as for the trypsin sensitivity assays) and ultracentrifuged to separate the microsomal-ER (pellet) from the cytosolic (supernatant) fraction (Gewurzet al., 2002). As shown in figure 28A, while the non-biotinylated material was present only in the microsomal fraction (as expected), the biotinylated one was localized both in the pellet and in the supernatant. In the soluble fraction, however, only a part of the deglycosylated and fully biotinylated MHC-Iα fraction could be detected, whereas the vast majority of biotinylated material appear to be still associated to the microsomal/ER fraction. This was true for all the glycosylated-biotinylated forms of MHC-Iα but also for part of the already deglycosylated-biotinylated molecules. The finding that part of the completely deglycosylated molecules were present both in the cytosol and still associated to the microsomal fraction has been previously reported by some authors for MHC-Iα (Wiertz et al., 1996b, Kikkert et al., 2001) and for other type-I membrane proteins such as TCRα chain and US11 (Tortorella et al., 1998; Baker and Tortorella, 2007); in this view it is not surprising that the glycosylated-biotinylated precursor was found totally associated to the ER pellet and not extracted to the cytosolic fraction.

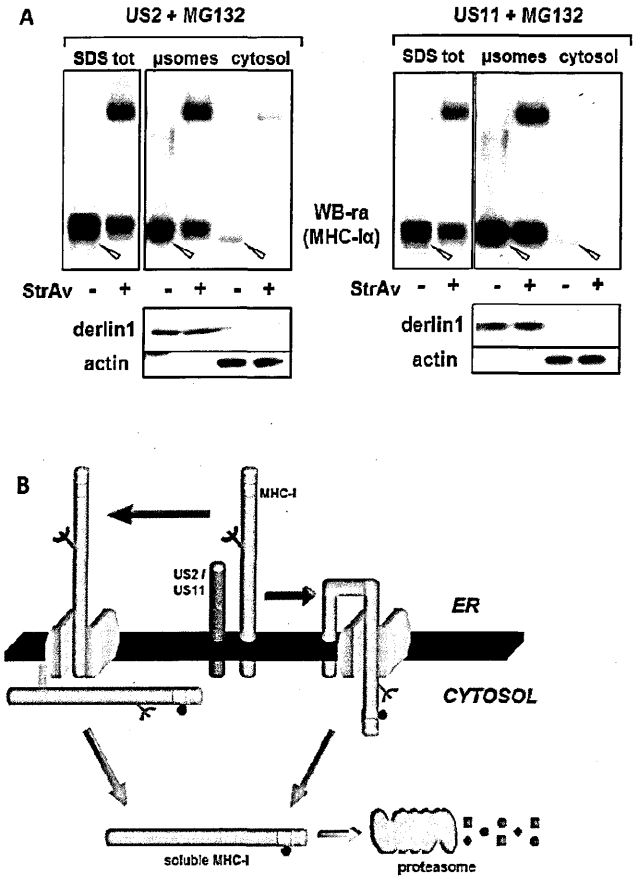

Figure 28. Cell fractionation of MHC-Iα. (A) WB-ra of SDS total cell extracts and µsomes (pellets) and cytosol (supernatants) obtained from mechanical cell lysates derived from 100.000xg fractions of cells expressing BAP-MHC-Iα, BirA and US2 or US11 and treated with 10µM MG132 for 16h, as indicated. All blots were developed with anti-SV5 mAb and where indicated, as a control of effective fractionation, with anti-derlin1 (ER-microsomal marker) or anti-actin (soluble-cytosolic marker) Open arrowheads indicate de-glycosylated molecules. (B) Possible representations of BAP-MHC-Iα dislocation, in the presence of BirA and US2 or US11, according to cell fractionation data. MHC-Iα is represented in light blue, BAP and SV5 sequences are symbolized respectively in red and green; biotin is indicated in violet.

To investigate the features of retrotranslocated-biotinylated MHC-Iα interactions with ER membranes present in the microsomal fraction we performed cell fractionation in a buffer enriched with 4.5 M urea. The use of denaturing buffers has an advantage to the use of 0.1 M Na_2CO_3, since protein-protein interactions which can resist to Na_2CO_3 treatment are destroyed in 4.5 M urea (Gewurz et al., 2002; Soriano et al., 1997). Several authors reported that incubation of cell-derived microsomes with urea causes the release of non-integral peripheral proteins from the membrane bilayer, while polypeptides imbedded within the bilayer are insensitive to such denaturant hypertonic conditions (Chen et al.,

1998; Gewurz et al., 2002; Baker and Tortorella, 2007). This was actually the case for the biotinylated MHC-Iα. Indeed, while even soluble ER proteins were fully extracted by the urea buffer (Fig. 29B), biotinylated MHC-Iα from the microsomal fraction was almost unaffected by this treatment (Fig. 29A), indicating that this retrotranslocated isoforms are still strongly embedded in the ER membrane or only partially dislocated, conceivably as indicated in figure 28B. Similar models for type-I membrane protein dislocation intermediates were already reported in the literature (i.e. Baker and Tortorella, 2007). However, it cannot be completely excluded that these forms of biotinylated MHC-Iα are pelleted in the microsomal fraction because are part or a heavy cytosolic complex resistant to urea and not due to association with membranes.

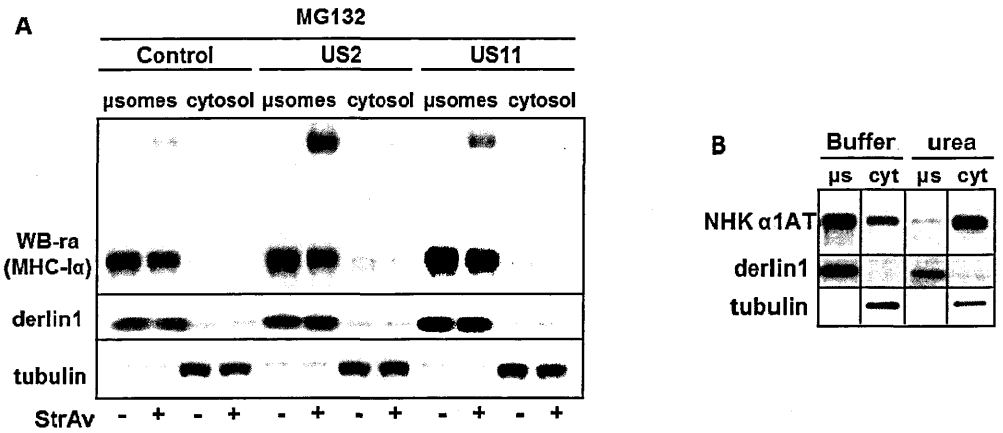

Figure 29. Cell fractionation of MHC-Iα in urea buffer. (A) WB-ra of SDS total cell extracts and µsomes (pellets) and cytosol (supernatants) obtained from mechanical cell lysates, in buffer containing 4.5M urea, derived from 100.000xg fractions of cells expressing BAP-MHC-Iα, BirA and US2 or US11 and treated with 10µM MG132 for 16h, as indicated. (B) WB of cells transfected with NHK-α1AT treated with MG132, lysed in control buffer or in urea buffer, as in (A), and fractionated by high speed centrifugation. All blots were developed with anti-SV5 mAb and where indicated, as a control of effective fractionation, with anti-derlin1 (ER-microsomal marker) or anti-tubulin (soluble-cytosolic marker).

2.5 The extracellular domain of biotinylated-glycosylated MHC-Iα is fully exposed to the cytosol.

In light of these results with fractionations and of the partially dislocated models proposed in the literature (i.e. Baker and Tortorella, 2007; Ye et al., 2005), we were interested in evaluating if only the N-terminus or all the MHC-I extracellular

portion is exposed to the cytosolic environment in the retrotranslocation intermediates detectable through our biotinylation assay. Thus we next used three version of MHC-Iα tagged with SV5 at the extreme C-terminus and with the BAP sequence located in different positions: i) immediately after the leader peptide (BAP-α1α2α3 MHC-Iα); ii) between domains α2 and α3 (α1α2-BAP-α3 MHC-Iα); iii) downstream of domain α3 and upstream of the α3-TM connecting peptide (α1α2α3-BAP-MHC-Iα) (Fig. 30A upper panel). In the second and third case the BAP sequence was inserted after the N-glycosylation site located in domain α1 (N110) and in the latter it was positioned just 13 amino acids upstream from the transmembrane domain. Such distance of around 30-40 Å in an extended coil conformation, should be enough to guarantee docking of BirA (i.e. other enzymes like oligosaccharyltransferase complex can recognize and glycosylate Asn located at least 12 amino acid from the transmembrane domain (Bause and Hettkamp, 1979) and biotinylation. The availability for biotinylation of all the new BAP-tagged molecules was verified in a control experiment expressing them together with sec-BirA (Fig. 30A).

After this preliminary test, the three different BAP-tagged MHC-Iα were co-expressed together with BirA, in the absence or presence of US2 or US11. As shown in figure 30A (lower panels) all these versions of MHC-Iα were degraded by the CMV immunoevasins (an higher decrease of α1α2α3-BAP-MHC-Iα was obtained with US2, as if the BAP tag in the middle of the molecule could favour US2 induced degradation) and all of them were likewise biotinylated by BirA. Taken together these results indicate a complete exposure of the MHC-Iα ectodomain to the cytosolic environment in the glycosylated ERAD intermediate. A possible interpretation of the glycosylated-biotinylated intermediates recovered in the absence of proteasomal inhibition is represented in figure 30B: partially dislocated MHC-Iα could have its ectodomain fully exposed to the cytosol but still somehow tethered to the ER membrane through the transmembrane domain in an "embedded conformation". The alternative possibility that in a fully stretched conformation the 13 amino acids between BAP and the transmembrane domain are sufficient to cross the ER membrane through a dislocation channel, leaving the MHC-Iα transmembrane correctly placed in a "bent conformation", is quite unlikely considering the 35–50 Å thickness of the membrane lipid bilayer (Khramtsov et al., 2008). In any case

our data do not exclude the possibility that MHC-Iα is retrotranslocated by means of small lipid droplets vesicles, a model already proposed few years ago where membrane proteins were suggested to be exposed to the cytosol maintaining their transmembrane domain into a single layer membrane, resembling classical lipid droplets (Ploegh, 2007).

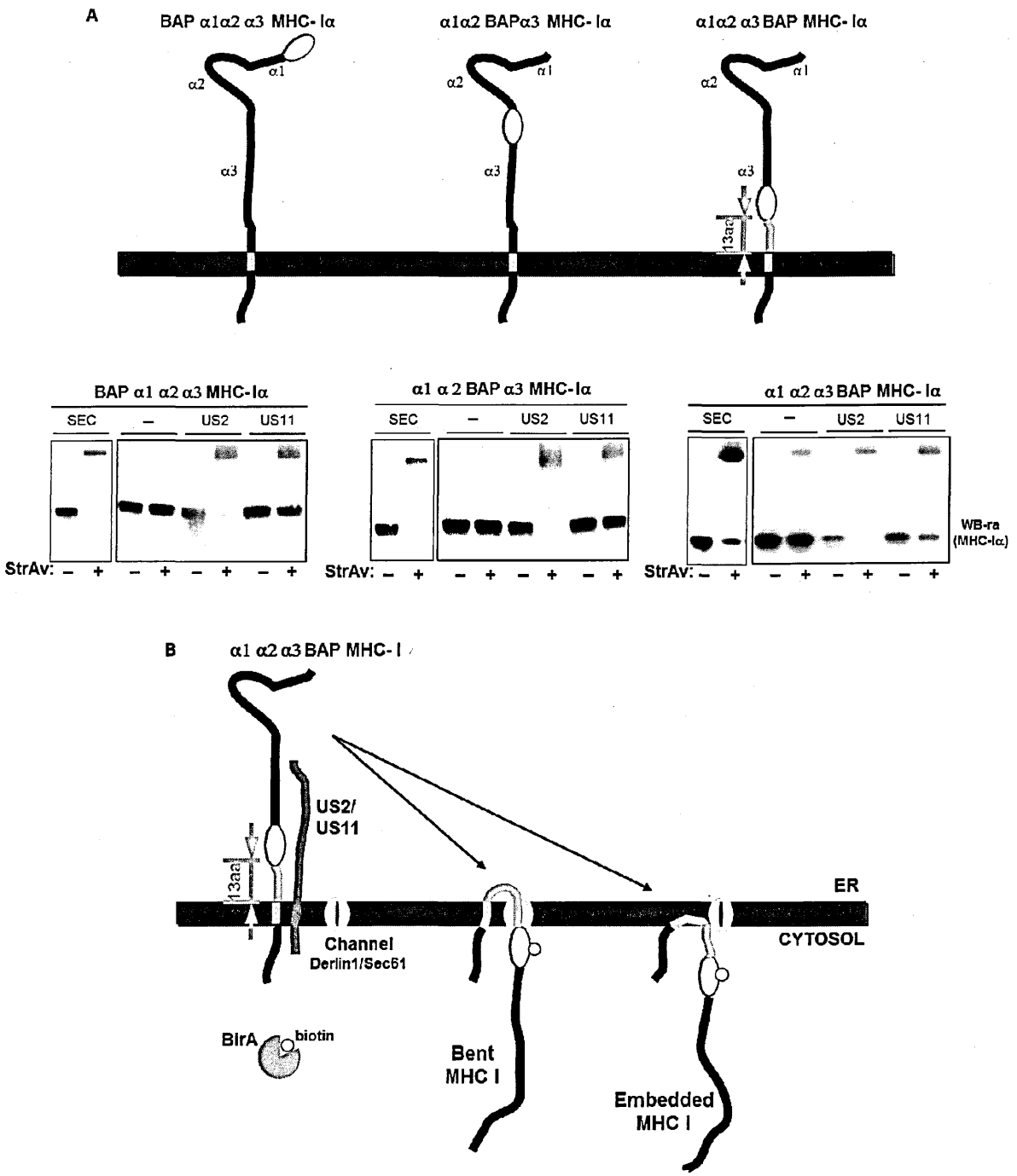

Figure 30. Biotinylated-glycosylated MHC-Iα ectodomain is fully dislocated to the cytosol. (A) Upper panel: organization of the three differently tagged MHC-Iα molecules. Lower

panel: WB-ra of extracts from cell expressing BirA together with the indicated BAP tagged form of MHC-Iα, co-transfected or not with US2 or US11. SEC indicates expression of sec-BirA. All blots were developed with anti-SV5 mAb (B) Schematic representation of MHC-Iα dislocation intermediates, according to results obtained with of α1α2α3-BAP-MHC-Iα through a channel dislocation model.

3. Retrotranslocation of secretory proteins

We next performed experiments with two different secretory model proteins, NHK-α1AT and Ig HC, which led to essentially equivalent conclusions to those with MHC-Iα. In figure 31A the secretion-incompetent mutant NHK-α1AT-BAP, tagged with SV5 and BAP at the C-terminus, was compared to the wild type protein. Compromised secretion of NHK-α1AT resulted in intracellular accumulation with a clear fraction of biotinylated molecules. In contrast, only a small fraction of intracellular α1AT-BAP was biotinylated, while the secreted material was, as expected, totally non-biotinylated. A smaller band of α1AT was also observed, and resulted to be biotinylated, likely representing a cytosolic fragment. In the presence of the proteasome inhibitor MG132 a band corresponding to de-glycosylated NHK-α1AT (confirmed by PNGaseF treatment, Fig. 31B) was detected, that was obviously fully biotinylated. However, as in the case of MHC-Iα, a fraction of glycosylated NHK-α1AT was also biotinylated. In addition, a smaller de-glycosylated band (because insensitive to PNGaseF) of NHK-α1AT mutant, which most likely corresponds to the same N-terminal deletion of α1AT shown in figure 31A, was fully biotinylated, consistent with cytosolic localization.

Also for NHK-α1AT the biotinylated fraction corresponded to cytosolically exposed molecules, as shown in figure 31C. When microsomes-containing lysates prepared from cells co-expressing NHK-α1AT and BirA were treated with trypsin, the non-biotinylated material was trypsin-resistant, as it corresponds to ER protected molecules, while the whole fraction of biotinylated molecules was trypsin-sensitive.

In contrast, when microsomal membranes were solubilized by detergent treatment (NP40), both biotinylated and non-biotinylated molecules became trypsin-sensitive. The biotinylated proteolytic fragments (containing SV5-BAP) generated by trypsin bound to StrAv and migrated as a smear roughly in the same position of NHK-α1AT (Fig. 31C left panel, lanes 4, 6). As shown in figure 31C right panel, following ultracentrifugation of microsomes-containing cell lysates only biotinylated NHK-α1AT localized to the cytosolic fraction, while in the microsomal pellet fraction (microsomes) both biotinylated and non-biotinylated molecules were found. Thus, together with the trypsin sensitivity

assay we concluded that the soluble NHK-α1AT ERAD model in part remains associated to the cytosolic face of ER membrane during ER to cytosol dislocation.

It has been demonstrated that for NHK disposal mannose trimming by ER mannosidases plays an important role (Hosokawa et al., 2001 and 2003). Indeed, when the mannosidase-I inhibitor Kifunensine was used in combination with the proteasomal inhibitor MG132 a reduced retrotranslocation was observed as compared to MG132 treatment alone (Fig. 31D). This was true considering both the biotinylation levels and the amount of deglycosylated material. This result further confirms the importance of mannose trimming for NHK exposure to the cytosolic environment and its degradation.

Expression of the second secretory model protein, Ig γHC-BAP (tagged similarly to NHK-α1AT at the C-terminus), in the absence of LC resulted in no secretion and in the appearance of a significant amount of intracellular biotinylated molecules. In contrast, co-expression with LC promoted, as expected, active secretion of non-biotinylated HC and a much reduced level of the intracellular biotinylated fraction, confirming that the presence of LC rescues HC from ERAD, reducing the extent of retro-translocation (Fig. 31E).

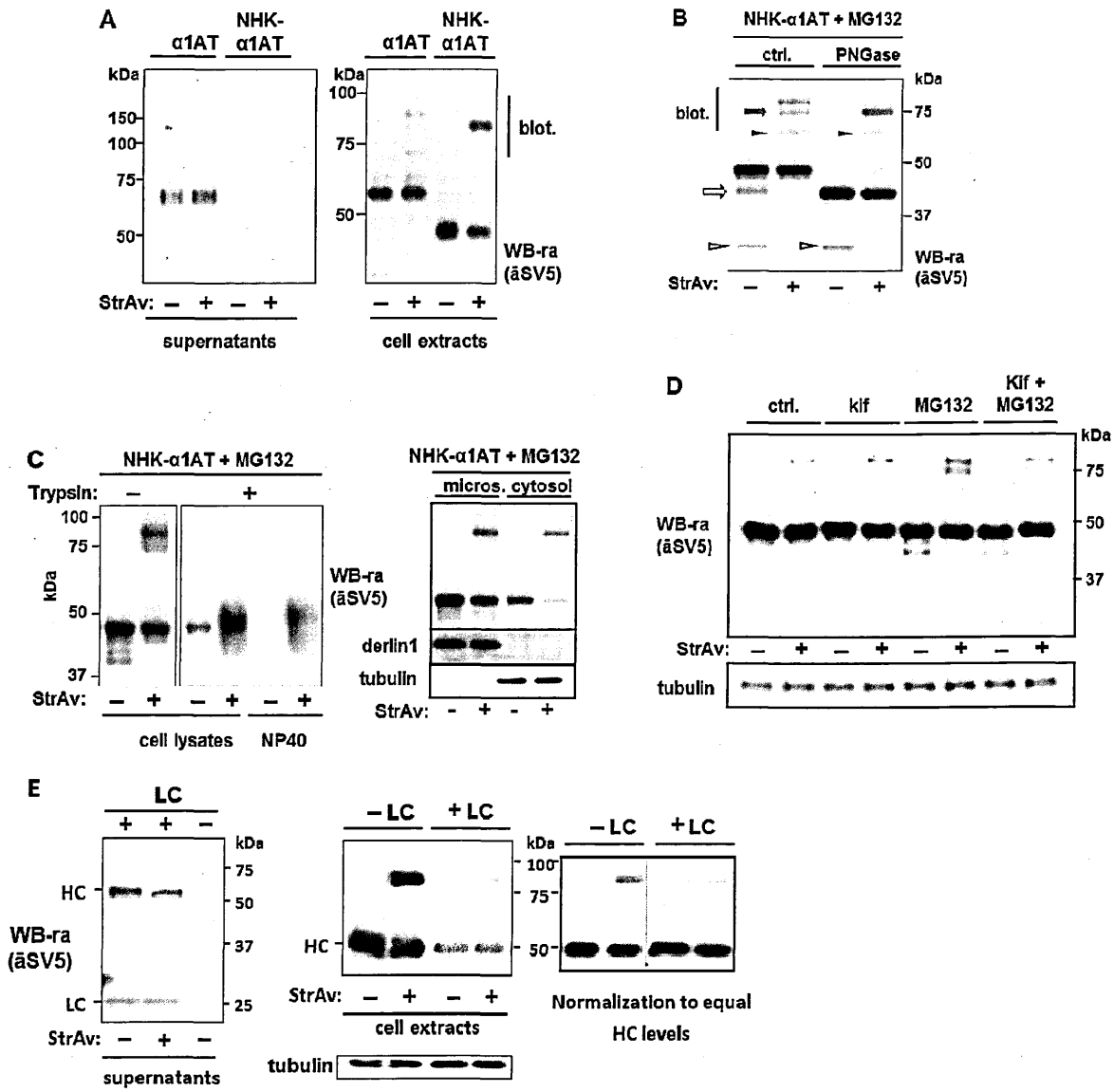

Figure 31. Retro-translocation of secretory proteins. (A) WB-ra of supernatants and/or cellular extracts of HEK293 cells co-transfected with α1AT-BAP or the mutant NHK-α1AT-BAP and cyt-BirA; (B), NHK-α1AT-BAP and cyt-BirA in the presence of MG132 (10μM for 16hours) and digested or not (mock) with PNGaseF. Open arrow and arrowheads indicate deglycosylated full-length NHK-α1AT-BAP and NHK-α1AT-BAP fragment, respectively, while filled arrow and arrowheads indicate the corresponding biotinylated bands. (C) WB-ra of microsomes-containing cell lysates derived from cells expressing NHK-α1AT-BAP and BirA and treated with MG132 (10μM for 16h) and, where indicated (left panel), digested with trypsin. NP40 indicates the same microsomes-containing lysates treated with detergent to solubilise ER membranes, thus making also luminal proteins accessible to trypsin. In the right panel is shown a high speed fractionation into microsomes (pellet) and cytosol (supernatant) of mechanical cells extract used for trypsin experiments. (D) Cell extracts from cells transfected with NHK-α1AT-BAP and BirA, treated as indicated with Kifunensine 100μM or MG132 10μM for 4 hours, and analyzed by WB-ra. (E) WB-ra of supernatants and cellular extracts from cells expressing HC-BAP (HC) and cyt-BirA with (+) or without (-) LC. All blots were developed with anti-SV5 or anti-tubulin; the LC in (D), left panel, was visualized because of the secondary anti-mouse IgG antibody used.

4. Retrotranslocation of calreticulin

Finally, we determined the level of biotinylation associated to the spontaneous retro-translocation of calreticulin (Crt) and compared to the dislocation-incompetent mutant (Crt-ΔC), which lacks the 115 residues long C-terminal portion. As shown in two different representative experiments in figure 32A, up to 30% of Crt was biotinylated, in agreement with active dislocation activity and with the relative abundance of dislocated Crt reported (Afshar et al., 2005). In contrast, less than 5% dislocation was observed for Crt-ΔC. As expected, however, both of them were almost fully biotinylated by sec-BirA (Fig. 32B. In addition, a number of smaller fragments (representing deletions from the C-terminus since the tag was at the N-terminus) was sometimes detected (Fig 32A, experiment 1) for Crt, but not for the Crt-ΔC mutant. These fragments appeared not to be generated by cytosolic proteases, since they were not biotinylated when co-expressed with cyt-BirA (the proximity of SV5 and BAP tags exclude that all this fragments had lost the BAP).

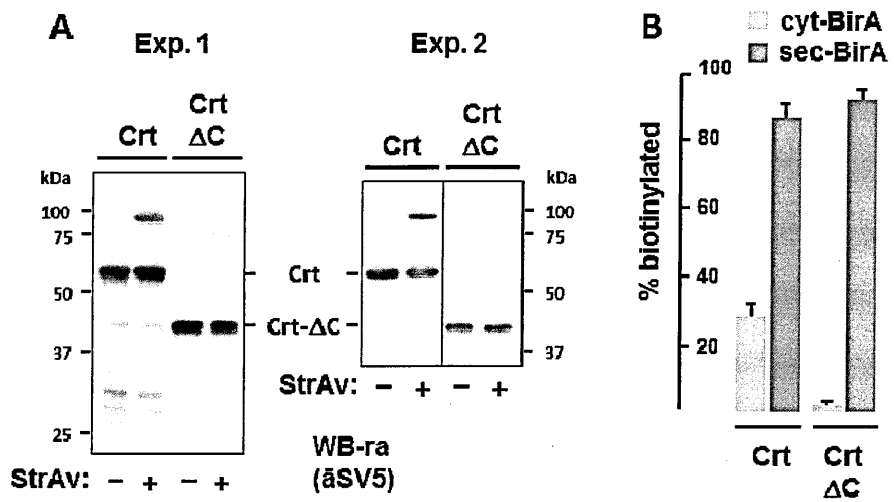

Figure 32. Retro-translocation of calreticulin. (A) WB-ra of cellular extracts (developed with anti-SV5 mAb) of HEK293 cells co-transfected with Crt or the mutant Crt-ΔC and cyt-BirA. Two representative different experiments are shown. (B) Quantification of the relative levels of biotinylation of Crt and Crt-ΔC (obtained from the WB-ra) when co-expressed with cyt-BirA or sec-BirA. Histograms show the results of three independent experiments; error bars indicate one standard deviation.

Taken together the data obtained with these different models demonstrated that BirA biotinylation of proteins within the secretory pathway (properly BAP-tagged on the ER luminal side) is highly specific for molecules that have been retro-translocated from the ER to the cytosol, thus representing a fast and reliable way to determine the extent of ER-to-cytosol retro-translocation.

5. Analysis of protein folding during dislocation

The availability of a sensitive method to clearly localize proteins during retro-translocation offers the opportunity to investigate some controversial aspect of this pathway. One of them is certainly the requirement for unfolding during dislocation (Bagola et al., 2010). Despite several reports stating the requirement of unfolding before retrotranslocation of protein substrates (Tsai et al., 2001; Ushioda et al., 2008; Tortorella et al., 1998; Fagioli et al., 2001), there are few examples of artificial substrates that seem to be dislocated as folded molecules (Fiebiger et al., 2002; Tirosh et al., 2003). These evidences seem to suggest, indirectly, that unfolding is not a prerequisite for retro-translocation.

During MHC-Iα dislocation induced by immunoevasins the protein is object of disulfide bonds reduction prior to deglycosylation, thus suggesting an unfolding step before engagement by the dislocation channel and the proteasomal degradation (Tortorella et al., 1998). However, since deglycosylation is a cytosolic event is also possible that the reduction takes place in the cytosol on already exposed but still glycosylated molecules. Indeed, when under proteasomal inhibition, we tested BAP tagged MHC-Iα in the presence of US2 we observed that the reduced isoforms of MHC-Iα consisted on both glycosylated and de-glycosylated molecules; moreover even the non-biotinylated and biotinylated material were reduced in the presence of the immunoevasin (Fig. 33, similar migration comparing MHC-Iα in US2 expressing cells in left (reducing) and right (non-reducing) panels). While comparing reducing and non-reducing conditions, a faster migrating band was present when MHC-Iα was expressed alone. This band corresponds to oxidized molecules, as is expected that oxidized globular Ig domains migrates faster than when they are reduced. As judge by decrease of this oxidized band between lane 1 and 2 of figure 33 right panel, it seems that MHC-Iα in control condition can be dislocated with folded disulphide bridges. This indication was recently confirmed in a recent paper (Wang et al., 2013), where, using our BirA method to study spontaneous MHC-Iα ERAD, they also report the presence of disulphide bonds in the biotinylated glycosylated fraction.

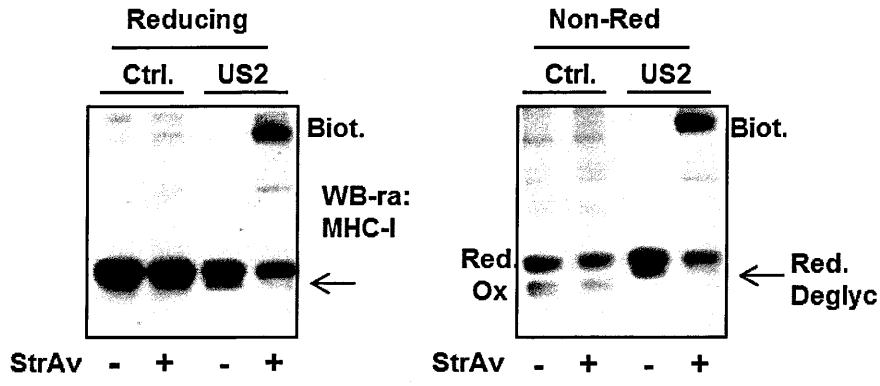

Figure 33. Disulphide bridges analysis of MHC-Iα. WB-ra of cell extracts from cells expressing BAP-MHC-Iα, BirA and US2 where indicated. Before lyses cell were treated 4 hours with 50μM MG132. Samples were lysed in the presence of 20mM NEM and separated by SDS-PAGE under reducing (sample buffer containing 0.1M DTT, left panel) or non-reducing conditions (sample buffer not containing DTT). All blots were developed with anti-SV5. Arrows indicate the position of reduced-deglycosylated MHC-Iα. Positions of reduced and non-reduced glycosylated isoform are also indicated.

5.1 Biotinylation of dislocated CD4 and Tetherin

For most of the models used before it is assumed that they are reduced before dislocation. To investigate the folding status during ERAD, we moved to two other proteins, CD4 and Tetherin uncharacterized about their redox status during retrotranslocation. While CD4 is a type I transmembrane protein (mostly monomeric), Tetherin is a homodimeric type II protein with a TM domain close to the N-terminus and a GPI anchor at the C-terminus.

Both CD4 and Tetherin can be induced to proteasomal degradation by the HIV-1 protein Vpu. The BAP tag was fused to ER luminal positions in both proteins, namely at the N-terminus for CD4 and in the C-terminal part, just upstream of the GPI anchor signal, for Tetherin (Fig. 34). A second tag SV5 was also included next to BAP to favour recognition. Vpu was also SV5-tagged at its N-terminus by fusing a leader peptide followed by the SV5-tag sequence.

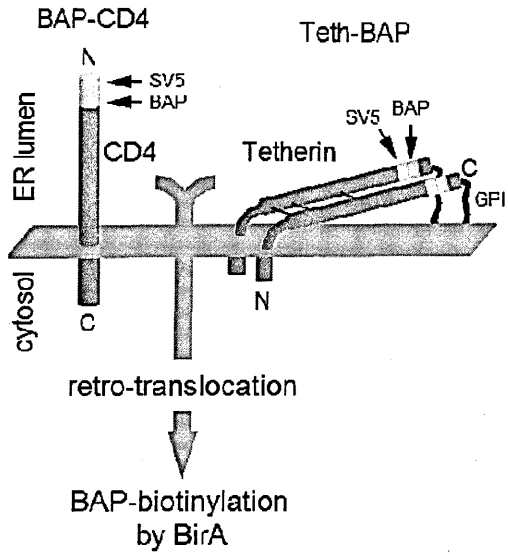

Figure 34. Scheme CD4 and Tetherin. CD4 and Tetherin were tagged with BAP in an ER-luminal position. The 11 amino acids-long SV5 tag is also shown. Only retrotranslocated BAP-tagged molecules are expected to be biotinylated by BirA.

The two proteins were independently co-expressed in HEK293T cells with BirA, both in the presence and absence of Vpu and, in the case of CD4, also with HIV-1 gp160 in order to obtain a stronger degradation effect (Willey et al., 1992). The degree of retro-translocation was determined again by monitoring the proportion of biotinylated molecules in a WB-ra.

5.1.1 Retro-translocation of CD4

In the case of CD4s some biotinylated-CD4 (b-CD4) (around 5%) was detected in the absence of Vpu, corresponding to spontaneous retro-translocation, as shown in a representative experiment in figure 35A. In contrast, when co-expressed with Vpu a substantial fraction of b-CD4 was evident (around 30%) only after proteasome inhibition with MG132, indicating accumulation of retro-translocated molecules directed to proteasomal degradation. A band of de-glycosylated CD4, a consequence of the cytosolic cellular PNGase, was also detected and, as expected, it was totally biotinylated. In addition, the b-CD4 fraction was composed of both de-glycosylated and EndoH-sensitive (ER-like) glycosylated molecules, consistent with the fact that ERAD substrates retro-

translocate from the ER (Fig. 35B).

Biotinylated CD4 corresponded to intracellular cytosolically localised molecules. In fact, immunoprecipitation of the mature membrane-exposed CD4 from cells first incubated with anti-SV5 and then washed and lysed was found essentially not biotinylated (Fig. 35C). When compared with a total cell extract under non-reducing conditions (Fig. 35C right panel), this membrane fraction was highly enriched in the minority homo-dimeric population of CD4, formed by interchain disulphide bridges between two of its cytosolic cysteines. These dimers have been recently shown to associate with tetraspanin-enriched microdomains in the plasma membrane (Fournier et al., 2010).

Trypsin-sensitivity assays performed on microsomes-containing cell lysates showed that b-CD4 was sensitive to trypsin, while the non-biotinylated material was trypsin-resistant, except for the predicted cleavage of the cytosolic C-terminal tail that produces a band of higher mobility (Fig. 35D).

As in the case of MHC-Iα, also for CD4 most of the biotinylated material, both glycosylated and deglycosylated, was found in the ER fraction (Fig. 35E). Complete dislocation to the cytosolic fraction was observed only for the deglycosylated-biotinylated fraction in the presence of proteasomal inhibition.

As a control, the amount of de-glycosylated CD4 accumulated in the presence of Vpu following MG132 treatment was not affected by the presence of BirA, ruling out interference of the BirA enzyme on retro-translocation (Fig. 35F).

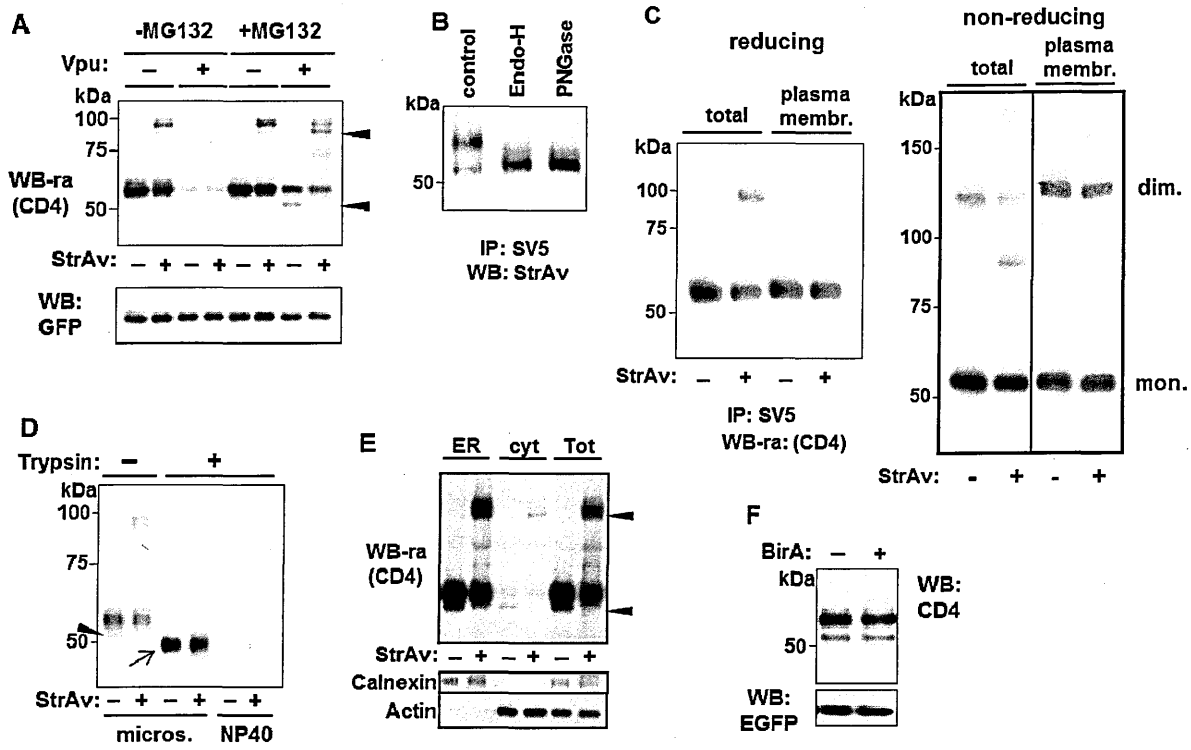

Figure 35: Biotinylation of BAP-tagged CD4. (A) WB-ra of BAP-tagged CD4. Extracts from HEK 293T cells co-transfected with BAP-CD4 and, where indicated, Vpu in the absence or presence of MG132 (5 µM for 12 hours) were run, blotted and developed with anti-SV5. Biotinylated molecules appear as retarded bands when run with StrAv. (B) Biotinylation of de-glycosylated and glycosylated CD4. CD4 from extracts of cells co-expressing Vpu in the presence of MG132 (5 µM for 12 hours) was immunoprecipitated with anti-SV5 and treated with Endoglycosidase H or PNGase. WB was developed with HRP-conjugated StrAv. (C) Plasma membrane displayed CD4 was not biotinylated. Membrane displayed CD4 in the presence of MG132 was immunoprecipitated with anti-SV5, and analysed in a WB-ra developed with anti-SV5 in a εSIP form under reducing and non-reducing conditions. (D) Trypsin-sensitivity assay. WB-ra of microsome containing cell lysates (microsomes) derived from cells expressing BAP-CD4 and Vpu and treated with MG132 (5 µM) for 12 hours before lysis. Where indicated, samples were incubated with trypsin. Arrow indicates CD4 with trypsin digested cytosolic C-terminal tail. (E) Cell fractionation through high speed centrifugation of mechanical cell lysates. Calnexin and actin were analyzed as ER and cytosolic markers respectively. (F) BirA does not interfere with CD4 retro-translocation. WB with anti-SV5 of BAP-CD4 from cells co-expressing Vpu, treated with MG132 (10 µM) for 4 hours in the presence or absence of BirA. Unless indicated, all samples were derived from cells co-transfected with BirA. WB of anti-EGFP was used as loading and transfection control. Arrowheads indicate deglycosylated CD4 isoforms.

Retrotranslocation of CD4 was also studied in pulse-chase [^{35}S]-Methionine labelling experiments, which showed the expected higher CD4 degradation and a progressive more extended biotinylation in the presence of Vpu in comparison to control samples (Fig. 36A). Moreover, only when Vpu was present a pattern

compatible with the reported ubiquitination in the CD4 cytosolic tail was clearly visible (Magadan et al., 2010). This material was detectable regardless of the presence of proteasomal inhibitors and only during short chase periods (Fig. 36A and B); in addition, in MG132 cells, where both glycosylated and deglycosylated isoforms of biotinylated-retrotranslocated material were present, the pattern of ubiquitin-like bands was mainly formed by the non-biotinylated CD4. This fraction likely represents molecules ubiquitinated in the cytosolic tail, targeted for retrotranslocation (because of the presence of Vpu), but still located in the ER lumen (because they are not biotinylated). Using image of figure 36A it was obtained the graph of figure 36C, where was calculated that the pattern of high molecular weight CD4 isoforms are retarded from unmodified CD4 and from each other of about 8.3-10 kDa, consistently with repeated addition of ubiquitin (the theoretical molecular weight of a ubiquitin monomer is 8.54 kDa). These data suggest a possible scenario in which CD4 molecules targeted to ERAD undergo a first round of ubiquitination on the cytosolic tail, followed by de-ubiquitination and then retrotranslocated to the cytosol, where can be deglycosylated and degraded.

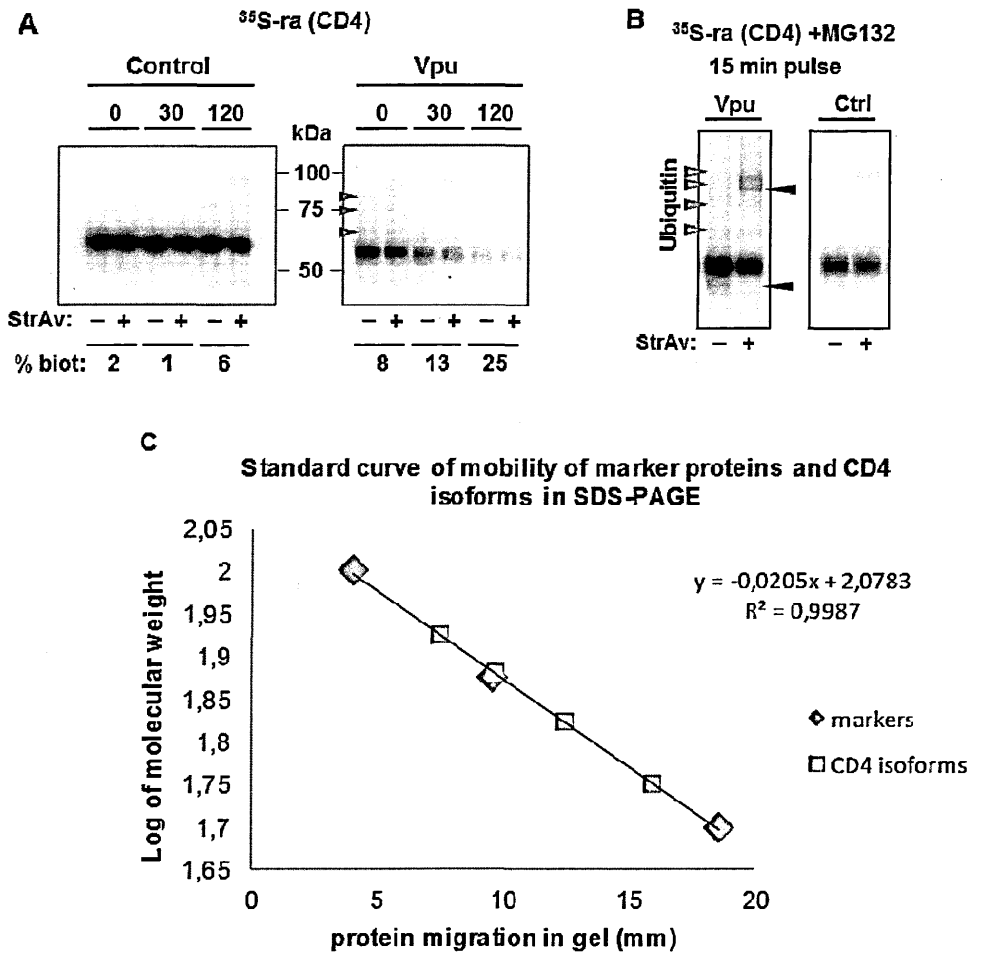

Figure 36. Pulse-chase labelling of CD4. (A) [^{35}S]-Methionine/Cysteine PAGE retardation assay of pulsed (15 minutes) and chased anti-SV5 immunoprecipitated cellular extracts of HEK293T cells co-transfected with BAP-CD4 and BirA and, where indicated, with vpu. Biotinylation percentage was calculated considering the difference between total CD4 and residual non-retarded material in the presence of StrAv. (B) Sample treated as in (A) from cells treated with MG132 10μM from starvation to lyses. Black arrowheads indicate deglycosylated CD4, pink ones are indicating ubiquitinated CD4 isoforms. (C) Standard curve of the distance travelled by each molecular marker protein in SDS-PAGE against log of molecular weight to estimate apparent mass of CD4 isoforms from data in (A). Linear relationship (R^2) and equation of the best-fit line from the markers standard data points are shown.

As discussed above for MHC-Iα, it has been previously proposed that for some ERAD substrates dislocation involves a step in which luminal domains are only partially exposed to the cytosolic side (Shamu et al., 2001; Okuda-Shimizu and Hendershot, 2007). However, using the BirA biotinylation system, we showed complete cytosolic exposure of the MHC-Iα ectodomain (Fig. 30). Using a similar approach to a protein with a related topology like CD4, we found that also in this case upon retro-translocation the whole luminal domain was completely exposed to the cytosolic side. An additional construct was used in which the BAP-tag was moved down to a position distant only 18 amino acids from the CD4 transmembrane domain on the luminal side. No differences in the relative retro-translocation levels were observed comparing membrane-proximal and membrane-distal BAP-tagged molecules (Fig. 37).

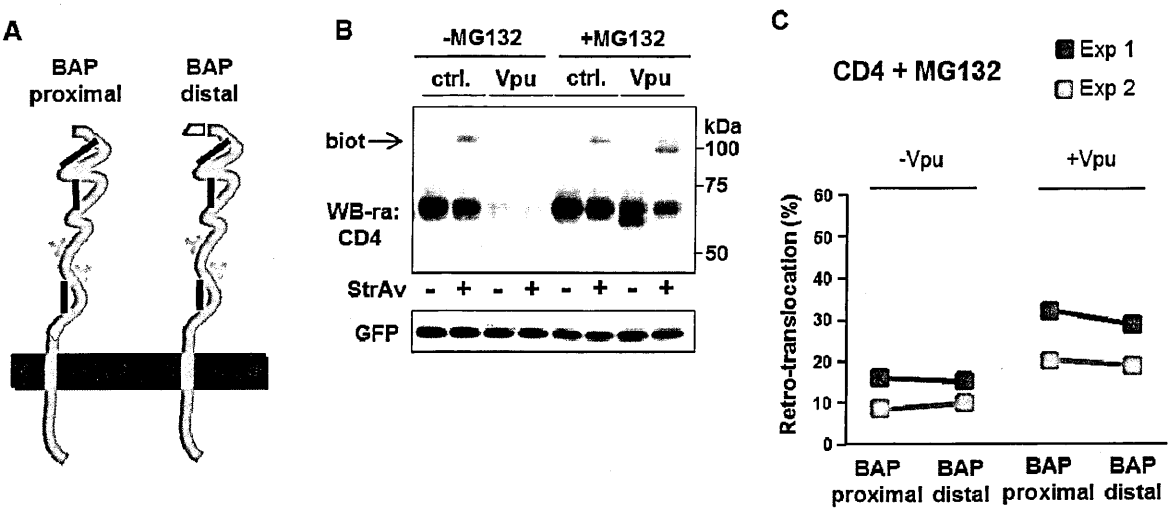

Figure 37. Cytosolic exposure of CD4 luminal domains. (A) Scheme of CD4 with the BAP tag positioned, proximal or distant from the transmembrane domain. (B) WB-ra of membrane proximal BAP-tagged CD4. Cell lysates were obtained from cells co-expressing Vpu, as indicated, and in absence or presence of MG132 (5 μM for 12 hours). (C) Quantification of retro-translocated fractions. Comparison of the relative levels of retro-translocated CD4 for molecules with the BAP tag in membrane-distal or membrane-proximal position, co-expressed with or without Vpu (in all cases in the presence of MG132 10 μM for 4 hours), expressed as percentage of total protein. The two different colours represent two independent experiments.

5.1.2 CD4 retrotranslocates with intrachain oxidised disulphide bonds

As all the CD4 ectodomain was exposed in the retrotranslocation intermediates detected, we next investigated the folding state of CD4 retro-translocated fractions by analysing the presence of disulphide bonds. To this end, total cellular extracts from cells co-expressing BirA, Vpu and CD4 were prepared in the presence of N-ethylmaleimide (NEM), to avoid possible post-lysis oxidation of reduced cysteines, and analysed in reducing and non-reducing WB-ra. In cells treated with MG132 both glycosylated and de-glycosylated b-CD4 accumulated and NEM alkylation was effective as caused a clear retardation of CD4 molecules. But this diverse migration was different between glycosylated and deglycosylated isoforms (Fig. 38A). Indeed, while both species are expected to be labeled by NEM because of the presence of cytosolic reduced cysteines, the observation that deglycosylated CD4 was bound by more NEM molecules than the glycosylated one suggested a different oxidation status for the two populations. This result was confirmed by analysis of samples in non-reducing and reducing conditions. Under non-reducing conditions most of the glycosylated CD4 showed a higher mobility than under reducing ones, because of the presence of oxidized intra-chain S-S bridges within the luminal domains. Interestingly, part of this fraction was biotinylated indicating that the retro-translocated glycosylated b-CD4 still contained oxidized disulphide bridges. In contrast, the biotinylated de-glycosylated fraction did not show mobility differences in reducing and non-reducing conditions, indicating that disulphide bonds were already reduced (Fig. 38B). To further confirm the presence of retro-translocated molecules with oxidized disulphide bonds, CD4 was immunoprecipitated with anti-SV5 and directly analysed in reducing and non-reducing WBs with HRP-conjugated StrAv to reveal only biotinylated molecules. As shown in figure 38C, the glycosylated b-CD4 (previously identified in figure 35B) clearly migrated with a lower mobility in reducing conditions, thus demonstrating that glycosylated CD4 was retro-translocated with disulphide bonds still formed. Therefore, dislocated CD4 molecules become reduced and de-glycosylated after reaching the cytosolic side. The same result was obtained after 2 hours of [^{35}S]-Methionine pulse labelling performed in the presence of MG132 (Fig. 38D).

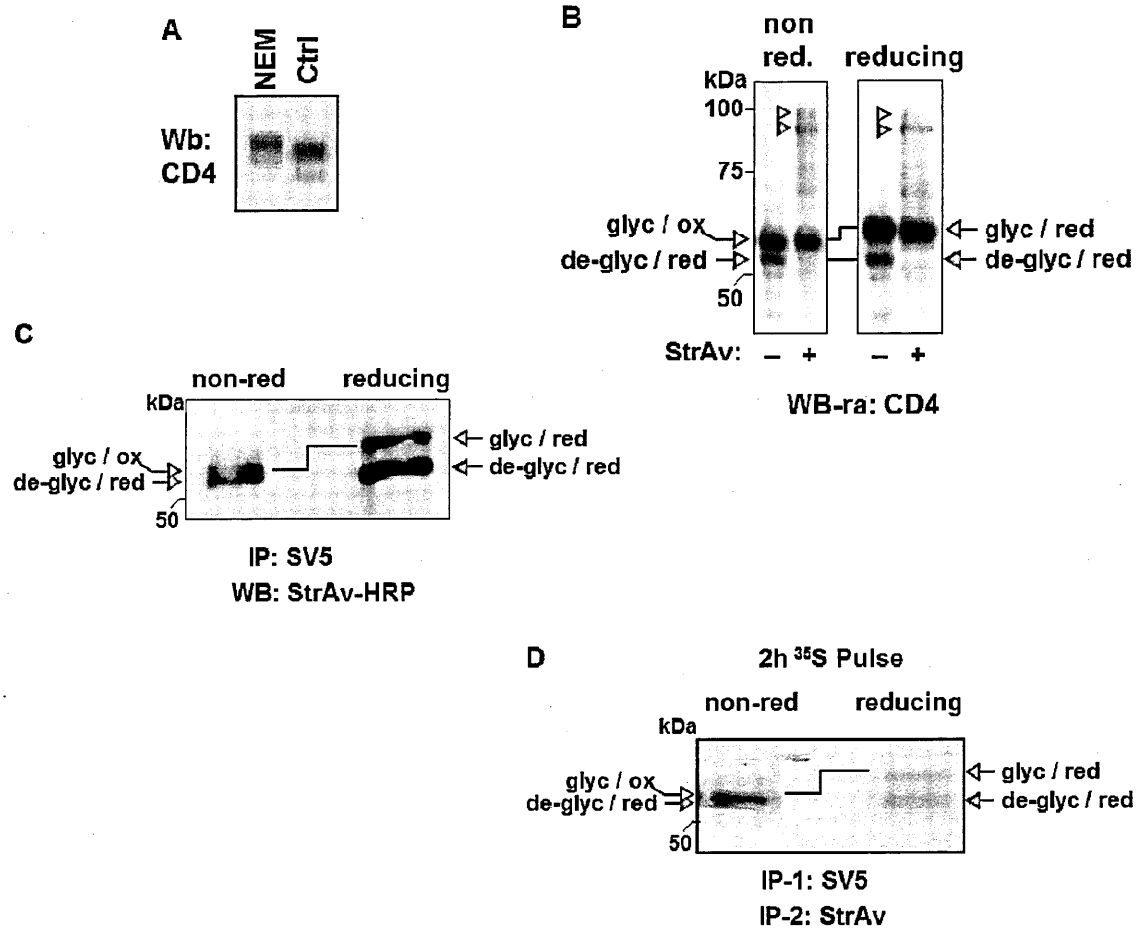

Figure 38. Retro-translocation of CD4 with oxidized disulphide bonds. (A) Wb of cell co-transfected with BAP-CD4 and Vpu. After MG132 treatment (5 μM for 12 hours), where indicated, to alkylate reduced cysteines, cells were incubated 5 minutes on ice with 30 mM NEM in PBS, before lyses in sample buffer enriched with 30 mM NEM. (B) Non-reducing WB-ra of BAP-tagged CD4. Cell lysates from cells co-transfected with Vpu, in the presence of MG132 (5 μM for 12 hours) were run in non-reducing (left) and reducing (right) conditions, blotted and developed with anti-SV5. Biotinylated and non-biotinylated fractions of glycosylated and de-glycosylated CD4 and their oxidation status are indicated with corresponding open and filled arrowheads and arrows. (C) WB of BAP-tagged CD4. CD4 was immunoprecipitated with anti-SV5 from cells expressing BirA and Vpu in the presence of MG132 and analysed in non-reducing (left) and reducing (right) conditions, blotted and developed with HRP-conjugated StrAv. (D) [^{35}S]-Methionine/Cysteine PAGE of 2hours pulse anti-SV5 immunoprecipitated cellular extracts of cells co-transfected as in (C) and treated with 10 μM MG132 during pulse. Biotinylated, glycosylated and de-glycosylated CD4 fractions and their oxidation status are indicated.

5.1.3 Retrotranslocation of Tetherin

In the case of Tetherin, spontaneous retro-translocation (i.e. in the absence of Vpu) was already apparent both in control cells and, with increased amounts, in MG132-treated cells (Fig. 39A). When co-expressed with Vpu, the relative level of biotinylated Tetherin compared with total Tetherin significantly increased (from around 10% to 35%). A more complex pattern of bands was observed for Tetherin, as it is a protein that undergoes several post-translational modifications, including two N-glycosylations (Asn65 and Asn92), the addition of a GPI anchor at the C-terminus with the corresponding cleavage of the hydrophobic terminal sequence, and the formation of homo-dimers covalently stabilised by three disulphide bonds (Cys53, Cys63 and Cys91). In the WBs, the upper set of bands (Fig. 39A, labelled as Golgi/membrane) corresponds mostly to cell surface-exposed molecules. This fraction immunoprecipitated from the membrane was not biotinylated, resistant to Endo-H and sensitive to PNGase (Fig. 39B). The set of bands showing an intermediate mobility (labeled ER-glyc in Fig. 39A) represents a relevant fraction that, because of its sensitivity to Endo-H (Figure 39C), corresponds to glycosylated molecules that have not yet trafficked through the Golgi. As for CD4, a significant part of this fraction was biotinylated (more than 70%). Only upon MG132 treatment, however, a lower set of bands corresponding to fully biotinylated de-glycosylated material (labeled de-glyc) became apparent. In microsomes-containing lysates biotinylated Tetherin, was trypsin-sensitive while non-biotinylated Tetherin was trypsin-resistant (Fig. 39D), while upon solubilisation with NP40 all Tetherin became sensitive to trypsin. In experiments of cell fractionation cell lysates were analysed by ultracentrifugation. Of note, part of the ER-glyc isoform of Tetherin was lost in the pellet of the first low speed centrifugation that removes non-lysed cells, nuclei and cellular debris (Fig. 39D and 39E). As shown in figure 39E, similarly to CD4 and MHC-Iα, most of retro-translocated Tetherin was associated with ER fraction, while only part of the deglycosylated material was fully soluble in the cytosolic fraction. A control experiment of no post-lysis biotinylation was performed. Cells transfected with only BirA or only Tetherin were mixed and lysed together. The BirA expressing cells contained also the MHC-Iα construct with a BAP on its cytosolic tail, as an internal control of BirA

activity. As shown in figure 39F, no biotinylation of Tetherin was observed, neither during lysis with sample buffer (SDS), nor during gentle mechanical lysis as in the case of cellular fractionation experiments. As expected, the control MHC-Iα was fully biotinylated in living cells. Thus, all the biotin-labelled material during cell fractionation experiments comes from the activity of BirA in living cells.

Controversial observations have been reported in relation to the degradation pathway followed by Tetherin and a role has been proposed also for the lysosomal/autophagy pathway (Douglas et al., 2009; Iwabu et al., 2009; Mitchell et al., 2009). To address this point, we analysed lysates derived from cells co-expressing Tetherin and Vpu that were treated either with MG132 or with chloroquine (CQ), an inhibitor of autophagy and lysosomal degradation (Yoon et al., 2010). CQ produced only a modest rescue of the total amount of intracellular protein (Fig. 39G). The fraction that increased upon CQ treatment was not biotinylated and not de-glycosylated. This was expected since molecules degraded by autophagy do not retro-translocate and remain in vesicular structures not accessible to cytosolic biotinylation and de-glycosylation before degradation within lysosomes. In contrast, a strong increase was observed when the proteasome was inhibited, with the appearance of biotinylated and de-glycosylated Tetherin. These results indicate that Tetherin is preferentially targeted to the proteasome, and only in part degraded through the lysosomal/autophagy pathway. A further control to demonstrate that biotinylated Tetherin represents the respective fraction of retro-translocated molecules was obtained co-transfecting a well secreted BAP-tagged scFv together with Tetherin and BirA. As shown in figure 39H after MG132 treatment, while Tetherin was highly biotinylated, the coexpressed scFv was not as a consequence of its localization within the secretory pathway.

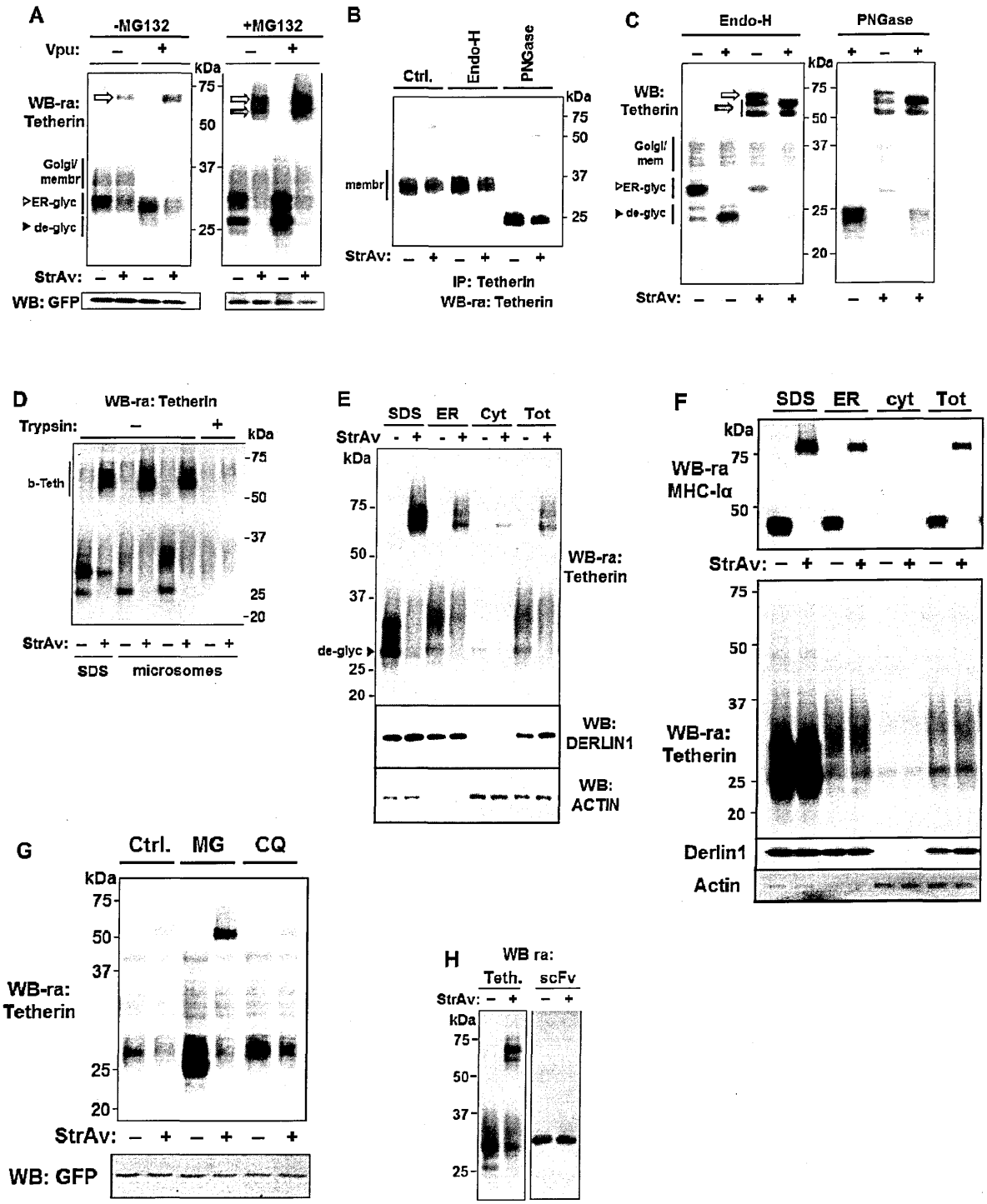

Figure 39. Biotinylation of BAP-tagged Tetherin. (A) Left panels: WB-ra of BAP-tagged Tetherin. Extracts from HEK 293T cells co-transfected with Tetherin-BAP and, where indicated, Vpu in the absence or presence of MG132 (5 μM for 12 hours) were run, blotted and developed with anti-SV5. Open and filled arrowheads indicate glycosylated and de-glycosylated Tetherin respectively, while open and filled arrows indicate the corresponding biotinylated (retarded) fractions. Right panel: cells were treated as in the left panels, but were cotransfected with BirA only where indicated. (B) Plasma membrane displayed Tetherin was not biotinylated.

Membrane displayed Tetherin was immunoprecipitated with anti-SV5, and the immunoprecipitates were digested with Endoglycosidase H or PNGase and analysed in a WB-ra developed with anti-SV5. Cells were co-transfected with Vpu. (C) Biotinylation of de-glycosylated and glycosylated Tetherin. WB-ra of cell lysates from cells co-expressing Tetherin and, where indicated, Vpu treated with MG132 (5 μM for 12 hours). Lysates were treated with Endoglycosidase H or PNGase, and the blot developed with anti-SV5. Open and filled arrowheads and arrows as in A. (D) Trypsin-sensitivity assay. WB-ra of microsome containing cell lysates (microsomes) derived from cells expressing Tetherin-BAP and Vpu and treated with MG132 for 3 hours before lysis. Where indicated, samples were incubated with trypsin. (E) WB-ra of cell fractionation through high speed centrifugation of mechanical cell lysates. Derlin1 and actin were analyzed as ER and cytosolic markers respectively. (F) Analysis of cell fractionation as in (E), performed after mixing of cells transfected with Tetherin or BirA and MHC-Iα tagged with the BAP in a cytosolic position. (G) WB-ra of Tetherin derived from cells treated with MG132 (10 μM) or CQ (50 μM) for 4 hours, as indicated. WB of anti-EGFP was used as loading and transfection control. (H) WB-ra of cell extracts from cells treated with MG132 after cotransfection with BirA, Tetherin and a BAP-tagged scFv. Tetherin expression was revealed by anti-SV5 mAb, while the scFv was detected by anti-roTag mAb.

5.1.4 Tetherin retrotranslocates with oxidised disulphide bonds

Tetherin is a type-II membrane protein with a peculiar topology, very different from the two other type I membrane proteins analyzed. To investigate whether also Tetherin presented its ectodomain completely exposed to the cytosolic side the BAP-tag was moved from the C-terminus close the GPI signal to a position 12 amino acids downstream of the transmembrane domain. Again no difference in the relative retro-translocation levels was observed when comparing transmembrane-proximal and transmembrane-distal BAP-tagged molecules (Fig. 40).

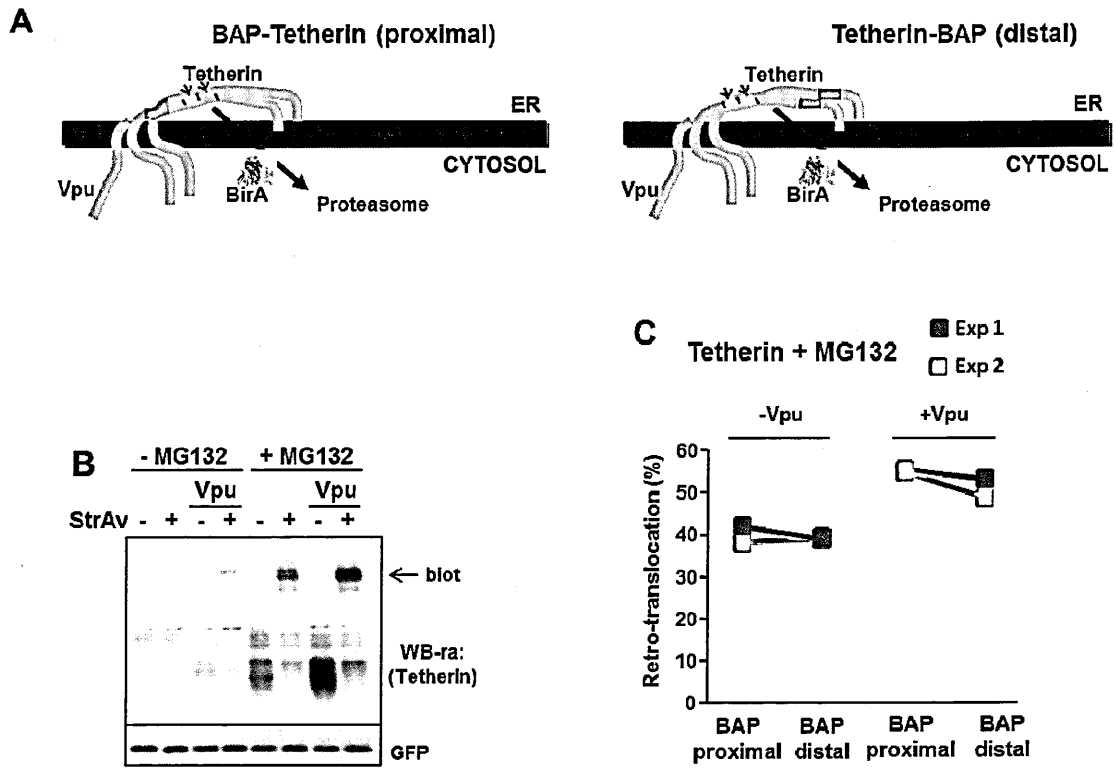

Figure 40. Cytosolic exposure of Tetherin luminal domains. (A) Scheme of Tetherin with the BAP tag positioned, proximal or distant from the transmembrane domain. (B) WB-ra of transmembrane proximal BAP-tagged Tetherin. Cell lysates were obtained from cells co-expressing Vpu, as indicated, and in absence or presence of MG132 (5 μM for 12 hours). (C) Quantification of retro-translocated fractions. Comparison of the relative levels of retro-translocated Tetherin for molecules with the BAP tag in membrane-distal or membrane-proximal position, co-expressed with or without Vpu (in all cases in the presence of MG132, 10 μM for 4 hours), expressed as percentage of total protein. The two different colours represent two independent experiments.

The results obtained suggested a complete exposure of dislocated Tetherin to the cytosolic milieu; thus, as Tetherin is known to form homo-dimers through cysteines oxidation, total cellular extracts from cells co-expressing BirA, Vpu and Tetherin were prepared in the presence of NEM, and analyzed for the presence of disulphide bonds in reducing and non-reducing WB-ra. In cells not treated with MG132 the biotinylated fraction under non-reducing conditions corresponded only to disulphide stabilised dimers (Fig. 41A left panel). This was independent of the presence or absence of Vpu, indicating that overexpressed Tetherin has an intrinsic tendency to spontaneous retro-translocation. Following proteasome inhibition, the level of biotinylated dimers increased and, in addition, totally biotinylated monomers accumulated. Accumulation of Tetherin monomers was observed only when the proteasome was inhibited but not in the presence of CQ (Fig. 41A middle panel). Thus reductions of Tetherin dimers into monomers appear to be a characteristic step of its cytosolic proteasomal degradation.

De-glycosylated material was evident in both dimeric and monomeric fractions. For comparison, the same samples analyzed in reducing conditions are also shown (Fig. 41A left panel). The presence of biotinylated dimers indicates that Tetherin retro-translocates with oxidized inter-chain S-S bridges. To further confirm this observation, cellular extracts from cells treated with MG132 in the presence and absence of Vpu were immunoprecipitated with anti-SV5 and analyzed in reducing and non-reducing WBs with StrAv-HRP (Fig. 41A right panel). To confirm the efficiency of alkylation of Tetherin cysteines (Fig. 41B left panel), sample treated with or without NEM were run in WB under non-reducing conditions; the presence of NEM caused a different migration of monomeric alkylated Tetherin isoforms and also prevented the formation of spurious hetero-dimers visible in the upper part of the gel. In addition, even when the ectodomain of this protein was expressed directly in the cytoplasm it did not form spontaneous homo-dimers (Fig. 41B middle panel). In contrast, as shown in figure 41B (right panel), when the same ectodomain was localised in the oxidizing environment of the ER lumen (by adding a leader signal peptide) only dimers were present. Furthermore, as for the full length Tetherin, monomeric material accumulated only after proteasomal inhibition. According to these results it is quite unlikely that the recovered biotinylated homo-dimeric Tetherin was formed by re-oxidation on the cytosolic side after retrotranslocation or

during sample preparation. An additional evidence to this point was obtained from [^{35}S]Methionine pulse-chase labelling experiments (Fig. 41C). After a 15 minutes pulse, all labeled Tetherin already appeared as a dimer with ER-like glycosylation (ruling out any mislocalization of the protein in the cytosol because of an unlikely inefficient ER targeting) and with a very small biotinylated fraction. After two hours chase, instead, part of the non biotinylated dimeric material was converted to the more mature Golgi/membrane isoforms (slower mobility) while an increased level of retro-translocated (biotinylated) dimers was apparent (from 11% after the pulse to around 30-35% after the chase). As expected, the biotinylated band was derived from the ER-like glycosylation isoform. The small amount of monomer, which appeared only during the chase, was also completely biotinylated. In addition, during the chase period the protein migrates faster than the ER-like glycosylation isoforms, suggesting, as in figure 41A, is that these isoforms are deglycosylated dimers. When samples from a stable cell line, co-expressing Tetherin and BirA, were tested in WB-ra the results obtained in transient transfection were confirmed. Indeed, despite an overall decreased biotinylation in the stable transfectants (a different ratio between mature and ER-like glycosylation forms) the biotin-labeled isoforms were all dimeric in the absence of proteasomal inhibitors, while with MG132 treatment the deglycosylated and biotinylated dimers and monomers were evident (Fig. 41D lane 3).

Taken together these results indicate that Tetherin retro-translocation initiates dislocating disulphide-bond stabilized dimers, which at a later stage become de-glycosylated, reduced to monomers, and finally degraded.

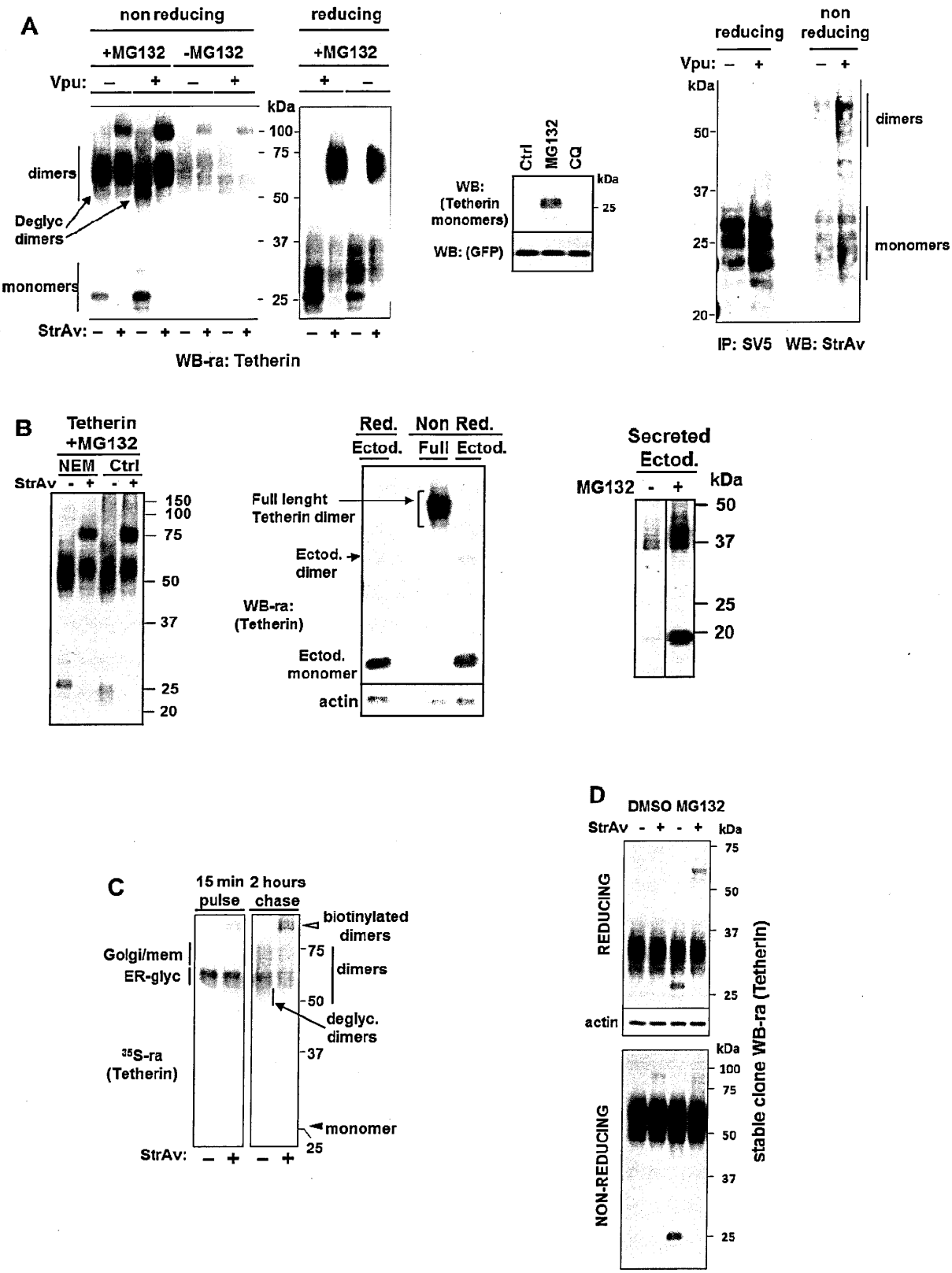

Figure 41. Retro-translocation of dimeric Tetherin. (A) Left panels: cell lysates from cells co-transfected with Vpu (where indicated), in the absence and presence of MG132 (5 μM for 12 hours) were run WB-ra in non-reducing and reducing conditions and developed with anti-SV5. Middle panel: WB of Tetherin derived from cells treated with MG132 (10 μM) or CQ (50 μM) for 4 hours, as indicated. WB of anti-EGFP was used as loading and transfection control. Right

panel: Tetherin was immunoprecipitated with anti-SV5 from cells co-expressing Vpu where indicated, in the presence of MG132 (5 μM for 12 hours) and analysed in non-reducing (left) and reducing (right) conditions, blotted and developed with HRP-conjugated StrAv. (B) Left panel: WB of cells transfected with Tetherin and treated with MG132 (5 μM for 12 hours). Where indicated cells were incubated 5 minutes on ice with 30 mM NEM in PBS before the lyses in sample buffer enriched with 30 mM NEM to alkylate reduced cysteines. Middle panel: Tetherin ectodomain was expressed in the cytosol of transfected cells. After NEM treatment cell lysates were analyzed in reducing and non-reducing condition. Full length Tetherin is shown as control of dimerization. Right panel: WB of non-reducing SDS-Page of cells extracts from cells treated or not with MG132, transfected with Tetherin ectodomain inserted in the ER lumen by means of a leader peptide. (C) [35S]-methionine pulse-chase labelling. Cells co-transfected with Tetherin were labeled for a 15 minutes pulse and then chased for 2 hours. MG132 (10 μM) was present from the beginning of the pulse. Tetherin was then immunoprecipitated with anti-SV5, run in a non-reducing PAGE retardation assay and developed by autoradiography. (D) Stable cell line expressing Tetherin and BirA was treated MG132 for 12hours where indicated. Samples were analyzed by WB-ra and run in reducing and non-reducing conditions.

The presence of deglycosylated dimeric Tetherin represents an independent proof, (from biotinylation) of the retrotranslocation of folded molecules. These deglycosylated dimeric isoforms were observed only in the presence of proteasomal inhibitors both in the WBs (Fig. 41A and D) and in the [^{35}S]-Methionine labelling experiments (Fig. 41C). Since the recombinant bacterial PNGase used in previous experiments does not work in non-reducing conditions, we took advantage of an inhibitor of the endogenous PNGase to confirm the identity of the supposed deglycosylated dimeric material. As shown in figure 42A, a 4 hour treatment with PNGase inhibitor, from one hour before addition of MG132 (3h), prevented the formation of the dimeric Tetherin isoforms (highlighted in the red square). Also the monomeric material in the presence of both chemicals was clearly retarded to more glycosylated isoforms compared to samples from cells treated with MG132 alone. The retardation of the supposed monomeric and dimeric deglycosylated isoforms in the presence of PNGase inhibitor is a strong evidence to confirm our interpretations.

In addition, preforming bi-dimensional non-reducing/reducing WBs in the absence of MG132 we observed two main isoform of Tetherin dimers (Fig. 42B upper left panel), and the only biotinylated was the one, which in the second reducing dimension co-migrated with the reduced ER-glycosylated Tetherin

reference (figure 42B lower left panel). In the presence of MG132 in addition to those two protein populations, which were again biotinylated only in the ER-glycosylated like fraction, several other isoform, all of them recognized also by StrAv-HRP, were present as monomers and dimers. In the second reducing dimension, those isoforms of different glycosylation showed a consistent mobility between monomeric and dimeric material (Figure 42B right panels). In fact, most of the species in the central part of the dimers, indicated as ER-glycosylated form, migrate to the same position of the glycosylated monomer. While faster dimeric isoforms, which in figure 42A were shown to be sensitive to PNGase inhibitor, after the reducing dimension showed a migration equivalent to the isoforms of de-glycosylated monomers. Altogether these data confirm the presence of de-glycosylated dimers, which represent a second independent criteria (in addition to biotinylation) supporting dislocation of Tetherin in a dimeric form.

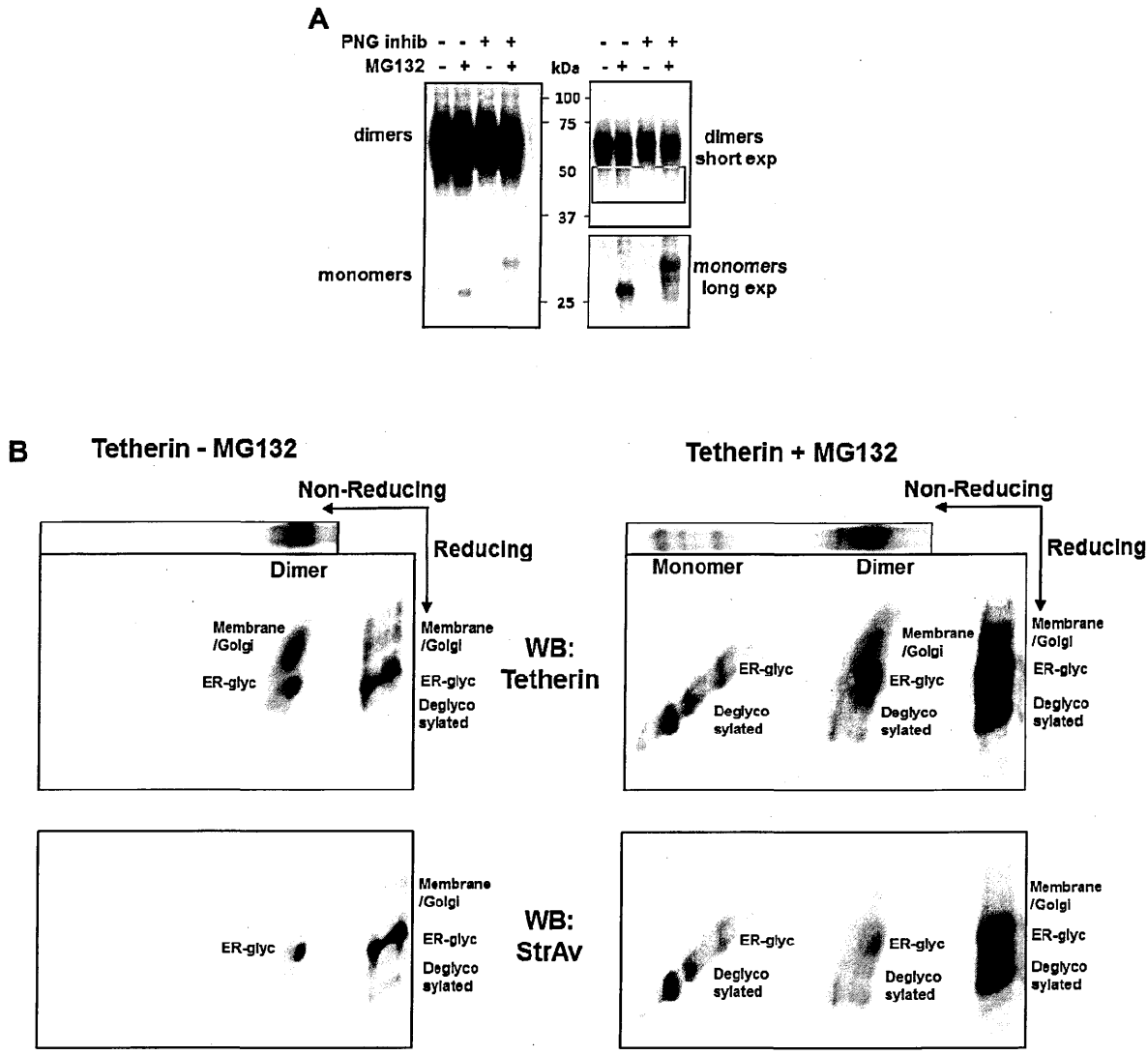

Figure 42. De-glycosylated Tetherin dimers. (A) WB of lysates from cells co-expressing Tetherin and BirA. Before lyses and where indicated, cells were treated for 4 hours with the PNGase inhibitor (Z-VAD-FMK 100μM) or with MG132 10μM for the last 3 hours, or after one hour with PNGase inhibitor cells were simultaneously treated for the last 3 hours with the proteasome inhibitor. Left panels showed different exposure times for Tetherin monomers and dimers. The red square highlights the isoforms sensible to the presence of PNGase inhibitor. (B) Bidimensional (non-reducing/reducing) analysis of Tetherin. Cellular lysates from cells cotransfected with Tetherin and BirA were treated (right panels) or not (left panels) with MG132 (5 μM for 12 hours), and analysed in a 2-D (non-reducing/reducing) WB and developed with anti-SV5 (upper panels) or HRP-conjugated StrAv (lower panels). The top panels show the same sample after the first non-reducing dimension. Our interpretation of the different Tetherin glycosylation species of monomers and dimers are indicated.

5.2 The non-secreted immunoglobulin κ light chain NS1

The immunoglobulin κ light chain (Ig-LC) NS1 is a soluble and non-glycosylated protein isolated from the NS1 plasmacytoma cell line and characterized as an ERAD model substrate when expressed in the absence of the Ig heavy chain (Ig-HC) (Leitzgen et al., 1997). However, this LC can completely fold, and be secreted when co-expressed with an H chain, assembling into a mature antibody molecule (Leitzgen et al., 1997). In the absence of Ig-HC it has been reported that the NS1 LC is bound to BiP in an almost 1:1 complex (Knittler and Haas, 1992).

The BiP binding site has been mapped to the N-terminal variable domain (V_L) of the protein. Interaction with BiP however occurs preferentially with the partially folded NS1 LC, an isoform in which the V_L domain is unfolded in a reduced form, while the C-terminal constant domain (C_L) is apparently still folded and not bound to BiP (Skowronek et al., 1998). Upon proteasomal inhibition a larger accumulation of this partially oxidised isoform was reported. The intra-chain disulphide bond (in the C_L domain) remains oxidized, while the one in the V_L domain is already reduced (Okuda-Shimizu and Hendershot, 2007). Based on this, and on the assumption that proteins need to be reduced in order to be retrotranslocated, a model of partial dislocation was proposed in which the reduced domain is exposed to the cytosolic side while the oxidised one is still in the ER lumen, until a tightly coupled final extraction and degradation. This model was further supported by the predominant ubiquitination of NS1 LC on the V_L domain (Okuda-Shimizu and Hendershot, 2007). However, on the light of our results with Tetherin and CD4, an alternative model compatible with complete dislocation of both domains can be envisaged. It has recently been shown that upon proteasomal inhibition the NS1 LC is released from the chaperone during the late ERAD steps and redirected into an ER quality control compartment (ERQC) from which BiP is excluded (Shenkman et al., 2013).

To explore the hypothesis of full NS1 retrotranslocation before proteasomal degradation the NS1 LC was tested with the BirA biotinylation system. A mutated NS1 LC, with the two Cys residues forming the intra-chain disulphide bridge in the C_L domain mutated to Ser (NS1C) was also analysed, as the stable folding of this domain might limit dislocation. In both proteins, wt NS1 and NS1C, the BAP tag was fused either at the N-terminus or at the C-terminus,

while the SV5 tag was always fused at the extreme carboxyterminal end (Fig. 43A). After co-transfection with BirA, we found biotinylation of NS1 LC bearing the BAP tag both at the N- and the C-terminus, with the latter form being even more biotinylated (Fig. 43B). Regarding the NS1C mutant we observed a biotinylation level similar to the wt, also for the N- and C-terminus tagged proteins. This means that the folding of the C_L domain does not impair retrotranslocation and that the dislocated molecules are completely exposed to the cytosol, in contrast to what was previously hypothesized (Okuda-Shimizu and Hendershot, 2007).

A second NS1 LC mutant, with all the Ser, Thr and Lys of the V_L were mutated to Ala (for S and T) or Arg (for K) and termed NS1STK- was also tested. NS1STK- was reported to be poorly ubiquitinated, much more stable than the wt and probably not retrotranslocated (Shimizu et al., 2010). We tested the effect of proteasomal inhibition on the wt and mutants with the BAP tag at the N- and C terminus (Fig. 43C and D). We observed, in all cases, a consistent increase in the amount of biotinylated material after MG132 treatment, with the non-biotinylated levels that remained almost the same as in the DMSO control; thus, in the presence of the proteasomal inhibitor, the rescued material was already retrotranslocated and corresponded to the amount that should have been degraded.

The NS1STK- mutant was found actually more expressed than the wild type and, in agreement with its reported stability, it was also less biotinylated considering the proportion of biotinylated material with respect to the total LC. Despite this, a relevant fraction of biotinylated NS1STK- molecules accumulated during the MG132 treatment indicating that also the more stable NS1STK- mutant can undergo retrotranslocation, although reduced, and be degraded by the proteasome.

When NS1 LC was run in non-reducing conditions two bands appeared. The main one was the faster migrating, corresponding to the fully oxidized form (ox-2). The slower migrating form that migrates close to the fully reduced NS1 LC and according to reported evidences (Chillarón and Haas, 2000; Okuda-Shimizu and Hendershot, 2007) represents the ox-1 form (with the S-S bridge in the C_L domain oxidised and the one in V_L reduced) was barely detected Fig. 43E). In the presence of MG132 both ox-1 and ox-2 isoforms accumulate. However, as previously reported (Chillaro and Haas 2000; Okuda-Shimizu and

Hendershot, 2007), the ox-1 form is highly stabilized during proteasomal inhibition indicating that it is degraded faster than ox-2. However, according to the BirA biotinylation assay, all the rescued material (ox1 and ox-2) was not located in the ER lumen, but in the cytosol as it was biotinylated. Thus NS1 LC is the third case of an oxidized-folded ERAD substrate completely exposed to the cytosolic environment before degradation. In the gel shown in figure 43E in samples from cells treated with MG132 high molecular weight material was observed in non-reducing conditions despite the presence of NEM during lysis and sample preparation. As a control, we co-transfected NS1 LC with the efficiently secreted BAP-tagged scFv (shown also in Fig. 43), a molecule structurally related to the LC. Despite the fact that both proteins are located within the secretory pathway, we observed retrotranslocation only of NS1 LC, also upon MG132 treatment, further demonstrating the specificity of the biotinylation assay (figure 43F).

Further demonstration that after retrotranslocation NS1 LC accumulates on the cytosol was obtained upon coexpression with the de-ubiquitinating enzyme OTU (a 169 amino acid long fragment of the polyprotein L of the Crimean Haemorrhagic Fever Virus (CHFV)) (Frias-Staheli et al., 2007; Ashour et al., 2009). As shown in figure 43G, strong stabilization of NS1 LC was observed. The rescued material was almost all biotinylated, as expected if the OTU enzyme removes ubiquitin molecules from the fully dislocated LC preventing proteasomal degradation. The NS1STK- mutant consistent with its higher stability and lower availability of ubiquitination sites was much less sensitive to the presence of OTU, yet a clear fraction was retrotranslocated confirming that, even if less efficiently than the wild type, also this mutant can be dislocated to the cytosol and, at least in part, to be a proteasomal substrate.

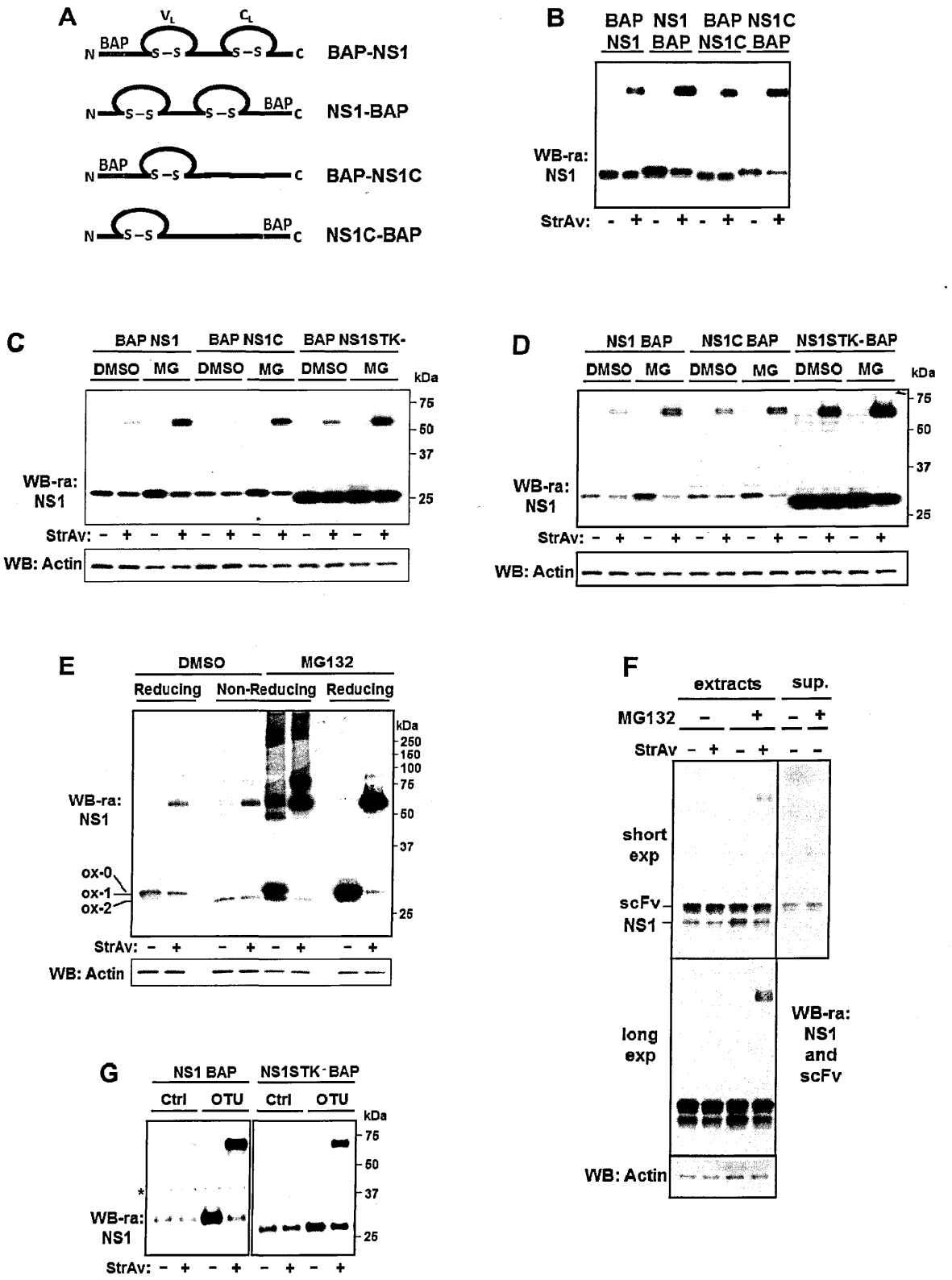

Figure 43. Retrotranslocation of NS1-LC. (A) Scheme of the four NS1 proteins tested. (B) WB-ra of cell extracts from cell cotransfected with BirA and, as indicated, one of the BAP-tagged NS1 illustrated in (A). (C) and (D) WB-ra of cell extracts from cells treated before lysis with MG132 10μM for 4hours, or DMSO as control. Cells were cotransfected with BirA and the indicated NS1 version. NS1STK⁻ is a NS1 mutant where all the Ser, Thr and Lys of the VL were

mutated to Ala or Arg. (E) WB-ra of cell extracts from cell transfected with NS1-BAP, treated or not with MG132 and run in non-reducing/reducing SDS-PAGE. Ox-0 indicates the fully reduced LC, ox-1 the LC oxidated only in the CL domain, while ox-2 shows the fully folded LC. (F) WB-ra of supernatants and cell extracts from cells co-transfected with BAP-NS1 and a BAP-tagged scFv and treated before lysis with MG132 10μM for 4 hours, or DMSO as control. Both proteins were detected by means of the SV5 antibody. (G) Cell extracts from cells co-transfected with BirA, NS1-BAP (wt or STK$^-$) and OTU or control vector as indicated. Asterisk shows a non-specific band revealed by this batch of anti-SV5 antibody. In every panel NS1 was detected by means of a SV5 tag fused to the C-terminus of all the NS1 versions tested.

6. The role of p97 ATPase activity in ERAD

The validated method to detect retrotranslocated molecules through biotinylation in living cells offered us the possibility to investigate the role of pivotal ERAD molecules during dislocation, such as the AAA-ATPase p97. It is generally thought that the p97 ATPase activity is required for retrotranslocation and proteasomal degradation (Ye et al., 2001). It is globally assumed that loss of p97 ATPase activity blocks ERAD by retaining substrates in the ER lumen or at least in partially dislocated forms not completely exposed to the cytosol. In this context, the ATPase activity of p97 is considered to be essential for extraction of proteins from the ER membranes. Also in the case of NS1, p97 activity was reported to be required for its degradation (Okuda-Shimizu and Hendershot, 2007). Thus, we initially investigated NS1 and other ERAD model substrates, co-transfecting them with BirA and either the wild type or the dominant negative ATPase incompetent mutant p97QQ which has the Glu 305 and 578 mutated into Gln (Ye et al., 2003). As shown in figure 44A, when NS1-BAP was co-expressed with p97QQ a large increase in the amount of NS1 was recovered from the cell extracts, in agreement with impaired degradation due to defective targeting of the substrate to the proteasome. This increased amount of protein, though, has always been generally interpreted as representing molecules accumulated in the ER lumen and unable to retrotranslocate to the cytosol. Surprisingly, however, most of NS1 was biotinylated (around 70-75%), indicating that it corresponded to molecules accumulated in the cytosol after retrotranslocation and not in the ER lumen. Remarkably, the amount of non-biotinylated material was almost the same as the one in cells without the mutant (empty control vector, indicated in figure 44 as -). Similar findings were obtained also for the NS1STK mutant, although in this case, as observed before upon proteasomal inhibition or induced de-ubiquitination, the p97QQ had a lower effect. Of note, although overexpression of wild type p97 caused a higher expression of NS1, the accumulated material was not biotinylated.

Furthermore, accumulation of retrotranslocated NS1 can also be clearly observed co-transfecting the deubiquitinase like CHFV OTU fragment, which deubiquitinates polyubiquitinated proteins (including ERAD substrates) making them unable to be engaged by the proteasome for degradation. As shown in figure 44B, accumulation of biotinylated NS1 and NS1STK- induced by OTU

was not impaired by the concomitant co-expression of p97QQ, strongly suggested that p97 activity is not required for effective retrotranslocation of NS1.

However, since these results were somehow surprising, the effect of p97QQ was also tested on NHK-α1A, a different model of a soluble ERAD substrate.

As shown in figure 44C, the results obtained are consistent with the ones with NS1. Indeed, in the presence of p97QQ, NHK-α1A showed impaired degradation and a large amount of biotinylated material (around 52%). As for NS1, no biotinylated NHK accumulated with wt-p97 despite the increased amounts of protein. In the presence of MG132, de-glycosylated NHK-α1A was detected in the control and p97-wt samples, which was totally biotinylated. Also a fraction of glycosylated molecules were biotinylated (a ratio of around 1:1 between glycosylated and de-glycosylated). In contrast, when co-expressed with p97QQ the large proportion of the biotinylated molecules (95%) corresponded to glycosylated material and very low amounts of de-glycosylated molecules were present. This is consistent with the well-known interaction p97 and the cytosolic PNGase (Li et al., 2006), and suggests that the p97 ATPase activity is required for efficient recruitment of PNGase towards the dislocated ERAD substrates.

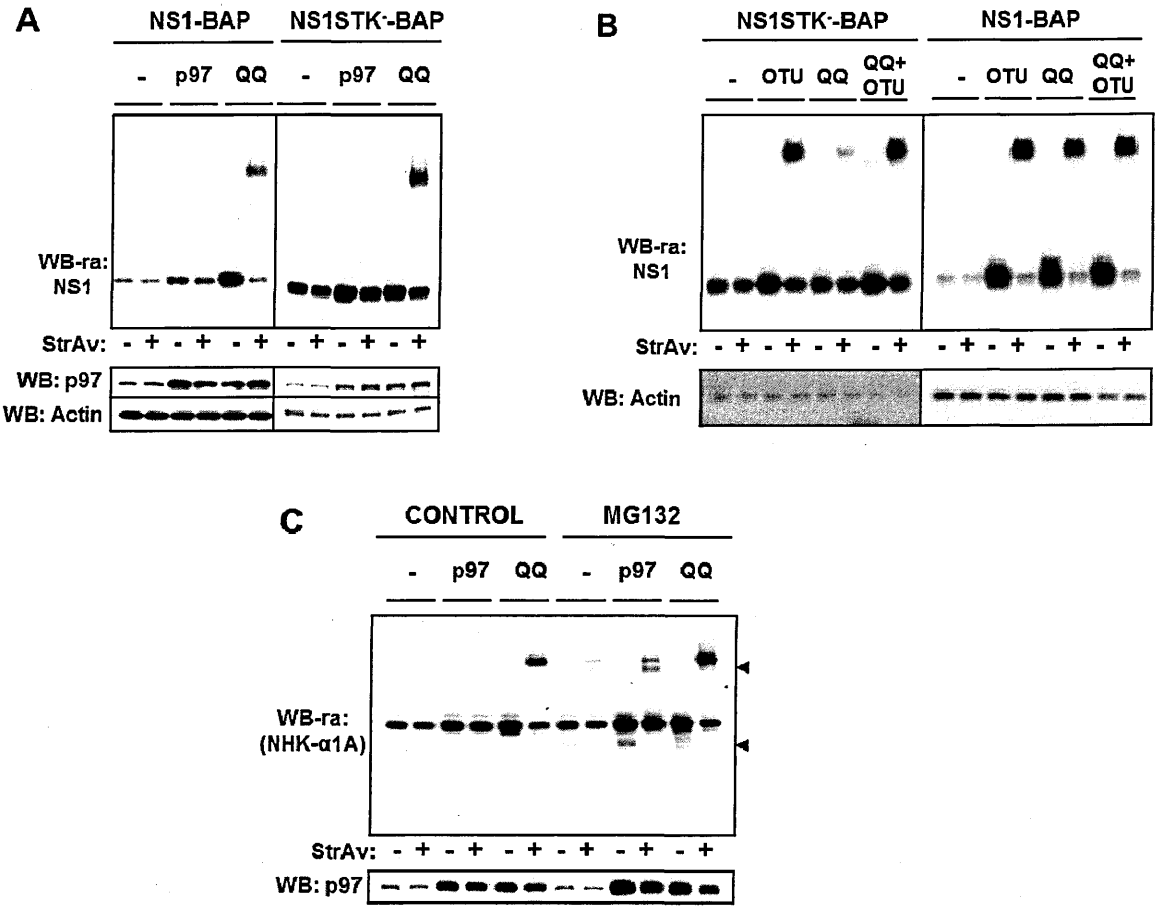

Figure 44. Effect of p97QQ on soluble ERAD model proteins. (A and B) WB-ra of cell extracts from cell cotransfected with BirA, the indicated BAP-tagged NS1, and empty control vector (-) or either wild type or ATPase incompetent p97 mutant (QQ); in (B) the effect of overexpression of OTU was evaluate. (C) WB-ra of cell extracts treated with MG132 10μM for 4 hours, or DMSO as control, before lysis. Cells were cotransfected with BirA, NHK-α1AT and as indicate with empty vector, wild type or mutant p97. Arrow heads indicate deglycosylated NHK-α1AT isoforms. In all blots NS1 and NHK-α1AT were detected by means of the SV5 tag fused to the C-terminus of them. Lower panels in (A), (B) and (C) visualize actin and p97 as control of loading and p97 overexpression.

Further confirmation that retrotranslocation does not require p97 activity was obtained with Tetherin, a membrane-bound ERAD model, which is efficiently targeted to proteasomal degradation either in the presence or absence of Vpu. Figure 45 shows the results of the effect of p97QQ on Tetherin retrotranslocation coexpressed with or without Vpu. The conclusion were similar to the soluble substrates, as the ATPase incompetent p97QQ caused strong protein stabilization, with almost all the accumulated material exposed to cytosolic biotinylation (Fig. 45A upper-left panel). Again, a reduced proportion of deglycosylated material was recovered in comparison with MG132 treatment

(figure 45A upper-right panel). Moreover, in non-reducing WB-ra (figure 45A lower panels) monomeric Tetherin was observed only when co-expressed with p97QQ in the absence of MG132, while upon proteasomal inhibition with MG132 monomers were found in all samples. As expected, all monomers were totally biotinylated and the ratio of glycosylated/deglycosylated was much higher when p97QQ was present, consistent with impaired PNGase recruitment.

As for NS1, also accumulation of biotinylated Tetherin promoted by OTU was not impaired by p97QQ as shown in reducing and non-reducing WB-ra (Fig. 45C), further confirming on-going retrotranslocation.

Collectively the data presented indicate that p97 ATPase activity is required for an efficient degradation and for an effective recruitment of PNGase, but not for the cytosolic exposure of ERAD substrates.

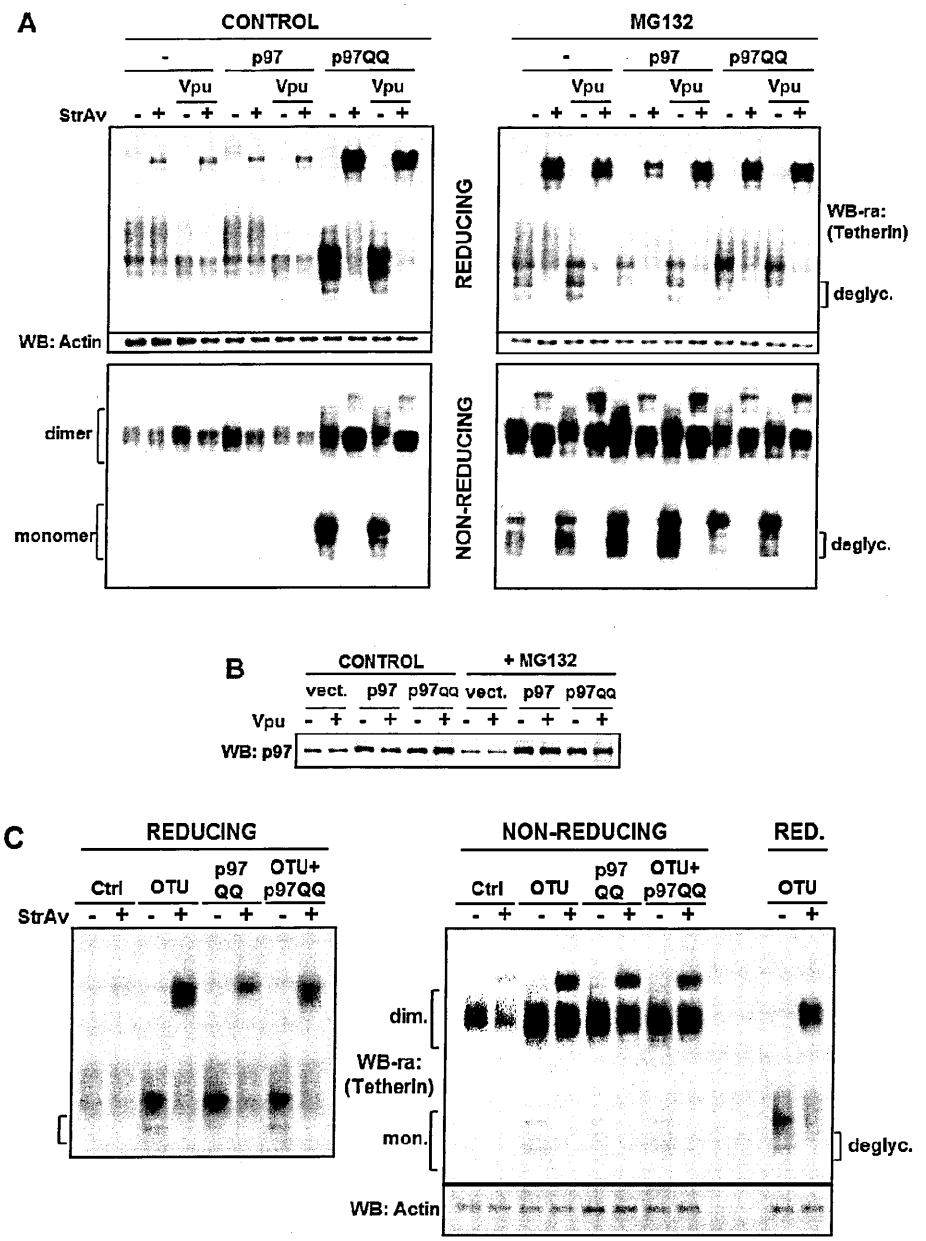

Figure 45. Effect of blocking p97 ATPase activity during Tetherin degradation. (A) WB-ra of cell extracts from cell cotransfected with BirA, Tetherin, and empty control vector (-) or either wild type or ATPase incompetent p97 mutant. (B) WB of p97 from cell extracts showed in (A). (C) Reducing (left panel) and non-reducing (right panel) WB-ra of cell extracts from cell cotransfected with BirA and Tetherin. Where indicated, cells were also cotransfected with OTU and p97QQ (QQ). Actin is used as loading control.

7. TEVp as second reporter of ER to cytosol retrotranslocation

To further support the findings obtained using the BirA-mediated biotinylation and to have more available tools in the field, we also investigated the possibility to use a different cytosolic enzyme to label retro-translocated proteins.

We focused on TEVp, the Nuclear Inclusion proteinase a (NIa-Pro) from Tobacco Etch Virus (TEV) (Phan et al., 2002), which is a 27kDa cysteine protease with a stringent specificity to the seven amino acid cleavage site (ENLYFQ/G), named here TS (TEV sequence), that led to the widespread use among the biotechnology industry as a reagent for endoproteolytic removal of affinity tags (Melker, 2000). While in viral infection full length NIa accumulates mainly in the nucleus of plant cells, the NIa-pro can be efficiently targeted to the cytoplasm (Ceriani et al., 1998).

The approach to exploit TEVp on ERAD was essentially the same adopted for BirA. TEVp was expressed in the cytoplasm to label by cleavage retrotranslocated molecules. For example, it was tested with an MHC-Iα tagged with the TS in the luminal domain and analysed its dislocation in the presence of the CMV immunoevasins (figure 46A). Preliminary experiments showed the need of a codon-optimized version of TEVp, due to the very low expression of the original viral protein. After 293T transfection no obvious toxicity or off target activity by the overexpressed protease was observed (Fig. 46B), also because its abundance in the cell is limited by its known self-cleavage activity (Parks et al., 1995 and Fig. 46C).

To evaluate compartment specificity of TEVp activity we created two MHC-Iα constructs with the SV5 and the roTag tags added respectively, at the N-terminus and the C-terminus to easily detect both, the full length and cleaved proteins. The TS was in one case positioned in the ER lumen downstream of the SV5 tag, while in the second it was located upstream of roTag in the MHC-Iα cytosolic tail.

As shown in figure 46C, when the TS was at the N-terminus no cleavage of the substrate protein was observed, indicating that the protease cannot enter in the lumen of the secretory pathway. In contrast, when the TS was positioned in the cytosolic tail, complete and efficient removal of the C-terminal roTag sequence took place in the presence of TEVp (Fig. 46C). This was confirmed taking advantage of the N-terminal SV5 tag that showed the expected faster migrating

MHC-Iα product (Fig. 46). Despite the high TEVp activity observed, the wild type protease was barely detected in cell extracts (Fig. 46C lower panel). As a control we expressed the C151A TEVp mutant, a completely inactive enzyme with the catalytic Cys mutated (Parks et al., 1995), which was totally unable to cleave both itself (as it was easily detected) and MHC-Iα (Fig. 46C lower panel).

7.1 TEVp in the analysis of MHC-Iα ERAD

Since the TEVp proteolytic activity compartment was restricted to the cytosol, we tested the enzyme as a reporter of ER to cytosol retrotranslocation.

The approach was analogue to what was previously done to evaluate BirA activity. An MHC-Iα construct with the SV5 and TS at the N-terminus and a roTag at the C-terminus was expressed in eukaryotic cells in the presence or absence of US2 and TEVp, treated with or without MG132 (4 hours) and then lysed with PAGE sample buffer in the presence of protease inhibitor cocktail, to avoid any post-lysis activity of the TEV protease.

As shown in figure 46D we observed the expected degradation of MHC-Iα in the presence of the immunoevasin and the stabilization of glycosylated and non-glycosylated molecules after proteasomal inhibition. In samples from cells expressing TEVp the amount of full length MHC-Iα was decreased. As expected, however, the cleaved forms could be revealed with anti-roTag. In figure 46D those species are shown highlighted in blue boxes and arrows, in cells treated with MG132 (glycosylated, cut MHC-Iα) and in cells coexpressing also US2 in the absence (glycosylated, cut MHC-Iα) and presence of MG132 (glycosylated, cut MHC-Iα and de-glycosylated cut MHC-Iα). These bands were absent both in the absence of TEV or in the WB developed with anti-SV5, as expected, since the SV5 tag is lost after TEVp cleavage. Thus, the data indicates that the efficiency of TEV resulted very similar to the one of BirA in recognizing retrotranslocated MHC-Iα molecules.

A direct challenge between the two reporter systems, based on BirA biotinylation and on TEVp proteolytic cleavage, was performed using an MHC-Iα tagged at the N-terminus with SV5, BAP and TS, and roTag at the C-terminus (Fig. 46E). This model molecule, when coexpressed with US2 and BirA raised the expected biotinylation levels (Fig. 46F left panel), while in the presence of

both the biotin ligase and TEVp all the biotinylated material disappeared (in this exposure the cleaved fragment was below the detection limit). When cells expressing US2 and MHC-Iα were treated with MG132 the typical pattern of glycosylated and deglycosylated MHC-Iα was observed. In the presence of BirA all the deglycosylated material and part of the glycosylated one were, as expected, retarded in the gel in the presence of StrAv. Instead, in the presence of TEVp complete cleavage of all the deglycosylated and part of the glycosylated MHC-Iα isoforms was observed (labelled in figure 46F in red, full length; blue, cut forms).

Of note, all the biotinylated material was cytosolically exposed and cleaved by TEVp resulting in faster migrating cleaved bands (Fig. 46F right panel).

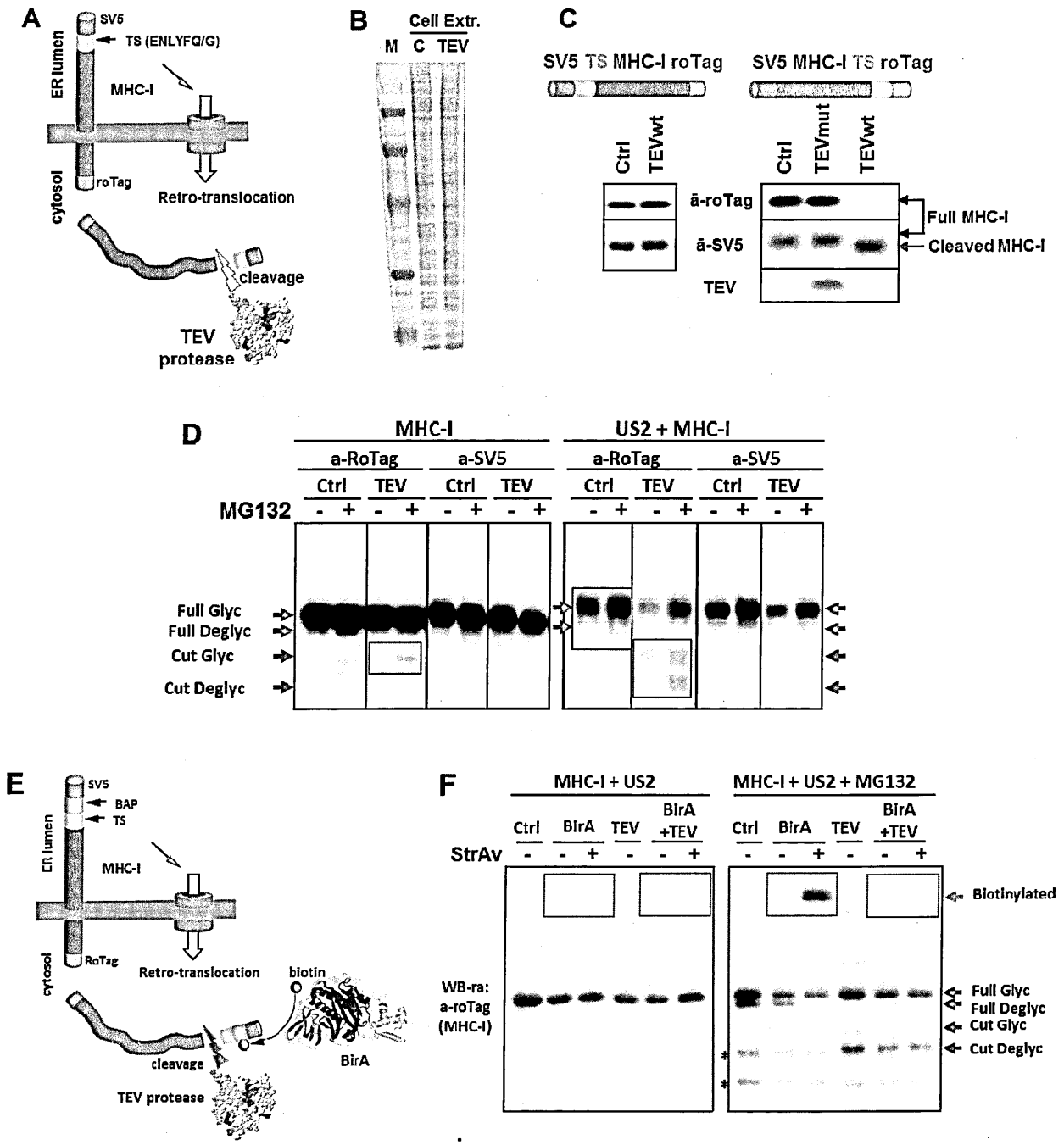

Figure 46. TEVp as ERAD reporter. (A) Schematic representation of TS/TEVp system applied to ERAD. (B) Comassie-blue staining of whole cell extracts from control (-) or TEVp transfected cells (+). Lane 1 (M) MW markers. (C) Scheme and WB analysis of MHC-Iα tagged with TS in ER luminal (left panel) or cytosolic locations (right panel). MHC-Iα was cotransfected as indicated with TEVp wild type (wt) or the C151A inactive mutant. (D) WB of cell extracts from cells expressing luminal TS tagged MHC-Iα cotransfected as indicated with US2 and TEVp. MG132 (25μM) was applied for four hours before cell lysis. (E) Schematic representation of the experiment shown in (F). (F) WB-ra of cell extracts from cells coexpressing MHC-Iα and US2. Where indicated cells were transfected with control empty vector (ctrl), TEVp or BirA. Proteasomal inhibition with MG132 (5μM) was performed for the last 16 hours.

7.2 TEVp and NS1 retrotranslocation

As the results of NS1STK- retrotranslocation measured by BirA biotinylation, were not in complete agreement with what has previously been published (inability to reach the cytosol) (Okuda-Shimizu and Hendershot, 2007), we decided to test it also with TEV/TS system. As shown in figure 47B NS1STK was C-terminally tagged with BAP, SV5, TS and roTag. This molecule expressed alone or together with BirA was present in a single band in WB analysis. After proteasomal inhibition a clear fraction was biotinylated, in agreement with the experiments described before (Fig. 47A). The co-expression with TEVp produced a faster migrating band, not detectable with the C-terminal roTag. This fraction actually corresponds to retrotranslocated material cleaved by TEVp, as when the two enzymes BirA and TEVp, were coexpressed, the cleaved NS1STK- was fully biotinylated. Moreover, the biotinylated retarded material in the presence of TEVp was detectable only with anti-SV5 and migrated faster than in the control with only BirA (absence of TEVp). This additional evidence demonstrates that BirA and TEVp recognized the same retrotranslocated molecules, as all the biotinylated material was also cleaved by TEVp and, likewise, all the non-cleaved material was not biotinylated.

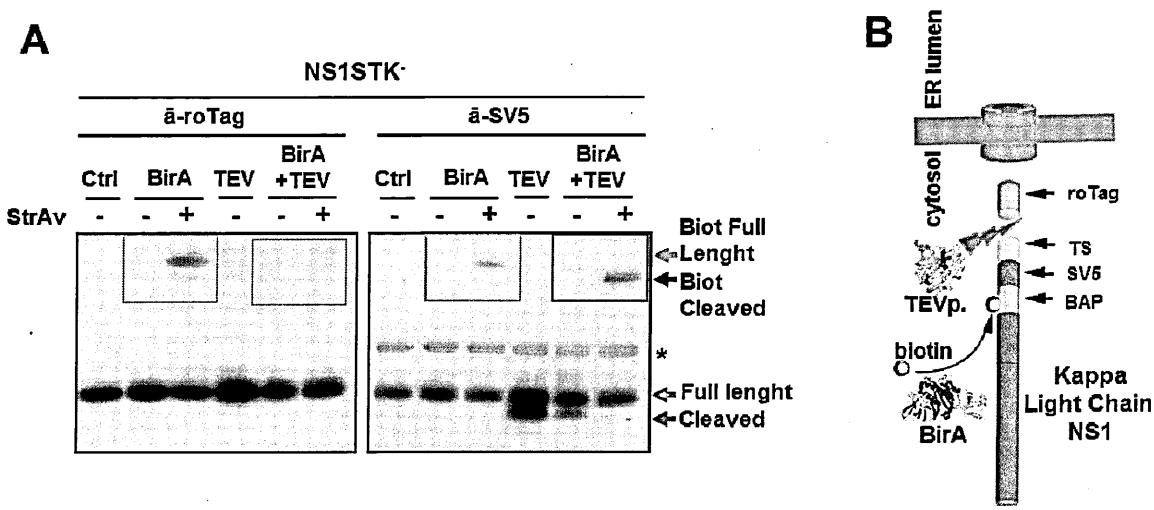

Figure 47. NS1STK- retrotranslocation. (A) WB-ra of cell extract from cells expressing NS1-STK. Where indicated cells were transfected with control empty vector (Ctrl), TEVp or BirA. Proteasomal inhibition with MG132 (5μM) was performed for the last 16 hours. (B) Schematic representation of the dislocated NS1STK- isoforms from the experiment shown in (A).

Taken together the results obtained demonstrate that the TS/TEV protease system represents an alternative to the BirA/BAP strategy for the efficient detection of ER to cytosol retrotranslocated proteins, strengthening our idea of using cytosolically localized enzymes with well-defined activities to monitor the localization of ERAD substrates during dislocation in living cells.

Discussion

Labelling of retrotranslocated proteins by biotinylation in living cells

Biotinylation of proteins, either chemical or enzymatic, is a widely used technology with a variety of applications in biological research. Enzymatic biotinylation offers the possibility to be implemented in living cells to achieve specific labelling of proteins that have been properly tagged with the 15 amino acid long biotin acceptor peptide BAP (Beckett et al., 1999), which contains a single lysine as biotin acceptor residue. The biotinylation in mammalian cells by the *E. coli* derived BirA is efficient, specific for the BAP peptide and results in a mono-biotinylated product. When BirA is coexpressed with a cytosolically localised protein, catalyses efficiently the complete biotinylation of the target (Predonzani et al., 2008). The same was observed in the case of the MHC-Iα-BAP, with the BAP tag localised to the cytosolic side of the ER membrane, which was completely biotinylated by BirA. Biotinylation is extremely stable, because the only de-biotinylating activity in cells takes place on short peptides derived from degraded proteins. De-biotinylation is the result of the activity of biotinidase, a class of enzymes that removes biotin from biocytin (Biotinyl-L-lysine (Wolf 2005)). Consistently, we did not observe a decrease in the amount of biotinylated proteins after incubation of lysates for several hours. Exploiting all these BirA's features and its cytosolic localization, we developed a method to specifically label molecules retrotranslocated from the ER to the cytosol in living cells.

Using four protein models (MHC-Iα, NHK-α1AT, HC, calreticulin), which are well-known examples of ER to cytosol dislocation substrates, we showed that BirA biotinylation identifies retro-translocated molecules for different proteins types (type-I membrane, soluble secretory and ER proteins). Taken together the data presented clearly demonstrate that only molecules exposed to the cytosolic environment, either soluble or still associated to the cytosolic side of the ER membrane, become BirA substrates and are consequently biotinylated. Biotin labelling allows precise quantification of the fraction of biotinylated molecules by diverse detection techniques (i.e. WB-ra, WB-StrAv-HRP and

ELISA), simplifying the determination of the level of retrotranslocation of a protein substrate in different conditions. Moreover, by this enzymatic biotinylation is possible to easily compare the relative folding and degradation efficiency of mutant proteins or of the same protein in different cells, as we have observed for MHC-Iα. For instance, whilst in HEK293 and HeLa cells US2 induces a higher level of MHC-Iα degradation than US11, in CHO cells US11 performs significantly better than US2. This difference can be explained because CHO cells are derived from a different organism (hamster) and, thus, is somehow expected that immunoevasins from human CMV could display a diverse phenotype in a non-human cell line.

Up to now, just a few user friendly biochemical techniques have been described for the detection of retro-translocated molecules, often in the presence of proteasome inhibitors to favour accumulation of the retrotranslocated proteins. Retrotranslocation of MHC-Iα and of other proteins is often identified as the fraction of cytosolic deglycosylated intermediates, which usually requires the use of proteasome inhibitors or the interference with cytosolic ERAD steps to accumulate (i.e. Blom et al., 2004; Hassink et al., 2006; Greenblatt et al., 2011). In contrast, BirA biotinylation method was able to detect a significant amount of biotinylated molecules of MHC-Iα as well as secretory NHK-α1AT and HC that were still glycosylated, without requiring the presence of proteasome inhibitors. Up to now it has been difficult to label or to prove glycosylated cytosolically exposed ERAD intermediates, but they are likely to be present in cells, because it is well-established that the localization of cellular PNGase is only in the cytosol and its activity is non-essential in ERAD (Bloom et al., 2004). Moreover, for some glycoproteins it is known that after retrotranslocation they are exposed to the cytosol and polyubiquitinated by cytosolic E3-ligases prior to be deglycosylated by the cellular PNGase (Jarosch et al., 2002; Yoshida and Tanaka, 2010).

A landmark for supporting this conclusion is the presence of cytosolic lectins such as Fbs1 and Fbs2, which can associate to SCF E3 ubiquitin ligases and form a complex that seems to target in the cytosol glycosylated protein, but not non-glycosylated ones (Yoshida et al., 2002 and 2005; Shenkman et al., 2013). Such findings indicate that glycoproteins can reside in the cytosol after retrotranslocation and be handled in several processes prior to eventual deglycosylation (proteasome can digest efficiently also glycosylated

polypeptides (Kario et al., 2008)) and final degradation. Reasonably, the biotinylation by overexpressed BirA is fast enough to label with biotin most of the retrotranslocated-glycosylated proteins during the first cytosolic ERAD steps. The existence of cytosolic E3-ligase-associated-lectins, their ability to bind cytosolically localized glycosylated misfolded proteins and their relevant role in ERAD (together to the non-essential role of PNGase in ERAD), strongly challenge, as not always reliable, the widely used method of evaluation of the fraction of retrotranslocated molecules only by means of their glycosylation/deglycosylation status.

Hence, by biotinylation in living cells it is possible to investigate the rate and extent of retro-translocation also for non-glycosylated proteins and regardless of the glycosylation status. Biotinylation of BAP-tagged proteins can be adapted to *in vitro* retro-translocation assays, being BirA widely used for *in vitro* applications.

In addition, the BirA method does not require cellular fractionations, which could always produce artifactual results. In fact, in our case cells are directly lysed in strong denaturing conditions, to avoid any post-lysis change in the ratio of biotinylated/non biotinylated substrates.

Accumulation of deglycosylated molecules seems to be a characteristic feature of different cells lines. In the case of MHC-Iα we noticed that in HEK293 cells the abundance of its deglycosylated fraction is less relevant than described IN U373 cells (Wiertz et al., 1996b), and similar to the non-classical class I molecule HFE in HEK293 cells (Vahdati-Ben Arieh et al. 2003).

In living cells BirA biotinylation appears to be very efficient in labelling recently retrotranslocated molecules, well before their deglycosylation.

Deglycosylated molecules are only detected following proteasome inhibition or interfering with late ERAD steps and, because of their cytosolic localization were completely biotinylated in our experiments. This suggests that deglycosylation is the rate-limiting step in the degradative pathway. According to the results obtained by means of BirA biotinylation quantifying retrotranslocation by considering only de-glycosylated molecules may result in underestimation of the extent of the dislocated fraction. Moreover, treatment of cells with proteasome inhibitors can lead to the activation of the unfolded protein response (UPR) as consequence of accumulation of misfolded proteins. A similar effect caused by the presence of biotin on our model proteins is quite

unlikely, as no obvious differences were recorded in experiments where biotinylation of BAP bearing proteins was prevented (performing experiments in the absence of biotin or of BirA) or allowed. UPR implies increased expression of proteins involved in protein folding, such as chaperones, and proteins directly participating in retro-translocation, such as SEL1L and Derlin proteins (Oda et al., 2006; Kaneko et al. 2007). Consistently, in our experiments treatment with proteasome inhibitors led to an increase in the amount of retro-translocated/biotinylated MHC-Iα molecules accumulated even in the absence of immunoevasins.

Even though biotinylated molecules can be directly revealed by assaying blotted membranes with StrAv, the retardation assay allows to simply and directly establish the extent of the biotinylated fraction by detecting the non-biotinylated population and the possible presence of fragments, which may also be not biotin-labeled, as observed for calreticulin. In this respect, it is not clear what those calreticulin fragments represent. They were all derived from deletions of the C-terminus (since the tag is N-terminally located) with similar or shorter lengths than the Crt-ΔC mutant, which lacks 115 amino acids. It is possible that these fragments were generated and retained in the ER, and not retro-translocated. Alternatively, they may result from the activity of lysosomal proteases participating in degradation of ER material as a consequence of autophagy (Ding and Yin 2008). Since calreticulin retrotranslocation appears to be of relevance for its nuclear activity, it may not be related to the turnover of the protein via proteasomal degradation. It thus remains an open question whether natural turnover of calreticulin involves preferentially autophagy rather than proteasomal degradation.

A further advantage of biotinylation is the possibility to affinity purify biotin-labeled molecules, making possible for instance the analysis by mass-spectrometry of retro-translocation intermediates.

In summary, the mono-biotinylation of cytosolically dislocated molecules represents a simple, quantitative and consistent way of determining the extent of ER to cytosol retrotranslocation of proteins in living cells.

Protein folding during retrotranslocation

The way in which secretory and membrane proteins that have entered the ERAD pathway cross the membrane barrier in order to be transported to the cytosol remains still obscure. Retro-translocation itself is frequently described as a step involving the unfolding of the polypeptide chain, followed by the actual extraction, probably through some sort of dislocation channel. Many hypotheses from different groups have indicated the translocon Sec61 (Wiertz et al., 1996a; Schmitz et al., 2000), the Derlin family proteins (Lilley and Ploegh, 2004; Sun et al., 2006), TRAM1 (Ng et al., 2010) and BAP31 (Wang et al., 2008) as possible components of this macromolecular structure. On the cytosolic side, the AAA ATPase VCP/p97 has been widely reported as necessary to provide energy for the entire process (Ye et al., 2001; Elkabetz et al., 2004; Carlson et al., 2006).

Taking advantage of BirA biotinylation for detection of molecules retro-translocated from the ER to the cytosol (Petris et al., 2011, Vecchi et al., 2012) we decided to investigate the folding state of the retro-translocated fractions of CD4 and Tetherin. Biotinylation in living cells has also been recently used to study spontaneous retro-translocation of MHC class I molecules and cytosolic/luminal localization of prion protein isoforms (Wang et al., 2013; Emerman et al., 2010).

When co-expressed with HIV-1 Vpu, CD4 and Tetherin are induced to enter the ERAD pathway (Mangeat et al., 2009; Magadan et al., 2010). For both proteins we showed that biotinylation identifies the population of retro-translocated molecules and established that overexpressed Tetherin preferentially follows the retro-translocation/proteasome pathway, even in the absence of Vpu. More interestingly, both proteins are actually retro-translocated with disulphide bridges still formed. While for CD4 the three disulphide bonds are intra-chain, within each of the three out of four extracellular Ig domains, for Tetherin three inter-chain disulphide bonds are formed between two parallel monomers. Hence, CD4 and Tetherin exit the ER as a partially folded molecule and as a dimer, respectively. This observation is particularly remarkable in the case of Tetherin also because of its double unusual N-terminal (TM domain) and C-terminal (GPI) anchorage to the membrane.

In general the folding status of retro-translocated molecules is controversial. Indeed several publications (both Reviews and original papers) have actually

addressed the problem of S-S bonds during retro-translocation. In many cases the need of a reduced substrate prior to dislocation was postulated, indirectly deduced, or presented as a step thought to be necessary or sometimes highlighted as a major open question (Hoseki et al., 2010; Hagiwara and Nagata 2012; Römisch 2005; Herbert et al., 2010; Feige and Hendershot 2011; Claessen et al., 2012; Hampton and Sommer 2012; Bagola et al., 2011; Okuda-Shimizu and Hendershot 2007; Vembar and Brodsky 2008). Conversely, our findings are a clear direct proof that different proteins retrotranslocate with intact S-S bonds. In literature there are few examples reported of artificial substrates that seem to be dislocated as folded molecules (Fiebiger et al., 2002; Tirosh et al., 2003). These evidences seem to suggest, in a very indirect way, that unfolding is not a prerequisite for crossing the ER lipid bilayer. It has recently been shown that the very large SV40 viral particle (30-40 nm in diameter), which dislocates from the ER to the cytosol to subsequently enter the nucleus, exits the ER as a complex assembly assisted by two ERAD-involved proteins, BiP and BAP31 (Geiger et al., 2011). A role for Derlin-2 has been also established during infection by mouse Polyomavirus, a virus similar to SV40 (Lilley et al., 2006).

CD4 and Tetherin are N-glycosylated. We found that for both proteins, a fraction of the biotinylated molecules retain their glycosylation state, in agreement with previous findings with MHC-Iα and NHK-α1AT (Blom et al., 2004; Petris et al., 2011) and consistently with the fact that the de-glycosylating activity in mammalian cells is provided by the cytosolic PNGase (Misaghi et al., 2004). This confirms that de-glycosylation appears to be the rate-limiting step of the process, since de-glycosylated biotinylated material only accumulates upon proteasome inhibition, while glycosylated biotinylated molecules are also detected without inhibition. In addition, we observed dislocated CD4 molecules that were still glycosylated and with disulphide bridges formed while all the de-glycosylated isoforms were found completely reduced, indicating that, in addition to de-glycosylation, also the reduction of this molecule takes place after dislocation. Interestingly, in the presence of Vpu during short [^{35}S]-Methionine labelling pulse we observed a pattern of CD4 bands which likely represents molecules ubiquitinated in the cytosolic tail (as described by Magadan et al., 2010), targeted for retrotranslocation but still located in the ER lumen, since they are not biotinylated. Thus, it is possible that CD4 molecules targeted to

ERAD undergo a first round of ubiquitination on the cytosolic tail, that trigger retrotranslocation, followed by fast deubiquitination as the biotinylated material glycosylated or deglycosylated is no more ubiquitinated. Then the cytosolically exposed CD4 should be further ubiquitinated and deubiquitinated for final proteasomal degradation. Interestingly CD4 can be ubiquitinated on multiple types of amino acids: Lys, Ser and Thr (Magadan et al., 2010). Based on the different amino acid on the substrate protein used for the first ubiquitin conjugation, and despite not yet reported, it could be speculated that some other residues other than the initial Met and the seven Lys of ubiquitin could be involved in the formation of polyubiquitin chains, as often is the same E3 enzyme that catalyse chain elongation. For example, exploiting the structures of the ubiquitin protein (pdb 2k39, Lange et al., 2008), some Thr and Ser (over all Thr 9, Thr 12, Ser20) are well exposed on the surface of the ubiquitin protein (Fig. 48), quite distant and directed to different directions respected to Met1 and the seven Lys used for the already known types of polyubiquitin chains (Fig. 48 and Fig. 8).

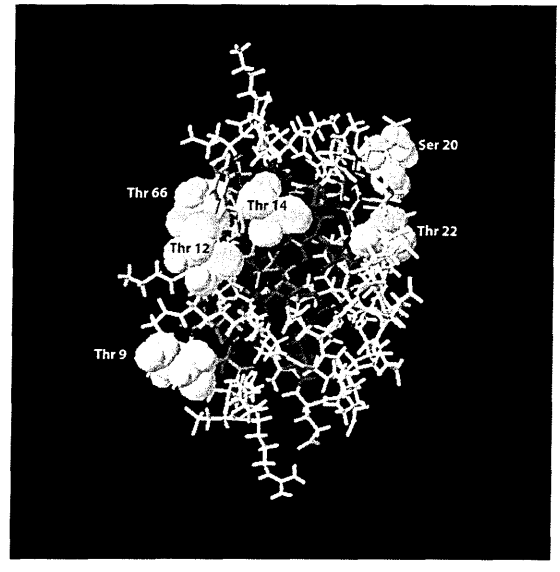

Figure 48. Ubiquitin structure . Adaptation of an ubiquitin molecular structure (a single ubiquitin subunit from polyubiquitin-C polyprotein) from pdb 2k39 (Lange et al., 2008), colours represent accessibility of the amino acid residues (yellow highly accessible, dark blue hidden amino acid side chain). In the crystal structure are labelled and indicated the exposed Ser and Thr residues in the surface of the ubiquitin structure; the other few other Thr, Ser and Tyr, present in the ubiquitin molecule, but hidden in the structures are not labelled. Of note no Cys residues are present in ubiquitin.

In the particular case of Tetherin, biotinylated dimers were in part also deglycosylated indicating that PNGase digestion can precede reduction.
However, not all proteins behave like CD4 and Tetherin. For example, we have observed reduction prior to dislocation when the MHC-I α chain is directed to degradation by the CMV immunoevasin US2, suggesting that different requirements may apply to different proteins. To this respect, a crucial role for the activity of the ER-resident oxidoreductases PDI and ERdj5 was reported for the MHC-I α chain (Tortorella et al., 1998) and for other ERAD substrates such as BACE457 and BACE457Δ (Molinari et al., 2002), the NHK α1-antitrypsin and the J chain of mouse IgM (Ushioda et al., 2008; Hagiwara et al., 2011). Indeed, a role for the redox potential during ERAD has been proposed (Tortorella et al., 1998; Hosokawa et al., 2006).

An interesting case is represented by the conditional non-secretory mouse Ig k-light chain NS1, for which the evidence indicates that, in the presence of MG132, one of the two intra-chain disulphide bonds (in the C_L domain) remains oxidized while the one in the V_L domain is already reduced and is the preferential ubiquitination site of the molecule (Okuda-Shimizu and Hendershot, 2007; Shimizu et al., 2010). In this case, a model of partial dislocation was proposed with the reduced domain exposed to the cytosolic side and the oxidised one still in the ER lumen, until its final extraction and degradation (Okuda-Shimizu and Hendershot, 2007). However, our results here presented, obtained by positioning the BAP at either the N- or C-terminus of the NS1-LC, pictured an alternative model compatible with complete dislocation to the cytosol of both domains and representing a third case of folded protein retrotranslocated without been fully reduced. In addition the influence of the folding state of the C_L domain challenged with the NS1C mutant was essentially not influent on the dislocation and stability of the protein.
The fact that some proteins retrotranslocate with both carbohydrate chains attached and intact disulphide bonds, poses a limit to an exit mechanism based on a simple protein channel, because of the high steric hindrance imposed by the sugar moieties and the globular or multimeric structure of the oxidized polypeptide. While the CD4 dislocated species is still represented by a monomeric chain, for Tetherin there are two transmembrane domains and two GPI anchors to deal with, thus making the whole process far more complex.

In any event, the minimal width of Ig domains, present both in CD4 and Ig LC, with disulphide bridges formed, and without considering the sugar moieties is of around 20-30 Å (Wu et al., 1997; Rudd et al., 1999). Similar values have been proven for the width of Tetherin dimers in the coiled-coil region (residues 68-138) (Hinz et al., 2010). The Sec61a channel is only 15-25 Å wide and during synthesis can accommodate the transport of non-glycosylated unfolded polypeptides of 5-8 Å (Van den Berg et al., 2004), suggesting that a pore at least four times as wide is needed. It has been proposed but not completely proved, that the Sec61 channel could form the retro-translocation pore by dynamically interacting with different molecular partners and thereby changing its permeability properties, adapting it not only to function in the opposite direction, but also to accommodate wide folded proteins (Kalies et al., 2005).

Pores of larger size such as the ones formed by perforin (130-300 Å wide) (Law et al., 2010; Praper et al., 2011), which allow the movement of granzymes of 45-50 Å width (Law et al., 2010) are large enough to compromise tight control of the transported material (Liu et al., 1995; Voskoboinik et al., 2006).

Therefore, our data suggest the existence of ways of exit from the ER alternative to a classical channel, operating for some ERAD substrates and possibly also for other structures, such as the significantly larger SV40 particles. Interestingly, import of some proteins into peroxisomes has been described to occur post-translationally (Rucktaschel et al, 2011), when the polypeptide has already undergone folding and quaternary interactions have been formed. For instance catalase, which enters the organelle as a mature tetramer in a receptor-mediated manner (Rachubinski and Subramani, 1995; McNew and Goodman, 1994 and 1996; Albertini et al, 1997) and the chloramphenicol acetyltransferase (CAT), which fused to a short peroxisomal targeting sequence enters in yeast and mammalian peroxisomes as a mature trimer (McNew and Goodman, 1994), indicate that folded and multimeric proteins can cross a lipid bilayer.

An alternative model for type-I transmembrane proteins, which does not consider dislocation as a pore-driven process has been suggested (Ploegh, 2007). The model postulated that extraction of the substrate could arise from the rearrangement of the ER membrane lipids leading to the formation of bicellar structures released in the cytosol. In this hypothesis formation of membrane complexes was proposed to involve lipid droplets, which are key

organelles for the metabolism of lipids in mammalian cells that are accumulated after the exposure of cells to high fatty acids levels (Murphy, 2001). These organelles are formed by lipid ester deposition between the two leaflets of the ER membrane, from where they bud in structures formed by a single layer of phospholipids (Brown, 2001; Tauchi-Sato et al., 2002; Martin and Parton, 2006). A possible involvement of lipids could overcome the evidences of the retrotranslocation of large folded proteins; indeed the extraction of small lipid vesicles should facilitate the handling of highly hydrophobic transmembrane domains, as in the case of MHC-I (Ploegh, 2007). To support this hypothesis two main clues may be that lipids droplet accumulates under proteasomal inhibition and apoliprotein B (ApoB), a transmembrane marker protein of lipid droplets, can be ubiquitinated and is a proteasomal substrate (Ohsaki et al., 2006). It could be interesting to address if also some viruses like polioma viruses and SV40, which are known to take advantage from the same set of proteins involved in extraction of misfolded glycoproteins (Lilley et al., 2006; Gilbert et al., 2006; Geiger et al., 2011) might be able to exploit this hypothetical lipid droplet pathway to leave the ER lumen. Recently, however, new experimental data has challenged this view, excluding a role for classical lipid droplets in ERAD for at least few substrates (Olzmann and Kopito, 2011). These evidences however do not exclude necessarily the involvement of transient lipid vesicles or membrane lipids rearrangements during the ERAD retrotranslocation step.

In conclusion, by means of BirA biotinylation we provided direct evidence that proteins can retrotranslocate from the ER to the cytosol with folded oxidised disulphide bridges. Our results therefore seriously challenge the prevalent view of a retro-translocation step involving transport of already denatured polypeptides and impose structural constraints to the molecular complex participating in the extraction phase.

Role of p97 ATPase in ERAD

The role of p97 in ERAD is believed to be the extraction of ubiquitinated substrates to the cytosol from the ER membrane and to occur prior to degradation, but after at least one round of substrate ubiquitination (Nakatsukasa et al., 2008; Ye et al., 2001; Ye et al., 2003; Ernst et al., 2011). This was proposed to be performed by p97 either by an active pulling of substrates through the hypothetical retrotranslocon, or even in an unknown manner across the lipid membrane, or by segregating the polypeptide that has already been liberated from the ER membrane (Nakatsukasa and Brodsky 2008).

p97, however, is an enzyme located in the cytosol or associated to the cytosolic side of the ER membrane when involved in ERAD, which interacts with both ubiquitinated and non-ubiquitinated proteins. Overall the predominant models foresee that, if p97 is not present or is inactive because of ATP depletion or inhibition of its ATPase activity, the ERAD substrates are not dislocated or only partially dislocated or not degraded, (i.e. Ye et al., 2001; Ye et al., 2003; Rabinovich et al., 2002; Okuda-Shimizu and Hendershot, 2007). But, it is striking that markers of cytosolic localization like ubiquitination and interaction with the p97 ATPase protein complex were always reported, in particular for soluble luminal proteins, as a partial dislocation of the model proteins (i.e. Ye et al., 2001; Rabinovich et al., 2002; Shimizu et al., 2010; Ernst et al., 2011 and 2009). This was primarily due to the accumulation of ERAD substrates, which largely associate even when ubiquitinated, to the pellet (microsomal/ER containing fraction) in cell fractionation experiments, and to an apparent resistance of part of the microsomal accumulated material to protease digestion. Consistently with this, since down regulation of p97 induces UPR, it has been interpreted as an indication that it is the consequence of accumulation of ERAD substrates in the ER lumen (i.e. Ye et al., 2001; Rabinovich et al., 2002; Ye et al., 2003; Elkabez et al., 2004). These evidences are certainly strong, but not necessarily conclusive. Because, during high speed centrifugation several particles, other than ER-derived vesicles and similar lipid compartments, end up in the pellet, such as mitochondria, proteasomes, ribosomes, and several other large protein complexes (Kalies et al., 2005; Greenblatt et al., 2011; Ackerman et al., 2006; Tang et al., 2011; Fujii et al.,

2012).

It is generally accepted that during ERAD one or more large protein complexes are formed (i.e. Ye et al., 2003; Christianson et al., 2011), some of them are located almost completely in the cytosolic side of the ER membrane, involving usually also transmembrane proteins (i.e. Ye et al., 2004; Lilley and Ploegh 2004; Christianson et al., 2011; Ernst et al., 2011 and 2009). Undoubtedly, proteins fully exposed to the cytosol might be abundantly tethered to the cytosolic side of the ER membrane (pellet fraction) by the strong interaction of the complex components to the latter (i.e. Greenblatt et al., 2011; Ernst et al., 2011 and 2009; Baker and Tortorella, 2007; Jarosh et al., 2002).

In a similar scenario the widely reported requirement of ATP and p97ATPase activity for protein dislocation (i.e.; Ye et al., 2001; Ye et al., 2003; Jarosh et al., 2002; Flierman et al., 2003) might be the simple result of the need of ATP hydrolysis for releasing of ERAD substrates from the p97 containing complex and for the eventual proteasomal degradation (which also need ATP hydrolysis to work), but not necessarily for the extraction from the lumen of the ER or from an hypothetical embedded intermediate in the ER membrane.

However, affecting p97 or proteasomal activity for a long period of time might cause a bottleneck and as a consequence is also possible that some of the ERAD substrates could accumulate in the ER lumen.

At any rate, there are two major problems for the interpretation of p97 published results, the first resides in the general semantic definition of what is actually the retrotranslocation step, while the second is the lack of reliable ways to establish protein localization between cytosolic and luminal compartments both in vitro and in living cells.

According to the literature the ER to cytosol retrotranslocation is the dislocation and solubilization of a ER membrane/luminal substrate to the cytosolic fraction before proteasomal degradation (Hampton and Sommer, 2012). But, for instance such definition is not adapted to ERAD substrates, which never appear soluble before proteasomal degradation (Okuda-Shimizu and Hendershot, 2007). There is a known association of a proteasomal population to the ER membrane (Kalies et al., 2005), which was proposed to degrade these substrates during or immediately after crossing of the membrane, for instance in the case of NS1-LC (Okuda-Shimizu and Hendershot, 2007).

Thus, it is important to discriminate whether p97 is necessary for crossing the

membrane (representing the actual retrotranslocation step) or to render the substrate soluble, a step that may not always be reached.

Moreover, in most ERAD models the solubilization of the proteins can be observed only when the proteasome is directly or indirectly inhibited (i.e. Ernst et al., 2011 and 2009; Wiertz et al., 1996a). Therefore, it could be considered that this effect may represent an artefact rather than a required step of the process, as this fraction is just the effect of proteasomal impairment and may result simply by the escape from degradation after disassembly of the ERAD complex.

The resistance in protease sensitivity assays, apart from being quite difficult to be properly performed and despite of being a strong localization criteria, does not necessarily demonstrate a luminal localization of the protein, even if controls with non-ionic detergent added to the sample allows a complete degradation. Indeed, polypeptides in protein complexes associated to membranes can be resistant to proteases, but could still be sensitive to detergents, favouring protease degradation. Of note, ERAD complexes resistant to non-ionic detergent solubilization are known (Greenblatt et al., 2011; Ernst et al., 2011).

It is generally believed that ubiquitination occurs prior to the interaction of the substrate with the p97 complex, which should provide the energy for extracting the unfolded protein in an ATP dependent manner (Ye et al., 2001; Jarosh et al., 2002; Shimizu et al., 2010). Our results using the p97QQ dominant negative mutant in retrotranslocation assays in living cells clearly challenge this predominant view, leading to different possible interpretations of the role of p97ATPase in ERAD.

The membrane-extracting role of p97 should rise per se serious perplexities in the case of soluble luminal proteins, since microsomal associated ubiquitinated fractions are a clear evidence of ER to cytosol dislocation. In this case a sort of ratcheting mechanism has been proposed, in which ubiquitination on the cytosolic side ensures that the soluble protein does not slip back into the lumen before it can be engaged by p97 (Shimizu et al., 2010). However, we found a clear large accumulation of biotinylated and non-ubiquitinated cytosolic NS1 LC in the presence of p97QQ indicating exposure of the protein to the cytosol. Similar results were obtained with NHK-α1AT that accumulated as biotinylated material when co-expressed with p97QQ. This retrotranslocated fraction was almost all glycosylated. Defects in deglycosylation efficiency of NHK-α1AT and

Tetherin co-expressed with p97QQ was also observed following proteasomal inhibition. This is consistent with the dominant negative effect on degradation of the impaired ATPase p97 mutant. It is possible that by blocking the ATPase activity (as in p97QQ) the link between the substrate recognition function performed by the regulating proteins associated to p97 N-terminus, and the effector function by proteins such as PNGase, bound to p97 C-terminus, is impaired. In fact, deep conformational changes are induced by the ATP hydrolysis (Rouilleret al., 2002; Davies et al., 2008). Moreover, PNGase was shown to interact simultaneously also with the shuttling factor HR23/Rad23 (Kamiya, et al., 2012), which is the direct link to transfer the substrate from p97/cdc48 to the proteasome (Richly et al., 2005). As it has been proposed that the p97 substrates are first recognized by substrate-recruiting cofactors and then processed by substrate-processing cofactors such as the PNGase (Rumpf and Jentsch, 2006), it can be envisaged that PNGase action occurs mainly downstream of p97. However, PNGase is known to interact also with Derlin1 (probably at the C-terminus between amino acids 187 and 251 (Katiyar et al., 2005)) and this can explain residual PNGase recruitment and activity. In view of this, it can be explained the inefficient deglycosylation observed also when p97QQ transfected cells were crossed to a proteasomal inhibition both in the case of NHK-α1AT and Tetherin.

Experiments with NHK-α1AT and Derlin1 mutants that do not interact with p97 because of the deletion of the SHP box motif (FxGxGQRn, where n is a non-polar residue), showed accumulation of deglycosylated NHK-α1AT substrate, demonstrating that disruption of the Derlin1/p97 interaction does not affect retrotranslocation and deglycosylation. (Greenblatt et al., 2011). Based on this and other data, it has been proposed that p97 activity is required in a step downstream of retrotranslocation and Derlin 1 involvement (Greenblatt et al., 2011).

Complete loss of Derlin1 or p97 ATPase functions might lead to a failure to disassemble ERAD complexes, preventing appropriate presentation of dislocated substrates to the proteasome, but is not directly involved in the retrotranslocation (membrane crossing) step.

Interestingly, the ERAD/retrotranslocation pathway is also involved in the cross presentation process in specialised antigen presenting cells, a mechanism that

remains poorly understood (Joffre et al., 2012). In cross presentation, exogenous antigens uptaken from the extracellular compartment are retrotranslocated from peculiar endosomes and phagosomes to the cytosol exploiting ERAD components like Sec61 and p97 before proteasomal degradation and reload of the resulting peptides on MHC-I molecules in the ER lumen (Joffre et al., 2012). It was proposed that functional p97 was required for the retrotranslocation of internalised antigens from those kind of phagosomes and thus for effective cross presentation (Ackerman et al., 2006). However, despite a clear major role for the p97 ATPase activity in cross presentation, the assays performed considered dislocation, strictly as the full cytosolic solubilization of the uptaken antigens. For example, in an interesting work (Ackerman et al., 2006) exit of the antigen (luciferase) from the internalisation endosomes was determined on the supernatant fraction after high speed centrifugation. In doing this, an already dislocated fraction associated to ER membranes in the presence of p97QQ, similarly to what was observed with our reporter systems, was completely excluded and not taken into consideration. It is therefore likely that, also in the dislocation of antigens in the cross presentation pathway, p97 acts not in the extraction from the ER lumen, but downstream in the solubilization and efficient degradation. In this scenario the pivotal role of p97 is maintained, but is just positioned a step after the retrotranslocation, intended as the crossing of the ER membrane and exposure to the cytosolic side.

More interesting is the dominant effect of coexpression of the CHFV OTU deubiquitinase with p97QQ: when expressed together the effect resembled the overexpression of OTU alone, which was a remarkable accumulation of retrotranslocated material both deglycosylated and not. This was observed considering the protein abundance, the biotinylation levels and the amount of deglycosylated material. Up to now there are 32 DUBs known, which can associate with p97 (Sowa et al., 2009). Some of them have opposite effects, for instance: Ataxin-3 seems to remove ubiquitin from ERAD substrates preventing degradation, while USP13 and YOD1 to favour degradation (Ernst et al., 2009; Sowa et al., 2009). The strong effect of CHFV OTU is similar to an inhibition of proteasomal degradation, but overcoming the decreased deglycosylation efficiency on ERAD substrates observed with p97QQ, even in OTU/p97

crossing experiments. Thus, OTU acts similar to Ataxin3 in preventing degradation and similar to the effect of the overexpression of the DUB protease domain of the Epstein-Barr Virus (EBV) large tegument protein (BPLF1). This deneddylase hydrolyses also K48 and K63 ubiquitin linkages, similar to CHFV OTU (Ernst et al., 2011; Frias-Staheli et al., 2007; Capodagli et al., 2011).

In experiments with the dominant negative mutant of the cytosolic deubiquitinase YOD1 (C160S), deglycosylation and efficient degradation of the soluble luminal ERAD model ribophorin-I was prevented. This result was interpreted as a halt of dislocation of the substrate (Ernst et al., 2009). In addition, accumulation of ubiquitinated proteins associated to p97 in the cytosol was interpreted as a halt on the dislocation reaction (Ernst et al., 2009). Upon EBV-DUB co-expression with the C160S mutant, deglycosylation was achieved. Therefore, the authors concluded that, because of the EBV-DUB de-ubiquitinase activity retrotranslocation was allowed to proceed. In this scenario both, ubiquitination and deubiquitination from the cytosolic side are steps needed for retrotranslocation. (Ernst et al., 2009 and 2011). and upstream of p97 activity.

However, in other cases this need of DUBs activity might not be required for retrotranslocation. For instance, MHC-Iα was found retrotranslocated (luminal domain exposed to the cytosol) by means of BirA biotinylation after treating cells with DUBs inhibitors (Wang et al., 2013) but, consistent with a role upstream of p97 and PNGase activity, the dislocated MHC-Iα was mainly glycosylated and associated with the pellet/microsomal fraction. The authors concluded that dislocation of MHC-Iα is dependent of DUB activity, while, the data suggest that they are required for solubilisation and efficient de-glycosylation. Of note, the dislocation of this molecule does not require ubiquitination on both its tail and ectodomain, but is needed for rapid proteasomal degradation, thus challenging any involvement of both the ubiquitination and deubiquitination of the substrate in the dislocation step. In addition, in this report (Wang et al., 2013) a chemical inhibitor of p97 ATPase activity (DBeQ) (Chou et al., 2011) caused 50% increase (biotinylation assay) in the accumulation of dislocated-glycosylated MHC-Iα. In experiments of double treatment with both DBeQ and proteasomal inhibitors both dislocated-glycosylated and deglycosylated MHC-Iα were clearly observed. The detected total dislocated fraction was almost equal to treatment with only proteasome inhibitor and the major difference was a diverse ratio

between glycosylated and deglycosylated retrotranslocated molecules. Strikingly, despite the results supported a post-dislocation role for p97 ATPase activity, it was concluded the opposite: that dislocation was dependent of p97 function. Again the pivotal problem might in part reside in a relevant semantic definition: whether a protein that left its original luminal localization and becomes exposed to the cytosol should be defined dislocated (dislocation = change of localization), as we believe, or not.

The similarities in deubiquitination specificity of EBV-DUB and CHFV OTU suggest a similar activity between the two. However, with OTU we observed a clear and efficient retrotranslocation/biotinylation of every ERAD model tested, indicating that OTU acts after the ER to cytosol dislocation.

Interestingly, most if not all of the known p97/Cdc48 ATPase dependent functions seem to be directly linked to the ability of the protein to bind to ubiquitinated proteins and to segregate them from their binding partners or to extract them from protein complexes (Liu and Ye, 2012). A role of p97 in regulating protein interactions (not associated with dislocation) at cell membrane was reported (Jentsch and Rumpf, 2007; Shcherbik and Haines, 2007). The general result is the separation of polypeptides from relatively large immobile subcellular structures, membrane associated or not (Liu and Ye, 2012). For this reason, p97 has been dubbed “segregase” (Jentsch and Rumpf, 2007). According to our data, this p97 segregase function on large multiprotein complexes is in agreement with our interpretation of a post dislocation role of p97 in ERAD.

A reporter system based on TEVp proteolytic activity

We found that expression of TEVp in the cytosol of mammalian cells allowed to discriminate the localization of the TS-tagged (TEVp cleavage site) domain between the ER luminal compartment and the cytosol. This feature allowed us to exploit TEVp catalytic activity to study ERAD and in particular the retrotranslocation step, with an approach similar to BirA biotinylation. In both cases we took advantage of the overexpression of cytosolically localised enzymes to quickly label dislocated proteins. BirA and TEVp are two completely unrelated proteins, being the first a cytoplasmic bacterial biotin ligase and the second a protease of a virus infecting plant cells (Beckett et al., 1999; Parks et al., 1995). However, they both share a considerable specificity towards their minimal target sequence and a comparable catalytic efficiency (K_m 0.025 mM, k_{cat} 0.2 (s^{-1}) in the case of BirA (Slavoff et al., 2011) and K_m 0.061 mM k_{cat} 0.16 (s^{-1}) in the case of TEVp (Kapust et al., 2001)). In parallel experiments with MHC-Iα and CMV immunoevasins we observed that the two reporter systems revealed similar levels of retrotranslocated molecules. The major difference was the requirement of transfecting four/five times more plasmid encoding TEVp than BirA, due to the well-known auto-cleavage of TEVp. Some TEVp more stable mutants described in the literature (Kapust et al. 2001) and tested in our laboratory were not more efficient than the wild type TEVp. Nevertheless, no obvious toxicity was observed in TEVp transfected cells, probably because of both, the specificity of the protease and the relatively low abundance of active enzyme. Our finding that, under optimal conditions in retrotranslocation experiments in living cells, TEVp and BirA labeled the same molecular fraction (almost all the biotinylated was cleaved and all the cleaved was biotinylated) strengthened the findings observed with BirA (and also the ones with TEVp) and in general the idea of using cytosolically localized enzymes as a way to detect retrotranslocated molecules in living cells.

This second method to label dislocated molecules in living cells offer new opportunities for biochemical and imaging approaches. For instance, the cleavage might be used to reveal an epitope previously hidden or to activate a quenched fluorescent protein. In addition the use of TEVp is simple, non-requiring treatment of cells with biotin or incubation with streptavidin as in the retardation assays for the quantification of the proportion of retrotranslocated

molecules.

Another advantage of TEVp system is the very limited size of its target sequence (only seven amino acids), which should minimally affect conjugated proteins and also does not contain any Lys, that are the most frequent ubiquitination sites.

Other than the very classical MHC-Iα/immunoevasins ERAD system used for the first validation of TEVp in labelling ER to cytosol retrotranslocated molecules, we focused on the NS1STK- mutant. With this protein our aim was to corroborate the results obtained by BirA biotinylation, which revealed that it was degraded by the proteasome at a lower rate compared to the wild type NS1. TEVp assays showed, in agreement with the biotinylation assay and with the published evidences, that NS1STK- was more stable but still degraded and ubiquitinated in the C_L domain (Shimizu et al., 2010). Moreover, TEVp confirmed our finding of the complete cytosolic localization of the C-terminus, thus indicating that the method can be used to analyse how protein substrates become exposed to the cytosolic milieu during dislocation.

Of note, BirA and TEVp are two independent techniques useful to analyse retrotranslocation of soluble non-glycosylated proteins, as demonstrated with NS1, which are the most difficult to study.

Another very interesting ERAD reporter system could be based on *E. coli* enzyme lipoic acid ligase (LplA). Engineered mutant of this ligase are capable of recognizing fluorescent substrates and catalysing, both in vitro and in living cells, their covalent conjugation to a short 13 amino acids long peptide (GFEIDKVWYDLDA) called LplA Acceptor Peptide-2 (LAP-2) and other related small tags (Uttamapinant, et al., 2010; Cohen et al., 2011). The small molecular size (39kDa) and enzymatic features of LplA and mutants in conjugating the natural substrates and fluorophores to the appropriate target sequences are similar to BirA and TEVp (Slavoff et al., 2011; Kapust et al., 2001). This enzyme was already used to label proteins with compartment specificity (Uttamapinant, et al., 2010; Cohen et al., 2011) and thus should be useful for replacing BirA or TEVp since should provide a simple fluorescent based assay. In particular it could be useful to be used in genome wide siRNAs screenings to identify essential ERAD components in the still obscure ER to cytosol retrotranslocation step. It would be however interesting to compare the efficiency of such a system

with the ones here described and with the two recently published techniques to analyse ERAD in intact cells, which are based on two different ways of fluorescence reconstitution of split GFP, either based on PNGase activity or not (Zhong and Fang, 2012; Grotzke et al., 2013), in particular considering that the fluorescence reconstitution is probably substantially slower than BirA, TEVp or LplA activity (Kerppola, 2009).

In general, this approach of expressing cytosolic reporter enzymes should be useful and easily applicable to evaluate several kind of movements from an extracellular/luminal compartments to the cytosol of appropriately tagged molecules, compounds or viruses.

Acknowledgments

Lara Vecchi and Marco Bestagno contributed to experiment for the validation of BirA system. Data on CD4 and Tetherin models were performed in collaboration with Antonio Casini and Linda Sasset. Data on TEVp system were performed in collaboration with Francesca Cesaratto. US2 and US11 plasmids were kindly provided by Domenico Tortorella. NS1 plasmids were a kind gift of Linda Hendershot, as the p97 and p97QQ plasmids. OTU plasmid was supplied by Adolfo García-Sastre.

References

Abbott J and Beckett D. Cooperative binding of the Escherichia coli repressor of biotin biosynthesis to the biotin operator sequence. Biochemistry. 1993; 32(37):9649-56.

Ackerman A.L., Giodini A., Cresswell P. A role for the endoplasmic reticulum protein retrotranslocation machinery during crosspresentation by dendritic cells. Immunity. 2006; 25:607–617.

Adachi, Y., Yamamoto, K., Okada, T., Yoshida, H., Harada, A., & Mori, K. ATF6 is a transcription factor specializing in the regulation of quality control proteins in the endoplasmic reticulum. Cell structure and function. 2008; 33(1):75–89.

Afshar N., Black B.E., Paschal B.M. Retrotranslocation of the chaperone calreticulin from the endoplasmic reticulum lumen to the cytosol. Mol Cell Biol. 2005; 25:8844-8853.

Ahluwalia N, Bergeron J.J., Wada I., Degen E., Williams D.B. The p88 molecular chaperone is identical to the endoplasmic reticulum membrane protein, calnexin. J Biol Chem. 1992; 267(15):10914-8.

Albertini M., Rehling P., Erdmann R., Girzalsky W., Kiel J.A., Veenhuis M., Kunau W.H. Pex14p, a peroxisomal membrane protein binding both receptors of the two PTS-dependent import pathways. Cell. 1997; 89:83-92.

Amzel L.M., and Poljak, R.J. Three-dimensional structure of immunoglobulins. Annu. Rev. Immunol. 1979; *48*:961–997.

Andrew A.J., Miyagi E., Strebel K. Differential effects of human immunodeficiency virus type 1 Vpu on the stability of BST-2/tetherin. J. Virol. 2011; 85:2611–2619.

Appenzeller-Herzog C. and Hauri H.P. The ER–Golgi intermediate compartment (ERGIC): in search of its identity and function. J. Cell Sci. 2006; 119:2173–2183.

Archibald J.M., Teh E.M., Keeling P.J. Novel Ubiquitin Fusion Proteins: Ribosomal Protein P1 and Actin. Journal of Molecular Biology. 2003; 328 (4):771-778.

Arnold S.M., Fessler L.I., Fessler J.H., Kaufman R.J. Two homologues encoding human UDP-glucose:glycoprotein glucosyltransferase differ in mRNA expression and enzymatic activity. Biochemistry. 2000; 39:2149-2163.

Ashok A., and Hegde R.S. Retrotranslocation of prion proteins from the endoplasmic reticulum by preventing GPI signal transamidation. Mol Biol Cell. 2008;19:3463–76.

Ashour J., Laurent-Rolle M., Shi P.-Y., García-Sastre A. NS5 of dengue virus mediates STAT2 binding and degradation. Journal of virology. 2009; *83*(11):5408–18.

Atreya C. D., Singh N.K., and Nakhasi H.L. The rubella virus RNA binding activity of human calreticulin is localized to the N-terminal domain. J. Virol. 1995; 69:3848–3851.

Avezov E., Frenkel Z., Ehrlich M., Herscovics A., Lederkremer G.Z. Endoplasmic reticulum (ER) mannosidase I is compartmentalized and required for N-glycan trimming to Man5-6GlcNAc2 in glycoprotein ER-associated degradation. Mol Biol Cell. 2008; 19:216-225.

Bagola K., Mehnert M., Jarosch E., Sommer T. Protein dislocation from the ER.Biochim Biophys Acta. 2011; 1808(3):925-36.

Baker B. M., and Tortorella D. Dislocation of an Endoplasmic Reticulum Membrane Glycoprotein Involves the Formation of Partially Dislocated Ubiquitinated Polypeptides. Journal of Biological Chemistry. 2007; *282*(37):26845–26856.

Baker R.T., Tobias J.W., Varshavsky A. Ubiquitin-specific proteases of Saccharomyces cerevisiae. J. Biol. Chem. 1992; 267:23364–23375.

Barel M.T., Ressing M., Pizzato N., van Leeuwen D., Le Bouteiller P., Lenfant F., Wiertz E.J.

Human cytomegalovirus-encoded US2 differentially affects surface expression of MHC class I locus products and targets membrane-bound, but not soluble HLA-G1 for degradation. J Immunol. 2003;171(12):6757-65.

Barker D.F., and Campbell A.M. The birA gene of Escherichia coli encodes a biotin holoenzyme synthetase. J Mol Biol. 1981;146:451-467.

Barlowe C. COPII-dependent transport from the endoplasmic reticulum. Curr Opin Cell Biol. 2002;14(4):417-22.

Baksh S., and Michalak M. Expression of calreticulin in Escherichia coli and identification of its Ca2+ binding domains. J. Biol. Chem. 1991; 266:21458–21465.

Baksh S., Spamer C., Heilmann C., Michalak M. Identification of the Zn2+ binding region in calreticulin. FEBS Lett. 1995;376:53–57.

Bause E., and Hettkamp H. Primary structural requirements for N-glycosylation of peptides in rat liver. FEBS Lett. 1979; 108(2):341-4.

Ballar P., Zhong Y., Nagahama M., Tagaya M., Shen Y., Fang S. Identification of SVIP as an endogenous inhibitor of endoplasmic reticulum-associated degradation. J Biol Chem. 2007; 282(47):33908-14.

Bannykh S.I., Rowe T., and Balch W.E. The organization of endoplasmic reticulum export complexes. J. Cell Biol. 1996; 135:19–35.

Baumeister W., Walz J., Zuhl F., Seemuller E. The proteasome: paradigm of a selfcompartmentalizing protease. Cell. 1998; 92:367-380.

Beckett D., Kovaleva E., Schatz P.J. A minimal peptide substrate in biotin holoenzyme synthetase-catalyzed biotinylation. Protein Sci. 1999; 8(4):921-9.

Bernasconi R., Galli C., Calanca V., Nakajima T., Molinari, M. Stringent requirement for HRD1, SEL1L, and OS-9/XTP3-B for disposal of ERAD-LS substrates. The Journal of cell biology. 2010; 188(2):223–35.

Bertolotti A., Zhang Y., Hendershot L., Harding H., Ron, D. Dynamic interaction of BiP and the ER stress transducers in the unfolded protein response. Nature Cell Biol. 2000; 2:326–332.

Besche H.C., Haas W., Gygi S.P., Goldberg A.L. Isolation of mammalian 26S proteasomes and p97/VCP complexes using the ubiquitin-like domain from HHR23B reveals novel proteasome-associated proteins. Biochemistry. 2009; 48(11):2538-49.

Bielli A., Haney C.J., Gabreski G., Watkins S.C., Bannykh S.I., Aridor, M. Regulation of Sar1 NH2 terminus by GTP binding and hydrolysis promotes membrane deformation to control COPII vesicle fission. J. Cell Biol. 2005; 171:919–924.

Biswas S., Katiyar S., Li G., Zhou X., Lennarz W.J., Schindelin H. The N-terminus of yeast peptide: N-glycanase interacts with the DNA repair protein Rad23. Biochem Biophys Res Commun. 2004; 323(1):149-55.

Blom D., Hirsch C., Stern P., Tortorella D., Ploegh H.L. A glycosylated type I membrane protein becomes cytosolic when peptide: N-glycanase is compromised. EMBO J. 2004; 23(3):650-8.

Bole D.G., Hendershot L.M., Kearney, J.F. Posttranslational association of immunoglobulin heavy chain binding protein with nascent heavy chains in nonsecreting and secreting hybridomas. J. Cell Biol. 1986; 102:1558–1566.

Bonifacino J.S., and Traub L.M. Signals for sorting of transmembrane proteins to endosomes and lysosomes. Annu. Rev. Biochem. 2003; 72:395-447.

Bordallo J., Plemper R.K., Finger A., Wolf D.H. Der3p/Hrd1p is required for endoplasmic reticulum-associated degradation of misfolded lumenal and integral membrane proteins. Mol

Biol Cell. 1998; 9(1):209-22.

Bose S., and Freedman R.B. Peptidyl prolyl cis-trans-isomerase activity associated with the lumen of the endoplasmic reticulum. Biochem J. 1994; 300(3):865-70.

Bour S., Schubert U., Strebel K. The human immunodeficiency virus type 1 Vpu protein specifically binds to the cytoplasmic domain of CD4: implications for the mechanism of degradation, J. Virol. 1995; 69:1510-1520.

Bour S., Perrin C., Akari H., Strebel K. The human immunodeficiency virus type 1 Vpu protein inhibits NF-kappa B activation by interfering with beta TrCP-mediated degradation of Ikappa B. J Biol Chem. 2001; 276(19):15920-8.

Bowers K., Pitcher C., Marsh M. CD4: a co-receptor in the immune response and HIV infection. Int J Biochem Cell Biol. 1997; 29(6):871-5.

Breyton C., Haase W., Rapoport T.A., Kühlbrandt W., Collinson I. Three-dimensional structure of the bacterial protein-translocation complex SecYEG. Nature. 2002; 418(6898):662-5.

Brown D.A. Seeing is believing: visualization of rafts in model membranes. Proc Natl Acad Sci U S A. 2001; 98(19):10517-8.

Budnik A., and Stephens D.J. ER exit sites – Localization and control of COPII vesicle formation. FEBS Letters. 2009; 583(23):3796–3803.

Cai H., Wang C.C., Tsou C.L. Chaperone-like activity of protein disulfide isomerase in the refolding of a protein with no disulfide bonds. J Biol Chem. 1994; 269(40):24550-2.

Cadwell K., and Coscoy L. Ubiquitination on nonlysine residues by a viral E3 ubiquitin ligase. Science. 2005; 309:127–130.

Capodagli G.C., McKercher M.A., Baker E.A., Masters, E.M., Brunzelle J.S., Pegan, S.D. Structural analysis of a viral ovarian tumor domain protease from the Crimean-Congo hemorrhagic fever virus in complex with covalently bonded ubiquitin. Journal of virology. 2011; 85(7):3621–30.

Caramelo J.J., Castro O.A., Alonso L.G., De Prat-Gay G., Parodi A.J. UDP-Glc:glycoprotein glucosyltransferase recognizes structured and solvent accessible hydrophobic patches in molten globule-like folding intermediates. Proc Natl Acad Sci U S A. 2003; 100(1):86-91.

Caramelo J.J., Parodi A.J. Getting in and out from calnexin/calreticulin cycles. J Biol Chem. 2008; 283(16):10221-5.

Carlson E.J., Pitonzo D., Skach W.R. p97 functions as an auxiliary factor to facilitate TM domain extraction during CFTR ER-associated degradation. EMBO J. 2006: 25:4557-4566.

Carpio M.A., López Sambrooks C., Durand E.S., Hallak M.E.. The arginylation-dependent association of calreticulin with stress granules is regulated by calcium. The Biochemical journal. 2010; 429(1):63–72.

Carroll S.M., Hampton R.Y. Usa1p is required for optimal function and regulation of the Hrd1p endoplasmic reticulum-associated degradation ubiquitin ligase. J Biol Chem. 2010; 285(8):5146-56.

Carvalho P., Goder V., Rapoport T.A. Distinct ubiquitin-ligase complexes define convergent pathways for the degradation of ER proteins. Cell. 2006;126(2):361-73.

Ceriani M.F., Marcos J.F., Hopp H.E., Beachy R.N. Simultaneous accumulation of multiple viral coat proteins from a TEV-NIa based expression vector. Plant Molecular Biology. 1998; 36:239-248.

Chang S.C., Momburg F., Bhutani N., Goldberg A.L. The ER aminopeptidase, ERAP1, trims precursors to lengths of MHC class I peptides by a "molecular ruler" mechanism. Proc Natl Acad Sci USA. 2005; 102(47):17107-12.

Chau V., Tobias J.W., Bachmair A., Marriott D., Ecker D.J., Gonda D.K., Varshavsky A. A multiubiquitin chain is confined to specific lysine in a targeted short-lived protein. Science. 1989; 243:1576–83.

Chapman-Smith A., and Cronan J.E. The enzymatic biotinylation of proteins: a post-translational modification of exceptional specificity. Trends in biochemical sciences. 1999; 24(9):359–63.

Chen X., Karnovsky A., Sans M.D., Andrews P.C., Williams J.A. Molecular characterization of the endoplasmic reticulum: Insights from proteomic studies. Proteomics. 2010; 10(22):4040-52.

Chen Y., Hu D., Yabe R., Tateno H., Qin S.Y., Matsumoto N., Hirabayashi J., Yamamoto K. Role of malectin in Glc(2)Man(9)GlcNAc(2)-dependent quality control of α1-antitrypsin. Molecular biology of the cell. 2011; 22(19):3559–70.

Chen X., Brown T., Tai P.C. Identification and characterization of protease-resistant SecA fragments: secA has two membrane-integral forms. J Bacteriol. 1998; 180(3):527-37.

Chevalier M.S., Daniels G.M., Johnson D.C. Binding of human cytomegalovirus US2 to major histocompatibility complex class I and II proteins is not sufficient for their degradation. J Virol. 2002; 76(16):8265-75.

Chevalier M.S., Johnson D.C. Human cytomegalovirus US3 chimeras containing US2 cytosolic residues acquire major histocompatibility class I and II protein degradation properties. J Virol. 2003; 77(8):4731-8.

Chillaròn J., and Haas I.G. Dissociation from BiP and Retrotranslocation of Unassembled Immunoglobulin Light Chains Are Tightly Coupled to Proteasome Activity. Molecular Biology of the Cell. 2000; 11:217–226.

Cho H.S., Mason K., Ramyar K.X., Stanley A.M., Gabelli S.B., Denney D.W. Jr., Leahy D.J. Structure of the extracellular region of HER2 alone and in complex with the Herceptin Fab. Nature. 2003; 421(6924):756-60.

Choi A.G., Wong J., Marchant D., Luo H. The ubiquitin-proteasome system in positive-strand RNA virus infection. Rev Med Virol. 20130; 23(2):85-96.

Chou T., Brown S.J., Minond D., Nordin B.E., Li K., Jones A.C., Chase P. Reversible inhibitor of p97, DBeQ, impairs both ubiquitin-dependent and autophagic protein clearance pathways. Proceedings of the National Academy of Sciences of the United States of America. 2011; 108(12):4834-4839.

Christianson J.C., Shaler T.A., Tyler R.E., Kopito R.R. OS-9 and GRP94 deliver mutant alpha1-antitrypsin to the Hrd1-SEL1L ubiquitin ligase complex for ERAD. Nat Cell Biol. 2008; 10:272-282.

Christianson J.C., Olzmann J.A., Shaler T.A., Sowa M.E., Bennett E.J., Richter C.M., Tyler R.E., Greenblatt E.J., Harper J., Kopito R.R. Defining human ERAD networks through an integrative mapping strategy. Nature cell biology. 2012; 14(1):93–105.

Ciechanover A., and Ben-Saadon, R. N-terminal ubiquitination: more protein substrates join in. Trends Cell Biol. 2004; 14, 103–106.

Ciechanover A. The ubiquitin proteolytic system: from a vague idea, through basic mechanisms, and onto human diseases and drug targeting. Neurology. 2006; 66(2 Suppl 1):S7-19.

Claessen J.H.L., Kundrat L., Ploegh, H.L. Protein quality control in the ER: balancing the ubiquitin checkbook. Trends in Cell Biology. 2012; 22(1):22–32.

Clerc S. Hirsch C., Oggier D.M., Deprez P., Jakob C., Sommer T., Aebi M. Htm1 protein generates the N-glycan signal for glycoprotein degradation in the endoplasmic reticulum. J Cell Biol. 2009; 184:159-172.

Cohen J.D., Thompson S., Ting A.Y. Structure-guided engineering of a Pacific Blue fluorophore ligase for specific protein imaging in living cells. Biochemistry. 2011; 50(38):8221-5.

Connoly T. and Gilmore R. Formation of a functional ribosome-membrane junction during translocation requires the participation of a GTP-binding protein. J Cell Biol. 1986; 103(6 Pt 1):2253-61.

Connoly T. and Gilmore R. GTP hydrolysis by complexes of the signal recognition particle and the signal recognition particle receptor. J Cell Biol. 1993; 123(4):799-807.

Contin R., Arnoldi F., Mano M., Burrone O.R. Rotavirus replication requires a functional proteasome for effective assembly of viroplasms. J Virol. 2011; 85(6):2781-92.

Cooper E. M., Cutcliffe C., Kristiansen T. Z., Pandey A., Pickart C. M., Cohen R. E. K63-specific deubiquitination by two JAMM/MPN+ complexes: BRISC-associated Brcc36 and proteasomal Poh1. EMBO journal. 2009; 28(6):621–31.

Corbett E.F., Michalak K.M., Oikawa K., Johnson S., Campbell I.D., Eggleton P., Kay C., Michalak M. The conformation of calreticulin is influenced by the endoplasmic reticulum lumenal environment. J. Biol. Chem. 2000; 275:27177–27185.

Cowan N.J., Secher D.S., Milstein C. Intracellular immunoglobulin chain synthesis in non-secreting variants of a mouse myeloma: detection of inactive light-chain messenger RNA. J Mol Biol. 1974; 90(4):691-701.

Credle J.J., Finer-Moore J.S., Papa F.R., Stroud R.M., Walter P. On the mechanism of sensing unfolded protein in the endoplasmic reticulum. Proceedings of the National Academy of Sciences of the United States of America. 2005; 102(52):18773–84.

Crise B., and Rose J.K. Identification of palmitoylation sites on CD4, the human immunodeficiency virus receptor. J. Biol. Chem. 1992; 267:13593–13597.

Crowley K.S., Reinhart G.D., Johnson A.E. The signal sequence moves through a ribosomal tunnel into a noncytoplasmic aqueous environment at the ER membrane early in translocation. Cell. 1993; 73(6):1101-15.

Crowley K.S., Liao S., Worrell V.E., Reinhart G.D., Johnson A.E. Secretory proteins move through the endoplasmic reticulum membrane via an aqueous, gated pore. Cell. 1994; 78(3):461-71.

Cyr D.M., and Hebert D.N. Protein quality control--linking the unfolded protein response to disease. Conference on 'From Unfolded Proteins in the Endoplasmic Reticulum to Disease'. EMBO Rep. 2009; 10(11):1206-10.

D'Arcy P., and Linder S. Proteasome deubiquitinases as novel targets for cancer therapy. Int J Biochem Cell Biol. 2012; 44(11):1729-38.

Davies J.M., Brunger A.T., Weis W.I. Improved structures of full-length p97, an AAA ATPase: implications for mechanisms of nucleotide-dependent conformational change. Structure. 2008; 16(5), 715–26.

Decca M.B., Carpio M.A., Bosc C., Galiano M.R., Job D., Andrieux A., Hallak, M.E. Post-translational arginylation of calreticulin : a new isospecies of calreticulin component of stress granules. J Biol Chem. 2007; 282(11):8237–8245.

DeLaBarre B., Brunger A.T. Nucleotide dependent motion and mechanism of action of p97/VCP. J Mol Biol. 2005; 347(2):437-52.

DeLaBarre B., Christianson J.C., Kopito R.R., Brunger A.T. Central pore residues mediate the p97/VCP activity required for ERAD. Mol Cell. 2006; 22(4):451-62.

Denisov A.Y., Maattanen P., Dabrowski C., Kozlov G., Thomas D.Y., Gehring K. Solution structure of the bb' domains of human protein disulfide isomerase. FEBS J. 2009; 276: 1440–1449.

Deprez P., Gautschi M., Helenius A. More than one glycan is needed for ER glucosidase II to allow entry of glycoproteins into the calnexin/calreticulin cycle. Molecular Cell. 2005 19:183–195.

Ding W.X., and Yin X.M. Sorting, recognition and activation of the misfolded protein degradation pathways through macroautophagy and the proteasome. Autophagy. 2008; 4:141-150.

Dong B., Niwa M., Walter P., Silverman R.H. Basis for regulated RNA cleavage byfunctional analysis of RNase L and Ire1p. RNA. 2001; 7(3):361-73.

Doss-Pepe E.W., Stenroos E.S., Johnson W.G., Madura K. Ataxin-3 interactions with rad23 and valosin-containing protein and its associations with ubiquitin chains and the proteasome are consistent with a role in ubiquitin-mediated proteolysis. Mol Cell Biol. 2003; 23(18):6469-83.

Dougherty W.G., and Parks T.D. Post-translational processing of the tobacco etch virus 49-kDa small nuclear inclusion polyprotein: identification of an internal cleavage site and delimitation of VPg and proteinase domains. Virology. 1991;183(2):449-56.

Douglas J.L., Gustin J.K., Viswanathan K., Mansouri M., Moses A.V., Früh K. The great escape: viral strategies to counter BST-2/Tetherin. PLoS Pathog. 2010; 6(5):e1000913.

Dubé M., Roy B.B., Guiot-Guillain P., Binette J., Mercier J., Chiasson A., Cohen E.A. (2010). Antagonism of tetherin restriction of HIV-1 release by Vpu involves binding and sequestration of the restriction factor in a perinuclear compartment. PLoS pathogens. 6(4), e1000856.

Dubè M., Bego M.G., Paquay C., Cohen É.A. Modulation of HIV-1 host interaction: role of the Vpu accessory protein, Retrovirology. 2010; 7:114.

Dul J.L., Aviel S., Melnick J., Argon Y. Ig light chains are secreted predominantly as monomers. J. Immunol. 1996; 157:2969–2975 70.

Eisenhaber B., Bork P., Eisenhaber F. Post-translational GPI lipid anchor modification of proteins in kingdoms of life: analysis of protein sequence data from complete genomes. Protein Eng. 2001; 14:17–25.

Elkabetz Y., Shapira I., Rabinovich E., Bar-Nun S. Distinct steps in dislocation of luminal endoplasmic reticulum-associated degradation substrates: roles of endoplamic reticulum-bound p97/Cdc48p and proteasome. J Biol Chem. 2004; 279:3980-3989.

Elsasser S., and Finley D. Delivery of ubiquitinated substrates to protein-unfolding machines. Nat Cell Biol. 2005; 7(8):742-9.

Elsasser S., Chandler-Militello D., Mueller B., Finley D. Rad23 and Rpn10 serve as alternative ubiquitin receptors for the proteasome. J Biol Chem. 2004; 279:26817–22.

Ellgaard L., Molinari M., Helenius A. Setting the standards: quality control in the secretory pathway. Science. 1999; 286(5446):1882-8.

Ellgaard L., and Ruddock L.W. The human protein disulphide isomerase family: substrate interactions and functional properties. Embo Rep. 2005; 6(1):28-32.

Emerman A.B., Zhang Z., Chakrabarti O., Hegde R.S. Compartment-Restricted Biotinylation Reveals Novel Features of Prion Protein Metabolism in Vivo. Mol Biol Cell. 2010; 21:4325–4337.

Ernst R., Mueller B., Ploegh H.L., Schlieker C. The otubain YOD1 is a deubiquitinating enzyme that associates with p97 to facilitate protein dislocation from the ER. Molecular cell. 2009;36(1):28-38.

Ernst R., Claessen J.H.L., Mueller B., Sanyal S., Spooner E., van der Veen A. G., Kirak O., Schlieker C.D., Weihofen W.A., Ploegh, H.L. Enzymatic blockade of the ubiquitin-proteasome pathway. PLoS biology. 2011;8(3):e1000605.

Evans E.A., Gilmore R., Blobel G. Purification of microsomal signal peptidase as a complex. Proc Natl Acad Sci U S A. 1986; 83(3):581-5.

Ewart G.D., Sutherland T., Gage P.W., Cox G.B. The Vpu protein of human immunodeficiency virus type 1 forms cation-selective ion channels, J. Virol. 1996; 70:7108–7115.

Fagioli C., Mezghrani A., Sitia R. Reduction of interchain disulfide bonds precedes the dislocation of Ig-mu chains from the endoplasmic reticulum to the cytosol for proteasomal degradation. J Biol Chem. 2001; 276(44):40962-7.

Feige M.J., Groscurth S., Marcinowski M., Shimizu Y., Kessler H., Hendershot L.M., Buchner J. An unfolded CH1 domain controls the assembly and secretion of IgG antibodies. Mol. Cell. 2009; 34(5):569–579.

Feige M.J., and Hendershot L.M. Disulfide bonds in ER protein folding and homeostasis. Current Opinion in Cell Biology. 2011; 23(2):167–175.

Feng M., Gu C., Ma S., Wang Y., Liu H., Han R., Gao J., Long Y., Mi H. Mouse FKBP23 mediates conformer-specific functions of BiP by catalyzing Pro117 cis/trans isomerization, Biochemical and Biophysical Research Communications. 2011; 408(4):537-40.

Fiebiger E., Story C., Ploegh H.L., Tortorella D. Visualization of the ER-to-cytosol dislocation reaction of a type I membrane protein. EMBO J. 2002; *21*(5):1041–1053.

Finley D. Recognition and processing of ubiquitin-protein conjugates by the proteasome. Annu Rev Biochem. 2009; 78:477-513.

Fliegel L., Burns K., MacLennan D.H., Reithmeier R.A., Michalak M. Molecular cloning of the high affinity calcium-binding protein (calreticulin) of skeletal muscle sarcoplasmic reticulum. J Biol Chem. 1989; 264(36):21522-8.

Flierman D., Ye Y., Dai M., Chau V., Rapoport T.A. Polyubiquitin serves as a recognition signal, rather than a ratcheting molecule, during retrotranslocation of proteins across the endoplasmic reticulum membrane. The Journal of biological chemistry. 2003; 278(37):34774–82.

Förster F., Lasker K., Nickell S., Sali A., Baumeister W. Toward an integrated structural model of the 26S proteasome. Molecular & cellular proteomics. 2010;. 9(8):1666–77.

Fournier M., Peyrou M., Bourgoin L., Maeder C., Tchou I., Foti M. CD4 dimerization requires two cysteines in the cytoplasmic domain of the molecule and occurs in microdomains distinct from lipid rafts. Molecular immunology. 2010; 47(16):2594–603.

Frenkel Z., Shenkman M., Kondratyev M., Lederkremer G.Z: Separate roles and different routing of calnexin and ERp57 in endoplasmic reticulum quality control revealed by interactions with asialoglycoprotein receptor chains. Mol Biol Cell. 2004;15:2133-2142.

Frias-Staheli N., Giannakopoulos N.V, Kikkert M., Taylor S.L., Bridgen A., Paragas J., Richt J.A., Rowland R.R., Schmaljohn C.S., Lenschow D.J., Snijder E.J., García-Sastre A., Virgin H.W. Ovarian tumor domain-containing viral proteases evade ubiquitin- and ISG15-dependent innate immune responses. Cell host & microbe. 2007; 2(6):404–16.

Frickel E. M., Riek R., Jelesarov I., Helenius A., Wuthrich K., Ellgaard L. TROSY-NMR reveals interaction between ERp57 and the tip of the calreticulin P-domain. Proc Nat Acad Sci U S A. 2002; 99(4):1954-1959.

Friedberg E.C., Lehmann A.R., Fuchs R.P. Trading places: how do DNA polymerases switch during translesion DNA synthesis? Mol. Cell. 2005; 18(5):499-505.

Fujii K., Kitabatake M., Sakata T., Ohno M. 40S subunit dissociation and proteasome-dependent RNA degradation in nonfunctional 25S rRNA decay. EMBO J. 2012; 31(11):2579–89.

Furman M.H., Loureiro J., Ploegh H.L., Tortorella D. Ubiquitinylation of the cytosolic domain of a type I membrane protein is not required to initiate its dislocation from the endoplasmic

reticulum. J Biol Chem. 2003; 278(37):34804-11.

Galan J.M., and Haguenauer-Tsapis R. Ubiquitin lys63 is involved in ubiquitination of a yeast plasma membrane protein. EMBO J. 1997 16(19), 5847-54.

Galli C., Bernasconi R., Soldà T., Calanca V., Molinari M. Malectin participates in a backup glycoprotein quality control pathway in the mammalian ER. PloSone. 2011; 6(1): e16304.

Garbi N., Tanaka S., van den Broek M., Momburg F., Hämmerling G.J. Accessory molecules in the assembly of major histocompatibility complex class I/peptide complexes: how essential are they for CD8(+) T-cell immune responses? Immunol Rev. 2005; 207:77-88.

Garbi N., Tiwari N., Momburg F., Hämmerling G.J. A major role for tapasin as a stabilizer of the TAP peptide transporter and consequences for MHC class I expression. Eur J Immunol. 2003; 33(1):264-73.

Geiger R., Andritschke D., Friebe S., Herzog F., Luisoni S., Heger T., Helenius A. BAP31 and BiP are essential for dislocation of SV40 from the endoplasmic reticulum to the cytosol. Nat Cell Biol. 2011;13:1305-1314.

Geraghty R.J., Talbot K.J., Callahan M., Harper W., Panganiban A.T: Cell typedependence for Vpu function. J Med Primatol. 1994; 23:146-150.

Germain R.N. MHC-dependent antigen processing and peptide presentation: providing ligands for T lymphocyte activation. Cell. 1994; 76:287-299.

Gething M.J. Role and regulation of the ER chaperone BiP. Semin Cell Dev Biol. 1999; 10(5):465-72.

Gewurz B.E., Gaudet R., Tortorella D., Wang E.W., Ploegh H.L., Wiley D.C. Antigen presentation subverted: Structure of the human cytomegalovirus protein US2 bound to the class I molecule HLA-A2. Proc Natl Acad Sci USA. 2001; 5;98(12):6794-9.

Gewurz B.E., Ploegh H.L., Tortorella D. US2, a human cytomegalovirus-encoded type I membrane protein, contains a non-cleavable amino-terminal signal peptide. J Biol Chem. 2002; 277(13):11306-13.

Gilbert J., Ou W., Silver J., Benjamin T. Downregulation of protein disulfide isomerase inhibits infection by the mouse polyomavirus. J. Virol. 2006; 80:10868–10870.

Glickman M.H., Rubin D.M., Coux O., Wefes I., Pfeifer G., Cjeka Z., Baumeister W., Fried V.A., Finley D. A subcomplex of the proteasome regulatory particle required for ubiquitin–conjugate degradation and related to the COP9-signalosome and eIF3. Cell. 1998; 94:615–623.

Goder V., Bieri C., Spiess M. Glycosylation can influence topogenesis of membrane proteins and reveals dynamic reorientation of nascent polypeptides within the translocon. J. Cell Biol. 1999; 147:257–266.

Goffinet C., Allespach I., Homann S., Tervo H.M., Habermann A., Rupp D., Oberbremer L., Kern C., Tibroni N., Welsch S., Krijnse-Locker J., Banting G., Krausslich H.G., Fackler O.T., Keppler O.T. HIV-1 antagonism of CD317 is species specific and involves Vpu-mediated proteasomal degradation of the restriction factor, Cell Host Microbe. 2009; 5:285–297.

Gold L.I., Eggleton P., Sweetwyne M.T., Van Duyn L.B., Greives M.R., Naylor S.M., Michalak M., Murphy-Ullrich J. E. Calreticulin: non-endoplasmic reticulum functions in physiology and disease. FASEB J. 2009; 24(3):665–683.

Goldberg A.L., Cascio P., Saric T., Rock K.L. The importance of the proteasome and subsequent proteolytic steps in the generation of antigenic peptides. Mol Immunol. 2002; 39:147–64.

Görlich D., Hartmann E., Prehn S., Rapoport T.A. A protein of the endoplasmic reticulum involved early in polypeptide translocation. Nature. 1992; 357(6373):47-52.

Görlich D., and Rapoport T.A. Protein translocation into proteoliposomes reconstituted from purified components of the endoplasmic reticulum membrane. Cell. 1993; 75(4):615-30.

Grenfell S.J., Trausch-Azar J.S., Handley-Gearhart P.M., Ciechanover A., Schwartz A.L. Nuclear localization of the ubiquitin-activating enzyme, E1, is cell-cycle-dependent. Biochem J 1994; 300(Pt 3):701-708.

Groisman B., Shenkman M., Ron E., Lederkremer G.Z. Mannose Trimming Is Required for Delivery of a Glycoprotein from EDEM1 to XTP3-B and to Late Endoplasmic Reticulum-associated Degradation Steps. J Biol Chem. 2011; 286(2):1292–1300.

Groll M., Ditzel L., Löwe J., Stock D., Bochtler M., Bartunik H.D., Huber R. Structure of 20S proteasome from yeast at 2.4 Å resolution. Nature. 1997; 386:463–471.

Groll M., Bajorek M., Kohler A., Moroder L., Rubin D.M., Huber R., Glickman M.HFinley., D. A gated channel into the proteasome core particle. Nat. Struct. Biol. 2000; 7(11):1062–1067.

Grotzke J.E., Lu Q., Cresswell P. Deglycosylation-dependent fluorescent proteins provide unique tools for the study of ER-associated degradation. Proceedings of the National Academy of Sciences of the United States of America. 2013; 110(9):3393–8.

Ha B.H., and Kim E.E. Structures of proteases for ubiqutin and ubiquitin-like modifiers. BMB reports. 2008; 41(6):435–43.

Haas IG, Wabl M. Immunoglobulin heavy chain binding protein. Nature. 1983 Nov 24-30;306(5941):387-9.

Hagiwara M., Maegawa K., Suzuki M., Ushioda R., Araki K., Matsumoto Y., Hoseki J., Nagata K., Inaba, K. Structural basis of an ERAD pathway mediated by the ER-resident protein disulfide reductase ERdj5. Mol Cell. 2011; 41:432-444.

Hagiwara M., and Nagata K. Redox-Dependent Protein Quality Control in the Endoplasmic Reticulum: Folding to Degradation. Antioxidants & Redox Signaling. 2012; 16(10):1119-1128.

Hamman B.D., Chen J.C., Johnson E.E., Johnson A.E. The aqueous pore through the translocon has a diameter of 40-60 A during cotranslational protein translocation at the ER membrane. Cell. 1997; 89(4):535-44.

Hampton R.Y., and Sommer T. Finding the will and the way of ERAD substrate retrotranslocation. Current opinion in cell biology. 2012; 24(4):460–6.

Hansen T.H., and Bouvier M. MHC class I antigen presentation: learning from viral evasion strategies. Nat Rev Immunol. 2009; 9(7):503-13.

Harding H.P., Zhang Y., Ron D. Protein translation and folding are coupled by an endoplasmic-reticulum-resident kinase. Nature. 1999; 397(6716):271-4.

Harding H.P., Zhang Y., Bertolotti A., Zeng H., Ron D. Perk is essential for translational regulation and cell survival during the unfolded protein response. Mol Cell. 2000;5(5):897-904.

Harding H.P., Calfon M., Urano F., Novoa I., Ron D. Transcriptional and translational control in the Mammalian unfolded protein response. Annu Rev Cell Dev Biol. 2002; 18:575-99.

Hassink G.C., Barel M.T., Van Voorden S.B., Kikkert M., Wiertz E.J. Ubiquitination of MHC class I heavy chains is essential for dislocation by human cytomegalovirus-encoded US2 but not US11. J Biol Chem. 2006; 281:30063-30071.

Haynes C.M., Caldwell S., Cooper A.A. An HRD/DER-independent ER quality control mechanism involves Rsp5p-dependent ubiquitination and ER-Golgi transport. J Cell Biol. 2002; 158:91-101.

Hatakeyama S., and Nakayama K.I. U-box proteins as a new family of ubiquitin ligases. Biochem Biophys Res Commun. 2003; 302:635-645.

Haze K., Yoshida H., Yanagi H., Yura T., Mori K. Mammalian transcription factor ATF6 is synthesized as a transmembrane protein and activated by proteolysis in response to endoplasmic reticulum stress. Mol Biol Cell. 1999; 10(11):3787-99.

Haze K., Okada T., Yoshida H., Yanagi H., Yura T., Negishi M., Mori K. Identification of the G13 (cAMP-response-element-binding protein-related protein) gene product related to activating transcription factor 6 as a transcriptional activator of the mammalian unfolded protein response. Biochem J. 2001; 355(Pt 1):19-28.

Heinrich S.U., Mothes W., Brunner J., Rapoport T.A. The Sec61p complex mediates the integration of a membrane protein by allowing lipid partitioning of the transmembrane domain.Cell. 2000;102(2):233-44.

Hengel H., Flohr T., Hämmerling G.J., Koszinowski U.H., Momburg F. Human cytomegalovirus inhibits peptide translocation into the endoplasmic reticulum for MHC class I assembly. J Gen Virol. 1996; 77(Pt 9):2287-96.

Henrichs T., Mikhaleva N., Conz C., Deuerling E., Boyd D., Zelazny A., Bibi E., Ban N., Ehrmann M. Target-directed proteolysis at the ribosome. Proc Natl Acad Sci USA. 2005; 102:4246–4251.

Hebert D.N., Bernasconi R., Molinari M. ERAD substrates: Which way out? Seminars in Cell & Developmental Biology. 2010; 21:526–532.

Hershko A., Heller H., Elias S., Ciechanover A. Components of ubiquitin-protein ligase system. Resolution, affinity purification, and role in protein breakdown. J. Biol. Chem. 1983; 258:8206–8214.

Hewitt, E. W. The MHC class I antigen presentation pathway: strategies for viral immune evasion. Immunology. 2003; 110:163-169.

Hicke L. Protein regulation by monoubiquitin. Nat Rev Mol Cell Biol. 2001; 2:195-201.

Hiller M.M., Finger A., Schweiger M., Wolf D.H. ER degradation of a misfolded luminal protein by the cytosolic ubiquitin-proteasome pathway. Science. 1996; 273(5282):1725-8.

Hinz A., Miguet N., Natrajan G., Usami Y., Yamanaka H., Renesto P., Hartlieb B., McCarthy A.A., Simorre J.P., Göttlinger H., Weissenhorn W. Structural basis of HIV-1 tethering to membranes by the BST-2/tetherin ectodomain. Cell Host Microbe. 2010; 7:314-323.

Hipp M.S., Kalveram B., Raasi S., Groettrup M., Schmidtke G. FAT10, a ubiquitinindependent signal for proteasomal degradation. Mol. Cell Biol. 2005; 25:3483–91.

Hirsch C., Gauss R., Horn S.C., Neuber O., Sommer, T. The ubiquitylation machinery of the endoplasmic reticulum. Nature. 2009; 458(7237):453–60.

Hirsch C., Blom D., Ploegh H.L. A role for N-glycanase in the cytosolic turnover of glycoproteins. EMBO J. 2003; 22(5):1036-46.

Hitchcock A.L., Krebber H., Frietze S., Lin A., Latterich M., Silver P.A. The conserved npl4 protein complex mediates proteasome-dependent membrane-bound transcription factor activation. Mol Biol Cell. 2001; 12(10):3226-41.

Hitt R., Wolf D.H. Der1p, a protein required for degradation of malfolded soluble proteins of the endoplasmic reticulum: topology and Der1-like proteins. FEMS Yeast Res. 2004; 4(7):721-9.

Ho S.C., Chaudhuri S., Bachhawat A., McDonald K., Pillai S. Accelerated proteasomal degradation of membrane Ig heavy chains. J Immunol. 2000; 164:4713–4719.

Hochstrasser M. Ubiquitin-dependent protein degradation. Annu Rev Genet 1996; 30, 405-439.

Hochstrasser M. Origin and function of ubiquitin-like proteins. Nature. 2009; 458(7237):422–9.

Hofle M., Linthicum S.D., Ioerger T. Analysis of diversity of nucleotide and amino acid distributions in the VD and DJ joining regions in Ig heavy chains. Mol. Immunol. 2000 37:827-835.

Hofmann K., and Bucher P. The UBA domain: a sequence motif present in multiple enzyme classes of the ubiquitination pathway. Trends Biochem Sci. 1996; 21(5):172-3.

Holaska J.M., Black B.E., Love D.C., Hanover J.A., Leszyk J., Paschal B.M. Calreticulin Is a receptor for nuclear export. J Cell Biol. 2001; 152:127-140.

Hollien J., and Weissman J.S. Decay of endoplasmic reticulum-localized mRNAs during the unfolded protein response. Science. 2006; 313(5783):104-7.

Horton R.E., and Vidarsson G. Antibodies and their receptors: different potential roles in mucosal defense. Front Immunol. 2013; 4:200.

Hoseki J., Ushioda R., Nagata K. Mechanism and components of endoplasmic reticulum associated degradation. J Biochem. 2010, 147(1):19–25.

Hosokawa N., Tremblay L.O., You Z., Herscovics A., Wada I., Nagata, K. Enhancement of endoplasmic reticulum (ER) degradation of misfolded Null Hong Kong alpha1-antitrypsin by human ER mannosidase I. Journal Biol Chem. 2003; 278(28):26287–94.

Hosokawa N., Wada I., Hasegawa K., Yorihuzi T., Tremblay L.O., Herscovics A., Nagata K. A novel ER alpha-mannosidase-like protein accelerates ER-associated degradation. EMBO reports. 2001; 2(5):415–22.

Hosokawa N., Wada I., Natsuka Y., Nagata K. EDEM accelerates ERAD by preventing aberrant dimer formation of misfolded alpha1-antitrypsin. Genes Cells. 2006; 11(5):465–76.

Hosokawa N., You Z., Tremblay L.O., Nagata K., Herscovics A. Stimulation of ERAD of misfolded null Hong Kong α1-antitrypsin by Golgi α1,2-mannosidases. Biochem Biophys Res Commun. 2007; 362:626–632.

Hosokawa N., Wada I., Nagasawa K., Moriyama T., Okawa K., Nagata K: Human XTP3-B forms an endoplasmic reticulum quality control scaffold with the HRD1-SEL1L ubiquitin ligase complex and BiP. J Biol Chem. 2008; 283:20914-20924.

Huard B. and Früh K. A role for MHC class I down-regulation in NK cell lysis of herpes virus-infected cells. Eur J Immunol. 2000; 30(2):509-15.

Hubbard S.C., and Robbins, P.W. Synthesis and processing of protein-linked oligosaccharides in vivo. J. Biol. Chem. 1979; 254:4568–4576.

Huber D., Boyd D., Xia Y., Olma M.H., Gerstein M., Beckwith J. Use of thioredoxin as a reporter to identify a subset of Escherichia coli signal sequences that promote signal recognition particle-dependent translocation. J Bacteriol. 2005a; 187(9):2983-91.

Huber D., Cha M.I., Debarbieux L., Planson A.G., Cruz N., López G., Tasayco M.L., Chaffotte A., Beckwith J. A selection for mutants that interfere with folding of Escherichia coli thioredoxin-1 in vivo. Proc Natl Acad Sci U S A. 2005b; 102(52):18872-7.

Hughes H., and Stephens D.J. Assembly, organization, and function of the COPII coat. Histochem Cell Biol. 2008;129:129–151.

Hussain A., Das S.R., Tanwar C., Jameel S. Oligomerization of the human immunodeficiency virus type I (HIV-1) Vpu protein - a genetic, biochemical and biophysical analysis. Virol. J. 2007; 4:81.

Iakova P., Wang G.L., Timchenko L., Michalak M., Pereira-Smith O.M., Smith J.R., Timchenko N.A. Competition of CUGBP1 and calreticulin for the regulation of p21 translation determines cell fate. EMBO J. 2004; 23:406–417.

Ireland B.S., Brockmeier U., Howe C.M., Elliott T., Williams D.B. Lectin-deficient calreticulin retains full functionality as a chaperone for class I histocompatibility molecules. Mol Biol Cell.

2008; 19:2413-2423.

Iwabu Y., Fujita H., Kinomoto M., Kaneko K., Ishizaka Y., Tanaka Y., Sata T., Tokunaga K. HIV-1 accessory protein Vpu internalizes cell-surface BST-2/tetherin through transmembrane interactions leading to lysosomes. J Biol Chem. 2009; 284(50):35060–72.

Iwawaki T., Hosoda A, Okuda T., Kamigori Y., Nomura-Furuwatari C., Kimata Y., Tsuru A., Kohno K. Translational control by the ER transmembrane kinase/ribonuclease IRE1 under ER stress. Nature cell biology. 2001; 3(2):158–64.

Jarosch E., Taxis C., Volkwein C., Bordallo J., Finley D., Wolf D. H., Sommer, T. Protein dislocation from the ER requires polyubiquitination and the AAA-ATPase Cdc48. Nat Cell Biol. 2002; 4:134-139.

Jentsch S., and Rumpf S. Cdc48 (p97): a "molecular gearbox" in the ubiquitin pathway? Trends in biochemical sciences. 2007; 32(1):6–11.

Joffre O.P., Segura E., Savina A., Amigorena S. Cross-presentation by dendritic cells. Nat Rev Immunol. 2012; 12(8):557-69.

Johnson D., and Travis J. Structural evidence for methionine at the reactive site of human alpha-1-proteinase inhibitor.J. Biol. Chem. 1978; 253:7142-7144.

Johnston S.C., Larsen C.N., Cook W.J., Wilkinson K.D. Hill C.P. Crystal structure of a deubiquiitnating enzyme (human UCH-L3) at 1.8 Å resolution. EMBO J. 1997; 16:3787-3796.

Jones T.R., Hanson L.K., Sun L., Slater J.S., Stenberg R.M., Campbell A.E. Multiple independent loci within the human cytomegalovirus unique short region down-regulate expression of major histocompatibility complex class I heavy chains. J Virol. 1995; 69(8):4830-41.

Jones T.R., Wiertz E.J., Sun L., Fish K.N., Nelson J.A., Ploegh H.L. Human cytomegalovirus US3 impairs transport and maturation of major histocompatibility complex class I heavy chains. Proc Natl Acad Sci USA. 1996; 93(21):11327-33.

Jonnalagadda S., Butt T.R., Monia B.P., Mirabelli C.K., Gotlib L., Ecker D.J., Crooke S.T. Multiple (alpha-NH-ubiquitin) protein endoproteases in cells. J. Biol. Chem. 1989; 264:10637–10642.

Kabat E. A., and Wu T. T. Identical V region amino acid sequences and segments of sequences in antibodies of different specificities. Relative contributions of VH and VL genes, minigenes, and complementary-determining regions to binding of antibody-combining sites. J. Immunol. 1991; 147:1709-1719.

Kalies K.U., Allan S., Sergeyenko T., Kröger H., Römisch K. The protein translocation channel binds proteasomes to the endoplasmic reticulum membrane.EMBO J. 2005; 24(13):2284-93.

Kamhi-Nesher S., Shenkman M., Tolchinsky S., Fromm S.V., Ehrlich R., Lederkremer G.Z. A novel quality control compartment derived from the endoplasmic reticulum. Mol Biol Cell. 2001; 12(6):1711-23.

Kamiya Y., Kamiya D., Yamamoto K., Nyfeler B., Hauri H.P., Kato K. Molecular basis of sugar recognition by the human L-type lectins ERGIC-53, VIPL, and VIP36. J Biol Chem. 2008; 283:1857-1861.

Kaneko M., Yasui S., Niinuma Y., Arai K., Omura T., Okuma Y., Nomura Y. A different pathway in the endoplasmic reticulum stress-induced expression of human HRD1 and SEL1 genes. FEBS Lett. 2007; 581:5355-5360.

Kaplun L., Tzirkin R., Bakhrat A., Shabek N., Ivantsiv Y., Raveh D. The DNA damage-inducible UbL-UbA protein Ddi1 participates in Mec1-mediated degradation of Ho endonuclease. Mol Cell Biol. 2005; 25(13):5355-62.

Kapust R.B., Tozsér J., Fox J.D., Anderson D.E., Cherry S., Copeland T.D., Waugh D.S.

Tobacco etch virus protease: mechanism of autolysis and rational design of stable mutants with wild-type catalytic proficiency. Prot. Eng. 2001; 14(12):993-1000.

Kario E., Tirosh B., Ploegh H.L., Navon A. N-linked glycosylation does not impair proteasomal degradation but affects class I major histocompatibility complex presentation. J Biol Chem. 2008; 283(1):244-54.

Katiyar S., Joshi S., Lennarz W.J. The retrotranslocation protein Derlin-1 binds peptide:N-glycanase to the endoplasmic reticulum. Mol Biol Cell. 2005; 16(10):4584-94.

Katiyar S., Li G., Lennarz W.J. A complex between peptide:N-glycanase and two proteasome-linked proteins suggests a mechanism for the degradation of misfolded glycoproteins. Proc Natl Acad Sci U S A. 2004; 101(38):13774-9.

Kerppola T.K. Visualization of molecular interactions using bimolecular fluorescence complementation analysis: characteristic of protein fragment complementation. Chem Soc Rev. 2009; 38(10), 2876–2886.

Kerscher O., Felberbaum R., and Hochstrasser M. Modification of proteins by ubiquitin and ubiquitin-like proteins. Annu. Rev. Cell Dev. Biol. 2006; 22:159–180.

Khalkhall Z., and Marshall R.D. Glycosylation of ribonuclease A catalysed by rabbit liver extracts. Biochem J. 1975; 146(2):299-307.

Khramtsov Y.V., Rokitskaya T.I., Rosenkranz A.A., Trusov G.A., Gnuchev N.V., Antonenko Y.N., Sobolev A.S. Modular drug transporters with diphtheria toxin translocation domain form edged holes in lipid membranes. J Control Release. 2008; 128(3):241-7.

Kikkert M., Hassink G., Barel M., Hirsch C., van der Wal F. J., Wiertz, E. Ubiquitination is essential for human cytomegalovirus US11-mediated dislocation of MHC class I molecules from the endoplasmic reticulum to the cytosol. Biochem J 2001; 358:369-377.

Kirkin V., McEwan D.G., Novak I., Dikic I. A role for ubiquitin in selective autophagy. Mol. Cell. 2009; 34:259–69.

Kirst M.E., Meyer D.J., Gibbon B.C., Jung R., Boston R.S. Identification and characterization of endoplasmic reticulum-associated degradation proteins differentially affected by endoplasmic reticulum stress. Physiol. 2005; 138(1):218-31.

Kisselev A.F., Akopian T.N., Woo K.M., Goldberg A.L. The sizes of peptides generated from protein by mammalian 26 and 20 S proteasomes. Implications for understanding the degradative mechanism and antigen presentation. J Biol Chem. 1999; 274:3363–71.

Knittler M. R., and Haas I. G. Interaction of BiP with newly synthesized immunoglobulin light chain molecules: cycles of sequential binding and release. The EMBO J. 1992;. 11(4):1573–81.

Kny M., Standera S., Hartmann-Petersen R., Kloetzel P.-M., and Seeger M. Herp regulates Hrd1-mediated ubiquitylation in a ubiquitin-like domain-dependent manner. J Biol Chem. 2011; 286(7):5151–6.

Kobayashi S., Uchiyama S., Sone T., Noda M., Lin L., Mizuno H., Matsunaga S. Fukui, K. Calreticulin as a new histone binding protein in mitotic chromosomes. Cytogenet. Genome Res. 2006; 115:10–15.

Kobayashi T., Wang J., Al-Ahmadie H., Abate-Shen C. ARF Regulates the Stability of p16 Protein Via REGγ-Dependent Proteasome Degradation. Mol Cancer Res. 2013; 11(8):828-33.

Koegl M.,Hoppe T., Schlenker S., Ulrich H.D., Mayer T.U., Jentsch S. A novel ubiquitination factor, E4, is involved in multiubiquitin chain assembly. Cell. 1999; 96:635-44.

Kokame K., Kato H., Miyata, T. Identification of ERSE-II, a new cis-acting element responsible for the ATF6 dependent mammalian unfolded protein response. J Biol. Chem. 2001; 276:9199-9205.

Komada M., and Kitamura N. The Hrs/STAM complex in the downregulation of receptor tyrosine kinases. J Biochem. 2005; 137(1):1-8.

Komander D., and Rape M. The ubiquitin code. Annual review of biochemistry 2012; 81:203–29.

Kondratyev M., Avezov E., Shenkman M., Groisman B., Lederkremer G.Z. PERK-dependent compartmentalization of ERAD and unfolded protein response machineries during ER stress. Exp Cell Res. 2007; 313:3395-3407.

Kostallas G., Löfdahl P.Å., and Samuelson P. Substrate profiling of tobacco etch virus protease using a novel fluorescence-assisted whole-cell assay. PloS One 2011; 6(1):e16136.

Kothe M., Ye Y., Wagner J.S., De Luca H.E., Kern E., Rapoport T.A., Lencer W.I. Role of p97 AAA-ATPase in the retrotranslocation of the cholera toxin A1 chain, a non-ubiquitinated substrate. J Biol Chem. 2005; 280(30):28127-32.

Kowarik M., Küng S., Martoglio B., Helenius A. Protein folding during cotranslational translocation in the endoplasmic reticulum. Mol Cell. 2002; 10(4):769-78.

Kozlov G., Määttänen P., Thomas D.Y., Gehring K. A structural overview of the PDI family of proteins. FEBS J: 2010; 277(19):3924-36.

Krause K., and Michalak M. Calreticulin. Cell. 1997; 88(4):439-43.

Krieg U.C., Walter P., Johnson A.E. Photocrosslinking of the signal sequence of nascent preprolactin to the 54-kilodalton polypeptide of the signal recognition particle. PNAS 1986; 83(22):8604-8.

Kunjappu M.J., and Hochstrasser M. Assembly of the 20S proteasome. Biochimica et biophysica acta. 2013; pii: S0167-4889(13)00099-2.

Kwon Y., Kashina A., Varshavsky A. Alternative splicing results in differential expression, activity, and localization of the two forms of arginyl-tRNA-protein transferase, a component of the N-end rule pathway. Mol Cell Biol. 1999;19:182–193.

Lange O.F., Lakomek N.A., Fares C., Schroder G.F., Walter K.F., Becker S., Meiler J., Grubmuller H., Griesinger C., de Groot B.L. Recognition dynamics up to microseconds revealed from an RDC-derived ubiquitin ensemble in solution. Science. 2008; 320:1471-1475.

Larsen C.N., Krantz B.A. and Wilkinson K.D. Substrate specificity of deubiquitinating enzymes: ubiquitin C-terminal hydrolases. Biochemistry. 1998; 37:3358-3368.

Lappi A.K., and Ruddock L.W. Reexamination of the role of interplay between glutathione and protein disulfide isomerase. J Mol Biol. 2011; 409(2):238-49.

Latres E., Chiaur D.S., Pagano M. The human F box protein beta-Trcp associates with the Cul1/Skp1 complex and regulates the stability of beta-catenin. Oncogene. 1999; 18:849-854.

Lavoie C., Paiement J. Topology of molecular machines of the endoplasmic reticulum: a compilation of proteomics and cytological data. Histochem Cell Biol. 2008; 129(2):117-28.

Law R.H., Lukoyanova N., Voskoboinik I., Caradoc-Davies T.T., Baran K., Dunstone M.A., D'Angelo M.E., Orlova E.V., Coulibaly F., Verschoor S., Browne K.A., Ciccone A., Kuiper M.J., Bird P.I., Trapani J.A., Saibil H.R., Whisstock J.C. The structural basis for membrane binding and pore formation by lymphocyte perforin. Nature. 2010; 468:447-451.

Lederkremer G.Z., Cheng Y., Petre B.M., Vogan E., Springer S., Schekman R., Walz T., Kirchhausen, T. Structure of the Sec23p/24p and Sec13p/31p complexes of COPII. Proc. Natl. Acad. Sci. USA. 2001; 98:10704–10709.

Lederkremer G.Z. Glycoprotein folding, quality control and ER-associated degradation. Current Opinion in Structural Biology. 2009; 19:515–523.

Lee Y.K., Brewer J.W., Hellman R., Hendershot L.M. BiP and immunoglobulin light chain cooperate to control the folding of heavy chain and ensure the fidelity of immunoglobulin assembly. Mol Biol Cell. 1999; 10:2209-2219.

Lee S.O., Cho K., Cho S., Kim I., Oh C., Ahn K. Protein disulphide isomerase is required for signal peptide peptidase-mediated protein degradation. The EMBO J. 2010; 29(2):363–75.

Lee M.J., Lee B.H., Hanna J., King R.W., Finley D. Trimming of ubiquitin chains by proteasome-associated deubiquitinating enzymes. Mol Cell Proteomics. 2011; 10(5):R110.003871.

Lee K., Neigeborn L., Kaufman R.J. The unfolded protein response is required for haploid tolerance in yeast. J Biol Chem. 2003; 278(14):11818-27.

Lee C.C., Perchiacca J.M., Tessier P.M. Toward aggregation-resistant antibodies by design. Trends Biotechnol. 2013;. pii: S0167-7799(13)00160-1.

Lehmann M., Rocha S., Mangeat B., Blanchet F., Uji-I H., Hofkens J., Piguet V. Quantitative multicolor super-resolution microscopy reveals tetherin HIV-1 interaction. PLoS pathogens. 2011; 7(12): e1002456.

Leitman J., Ron E., Ogen-shtern N., Lederkremer, G.Z. Compartmentalization of endoplasmic reticulum quality control and ER-associated degradation factors. DNA Cell Biol. 2013; 32(1):2–7.

Leitzgen K., Knittler M.R., Haas I.G. Assembly of immunoglobulin light chains as a prerequisite for secretion. A model for oligomerization-dependent subunit folding. J. Biol. Chem. 1997; 272:3117–3123.

Lenburg M.E., and Landau N.R. Vpu-induced degradation of CD4: requirement for specific amino acid residues in the cytoplasmic domain of CD4. J. Virol. 1993; 67:7238–7245.

Lencer W. I., and Tsai B. The intracellular voyage of cholera toxin: going retro. Trends Biochem. Sci. 2003; 28:639-645.

Leonhardt R.M., Keusekotten K., Bekpen C., Knittler M.R. Critical role for the tapasin-docking site of TAP2 in the functional integrity of the MHC class I-peptide-loading complex. J Immunol. 2005; 175(8):5104-14.

Li W., Tu D., Brunger A.T., Ye Y. A ubiquitin ligase transfers preformed polyubiquitin chains from a conjugating enzyme to a substrate. Nature 2007; 446:333-37.

Li G., Zhao G., Zhou X., Schindelin H., Lennarz W.J. The AAA ATPase p97 links peptide N-glycanase to the endoplasmic reticulum-associated E3 ligase autocrine motility factor receptor. Proc Natl Acad Sci U S A. 2006; 103(22):8348-53.

Lilie H., Rudolph R., Buchner J. Association of antibody chains at different stages of folding: prolyl isomerization occurs after formation of quaternary structure. J. Mol. Biol. 1995; 248-190–201.

Lilley B.N., and Ploegh H.L. A membrane protein required for dislocation of misfolded proteins from the ER. Nature. 2004; 429(6994):834-40.

Lilley B.N., Ploegh H.L. Viral modulation of antigen presentation: manipulation of cellular targets in the ER and beyond. Immunol Rev. 2005; 207:126-44.

Lilley B.N., Ploegh H.L. Multiprotein complexes that link dislocation, ubiquitination, and extraction of misfolded proteins from the endoplasmic reticulum membrane. Proc Natl Acad Sci U S A. 2005; 102(40):14296-301.

Lilley B.N., Gilbert J.M., Ploegh H.L., Benjamin T.L. Murine polyomavirus requires the endoplasmic reticulum protein Derlin-2 to initiate infection. J. Virol. 2006; 80:8739–8744.

Lin A., Xu H., Yan W. Modulation of HLA expression in human cytomegalovirus immune evasion. Cell Mol Immunol. 2007; 4(2):91-8.

Lin W., Bailey S.L., Ho H., Harding H.P., Ron D., Miller S.D., Popko B. The integrated stress response prevents demyelination by protecting oligodendrocytes against immune-mediated damage. J Clin Invest. 2007; 117(2):448-56.

Lippincott-Schwartz J., Bonifacino J.S., Yuan L.C., Klausner R.D. Degradation from the endoplasmic reticulum: disposing of newly synthesized proteins. Cell. 1988; 54(2):209-20.

Liu Y., Choudhury P., Cabral C.M., Sifers, R.N. Oligosaccharide modification in the early secretory pathway directs the selection of a misfolded glycoprotein for degradation by the proteasome. J. Biol. Chem. 1999; 274:5861–5867.

Liu C.C., Walsh C.M., Young J. D. Perforin: structure and function. Immunol Today. 1995; 16:194-201.

Liu Y., and Ye Y. Roles of p97-associated deubiquitinases in protein quality control at the endoplasmic reticulum. Curr Protein Pept Sci. 2012; 13(5):436-46.

Livnah O., Bayer E.A., Wilchek M., Sussman J.L. Three-dimensional structures of avidin and the avidin-biotin complex. Proc Natl Acad Sci U S A. 1993; 90(11):5076-80.

Lomas D. A., and Mahadeva R. Alpha1-antitrypsin polymerization and the serpinopathies: pathobiology and prospects for therapy. J. Clin. Invest. . 2002; 110:1585–1590.

Lorenzo M.E., Ploegh H.L., Tirabassi R.S. Viral immune evasion strategies and the underlying cell biology. Semin Immunol. 2001; 13(1):1-9.

Lotti L.V., Torrisi M.R., Erra M.C., Bonatti S. Morphological analysis of the transfer of VSV ts-045 G glycoprotein from the endoplasmic reticulum to the intermediate compartment in vero cells. Exp Cell Res. 1996; 227(2):323-31.

Loureiro J., Lilley B.N., Spooner E., Noriega V., Tortorella D., Ploegh H.L. Signal peptide peptidase is required for dislocation from the endoplasmic reticulum. Nature. 2006; 441(7095):894-7.

Luirink J., and Sinning I. SRP-mediated protein targeting: structure and function revisited. Biochim Biophys Acta. 2004; 1694(1-3):17-35.

Lütcke H., High S., Römisch K., Ashford A.J., Dobberstein B. The methionine-rich domain of the 54 kDa subunit of signal recognition particle is sufficient for the interaction with signal sequences. EMBO J. 1992; 11(4):1543-51.

Maeda Y., and Kinoshita T. Structural remodeling, trafficking and functions of glycosylphosphatidylinositol-anchored proteins. Progress in lipid research. 2011; 50(4):411–24.

Magadan J.G., Pérez-Victoria F.J., Sougrat R., Ye Y., Strebel K., Bonifacino J.S. Multilayered mechanism of CD4 downregulation by HIV-1 Vpu involving distinct ER retention and ERAD targeting steps. PLoS Pathog. 2010; 6:e1000869.

Margottin F., Bour S.P., Durand H., Selig L., Benichou S., Richard V., Thomas D., Strebel K., Benarous R. A novel human WD protein, h-beta TrCp, that interacts with HIV-1 Vpu connects CD4 to the ER degradation pathway through an F-box motif. Mol. Cell. 1998; 1:565–574.

Maldarelli F., Chen M.Y., Willey R.L., Strebel K. Human immunodeficiency virus type 1 Vpu protein is an oligomeric type I integral membrane protein. J.Virol. 1993; 67:5056-5061.

Malhotra J.D., and Kaufman R.J. The endoplasmic reticulum and the unfolded protein response. Semin Cell Dev Biol. 2007; 18(6):716-31.

Mancini R., Fagioli C., Fra A.M., Maggioni C., Sitia R. FASEB J. 2000; 14:769–778.

Mangeat B., Gers-Huber G., Lehmann M., Zufferey M., Luban J., Piguet V. HIV-1 Vpu neutralizes the antiviral factor Tetherin/BST-2 by binding it and directing its beta-TrCP2-dependent degradation. PLoS Pathog. 2009; (9):e1000574.

Margottin F., Benichou S., Durand H., Richard V., Liu L.X., Gomas E., Benarous R. Interaction between the cytoplasmic domains of HIV-1 Vpu and CD4: role of Vpu residues involved in CD4 interaction and in vitro CD4 degradation. Virology. 1996; 223:381–386.

Martin S., and Parton R.G. Lipid droplets: a unified view of a dynamic organelle. Nat Rev Mol Cell Biol. 2006; 7(5):373-8.

Martin V., Groenendyk J., Steiner S.S., Guo L., Dabrowska M., Parker J.M., Muller-Esterl W., Opas M. Michalak M. Identification by mutational analysis of amino acid residues essential in the chaperone function of calreticulin. J. Biol. Chem. 2006; 281;2338–2346.

Martoglio B., Hofmann M.W., Brunner J., Dobberstein B. The protein-conducting channel in the membrane of the endoplasmic reticulum is open laterally toward the lipid bilayer. Cell. 1995; 81(2):207-14.

Matlack K.E., Misselwitz B., Plath K., Rapoport T.A. BiP acts as a molecular ratchet during posttranslational transport of prepro-alpha factor across the ER membrane. Cell. 1999; 97(5):553-64.

Matsumoto M.L., Wickliffe K.E., Dong K.C., Yu C., Bosanac I., Bustos D., Phu L., Kirkpatrick D.S., Hymowitz S.G., Rape M., Kelley R.F., Dixit V.M. K11-linked polyubiquitination in cell cycle control revealed by a K11 linkage-specific antibody. Mol. Cell. 2010; 39:477–84.

Mayer M.P.,and Bukau B. Hsp70 chaperones: cellular functions and molecular mechanism. Cell Mol Life Sci. 2005; 62(6):670-84.

Mayer M., Kies U., Kammermeier R., Buchner J. BiP and PDI cooperate in the oxidative folding of antibodies in vitro. J Biol Chem. 2000; 275(38):29421-5.

McConnell E., Lass A., Wójcik C. Ufd1-Npl4 is a negative regulator of cholera toxin retrotranslocation. Biochem Biophys Res Commun. 2007; 355(4):1087-90.

McConville M.J., and Ferguson M.A. The structure, biosynthesis and function of glycosylated phosphatidylinositols in the parasitic protozoa and higher eukaryotes. Biochem. J. 1993; 294:305–324.

McCormick-Davis C., Dalton S.B., Singh D.K., Stephens E.B. Comparison of Vpu sequences from diverse geographical isolates of HIV type 1 identifies the presence of highly variable domains, additional invariant amino acids, and a signature sequence motif common to subtype C isolates. AIDS Res. Hum. Retroviruses. 2000; 16:1089-1095.

McDowell G.S., and Philpott A. Non-canonical ubiquitylation: Mechanisms and consequences. The international journal of biochemistry & cell biology. 2013; 45(8): 1833–42.

McLaughlin S.H., and Bulleid N.J. Thiol-independent interaction of protein disulphide isomerase with type X collagen during intra-cellular folding and assembly. Biochem J. 1998; 331 (Pt 3):793-800.

McNew J.A., and Goodman J.M. The targeting and assembly of peroxisomal proteins: some old rules do not apply. Trends Biochem Sci. 1996; 21:54-58.

McNew J.A., and Goodman J.M. An oligomeric protein is imported into peroxisomes in vivo. J Cell Biol. 1994; 127:1245-1257.

Mehnert T., Lam Y.H., Judge P.J., Routh A., Fischer D., Watts A., Fischer W.B. Towards a mechanism of function of the viral ion channel Vpu from HIV-1. J Biomol Struct Dyn. 2007; 24(6):589-96.

Melker K. A modular set of prokaryotic and eukaryotic expression vectors. Anal Biochem. 2000; 277:109-120.

Mesaeli N., Nakamura K., Zvaritch E., Dickie P., Dziak E., Krause K.H., Opas M., MacLennan D.H. Michalak M. Calreticulin is essential for cardiac development. J Cell Biol. 1999; 144:857-868.

Messick T.E., Russell N.S., Iwata A.J., Sarachan K.L., Shiekhattar R., Shanks J.R.,Reyes-Turcu F.E., Wilkinson K.D., Marmorstein R. Structural basis for ubiquitin recognition by the Otu1 ovarian tumour domain protein. J Biol Chem. 2008; 283:11038-11049.

Meusser B., Hirsch C., Jarosch E., Sommer T. ERAD: the long road to destruction. Nat Cell Biol. 2005; 7(8):766-72.

Metzger M.B., Pruneda J.N., Klevit R.E., Weissman A.M. RING-type E3 ligases: Master manipulators of E2 ubiquitin-conjugating enzymes and ubiquitination. Biochim Biophys Acta. 2013; pii: S0167-4889(13)00216-4.

Metzger M.B., and Weissman A.M. Working on a chain: E3s ganging up for ubiquitylation. Nature Cell Biology. 2010; 12(12):1124-6.

Michalak M., Corbett E.F., Mesaeli N., Nakamura K., Opas M. Calreticulin: one protein, one gene, many functions. Biochem J. 1999; 292:281–292.

Michalak M., Groenendyk J., Szabo E., Gold L.I., Opas M. Calreticulin, a multi-process calcium-buffering chaperone of the endoplasmic reticulum. Biochem. J. 2009; 417:651–666.

Miller E., Antonny B., Hamamoto S., Schekman R. Cargo selectioninto COPII vesicles is driven by the Sec24p subunit. EMBO J. 2002; 21:6105–6113.

Miller E.A., Beilharz T.H., Malkus P.N., Lee M.C., Hamamoto S., Orci L., Schekman R. Multiple cargo binding sites on the COPII subunit Sec24p ensure capture of diverse membrane proteins into transport vesicles. Cell. 2003; 114(4):497-509.

Misaghi S., Pacold M., Blom D., Ploegh H., Korbel G. Using a small molecule inhibitor of peptide: -glycanase to probe its role in glycoprotein turnover. Chemistry & Biology. 2004; 11(12):1677–1687.

Misselwitz B., Staeck O., Rapoport T.A. J proteins catalytically activate Hsp70 molecules to trap a wide range of peptide sequences. Mol Cell. 1998; 2(5):593-603.

Mitchell R.S., Katsura C., Skasko M.A., Fitzpatrick K., Lau D., Ruiz A., Stephens E.B., Margottin-Goguet F., Benarous R., Guatelli J.C. Vpu antagonizes BST-2-mediated restriction of HIV-1 release via beta-TrCP and endo-lysosomal trafficking. PLoS pathogens. 2009; 5(5), e1000450.

Mizobuchi N., Hoseki J., Kubota H., Toyokuni S., Nozaki J.,. Naitoh M., Koizumi A., Nagata K. ARMET is a soluble ER protein induced by the unfolded protein response via ERSE-II element. Cell Struct Funct. 2007; 32(1):41-50.

Molinari M., Calanca V., Galli C., Lucca P., Paganetti P. Role of EDEM in the release of misfolded glycoproteins from the calnexin cycle. Science. 2003; 299(5611):1397-400.

Molinari M. N-glycan structure dictates extension of protein folding or onset of disposal. Nature Chemical Biology. 2007; 3(6):313-320.

Molinari M., Galli C., Piccaluga V., Pieren M., Paganetti P. Sequential assistance of molecular chaperones and protein degradation from the ER. J Cell Biol. 2002; 158(2):247-57.

Momburg F., and Tan P. Tapasin-the keystone of the loading complex optimizing peptide binding by MHC class I molecules in the endoplasmic reticulum. Mol Immunol. 2002; 39(3-4):217-33.

Mueller B., Lilley B.N., Ploegh H.L. SEL1L, the homologue of yeast Hrd3p, is involved in protein dislocation from the mammalian ER. J Cell Biol. 2006; 175(2):261-70.

Mukhopadhyay D., and Riezman H. Proteasome-independent functions of ubiquitin in endocytosis and signaling. Science. 2007; 315:201–5.

Murphy D.J. The biogenesis and functions of lipid bodies in animals, plants and microorganisms. Prog Lipid Res. 2001; 40(5):325-438.

Nagasawa K., Higashi T., Hosokawa N., Kaufman R.J., Nagata K. Simultaneous induction of the four subunits of the TRAP complex by ER stress accelerates ER degradation. EMBO Rep. 2007; 8(5):483-9.

Nakatsukasa K., and Brodsky J.L. The recognition and retrotranslocation of misfolded proteins from the endoplasmic reticulum. Traffic. 2008; 9(6):861-70.

Neil S.J., Eastman S.W., Jouvenet N., Bieniasz P.D. HIV-1 Vpu promotes release and prevents endocytosis of nascent retrovirus particles from the plasma membrane. PLoS Pathog. 2006; 2:e39.

Neil S.J., Sandrin V., Sundquist W.I., Bieniasz P.D. An interferon-alpha-induced tethering mechanism inhibits HIV-1 and Ebola virus particle release but is counteracted by the HIV-1 Vpu protein. Cell Host Microbe. 2007; 2:193-203.

Ng C.L., Oresic K., Tortorella D. TRAM1 is involved in disposal of ER membrane degradation substrates. Exp Cell Res. 2010; 316(13):2113-22.

Ng D.T., Brown J.D., Walter P. Signal sequences specify the targeting route to the endoplasmic reticulum membrane. J Cell Biol. 1996; 134(2):269-78.

Ng F.W., Nguyen M., Kwan T., Branton P.E., Nicholson D.W., Cromlish J.A., Shore G.C. p28 Bap31, a Bcl-2/Bcl-XL- and procaspase-8-associated protein in the endoplasmic reticulum. J Cell Biol. 1997; 139(2):327-38.

Ng W., Sergeyenko T., Zeng N., Brown J.D., Römisch, K. Characterization of the proteasome interaction with the Sec61 channel in the endoplasmic reticulum. Journal of cell science. 2007; 120(Pt 4):682–91.

Nilsson I.M., and von Heijne G. Determination of the distance between the oligosaccharyltransferase active site and the endoplasmic reticulum membrane. J Biol Chem. 1993; 268(8):5798-801.

Ninagawa S., Okada T., Takeda S., Mori, K. SEL1L is required for endoplasmic reticulum-associated degradation of misfolded luminal proteins but not transmembrane proteins in chicken DT40 cell line. Cell Struct Funct. 2011; 36(2):187–195.

Oda Y., Hosokawa N., Wada I., Nagata K. EDEM as an acceptor of terminally misfolded glycoproteins released from calnexin. Science. 2003; 299(5611):1394-7.

Oda Y., Okada T., Yoshida H., Kaufman R.J., Nagata K., Mori K. Derlin-2 and Derlin-3 are regulated by the mammalian unfolded protein response and are required for ER-associated degradation. J Cell Biol. 2006; 172(3):383-93.

Ohsaki Y., Cheng J., Fujita A., Tokumoto T., Fujimoto T. Cytoplasmic lipid droplets are sites of convergence of proteasomal and autophagic degradation of apolipoprotein B. Mol Biol Cell. 2006; 17(6):2674-83.

Okuda-Shimizu Y., and Hendershot L.M. Characterization of an ERAD pathway for non-glycosylated BiP substrates which requires Herp. Mol Cell. 2007; 28(4):544–554.

Olivari S., Cali T., Salo K.E., Paganetti P., Ruddock L.W., Molinari M. EDEM1 regulates ER-associated degradation by accelerating de-mannosylation of folding-defective polypeptides and by inhibiting their covalent aggregation. Biochem Biophys Res Commun. 2006; 349(4):1278-84.

Oliver J.D., Roderick H.L., Llewellyn D.H. High S. ERp57 functions as a subunit of specific complexes formed with the ER lectins calreticulin and calnexin. Mol Biol Cell. 1999; 10,2573-2582.

Olzmann J.A., and Kopito R.R. Lipid droplet formation is dispensable for endoplasmic reticulum-associated degradation. J Biol Chem. 2011; 286:27872-27874.

Omura T., Kaneko M., Onoguchi M., Koizumi S., Itami M., Ueyama M., Okuma Y., Nomura Y. Novel functions of ubiquitin ligase HRD1 with transmembrane and proline-rich domains. J

Pharmacol Sci. 2008a; 106(3):512-9.

Omura T., Kaneko M., Tabei N., Okuma Y., Nomura Y. Immunohistochemical localization of a ubiquitin ligase HRD1 in murine brain. J Neurosci Res. 2008b; 86(7):1577-87.

Oresic K., Noriega V., Andrews L., Tortorella D. A structural determinant of human cytomegalovirus US2 dictates the down-regulation of class I major histocompatibility molecules. J Biol Chem. 2006; 281(28):19395-406.

Orlean P., and Menon A.K. Thematic review series: lipid posttranslational modifications. GPI anchoring of protein in yeast and mammalian cells, or: how we learned to stop worrying and love glycophospholipids. J Lipid Res. 2007; 48:993–1011.

Osborne A.R., and Rapoport T.A. Protein translocation is mediated by oligomers of the SecY complex with one SecY copy forming the channel. Cell. 2007; 129(1):97-110.

Paetzel M., Karla A., Strynadka N.C., Dalbey R.E. Signal peptidases. Chem Rev. 2002; 102(12):4549-80.

Pan S., Cheng X., Sifers R.N. Golgi-situated endoplasmic reticulum α-1, 2-mannosidase contributes to the retrieval of ERAD substrates through a direct interaction with γ-COP. Mol Biol Cell. 2013; 24(8):1111-21.

Panter S., Thomson R., de Bruxelles G., Laver D., Trevaskis B., Udvardi M. Identification with proteomics of novel proteins associated with the peribacteroid membrane of soybean root nodules. Mol Plant Microbe Interact. 2000; 13(3):325-33.

Panzner S., Dreier L., Hartmann E., Kostka S., Rapoport T.A. Posttranslational protein transport in yeast reconstituted with a purified complex of Sec proteins and Kar2p. Cell. 1995; 81(4):561-70.

Parks T.D., Howard E.D., Wolpert T.J., Arp D.J., Dougherty W.G.. Expression and purification of a recombinant tobacco etch virus NIa proteinase: biochemical analyses of the full-length and a naturally occurring truncated proteinase form. Virology. 1995; 210(1):194-201.

Parks T.D., Leuther K.K., Howard E.D., Johnston S.A., Dougherty W.G. Release of proteins and peptides from fusion proteins using a recombinant plant virus proteinase. Anal. Biochem. 1994; 216:413–417.

Paquet M.E., Cohen-Doyle M., Shore G.C., Williams D.B. Bap29/31 influences the intracellular traffic of MHC class I molecules. J Immunol. 2004; 172(12):7548-55.

Parodi A.J. Protein glucosylation and its role in protein folding. Annu Rev Biochem. 2000; 69:69-93.

Pauli A., Althoff F., Oliveira R.A., Heidmann S., Schuldiner O., Lehner C.F., Dickson B.J., Nasmyth K. Cell-type-specific TEV protease cleavage reveals cohesin functions in Drosophila neurons. Dev Cell. 2008; 14:239–251.

Paulick M.G., and Bertozzi C.R. The glycosylphosphatidylinositol anchor: a complex membrane-anchoring structure for proteins. Biochemistry. 2008; 47(27):6991-7000.

Peaper D.R., Wearsch P.A., Cresswell P. Tapasin and ERp57 form a stable disulfide-linked dimer within the MHC class I peptide-loading complex. EMBO J. 2005; 24(20):3613-23.

Peaper D.R., and Cresswell P. Regulation of MHC class I assembly and peptide binding. Annu Rev Cell Dev Biol. 2008a; 24:343-68.

Peaper D.R., Cresswell P. The redox activity of ERp57 is not essential for its functions in MHC class I peptide loading. Proc Natl Acad Sci U S A. 2008b; 105(30):10477-82.

Pearse B.R., Gabriel L., Wang N., Hebert D.N. A cell-based reglucosylation assay demonstrates the role of GT1 in the quality control of a maturing glycoprotein. J Cell Biol. 2008: 181:309-320.

Pelham H.R. The retention signal for soluble proteins of the endoplasmic reticulum. Trends Biochem Sci. 1990; 15(12):483-6.

Perez-caballero D., Zang T., Ebrahimi A., Mcnatt M.W., Gregory D.A., Johnson M.C., Bieniasz P.D. Tetherin inhibits HIV-1 release by directly tethering virions to cells. Cell. 2010; 139(3):499–511.

Petrescu A.J., Milac A.L., Petrescu S.M., Dwek R.A., Wormald M.R. Statistical analysis of the protein environment of N-glycosylation sites: implications for occupancy, structure, and folding. Glycobiology. 2004; 14(2):103-14.

Phan J., Zdanov A., Evdokimov A.G., Tropea J.E., Peters H.K., Kapust R.B., Li M., Wlodawer A., Waugh D S. Structural basis for the substrate specificity of tobacco etch virus protease. The Journal of biological chemistry. 2002; 277(52):50564–72.

Pickart C.M. Mechanisms underlying ubiquitination. Annu. Rev. Biochem. 2001; 70:503–533

Pickart C.M., and Cohen R.E. Proteasomes and their kin: proteases in the machine age. Nat Rev Mol Cell Biol. 2004; 5:177-187

Pickart C.M., and Eddins M.J. Ubiquitin: structures, functions, mechanisms. Biochimica et biophysica acta. 2004; 1695(1-3):55–72.

Pickart C. M., and Fushman D. Polyubiquitin chains: polymeric protein signals. Curr Opin Chem Biol. 2004; 8:610-6.

Pincus D., Chevalier M.W., Aragón T., van Anken E., Vidal S.E., El-Samad H., Walter P. BiP binding to the ER-stress sensor Ire1 tunes the homeostatic behavior of the unfolded protein response. PLoS Biol. 2010; 8(7):e1000415.

Pinder J.B., Attwood K.M., Dellaire G. Reading, writing, and repair: the role of ubiquitin and the ubiquitin-like proteins in DNA damage signaling and repair. Front Genet. 2013; 4:45.

Plath K., and Rapoport T.A. Spontaneous release of cytosolic proteins from posttranslational substrates before their transport into the endoplasmic reticulum. J Cell Biol. 2000; 151(1):167-78.

Ploegh H.L. Viral strategies of immune evasion. Science. 1998; 280(5361):248-53.

Ploegh H.L. A lipid-based model for the creation of an escape hatch from the endoplasmic reticulum. Nature. 2007; 448(7152):435-8.

Pool MR. A trans-membrane segment inside the ribosome exit tunnel triggers RAMP4 recruitment to the Sec61p translocase. J Cell Biol. 2009 Jun 1;185(5):889-902.

Praper T., Sonnen A., Viero G., Kladnik A., Froelich C.J., Anderluh G., Dalla Serra M., Gilbert R.J. Human perforin employs different avenues to damage membranes. J Biol Chem. 2011; 286: 2946-2955.

Predonzani A., Arnoldi F., López-Requena A., Burrone O.R. In vivo site-specific biotinylation of proteins within the secretory pathway using a single vector system. BMC Biotechnol. 2008; 8:41.

Preiss T., and Hentze M.W., Starting the protein synthesis machine: eukaryotic translation initiation. Bioessays. 2003; 25(12):1201-11.

Promlek T., Ishiwata-Kimata Y., Shido M., Sakuramoto M., Kohno K., Kimata Y. Membrane aberrancy and unfolded proteins activate the endoplasmic reticulum stress sensor Ire1 in different ways. Mol. Biol. Cell. 2011; 22(18):3520-32.

Quan E.M., Kamiya Y., Kamiya D., Denic V., Weibezahn J., Kato K., Weissman J.S. Defining the glycan destruction signal for endoplasmic reticulum-associated degradation. Mol Cell. 2008; 32:870-877.

Querol-Audi J., Sun C., Vogan J.M., Smith M.D., Gu Y., Cate J.H., Nogales E. Architecture of

Human Translation Initiation Factor 3. Structure. 2013. 21(6):920-928.

Raasi S., and Wolf D.H. Ubiquitin receptors and ERAD: a network of pathways to the proteasome. Semin Cell Dev Biol. 2007; 18(6):780-91.

Rabinovich E., Kerem A., Fröhlich K.U., Diamant N., Bar-Nun S. AAA-ATPase p97/Cdc48p, a cytosolic chaperone required for endoplasmic reticulum-associated protein degradation. Mol Cell Biol. 2002; 22(2):626-34.

Rachubinski R.A., and Subramani S. How proteins penetrate peroxisomes. Cell. 1995; 83(4):525-8.

Rapoport T.A., Jungnickel B., Kutay U. Protein transport across the eukaryotic endoplasmic reticulum and bacterial inner membranes. Annu Rev Biochem. 1996; 65:271-303.

Rapoport T.A., Goder V., Heinrich S.U., Matlack K.E. Membrane-protein integration and the role of the translocation channel. Trends Cell Biol. 2004; 14:568–575.

Rapoport T.A. Protein translocation across the eukaryotic endoplasmic reticulum and bacterial plasma membranes. Nature. 2007; 450(7170):663-9.

Reilly D., Larkin D., Devocelle M., Fitzgerald D.J., Moran N. Calreticulin-independent regulation of the platelet integrin alphaIIbbeta3 by the KVGFFKR alphaIIb-cytoplasmic motif. Platelets 2004; 15(1):43–54.

Reits E.A., Benham A.M., Plougastel B., Neefjes J., Trowsdale J. Dynamics of proteasome distribution in living cells. EMBO J. 1997; 16:6087–6094.

Römisch K. Endoplasmic reticulum-associated degradation. Annual Review of Cell and Developmental Biology. 2005; 21:435–56.

Ron D., and Walter P. Signal integration in the endoplasmic reticulum unfolded protein response. Nat Rev Mol Cell Biol. 2007; 8(7):519-29.

Rouiller I., DeLaBarre B., May A.P., Weis W.I., Brunger A.T., Milligan R.A., Wilson-Kubalek E.M. Conformational changes of the multifunction p97 AAA ATPase during its ATPase cycle. Nature structural biology. 2002; 9(12):950–7.

Rucktaschel R., Girzalsky W., Erdmann R. Protein import machineries of peroxisomes. Biochim Biophys Acta. 2011; 1808:892-900.

Rudd P.M., Wormald M.R., Stanfield R.L., Huang M., Mattsson N., Speir J.A., DiGennaro J.A., Fetrow J.S., Dwek R.A., Wilson I.A. Roles for glycosylation of cell surface receptors involved in cellular immune recognition. J Mol Biol. 1999; 293:351-366.

Rumpf S., and Jentsch S. Functional division of substrate processing cofactors of the ubiquitin-selective Cdc48 chaperone. Mol Cell. 2006; 21:261–269.

Russell S.J., Ruddock L.W., Salo K.E., Oliver J.D., Roebuck Q.P., Llewellyn D.H., Roderick H.L., Koivunen P., Myllyharju J., High S. The primary substrate binding site in the b' domain of ERp57 is adapted for endoplasmic reticulum lectin association. J Biol Chem. 2004; 279:18861-18869.

Saeki Y., Kudo T., Sone T., Kikuchi Y., Yokosawa H., Toh-e A., Tanaka K. Lysine 63-linked polyubiquitin chain may serve as a targeting signal for the 26S proteasome. EMBO J. 2009; 28:359–71.

Saeki Y., Sone T., Toh-e A., Yokosawa H. Identification of ubiquitin-like protein-binding subunits of the 26S proteasome. Biochem Biophys Res Commun. 2002; 296(4):813-9.

Sakai H., Tokunaga K., Kawamura M., Adachi A. Function of human immunodeficiency virus type 1 Vpu protein in various cell types. J Gen Virol. 1995; 76(Pt 11):2717-2722.

Sambrook J., Fritsch E.F., Maniatis T. Molecular Cloning. A laboratory manual. New York: Cold Spring Harbor Laboratory Press. (1989).

Sambrooks C.L., Carpio M.A., Hallak M.E. Arginylated Calreticulin at Plasma Membrane Increases Susceptibility of Cells to Apoptosis. J Biol Chem. 2012; 287(26):22043–22054.

Sanches M., Alves B.S., Zanchin N.I., Guimarães B.G. The crystal structure of the human Mov34 MPN domain reveals a metal-free dimer. J Mol Biol. 2007; 370(5):846-55.

Saric T., Chang S.C., Hattori A., York I.A., Markant S., Rock K.L., Tsujimoto M., Goldberg A.L. An IFN-gamma-induced aminopeptidase in the ER, ERAP1, trims precursors to MHC class I-presented peptides. Nat Immunol. 2002; 3(12):1169-76.

Satoh A., Warren G. In situ cleavage of the acidic domain from the p115 tether inhibits exocytic transport. Traffic. 2008; 9:1522–1529.

Saveanu L., Carroll O., Lindo V., Del Val M., Lopez D., Lepelletier Y., Greer F., Schomburg L., Fruci D., Niedermann G., van Endert P.M. Concerted peptide trimming by human ERAP1 and ERAP2 aminopeptidase complexes in the endoplasmic reticulum. Nat Immunol. 2005; 6(7):689-97.

Sayeed A., and Ng D.T. Search and destroy: ER quality control and ER-associated protein degradation. Crit Rev Biochem Mol Biol. 2005; 40(2):75-91.

Schauber C., Chen L., Tongaonkar P., Vega I., Lambertson D., Potts W., Madura K. Rad23 links DNA repair to the ubiquitin/proteasome pathway. Nature. 1998; 391(6668):715-8.

Schmidt M., Hanna J., Elsasser S., Finley D. Proteasome-associated proteins: regulation of a proteolytic machine. Biol Chem. 2005; 386(8):725-37.

Schmitz A., Herrgen H., Winkeler A., Herzog V. Cholera toxin is exported from microsomes by the Sec61p complex. J Cell Biol. 2000; 148(6):1203-12.

Schreiber A., and Peter M. Substrate recognition in selective autophagy and the ubiquitin-proteasome system. Biochim Biophys Acta. 2013; pii: S0167-4889(13)00120-1.

Schröder M., and Kaufman R.J. The mammalian unfolded protein response. Annu Rev Biochem. 2005; 74:739-89.

Schubert U., Henklein P., Boldyreff B., Wingender E., Strebel K., Porstmann T. The human immunodeficiency virus type 1 encoded Vpu protein is phosphorylated by casein kinase-2 (CK-2) at positions Ser52 and Ser56 within a predicted alpha-helix-turn-alpha-helix-motif. J. Mol. Biol. 1994; 236:16–25.

Schubert U., Clouse K.A., Strebel K. Augmentation of virus secretion by the human immunodeficiency virus type 1 Vpu protein is cell type independent and occurs in cultured human primary macrophages and lymphocytes. J Virol. 1995; 69:7699-7711.

Schulman B.A., Harper J.W. Ubiquitin-like protein activation by E1 enzymes: the apex for downstream signalling pathways. Nat Rev Mol Cell Biol. 2009; 10(5):319-31.

Schulze A., Standera S., Buerger E., Kikkert M., van Voorden S., Wiertz E., Koning F., Kloetzel P.M., Seeger M. The ubiquitin-domain protein HERP forms a complex with components of the endoplasmic reticulum associated degradation pathway. J Mol Biol. 2005; 354:1021–1027.

Shaffer K.L., Sharma A., Snapp E.L. Hegde R.S. Regulation of protein compartmentalization expands the diversity of protein function. Dev. Cell. 2005; 9:545–554.

Shamu C.E., Flierman D., Ploegh H.L., Rapoport T.A., Chau V. Polyubiquitination is required for US11-dependent movement of MHC class I heavy chain from endoplasmic reticulum into cytosol. Mol Biol Cell. 2001; 12(8):2546-55.

Shcherbik N., and Haines D.S. Cdc48p(Npl4p/Ufd1p) binds and segregates membrane-anchored/tethered complexes via a polyubiquitin signal present on the anchors. Molecular cell. 2007; 25(3):385–97.

Shenkman M., Groisman B., Ron E., Avezov E., Hendershot L.M., Lederkremer, G.Z. A shared endoplasmic reticulum-associated degradation pathway involving the EDEM1 protein for glycosylated and nonglycosylated proteins. J Biol Chem. 2013; 288(4):2167–2178.

Shimizu Y., Okuda-shimizu Y., Hendershot L.M. Ubiquitylation of an ERAD substrate occurs on multiple types of amino acids. Molecular Cell. 2010; 40(6):917–926.

Sifers R.N., Brashears-Macatee S., Kidd V.J., Muensch H., Woo S.L. A frameshift mutation results in a truncated alpha 1-antitrypsin that is retained within the rough endoplasmic reticulum. J Biol Chem. 1988; 263(15):7330–5.

Simon S.M., and Blobel G. A protein-conducting channel in the endoplasmic reticulum. Cell. 1991; 65(3):371-80.

Skowronek M.H., Hendershot L.M., Haas I.G.. The variable domain of nonassembled Ig light chains determines both their half-life and binding to the chaperone BiP. Proc. Natl. Acad. Sci U. S. A. 1998; 95(4):1574–8.

Slavoff S. A., Liu D.S., Cohen J.D., Ting A.Y. Imaging protein-protein interactions inside living cells via interaction-dependent fluorophore ligation. Journal of the American Chemical Society. 2011; 133(49):19769–76.

Smith D.M., Kafri G., Cheng Y., Ng D., Walz T., Goldberg A.L. ATP binding to PAN or the 26S ATPases causes association with the 20S proteasome, gate opening, and translocation of unfolded proteins. Mol Cell. 2005; 20:687-98.

Soriano S., Thomas S., High S., Griffiths G., D'santos C., Cullen P., Banting G. Membrane association, localization and topology of rat inositol 1,4,5-trisphosphate 3-kinase B: implications for membrane traffic and Ca2+ homoeostasis. Biochem J. 1997; 324 (Pt 2):579-89.

Sousa M., and Parodi A.J. The molecular basis for the recognition of misfolded glycoproteins by the UDP-Glc:glycoprotein glucosyltransferase. EMBO J. 1995; 14:4196-4203.

Sowa M.E., Bennett E.J., Gygi S.P., Harper J.W. Defining the human deubiquitinating enzyme interaction landscape. Cell. 2009; 138(2):389-403.

Spiliotis E.T., Pentcheva T., Edidin M. Probing for membrane domains in the endoplasmic reticulum: retention and degradation of unassembled MHC class I molecules. Mol Biol Cell. 2002; 13:1566–81.

Strachan J., Roach L., Sokratous K., Tooth D., Long J., Garner T.P., Searle M.S., Oldham N.J., Layfield R. Insights into the molecular composition of endogenous unanchored polyubiquitin chains. J Proteome Res. 2012; 11(3):1969-80.

Stagg H.R., Thomas M., van den Boomen D., Wiertz E.J., Drabkin H.A., Gemmill R.M., Lehner P.J. The TRC8 E3 ligase ubiquitinates MHC class I molecules before dislocation from the ER. J Cell Biol. 2009; 186(5):685-92.

Stirling C.J., and Lord J.M. Quality control: linking retrotranslocation and degradation.Curr Biol. 2006; 16(24):R1035-7.

Strebel K. HIV-1 Vpu - an ion channel in search of a job. Biochim Biophys Acta. 2013; pii: S0005-2736(13)00218-6

Sun C., Liang J., Shi R., Gao X., Zhang R., Hong F., Yuan Q., Wang S. Tobacco etch virus protease retains its activity in various buffers and in the presence of diverse additives. Protein Expr Purif. 2012; 82(1):226–31.

Sun F., Zhang R., Gong X., Geng X., Drain P.F., Frizzell R.A. Derlin-1 promotes the efficient degradation of the cystic fibrosis transmembrane conductance regulator (CFTR) and CFTR folding mutants. J Biol Chem. 2006; 281(48):36856-63.

Suzuki T., Park H., Hollingsworth N.M., Sternglanz R., Lennarz W.J. PNG1, a yeast gene encoding a highly conserved peptide:N-glycanase. J Cell Biol. 2000; 149(5):1039-52.

Suzuki T., Park H., Lennarz W.J. Cytoplasmic peptide:N-glycanase (PNGase) in eukaryotic cells: occurrence, primary structure, and potential functions. FASEB J. 2002; 16(7):635-41.

Suzuki T., Park H., Till E.A., Lennarz W.J. The PUB domain: a putative protein-protein interaction domain implicated in the ubiquitin-proteasome pathway. Biochem Biophys Res Commun. 2001; 287(5):1083-7.

Swiecki M., Scheaffer S.M., Allaire M., Fremont D.H., Colonna M., Brett T.J. Structural and biophysical analysis of BST-2/tetherin ectodomains reveals an evolutionary conserved design to inhibit virus release. J Bioll Chem. 2011;. 286(4): 2987–97.

Tang F., Wang B., Li N., Wu Y., Jia J., Suo T., Chen Q., Liu Y.J., Tang J. RNF185, a novel mitochondrial ubiquitin E3 ligase, regulates autophagy through interaction with BNIP1. PloS one. 2011; 6(9):e24367.

Tanno H., and Komada M. The ubiquitin code and its decoding machinery in the endocytic pathway. J Biochem. 2013; 153(6):497-504.

Tauchi-Sato K., Ozeki S., Houjou T., Taguchi R., Fujimoto T. The surface of lipid droplets is a phospholipid monolayer with a unique Fatty Acid composition. J Biol Chem. 2002; 277(46):44507-12.

Taxis C., Stier G., Spadaccini R., Knop M. Efficient protein depletion by genetically controlled deprotection of a dormant N-degron. Mol Syst Biol. 2009; 5(267):267.

Taxis C., Hitt R., Park S.H., Deak P.M., Kostova Z., Wolf D.H. Use of modular substrates demonstrates mechanistic diversity and reveals differences in chaperone requirement of ERAD. J Biol Chem. 2003; 278(38):35903-13.

Thrower J.S., Hoffman L., Rechsteiner M., Pickart C.M. Recognition of the polyubiquitin proteolytic signal. EMBO J. 2000; 19:94-102.

Timchenko L.T., Iakova P., Welm A.L., Cai Z.J., Timchenko N.A. Calreticulin interacts with C/EBPalpha and C/EBPbeta mRNAs and represses translation of C/EBP proteins. Mol. Cell. Biol. 2002; 22:7242–7257.

Tirosh B., Furman M.H., Tortorella D., Ploegh H.L. Protein unfolding is not a prerequisite for endoplasmic reticulum-to-cytosol dislocation. J Biol Chem. 2003; 278(9):6664-72.

Tirosh B., Iwakoshi N.N., Lilley B.N., Lee A.H., Glimcher L.H., Ploegh H.L. Human cytomegalovirus protein US11 provokes an unfolded protein response that may facilitate the degradation of class I major histocompatibility complex products. J Virol. 2005; 79(5):2768-79.

Tortorella D., Story C.M., Huppa J.B., Wiertz E.J., Jones T.R., Bacik I., Bennink J.R., Yewdell J.W., Ploegh H.L. Dislocation of Type I Membrane Proteins from the ER to the Cytosol Is Sensitive to Changes in Redox Potential. J Cell Biol. 1998; 142(2):365–76.

Tokarev A.A., Munguia J., Guatelli .JC. Serine-threonine ubiquitination mediates downregulation of BST-2/tetherin and relief of restricted virion release by HIV-1 Vpu. J Virol. 2011; 85(1):51-63.

Trombetta E.S., Simons J.F., Helenius A. Endoplasmic reticulum glucosidase II is composed of a catalytic subunit, conserved from yeast to mammals, and a tightly bound noncatalytic HDEL-containing subunit. J Biol Chem. 1996; 271(44):27509-16.

Tsai B., Rodighiero C., Lencer W.I., Rapoport T.A. Protein disulfide isomerase acts as a redox-dependent chaperone to unfold cholera toxin. Cell. 2001; 104:937–948.

Tsai B., Ye Y., Rapoport T.A. Retro-translocation of proteins from the endoplasmic reticulum into the cytosol. Nat Rev Mol Cell Biol. 2002; 3(4):246–55.

Tu Y., Chen C., Pan J., Xu J., Zhou Z.G., Wang C.Y. The Ubiquitin Proteasome Pathway (UPP) in the regulation of cell cycle control and DNA damage repair and its implication in tumorigenesis. Int J Clin Exp Pathol. 2012; 5(8):726-38.

Ushioda R., Hoseki J., Araki K., Jansen G., Thomas D.Y., Nagata K. ERdj5 is required as a disulfide reductase for degradation of misfolded proteins in the ER. Science. 2008; 321:569-572.

Uttamapinant C., White K. A., Baruah H., Thompson S., Fernández-suárez M., Puthenveetil S., Ting, A. Y. A fluorophore ligase for site-specific protein labeling inside living cells. Proc Natl Acad Sci U S A. 2010; 107(24):10914-9.

Vahdati-Ben Arieh S., Laham N., Schechter C., Yewdell J.W., Coligan J.E., Ehrilich R. A single viral protein HCMV US2 affects antigen presentation and intracellular iron homeostasis by degradation of classical HLA class I and HFE molecules. Blood. 2003; 101:2858-2864.

Van Damme N., Goff D., Katsura C., Jorgenson R.L., Mitchell R., Johnson M.C., Stephens E.B., Guatelli J. The interferon-induced protein BST-2 restricts HIV-1 release and is downregulated from the cell surface by the viral Vpu protein. Cell Host Microbe. 2008; 3:245-252.

Van den Berg B., Clemons W.M.Jr., Collinson I., Modis Y., Hartmann E., Harrison S.C., Rapoport T.A. X-ray structure of a protein-conducting channel. Nature. 2004; 427(6969):36-44.

Vanhove M., Usherwood Y.K., Hendershot L.M. Unassembled Ig heavy chains do not cycle from BiP in vivo but require light chains to trigger their release. Immunity. 2001; 15:105–114.

Van Wijk S.J., and Timmers H.T. The family of ubiquitin-conjugating enzymes (E2s): deciding between life and death of proteins. FASEB J. 2010; 24(4):981-93.

Varshavsky A. Regulated protein degradation. Trends Biochem Sci. 2005; 30:283-286.

Vashist S., and Ng D.T. Misfolded proteins are sorted by a sequential checkpoint mechanism of ER quality control. J Cell Biol. 2004; 165(1):41-52.

Vembar S.S., and Brodsky J.L. One step at a time: endoplasmic reticulum-associated degradation. Nat Rev Mol Cell Biol. 2008; 9(12):944-57.

Verma R., Oania R., Graumann J., Deshaies R.J. Multiubiquitin chain receptors define a layer of substrate selectivity in the ubiquitin-proteasome system. Cell. 2004; 118(1):99-110.

Vincent M.J., Raja N.U., Jabbar M.A. Human immunodeficiency virus type 1 Vpu protein induces degradation of chimeric envelope glycoproteins bearing the cytoplasmic and anchor domains of CD4: role of the cytoplasmic domain in Vpu-induced degradation in the endoplasmic reticulum. J Virol. 1993; 67:5538-5549.

Voges, D., Zwickl, P. & Baumeister, W. The 26S proteasome: a molecular machine designed for controlled proteolysis. Annu Rev Biochem. 1999; 68:1015-1068.

Voskoboinik I., Smyth M.J., Trapani J.A. Perforin-mediated target-cell death and immune homeostasis. Nat Rev Immunol. 2006; 6:940-952.

Wada I., Rindress D., Cameron P.H., Ou W.J., Doherty J.J. 2nd, Louvard D., Bell A.W., Dignard D., Thomas D.Y., Bergeron J.J. SSR alpha and associated calnexin are major calcium binding proteins of the endoplasmic reticulum membrane. J Biol Chem. 1991 Oct 15;266(29):19599-610.

Wahlman J., DeMartino G.N., Skach W.R., Bulleid N.J., Brodsky J.L., Johnson A.E. Real-time fluorescence detection of ERAD substrate retrotranslocation in a mammalian in vitro system. Cell. 2007; 129(5):943-55.

Wakana Y., Takai S., Nakajima K., Tani K., Yamamoto A., Watson P., Stephens D.J., Hauri H.P., Tagaya M. Bap31 is an itinerant protein that moves between the peripheral endoplasmic reticulum (ER) and a juxtanuclear compartment related to ER-associated degradation. Mol Biol Cell. 2008; 19:1825–36.

Walter P., and Ron D. The unfolded protein response: from stress pathway to homeostatic regulation. Science 2011; 334(6059):1081–6.

Wang X., Yu Y.Y., Myers N., Hansen T.H. Decoupling the Role of Ubiquitination for the Dislocation vs. Degradation of Major Histocompatibility Complex (MHC) Class I Proteins during Endoplasmic Reticulum-associated Degradation (ERAD). J Biol Chem. 2013; 288(32):23295-306.

Wang X., Herr R.A., Chua W.J., Lybarger L., Wiertz E.J., Hansen T.H. Ubiquitination of serine, threonine, or lysine residues on the cyto- plasmic tail can induce ERAD of MHC-I by viral E3 ligase mK3. J. Cell Biol. 2007; 177:613–624.

Wang B., Heath-Engel H., Zhang D., Nguyen N., Thomas D.Y., Hanrahan J.W., Shore G.C. BAP31 interacts with Sec61 translocons and promotes retrotranslocation of CFTRDeltaF508 via the derlin-1 complex. Cell. 2008; 133(6):1080-92.

Weihofen A., Binns K., Lemberg M.K., Ashman K., Martoglio B. Identification of signal peptide peptidase, a presenilin-type aspartic protease. Science. 2002; 296(5576):2215-8.

Welply J.K., Shenbagamurthi P., Lennarz W.J., Naider F. Substrate recognition by oligosaccharyltransferase. Studies on glycosylation of modified Asn-X-Thr/Ser tripeptides. J Biol Chem. 1983; 258(19):11856-63.

Wertz I.E., O'Rourke K.M., Zhou H., Eby M., Aravind L., Seshagiri S., Wu P., Wiesmann C., Baker R., Boone D.L., Ma A., Koonin E.V., Dixit V.M. De- ubiquitination and ubiquitin ligase domains of A20 downregulate NF- kB signalling. Nature. 2004; 430:694–699.

Wessels H.P., and Spiess M. Insertion of a multispanning membrane protein occurs sequentially and requires only one signal sequence. Cell. 1988; 55(1):61-70.

Wei N., Serino G., Deng X.W. The COP9 signalosome: more than a protease. Trends Biochem Sci. 2008; 33(12):592-600.

White I.J., Souabni A., Hooper N.M. Comparison of the glycosyl-phosphatidylinositol cleavage/attachment site between mammalian cells and parasitic protozoa. Journal of cell science. 2000; 113 (Pt 4):721–7.

Wesolowski J., Alzogaray V., Reyelt J., Unger M., Juarez K., Urrutia M., Cauerhff A., Danquah W., Rissiek B., Scheuplein F., Schwarz N., Adriouch S., Boyer O., Seman M., Licea A., Serreze D.V., Goldbaum F.A., Haag F., Koch-Nolte F. Single domain antibodies: promising experimental and therapeutic tools in infection and immunity. Medical microbiology and immunology. 2009; 198(3), 157–74.

Whitby F.G., Masters E.I., Kramer L., Knowlton J.R., Yao Y., Wang C.C., Hill C.P. Structural basis for the activation of 20S proteasomes by 11S regulators. Nature. 2000; 408:115–120.

Wiertz E.J., Jones T.R., Sun L., Bogyo M., Geuze H.J., Ploegh H.L. The human cytomegalovirus US11 gene product dislocates MHC class I heavy chains from the endoplasmic reticulum to the cytosol. Cell. 1996b; 84:769-779

Wiertz E.J., Tortorella D., Bogyo M., Yu J., Mothes W., Jones T.R., Rapoport T.A., Ploegh H.L. Sec61-mediated transfer of a membrane protein from the endoplasmic reticulum to the proteasome for destruction. Nature. 1996a; 384(6608):432-8.

Wilbourn B., Nesbeth D.N., Wainwright L.J., Field M.C. Proteasome and thiol involvement in quality control of glycosylphosphatidylinositol anchor addition. Biochem J. 1998; 332(Pt 1):111–8.

Wilkinson B.M., Purswani J., Stirling C.J. Yeast GTB1 encodes a subunit of glucosidase II required for glycoprotein processing in the endoplasmic reticulum. J Biol Chem. 2006; 281(10):6325-33.

Wilkinson C.R., Wallace M., Morphew M., Perry P., Allshire R., Javerzat J.P., McIntosh J.R., Gordon C. Localization of the 26S proteasome during mitosis and meiosis in fission yeast. EMBO J. 1998; 17:6465–6476.

Willey R.L., Maldarelli F., Martin M. A., Strebel K. Human immunodeficiency virus type 1 Vpu protein regulates the formation of intracellular gp160-CD4 complexes. J Virol. 1992; 66:226-234.

Williams D.B. Beyond lectins: the calnexin/calreticulin chaperone system of the endoplasmic reticulum. J Cell Sci. 2006; 119(Pt 4):615-23.

Wilson K.C., Center D.M., Cruikshank W.W. The effect of interleukin-16 and its precursor on T lymphocyte activation and growth. Growth Factors. 2004; 22(2):97-104.

Wolf B. Biotinidase: its role in biotinidase deficiency and biotin metabolism. The J Nutr Biochem. 2005; 16(7):441–5.

Wu H., Kwong P.D., Hendrickson W. A. Dimeric association and segmental variability in the structure of human CD4. Nature. 1997; 387:527-530.

Yamamoto K., Yoshida H., Kokame K., Kaufman R.J., Mori K. Differential contributions of ATF6 and XBP1 to the activation of endoplasmic reticulum stress-responsive cis-acting elements ERSE, UPRE and ERSE-II. J. Biochem. 2004; 136:343–350.

Yamamoto K., Sato T., Matsui T., Sato M., Okada T., Yoshida H., Harada A., Mori K. Transcriptional induction of mammalian ER quality control proteins is mediated by single or combined action of ATF6alpha and XBP1. Dev Cell. 2007; 13(3):365-76.

Yan A., Ahmed E., Yan Q., Lennarz W.J. New findings on interactions among the yeast oligosaccharyl transferase subunits using a chemical cross-linker. J Biol Chem. 2003; 278(35):33078-87

Yan A., and Lennarz W.J. Unraveling the mechanism of protein N-glycosylation. J Biol Chem. 2005; 280(5):3121-4.

Yao T., and Cohen R.E. A cryptic protease couples deubiquitination and degradation by the proteasome. Nature. 2002; 419:403–7.

Ye Y., Meyer H.H., Rapoport T.A. The AAA ATPase Cdc48/p97 and its partners transport proteins from the ER into the cytosol. Nature. 2001; 414(6864):652-6.

Ye Y., Meyer H.H., Rapoport T.A. Function of the p97-Ufd1-Npl4 complex in retrotranslocation from the ER to the cytosol: dual recognition of nonubiquitinated polypeptide segments and polyubiquitin chains. The Journal of cell biology. 2003; 162(1), 71–84.

Ye J., Rawson R.B., Komuro R., Chen X., Davé U.P., Prywes R., Brown M.S., Goldstein J.L. ER stress induces cleavage of membrane-bound ATF6 by the same proteases that process SREBPs. Mol Cell. 2000; 6(6):1355-64.

Ye Y., Shibata Y., Kikkert M., van Voorden S., Wiertz E., Rapoport T.A. Recruitment of the p97 ATPase and ubiquitin ligases to the site of retrotranslocation at the endoplasmic reticulum membrane. Proc Natl Acad Sci U S A. 2005; 102(40):14132-8.

Ye Y, Shibata Y, Yun C, Ron D, Rapoport TA. A membrane protein complex mediates retro-translocation from the ER lumen into the cytosol. Nature. 2004 Jun 24;429(6994):841-7.

Yocupicio-Monroy R.M., Medina F., Reyes-del Valle J., del Angel R.M.. Cellular proteins from human monocytes bind to dengue 4 virus minus-strand 3' untranslated region RNA. J Virol. 2003; 77:3067–3076.

Yoon G.S., Lee H., Jung Y., Yu E., Moon H.B., Song K., Lee, I. Nuclear matrix of calreticulin in hepatocellular carcinoma. Cancer Res. 2000; 60:1117–1120.

Yoshida H., Haze K., Yanagi H., Yura T., Mori K. Identification of the cis-acting endoplasmic reticulum stress response element responsible for transcriptional induction of mammalian glucose-regulated proteins. Involvement of basic leucine zipper transcription factors. J Biol Chem. 1998; 11; 273(50):33741-9.

Yoshihisa T., Barlowe C., Schekman R. Requirement for a GTPaseactivating protein in vesicle budding from the endoplasmic reticulum. Science. 1993; 259:1466–1468.

Yoshida Y., Adachi E., Fukiya K., Iwai K., Tanaka K. Glycoprotein-specific ubiquitin ligases recognize N-glycans in unfolded sub- strates. EMBO Rep. 2005; 6:239–244.

Yoshida Y., Chiba T., Tokunaga F., Kawasaki H., Iwai K., Suzuki T., Ito Y., Matsuoka K., Yoshida M., Tanaka K., Tai T. E3 ubiquitin ligase that recognizes sugar chains. Nature. 2002; 418: 438–42.

Yoshida H., Matsui T., Yamamoto A., Okada T., Mori K. XBP1 mRNA is induced by ATF6 and spliced by IRE1 in response to ER stress to produce a highly active transcription factor. Cell. 2001; 107:881–891.

Yoshida Y., and Tanaka K. Lectin-like ERAD players in ER and cytosol. Biochimica et biophysica acta. 2010; 1800(2):172–80.

Yoshimura T., Kameyama K., Takagi T., Ikai A., Tokunaga F., Koide T., Tanahashi N., Tamura T., Cejka Z., Baumeister W., Tanaka K., Ichihara A. Molecular characterization of the "26S" proteasome complex from rat liver. J Struct Biol. 1993; 111:200-211.

Zehner M., and Burgdorf S. Regulation of antigen transport into the cytosol for cross-presentation by ubiquitination of the mannose receptor. Mol Immunol. 2013; 55(2):146-8.

Zhao G., Zhou X., Wang L., Li G., Schindelin H., Lennarz, W. J. Studies on peptide:N-glycanase-p97 interaction suggest that p97 phosphorylation modulates endoplasmic reticulum-associated degradation. Proceedings of the National Academy of Sciences of the United States of America. 2007; 104(21):8785–90.

Zhang X.B., Wang Y., Li H., Zhang W.Q., Wu D., Mi H.F. The mouse FKBP23 binds to BiP in ER and the binding of C-terminal domain is interrelated with Ca^{2+} concentration FEBS Lett. 2004; 559:57–60.

Zhong Y., and Fang S. Live cell imaging of protein dislocation from the endoplasmic reticulum. J Biol Chem. 2012; 287(33):28057–66.